Abwao, Stephen Indieka (2012) *Translational control of abiotic stress responses in Arabidopsis thaliana.* PhD thesis.

http://theses.gla.ac.uk/3502/

Copyright and moral rights for this thesis are retained by the author

A copy can be downloaded for personal non-commercial research or study, without prior permission or charge

This thesis cannot be reproduced or quoted extensively from without first obtaining permission in writing from the Author

The content must not be changed in any way or sold commercially in any format or medium without the formal permission of the Author

When referring to this work, full bibliographic details including the author, title, awarding institution and date of the thesis must be given

Glasgow Theses Service
http://theses.gla.ac.uk/
theses@gla.ac.uk

Translational Control of Abiotic Stress Responses in *Arabidopsis thaliana*

Abwao Stephen Indieka

Thesis Submitted for the Degree of

Doctor of Philosophy

School of Life Sciences

Institute of Molecular, Cell and Systems Biology

University of Glasgow

October 2011

© A.S. Indieka

Abstract

A detailed understanding of the mechanisms by which plants sense and respond to major environmental stress factors will significantly contribute towards the prospects of developing crops capable of yielding well over a wider geographical range, including marginalised lands. One of the important stress response mechanisms in eukaryotes is mediated through phosphorylation of the eIF2α-subunit (serine 51/56) by specific kinases, namely double stranded RNA activated protein kinase (PKR), General Control Non-repressible 2 protein kinase (GCN2), Pancreatic eIF2α kinase (PERK) and Heme-regulated inhibitor protein kinase (HRI). This mechanism is a highly conserved phenomenon in eukaryotes and occurs in response to various stress conditions. Unlike in yeast and mammals, the mechanism is however not well established in higher plants, although its components such as eIF2α and GCN2 kinase have been identified in plants. The objective of the study reported herein was therefore to elucidate this mechanism in *Arabidopsis*, a model plant species.

Initially the presence of yeast GCN2 kinase (ScGCN2), human PKR (HsPKR), human HRI (HsHRI) and human PERK (HsPERK) kinase homologues in *Arabidopsis* and Viridiplantae (green plants and algae) was evaluated through homology and phylogenetic analysis using TAIR10 and NCBI protein sequences, respectively. *Arabidopsis* lacked homologues of HsPKR, HsHRI and HsPERK however the presence of ScGCN2 homologue, herein referred to as AtGCN2 (*Arabidopsis* GCN2 kinase), was confirmed. Further evaluation of translation control mechanism through phosphorylation of AteIF2α (*Arabidopsis* eukaryotic initiation factor 2 α-sub-unit) was conducted using *Atgcn2-1* null mutant plants (plants expressing a copy of truncated non-functional AtGCN2 kinase). Unlike WT Col-0, the *Atgcn2-1* seedlings failed to induce phosphorylation of AteIF2α after exposure to amino acid starvation (150 µM glyphosate), NaCl (50 and 100 mM), heat (37^{o}C) and cold (4^{o}C) acclimation. On the other hand no strong phenotype of *Atgcn2-1* was observed under optimal growth conditions and NaCl stress, except seedlings had relatively shorter roots compared with WT Col-0 seedlings. Failure of *Atgcn2-1* seedlings to induce phosphorylation of AteIF2α Ser 56, after exposure to various stress confirmed that *Arabidopsis* possesses only one GCN2 kinase, as is in the case of yeast, and unlike mammalian systems. Further characterisation was

conducted by exposing WT Col-0, *Atgcn2-1*, *jar-1* and *NahG* seedling to biotic stress; Cauliflower Mosaic Virus (CaMV) and *Pseudomonas syringae* DC3000 (*P. syringae*) and positive control treatment using 150 µM glyphosate. The *jar-1* and *NahG* seedlings are mutants defective in jasmonate and salicylic pathways, respectively. Inoculation with CaMV and *P. syringae* failed to induce phosphorylation of AteIF2α, unlike glyphosate. These results suggested that activation of the AtGCN2 kinase may be independent of jasmonate and salicylic pathways.

Due to lack of a strong *Atgcn2-1* phenotype, two mutants expressing AtGCN2 under the control of a 35S promoter, namely *p35S:AtGCN2* and *p35S:GFP:AtGCN2* were generated for further characterisation and localisation of AtGCN2 kinase, respectively. For characterization experiments the *p35S:AtGCN2* seedlings were subjected to salinity stress, osmotic stress and temperature shock. In localisation experiments, GFP activities were assessed in non-stressed 7-day old *p35S:GFP:AtGCN2* seedlings. During characterisation, higher germination rates were generally obtained with *p35S:AtGCN2* and *Atgcn2-1* compared with WT Col-0 seeds on ½ MS media containing NaCl, KCl and mannitol. On media infused with PEG6000 however *p35S:AtGCN2* had the lowest germination rates. There were also no strong *p35S:AtGCN2* phenotypes observed, except for increased root growth compared with WT Col-0 and *Atgcn2-1* seedlings. In contrast, *Atgcn2-1* seedlings subjected to PEG6000 osmotic stress had the highest increase in root growth compared with both WT Col-0 and *p35S:AtGCN2* seedlings. On the other hand localisation of the GFP:AtGCN2 fusion protein was observed in the root and shoot tip tissues of *p35S:GFP:AtGCN2* seedlings. The results obtained with *Atgcn2-1* and *p35S:AtGCN2* seedlings suggested that mutation of *Atgcn2* produced root phenotypes. There were no significant differences in the survival of all the three genotypes when seedlings were subjected to heat shock stress. In cold shock experiments however *Atgcn2-1* survival was significantly ($p<0.05$) lower than that of WT Col-0 and *p35S:AtGCN2* seedlings, thus suggesting that null mutation of *Atgcn2* increased susceptibility of seedlings to cold shock.

The homologues of the yeast General Control Non-repressible 4 (ScGCN4) and human Activating Transcriptional Factor 4 (HsATF4), that are activated, when yeast and mammalian eIF2α is phosphorylated, respectively are yet to be identified in plants. To identify putative *Arabidopsis* ScGCN4 and HsATF4 homologues both *in vitro* and *in silico* approaches were explored. *In vitro* translation experiments using Wheat Germ Lysate (WG) mimicking plant translation under stress (WGeIF2α-P) and non-stress (WGeIF2α) conditions were conducted. To mimic stress conditions mPKR kinase was added into the translation reaction and significantly inhibited protein synthesis compared to control treatment. However, due to technical difficulties it was not possible to identify all translated transcripts under stress conditions (WGeIF2α-P) thereby identifying potential *Arabidopsis* ScGCN4 and HsATF4 homologues. This prompted the use of *in silico* tools to identify putative *Arabidopsis* homologues of ScGCN4 and HsATF4 using the FivePrime Viewer programme (Shaun, 2008). A total of 99 TAIR10 transcripts with 5′ upstream Open Reading Frames (uORFs) were identified and only two transcripts, AT4G31590.1 and AT1G58120.1, were identified as putative homologues of ScGCN4 and non for HsATF4. The AT4G31590.1 and AT1G58120.1 transcripts encode for proteins involved in cellulose synthase/ gylcosyl transferase and methyl transferase activities, respectively. Although these genes are involved in key plant growth and developmental activities, there is need to assess translation control of their main open reading frame (mORF) by uORFs through phosphorylation of AteIF2α.

Overall the data presented in this study suggest that stress response translation regulation mechanism mediated by phosphorylation of eIF2α is present in *Arabidopsis*. Plants are known, however, to carry out unique biological processes such as photosynthesis and cellulose biosynthesis that other eukaryotes lack. It would therefore not be surprising for them to have translation regulation mechanisms like other eukaryotes but with unique differences.

Table of Contents

List of Tables

List of Figures

List of Appendices

Acknowledgement

I would like to acknowledge my supervisor Dr. Peter J. Dominy for providing me with the opportunity to pursue PhD at University of Glasgow through William Stewart Bursary, and for his continual support, constructive discussion, encouragement, and guidance throughout my PhD research. I want thank my colleagues Naeem Shawani, Scott Ramsay, Shawn Webb and Augustina Nurcahayanti (Antin) for their company and friendship. Special thanks to Dr. Jillian Price and Jim Jardine for their assistance, ideas and weaning me into the PJD group, and my PhD research topic and techniques. I also thank members of the Arnott lab present and past for their assistance, especially Mai-Britt Jensen, Craig Carr, and Liz O'Donnel for their continuous help and kindness. Lots of thanks go to Dr. Andrew Love for his advice, assistance, and for providing CaMV and *P. syringae* DC3000 pathogens and the *Jar-1* and *NahG Arabidopsis* mutants. Special thanks go to Dr. John Christie for his friendship, advice and assistance on expression and purification of recombinant proteins. I am highly indebted to Dr. Gramme Conn of University of Manchester, for providing mPKR expression construct used in this study. I am also very grateful to Prof. Jesse Machuka of Kenyatta University, Nairobi, Kenya for allowing me to undertake part of my research in his laboratory, for his encouragement, and advice on experiments and thesis. I also thank members of Kenyatta University, Plant Transformation Laboratory for their support, especially Dr. Allan Jalemba, Duncan Odhiambo, Catherine Taracha and others, for their constructive discussions and help. Finally, I would like to thank to my beloved wife Lydia Wamalwa-Indieka for her love, patience, valuable support, prayers and encouragement throughout my PhD study. Lastly I would like to thank my mother and father, my brothers Ekongo, Abisai and Osome for their prayers and encouragement.

Declaration

I declare that this thesis has been written in accordance with the University regulations. All work presented in this thesis were performed by the author Abwao Stephen Indieka, unless otherwise stated and has not been submitted for a degree at any other institution.

Abbreviations

48S-PIC	48S-pre-initiation complex
ABA	Abscisic acid
ANOVA	Analysis of variance
ASALs	Arid and semi-arid
AteIF2α	*Arabidopsis* eukaryotic initiation factor 2-α subunit
ATF4	Activating transcriptional factor 4
AtmRNA	*Arabidopsis* mRNA
ATP	Adenosine triphosphate
bZIP	Basic leucine zipper
c.f.u	Colony forming units
CaMV	Cauliflower mosaic virus
CBFs	C-repeat binding factors
cDNA	Complementary DNA
Col-0	Columbia-0
CT-domian	C- terminal domain
DNA	Deoxyribonucleic acid
DRE	Dehydration-responsive elements
DTT	Dithiotheitol
dsRBD	Double stranded RNA binding domain
dsRNA	Double stranded RNA
eIF2α	Eukaryotic initiation factor 2-α subunit
eIF3	Eukaryotic initiation factor 3
ET	Ethylene
FAO	United Nation Food and Agriculture Organisation
FOX	Full-length cDNA over-expressing
GCN2	General control non-derepressible 2
GCN4	General control non-derepressible 4
GDP	Guanosine diphosphate
GFP	Green fluorescent protein
GTP	Guanosine triphosphate
His	Histidine
HisRS	Histidyl-tRNA synthetase
HsGCN2	Human GCN2
HsPERK	Human PERK
HsPKR	Human PKR
HR	Hypersensitive response
HRI	Heme-regulated inhibitor protein kinase
HsATF4	Human activating transcriptional factor 4
HSF	Heat stress factors
HsHRI	Human HRI
HSP90	Heat shock Protein 90;
PERK	Pancreatic eIF2-α protein kinase
PKR	Double stranded RNA-activated protein kinase
HSP	Heat shock proteins
IPTG	Isopropyl-b-D-thiogalactopyranoside
IRE	Iron-responsive element
IRES	Internal ribosome entry sites
ISR	Induced systemic resistance
JA	Jasmonic acid

KCl	Potassium chloride
MAPK	Mitogen-activated protein kinases
met-tRNA$_i^{Met}$	Methionyl initiator methionine transfer RNA
mORF	Main open reading frame
mRNA	Messenger RNA
MS	Murashige and Skoog
NaCl	Sodium chloride
ORF	Open reading frame
PABP	Poly(A)binding proteins
PCR	Polymerase chain reaction
PIC	Pre-initiation complex
pPKR	Plant PKR
QRT-PCR	Quantitative reverse transcript polymerase chain reaction
RNA	Ribonucleic acid
RNAi	RNA interference
ROS	Reactive oxygen species
RT-PCR	Reverse transcription PCR
SA	Salycilic acid;
SAR	Systemic acquired resistance
ScGCN2	*Saccharomyces cerevisiae* GCN2
ScGCN4	*Saccharomyces cerevisiae*, GCN4
siRNA	Short interfering RNA duplexes
TC	Ternary complex
T-DNA	Transfer DNA
TE	Tris EDTA
TF	Transcriptional factors
uORFs	Upstream open reading frames
UTRs	Un-translated regions
v/v	Volume per volume (expressed as percentage)
w/v	Weight per volume (expressed as percentage)
WG	Wheat germ lysate
WGeIF2α	Wheat germ eIF2α
WT	Wild type
WUE	Water use efficiency

1 Chapter 1: Introduction

1.1 Environmental Stress and Crop Production

The World population is estimated to increase by 50%, reaching 9.1 billion in 2050 compared to 6.7 billion in 2009 (Wang *et al.*, 2003). This population increase will put enormous pressure on agriculture and other ecosystem services (FAO, 2009). The problem of food production to feed the increasing population will be exacerbated by climate change. This will significantly affect basic elements of food production in particular water and soil fertility thereby altering the conditions for growing crops (Thuiller *et al.*, 2005). In addition to population increase, it has been projected that more than 50% of arable land may be lost due to salinity, drought and extreme temperature by 2050 (Wang *et al.*, 2003). Therefore the greatest challenge to global agriculture will be to increase land for food production. One of the strategies for addressing the problem of loss of arable land is the development of stress tolerant crops. These crops will also facilitate bringing marginal land into agricultural production.

The discovery of genes associated with plant stress-response is an ongoing effort. However the development of transgenic plants for robust stress-tolerant traits has been difficult to achieve. This is due to the complex nature of the traits associated with abiotic stress-response events. Nonetheless manipulation of stress-response components, such as transcription factors (TFs) and other upstream signalling modulators can result in significant improvement of stress tolerance in plants (Hai Lan *et al.*, 2001; Saijo *et al.*, 2001; Wang *et al.*, 2003). Ideally, genetically modified crops should have the capability of tolerating stress without affecting yields (Wang W.X *et al.*, 2001). On that note, there are encouraging reports where knowledge gained from functional genomic studies in *Arabidopsis* have been employed in the development of transgenic drought tolerant maize and rice (Karaba *et al.*, 2007; Nelson *et al.*, 2007).

1.2 Genetic Engineering of Plants for Stress Tolerance

Biotic and abiotic stresses pose a serious threat to crop production around the world. Farmers and scientists have acknowledged that often environmental stresses occur simultaneously, resulting in serious damage to crop production (Mittler, 2006) For example, during heat stress plants most often also experience drought, high photo irradiance, salinity, and mineral toxicity stresses (Moffat, 2002). Earlier biotechnological programmes on development of stress tolerant crops had relied mainly on single gene manipulation. These programmes attained limited success, since genes manipulated may have only been involved in a single event in a stress-response pathway (Flowers, 2004). There have been attempts to study the effects of different environmental-stresses simultaneously to mimic field conditions. This is demonstrated by studies on *Arabidopsis* exposed to heat and drought stress concurrently. These studies have revealed that less than 10% of the genes regulated during dual stress (heat and drought) treatment overlapped with those of individual stress treatment (Rizhsky *et al.*, 2004). These results clearly show that plant responses to multiple stresses are unique and thus cannot be predicted entirely from single stress studies. In the recent past, large scale genomic (transcriptomic, proteomic and metalabolomic) studies have been undertaken with regard to environmental stresses. These studies have generated a tremendous amount of data with greater insight into how plants respond to stresses (Westernack, 2007). Therefore, understanding plant responses to a combination of different stress factors will be critically important in developing stress tolerant crops.

1.3 Functional Genomics

There are two strategies that are generally employed to dissect functions of gene products namely, forward and reverse genetics. Forward genetics is phenotype driven, where one observes at the phenotype of a mutant based on the disruption of a particular gene. To date it has been the most successful approach to study functions of gene products. The assumption is that the function of a product of the mutated gene is inferred from what the mutant does differently when compared with wild-type lines. Forward genetic studies in *Arabidopsis* have been facilitated by disruption of genes through insertional

mutagenesis by T-DNA or transposons (McElver *et al.*, 2001; Thorneycroft *et al.*, 2001). Mutants are then screened for phenotypes, such as resistance to biotic or abiotic stresses. The aim of such screen is to finds gene(s) involved for a particular trait, thus referred to as a 'genetic screen'. Apart from insertional mutation, many genes and pathways in *Arabidopsis* have been dissected using forward genetic screens through gain-of-function mutation as primary screening tool (Ichikawa *et al.*, 2003; Kuromori *et al.*, 2009). Apart from ectopic expression of gene of interest in *Arabidopsis*, gain-of-function mutants have also been generated through activation tagging (Weigel *et al.*, 2000; Weigel & Glazebrook, 2006).

Reverse genetics studies typically start with a known gene of interest followed by assaying and identification of phenotypes due to its modification. In *Arabidopsis*, the reverse genetics approach entails disruption of the endogenous wild-type genes through insertion mutation to generate null-mutants. *Arabidopsis* genome has been sequenced (26,000 genes), however the function of the product of these genes and resulting phenotype caused by mutation of most of these genes is still unknown (Thorneycroft *et al.*, 2001). Though understanding their function is a major challenge, reverse genetics provide prospects in which their functions can be determined (Sessions *et al.*, 2002). On the other hand, sequence homology can help predict the function of a gene product; however there are many genes without sufficient homology to characterize these genes. Nonetheless sequence homology as a reverse genetics technique can reveal general functions of a gene of interest product (Sasaki *et al.*, 2002); though the precise function of cannot necessarily be determined from it alone. Although reverse genetic approaches in *Arabidopsis* have heavily relied on null mutation by T-DNA and transposon insertion, gene silencing through RNA interference has also been employed when insertional mutation is not efficient or more than 1 gene product needed to be silenced (Thorneycroft *et al.*, 2001; Wielopolska *et al.*, 2005).

1.4 Loss-of-Function Mutation

1.4.1 Insertional Mutagenesis

Arabidopsis loss-of-function mutants (null mutants) are generated by insertion of a transposon element or T-DNA into the structural gene; whether into an intron or an exon (Sessions *et al.*, 2002). The insertion disrupts the expression a particular gene and the resulting change leads either to it not being translated into RNA or into a functional protein. The reversal of null mutation generated by T-DNA insertions in wild type is fairly minimal, and therefore, they can be crossed with other null mutants to generated double or multiple mutations (Zhang *et al.*, 2003). Null mutation is an important tool in dissecting genes, because it provides a direct route to determine functions of gene products *in planta*. The effects of gene deficiency on the ability of the organism to function can be monitored (Krysan *et al.,* 1999). In addition, null mutation can produce clear phenotypes, thereby revealing new information about old pathways or function(s) of individual members of multigene families (Thorneycroft *et al.*, 2001). It can therefore provide a starting point for genetic manipulation of plants; however, it can sometimes produce unexpected phenotypes that are difficult to interpret in terms of functions of the gene product. This is because most genetic mutations through T-DNA or transposon insertion alter the gene sequence resulting in truncated transcripts that produce proteins with no or altered function (Hartwell *et al.,* 2008). The other limitation of loss-of-function mutation is that, in stress-response screens null-mutants are generally hypersensitive to stress and are usually lost, thereby limiting further experimentation.

1.4.2 Gene Silencing

In order to study functions of a gene product it is apparent that one has to induce mutation on that specific gene. As discussed earlier, insertional mutagenesis has played a key role in gene analysis through gain- or loss-of-function approaches. The usefulness of these approaches however may be limited because of their restriction mainly to model plant species and length of time required to generate mutants (Kuromori *et al.*, 2009). In addition,

polyploidy and genetic redundancy due to multigene family makes it difficult to study functions of gene products especially through loss-of-function mutation (McElver *et al.*, 2001). Apart from insertional mutations, post transcription gene silencing (RNA interference) has been used efficiently to study gene products. It has been used successfully to overcome problems encountered in dissecting gene through insertional mutations (Wielopolska *et al.*, 2005).

Gene silencing is achieved when double stranded RNA (dsRNA) is processed into short interfering RNA duplexes (siRNA) which guide RNA silencing through specific and distinct mechanisms (Meister & Tuschl, 2004). In siRNA silencing mechanism, the dsRNA is detected by the host genome as unusual and thus cleaved by dicer-like enzymes into two distinct classes of siRNA namely, 21-mers and 24-mers which are involved in degradation of mRNA, and systemic methylation of DNA (Hamilton *et al.,* 2002). siRNA silencing allows silencing of one, several, or all members of multigene families or homologous gene copies in polyploids by targeting sequences that are unique or shared by several genes (Miki *et al.,* 2005). This is of great importance for functional genomic studies in plants such as hexaploid wheat, where most of the genes are in at least three homologous copies; insertional mutation is not effective in dissecting gene products in such situations (Travella *et al.,* 2006). Systems for studying gene silencing designed for monocots and dicots are already in place, including for genes which may be lethal at gamete or embryo level, where inducible promoter systems have been employed (Wielopolska *et al.,* 2005).

1.5 Gain-of-Function Mutation

Gain-of-function screens are primary tools employed to dissect gene function in circumstances where loss-of-function screen is inefficient. As discussed in the preceding section, this is mainly due to problems associated with gene redundancy and for genes whose loss-of-function lead to embryonic or gametophytic lethality (Wielopolska *et al.*, 2005; Kuromori *et al.*, 2009). The Gain-of-function approach is key in dissecting gene product, especially if their ectopic activation is compatible with the survival of the organism (Weigel *et al.*, 2000). Gain-of-function phenotype can be brought about by mutation in the coding region, resulting in constitutive expression of the gene or by mutation

that alters the level or pattern of gene expression (Chang *et al.*, 1993). Mutation can be brought about by chromosomal rearrangement or by activation tagging where the gene is brought under the control of new promoters or enhancers. Unlike loss-of-function mutations, gain-of-function mutations cause a dominant mutation especially during the T_1 generation (Weigel & Glazebrook, 2006). In addition, one member of a gene family can produce a phenotype without interfering with other members of the family; especially for functionally redundant genes belonging to a gene family (Nakazawa *et al.*, 2003). Since gain-of-function mutation is dominant and mutants are usually isolated as hyper tolerant individuals, they can be rescued from stress screens and used for subsequent experimentation. The common techniques in gain-of-function mutation screens are ectopic expression of genes of interest, activation-tagging, and the FOX hunting system.

1.5.1 Ectopic Expression

Gain-of-function mutation can be achieved by placing a gene of interest under the control of a constitutive promoter. This form of gene expression is commonly referred to as ectopic expression and may provide a phenotype that can be used to determine the function(s) of the product of the gene of interest (Aoyama *et al.*, 1995). Furthermore ectopic expression can be used to study genes by examining the sub-cellular localisation of the corresponding protein. This is usually achieved by using a chimeric gene fusion constructs with reporter genes. The location of the reporter protein in a sub-cellular compartment often provides additional supporting evidence for the function of the gene product (Karimi *et al.*, 2007). However problems can be encountered with ectopic expressions. These are masking of tissue specific effects and can cause gene lethality or even sterility. Under such circumstances, controlling the expression of the gene of interest using an inducible promoter is vital (Pino *et al.*, 2007). Several inducible promoters have been employed in such circumstances, these include heat-shock promoters and other chemically induced promoters such oestrogen-responsive promoters (Coca *et al.*, 1996; Curtis & Grossniklaus, 2003). It is well known that there are genes which are normally expressed at a certain point of a plant's life cycle. In such circumstances the use of inducible

promoters also comes in handy if there is need to use ectopic expression to characterize such genes (Curtis & Grossniklaus, 2003).

1.5.2 Activation-tagging

Activation tagging is a gain-of-function mutation technique where transcriptional enhancers such as *CaMV 35S* are placed on T-DNA or transposons. The insertion of T-DNA containing enhancers into the genome induces constitutive transcription of genes near the insert from a distance of 0.38Kb to 3.6kb (Weigel *et al.,* 2000; Tani *et al.,* 2004). Transcriptional enhancers however have been shown to activate the expression of genes located up to 10.7kb from the activation enhancers (Nakazawa *et al.,* 2003). Activation-tagging generates mutants that are dominant and thus can be rescued and the gene responsible identified. Unlike other gain-of-function mutation approaches, activation-tagging is advantageous, since activation of a single dominant allele can reveal the function of a redundant gene (Hartwell *et al.,* 2008). On the other hand activation-tagging can also be used for identification of novel genes; since the integration of the transcriptional enhancers may activate the coding and non-coding sequences flanking the site of insertion (Weigel *et al.,* 2000). There are however disadvantages of using T-DNA in activation-tagging. This is because T-DNA insertions are complex and can sometimes be characterized by multiple insertions, tandem copies or even truncated T-DNAs, thereby making molecular analysis of the insertion difficult (Tax & Vernon, 2001). To circumvent this problem, a single copy transposon-tagging system was developed (Tissier *et al.,* 1999). There are other activation-tagging systems available such as pEnLOX/pCre system (Pogorelko *et al.,* 2008). This system has successfully been used to revert mutants to a wild-type genotype through the removal of *CaMV 35S* enhancers. This system has been recognised as a convenient method for identifying the corresponding gene(s) for a particular phenotype generated through activation-tagging (Kuromori *et al.,* 2009).

1.5.3 FOX Hunting System

Activation-tagging mutagenesis can be a very useful technique in characterising novel genes however there are some disadvantages in using activation-tagging. As discussed in the preceding section, one of the problems associated with this technique is that the effect of gene activation by a transcriptional enhancer is not restricted to one gene and may sometimes cause transcription of several genes resulting in a complex phenotype. Hence it is difficult to identify gene(s) corresponding to the particular phenotype obtained (Ichikawa *et al.,* 2003). The effect of influencing transcription of genes flanking the T-DNA insertion is supported by the findings that enhancers can activate the expression of genes located up to 10.7kb from the insertion site (Nakazawa *et al.,* 2003). In order to by-pass this problem the Full-length cDNA Over-eXpressing (FOX hunting) system was developed (Ichikawa *et al.,* 2006). The FOX hunting system is a gain-of-function system where normalised full-length cDNA expression libraries that are independently expressed under a *CaMV 35S* promoter and a nos terminator are introduced into the plant genome. Unlike activation-tagging, the FOX hunting system eliminates phenotype complexity due to multiple gene expression. This is because it utilizes normalised full-length cDNAs that are expressed in the correct orientation under the control of a promoter and a terminator. In addition, the FOX hunting system can be of choice when one wants to identify phenotypes associated with splice variants individually (Ichikawa *et al.,* 2006). Another advantage that the FOX system shares with all the gain-of-function mutations is that it causes a dominant phenotype and thus the generated lines can be rescued and screened for phenotypes. FOX hunting system has been employed in rice to elucidate a large population of rice genes for the purposes of identifying agriculturally useful genes (Nakamura *et al.,* 2007).

1.6 Gene Expression and Regulation

Generally alterations in the protein profile of tissues involves two main steps namely, transcription and translation. During transcription, the information carried on DNA is copied on to messenger RNA (mRNA), which is then matured by removal of non-coding region (introns) through splicing. Maturation also involves addition of 7-methyl-guanosine (m7G) on the 5′ and poly-A tail on the 3′ end of

the mRNA. Transcription and maturation occurs in the nucleus and mRNA is then translocated into the cytoplasm for translation. Matured mRNAs contain sequences that are organised in groups of three bases referred to as codons. There are 4 nucleotide bases and 64 possible codons, of which 61 of them specify amino acids. The other three codons UAA, UAG and UGA specify termination of protein synthesis, whereas AUG encodes methionine amino acid, which also signals the beginning of protein synthesis. During translation, mature mRNAs are decoded into proteins, which are molecules that are directly involved in various cellular functions. The process of DNA transcription and mRNA translation is referred to as protein expression. On the other hand controlling the efficiency of mRNAs translation (transcripts) of into proteins is referred to as translation regulation.

A series of codons on mRNA starting with AUG and ending with a stop codon (UAA or UAG or UGA) is referred to as open reading frame (ORF). In most genes, the mRNAs contain regions flanking the 5′ and 3′ ends of the ORF, termed as un-translated regions (UTRs). The UTRs are involved in regulating translation of mRNAs, apart from modulating translocation of mRNA out of the nucleus, sub-localization, and mRNA stability (Mignone *et al.*, 2002). The key translation regulatory elements located in the 5′ UTRs of eukaryotic mRNAs are; secondary structures (hairpin loop), internal ribosome entry sites (IRES), upstream open reading frames (uORFs) and m7G cap (Hinnebusch, 1997a; Mignone *et al.*, 2002; Wilkie *et al.*, 2003). The translation regulatory elements on 5′ and 3′ are shown in Figure 1.1 (Mignone *et al.*, 2002).

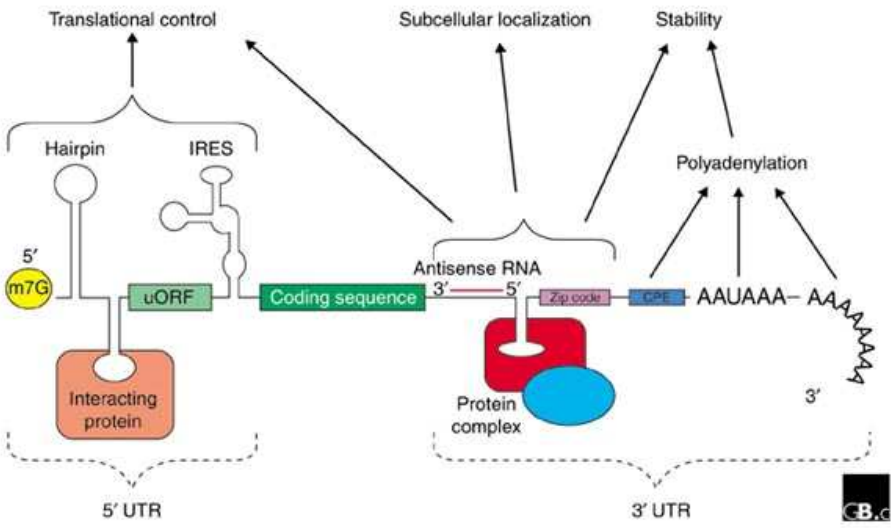

Figure 1.1. A schematic illustration of eukaryotic mRNA depicting translation regulatory elements in 5′ and 3′ UTRs (Mignone *et al.*, 2002). Annotations 5′ to 3′: UTR, un-translated region: m7G, 7-methyl-guanosine cap: hairpin, Interacting protein form hairpin-like secondary structure: uORF, upstream open reading frame: IRES, internal ribosome entry site: AAUAAA, poly (A).

1.7 Translation Initiation

Translation of mRNA commences when the 60S ribosomal subunit assembles with 48S subunit after scanning from the 7-methylguanosine (m7G) cap in the 5′-3′ direction for the start codon of the mRNA main Open Reading Frame (mORF). Translation of mRNAs into proteins is not a simple direct pair-to-pair correspondence of the mRNA nucleotides and amino acids. This is due to the fact that, there are only four different nucleotides and twenty possible amino acids. Therefore, translation of mRNA into proteins follows a rule referred to as the genetic code, which consists of codons (Albert *et al.*, 2002). The generally accepted mode of translation is the "scanning translation model", which entails three main steps. These steps are, (i) binding of the 43S ribosomal complex (eIF2.GTP.met-tRNA$_i^{Met}$) to the 5′ m7G cap of mRNA to form 48S ribosomal subunit, that scans the mRNA UTRs in the 5′ to 3′ direction for a start codon, (ii) the assembly of 60S ribosomal subunit at the start codon followed by translation of the mORF, (iii) termination of translation (Kozak, 1978; Pestova & Kulopaeva,

2002). Ideally, translation initiation begins with the formation of the pre-initiation complex (PIC), where met-$tRNA_i^{Met}$ is recruited by eIF2, coupled with GTP (eIF2.GTP) to form eIF2.GTP.met-$tRNA_i^{Met}$ ternary complex (TC). Then TC binds onto 40S ribosomal subunit facilitated by eIF1, 1A and eIF3, to form 43S pre-initiation complex (43S-PIC) (Asano & Sachs, 2007). Through facilitation of eIF4F, 4A, 4B and poly(A) binding proteins, the 43S-PIC then binds to the 5′ capped end of the mRNA to form 48S-PIC, which scans the mRNA for a start codon (Kozak, 1983; Albert *et al.*, 2002; Hinnebusch, 2005, 2006).

1.8 Eukaryotic Translation Initiation Factors

Eukaryotic translation initiation factors (eIFs) perform various functions at multiple steps (Fig. 1.2). They facilitate binding of met-$tRNA_i^{Met}$ and mRNA to 40S ribosomal subunit (48S PIC), scanning and selection of the start codon on mRNA, and joining of the 60S subunit to form the translation machinery (Pestova *et al.,* 2007). A number of eIFs associated with PIC has been identified in yeast, plants and mammals, these are; eIF1, eIF1A, eIF2, eIF2B, eIF3, eIF4F, eIF5 and eIF5B (Pestova & Kolupaeva, 2002; Asano & Sachs, 2007). The eIF1 and eIF1A are small polypeptides involved in multiple aspects of translation initiation. They facilitate recruitment of the TC on to the 40S ribosomal subunit (Singh *et al.,* 2004; Cheung *et al.,* 2007). They also play an important role in regulating the 48S-PIC during start codon selection, by blocking non-AUG start codons (Maag *et al.,* 2005). In addition, eIF1 is thought to control hydrolysis of GTP in the TC by eIF5 (GTPase activator) as a result of codon anti-codon pairing during translation initiation (Algire *et al.,* 2005; Majumdar & Maitra, 2005).

Among all the eIFs, eIF2 and eIF3 are well characterized multi-meric factors that bind directly to met-$tRNA_i^{Met}$ and the 40s subunit, respectively, to form 43S ribosomal subunit. The eIF2 is a trimeric factor, with α, ß and γ subunits, and can bind either GTP or GDP. However, it is only able to carry out its function of recruiting and binding met-$tRNA_i^{Met}$ to the 40S ribosomal subunit, when bound to GTP (Zhang *et al.*, 2003; Hinnebusch, 2005). On the other hand, eIF3 is a large multi-subunit factor, which binds to the 40S ribosomal subunit and consequently impedes its association with the 60S ribosomal subunit (Cheung *et al.,* 2007).

Its association with the 40S ribosomal subunit stimulates binding of the TC; though there is no evidence of direct interaction with eIF2. Its stimulatory effects on TC binding to 40S subunit may be due to other eIFs or allosteric alteration of the 40S subunit (Asano *et al.*, 2000).

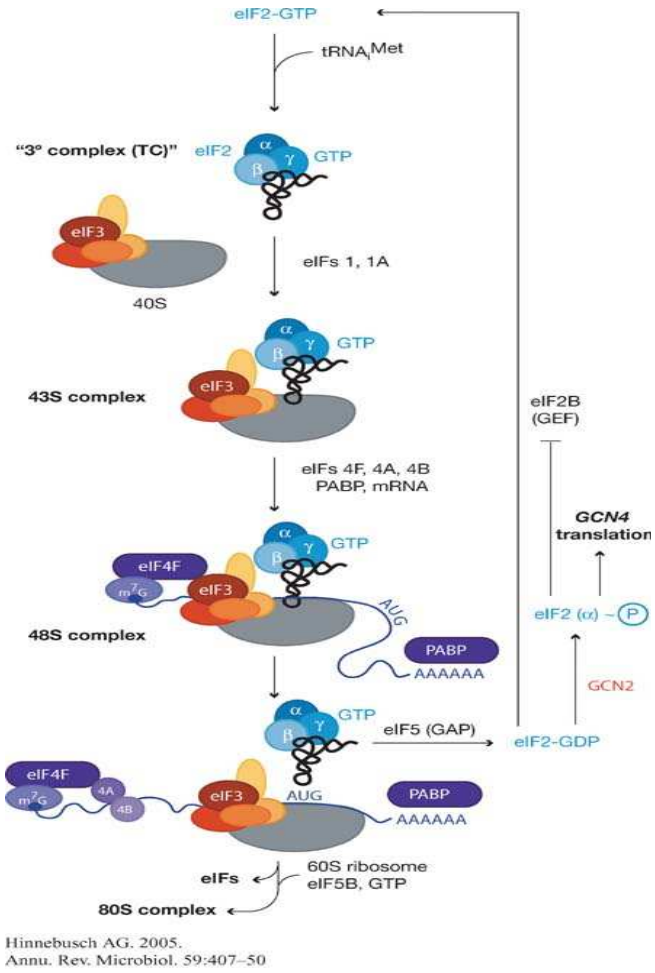

Figure 1.2. A schematic representation of translation initiation pathway (Hinnebusch, 2005). Steps depicting sequential facilitation of eIF(s), beginning with the recruitment of met-tRNA$_i^{Met}$ by eIF2.GTP to the formation of the ternary complex (TC), 43S and 48S pre-initiation complex (PIC), and hydrolysis of eIF2.GTP to eIF2.GDP by eIF5.

The eIF4F facilitates the binding of 5′ cap of the mRNA to the 43S-PIC. It consists of three subunits; an ATPase/RNA helicase (eIF4A), a cap binding protein (eIF4E) and a large modular protein (eIF4G) (Lamphear *et al.*, 1995; Imataka & Sonenberg, 1997; Lomakin *et al.*, 2000). Requirements for active eIF4A subunit is consistent with ATP-dependent restructuring of the 5′ mRNA

cap-proximal region by eIF4F, to provide attachment site for 43S complex (Ray *et al.*, 1985). The eIF5 mediates hydrolysis of GTP bound to the TC (eIF2α subunit) to GDP by GTPase activating protein. In this regard, there is strong evidence indicating interaction of eIF5, eIF1 and eIF3 in yeast (Naranda *et al.*, 1996; Phan *et al.*, 1998). Furthermore, eIF5 and eIF1 interacting with all the subunits of eIF2, are involved in accurate recognition of the initiation codon in yeast (Asano *et al.*, 2000). On base pairing of the anti-codon of met-$tRNA_i^{Met}$ with the start codon (AUG), the GTP bound to the TC is hydrolyzed to GDP, releasing eIF2.GDP. At the same time, eIFs are released leaving the met-$tRNA_i^{Met}$ positioned at the start codon and on the A-site of the ribosome. The 60S ribosomal subunit then joins to form the 80S initiation complex, facilitated by eIF5B (Asano & Sachs, 2007). After eIF2.GDP has been released, a guanine exchange factor eIF2B recycles GDP to GTP and eIF2.GTP is then able to recruit a new met-$tRNA_i^{Met}$ for another cycle of translation initiation.

1.9 Translation Control Structures in the 5′ UTR

1.9.1 Internal Ribosome Entry Site (IRES)

As discussed earlier (section 1.8), the scanning translation model is the generally accepted mode of mRNA translation (Kozak, 1978). However, there are some mRNAs, in which translation initiation is independent of 5′ m7G cap. These mRNAs possess structures referred to as internal ribosome entry sites (IRES). These sites allow the assembly of translation machinery and translation initiation to occur without associating with 5′ m7G cap (Mignone *et al.*, 2002; Fernandez *et al.*, 2005; Kozak, 2005). The IRESs are structures consisting of about 25-110 nucleotide sequences and are located in the 5′ UTR of mRNA (see Fig. 1.1). It has been hypothesised that IRES elements have distinctive secondary or even tertiary structures. Cellular mRNAs encoding proteins involved in stress survival are thought to contain IRESs (Kozak, 1991; Kozak, 2005).

1.9.2 RNA Hairpin Loop and Trans-acting Sequences

The RNA hairpin loops are secondary structure in the 5′ UTRs that also play an important role in regulation mORF translation. There is experimental evidence suggesting that the stability of hairpin loop structures significantly decreases translation of mORF. Their effects on inhibiting translation however are usually alleviated by increase in the eIF4F factor subunit eIF4A (Mignone *et al.*, 2002). The association of eIF4F with other translation initiation factors promotes the unwinding of the RNA hairpin loop secondary structure thereby enhancing translation of mORF (Pesole *et al.,* 2001; Mignone *et al.,* 2002). On the other hand, the trans-acting sequences are those sequence elements that are targets of RNA binding proteins. These RNA-binding proteins induce mRNA to form hairpin secondary structures which in turn inhibit translation of mORF by interfering with the scanning process (Kozak, 2005). An example of an mRNA trans-acting sequence is the iron-responsive element (IRE) found in mRNA encoding iron metabolism in mammals. The IRE inhibits translation through iron-dependent binding of iron regulatory proteins resulting in formation of hairpin secondary structures with helical distortion that impede normal scanning translation process (Ke *et al.,* 2000).

1.9.3 Upstream Open Reading Frames (uORFs)

A uORF is identified by the presence of a start and a stop codon in the 5′ UTRs upstream of the mORF. Transcribed uORFs are known to regulate translation of the mORF (Hinnebusch, 1997b; Vilela *et al.*, 1999; Kozak, 2005) and in eukaryotes, most of the transcripts containing transcribed uORFs encode for proteins that are involved in key metabolic pathways (Vattem & Wek, 2004; Hinnebusch, 2005). The most notable are GCN4 and ATF4 transcription activators that are involved in regulation of protein synthesis due to environmental and cellular stresses in yeast and mammals, respectively (Hinnebusch, 2005; Carnevalli *et al.,* 2006). Nonetheless there are reports suggesting that some genes that do not code for transcriptional activators also posses' uORFs that are not regulatory (Krummeck *et al.,* 1991; Morris & Gaballe, 2000). Translation of eukaryotic mRNA generally follows the scanning model as discussed in section 1.7. However for mRNA with regulatory uORFs, translation

of the mORF is more complex than stated in the scanning model, since the first AUG is not the genuine start codon for the mORF. Therefore the assembled translation machinery translates the first uORF then skips one or more AUGs (uORFs) before translation of the mORF. This form of translation is referred to as 'leaky scanning' and has been attributed to a lack of optimum sequences around the start codon (Kozak, 1978, 1987a, b). In this model, translation machinery recognises the start codons of the uORFs, then translation either terminates and then reinitiates at mORF, or terminates and leaves the mRNA consequently reducing translation efficiency of the mORF (Morris & Gaballe, 2000; Meijer & Thomas, 2002). This mode of translational control by uORFs is well established in yeast and mammalian systems (Hinnebusch, 1997b; Kochetov *et al.*, 2008).

1.10 Plant Genes with Regulatory uORFs

Translation control of transcripts by uORFs has been investigated for a number of plant genes. Similar to yeast and mammals, plant genes with regulatory uORFs also encode important regulators of cell cycle and transcriptional activators (Futterer & Hohn, 1992). The notable plant genes containing regulatory uORFs include plasma membrane H^+-ATPase genes. In plants and fungi the primary force that drives ion transport and solutes across the plasma membrane is the proton gradient generated by H^+-ATPases that are embedded in plasma membrane. The regulatory nature of uORFs in H^+-ATPase genes has been demonstrated using *Nicotiana plumaginifolia* H^+-ATPase gene (*PMA3*), using tobacco protoplasts (Lukaszewicz *et al.*, 1998). Maize also contains transcripts with regulatory uORFs, such as OPAQUE2 gene. The 258-nucleotide 5′ UTR region of OPAQUE2 mRNA contains three uORFs encoding 3, 21, and 20 amino acid, and their disruption stimulates translation of the *opaque2* mORF (Lohmer *et al.*, 1993). Furthermore maize Lc gene, a member of the R/B transcriptional activators family has a single regulatory uORF of 38 amino acids, unlike the OPAQUE2 gene. The uORF in the maize Lc gene causes inefficient re-initiation of the translation machinery at the mORF under optimal conditions (Damiani & Wessler, 1993). In *Arabidopsis*, translation initiation factor 3 subunit h (eIF3h) also has regulatory uORFs (Kim *et al.*, 2004).

1.11 Plant Stress Response

Plant growth, survival and regulation of key metabolic events are dependent on the perception and response to stress. These responses may be immediate or may take days or weeks, as is the case for temperature stress (Penfield, 2008). Plants have evolved mechanisms to alleviate prolonged stress exposure. This includes elaborate systems to perceive external stress cues that allow sufficient response. Several biotic and abiotic stress response pathways have been identified in plants, these include hormone signalling pathways regulated by abscisic acid (ABA), salicylic acid (SA), jasmonic acid (JA) and ethylene (ET), as well as reactive oxygen species (ROS) pathways (Bostock, 2005; Lorenzo & Solano, 2005; Mauch-Mani & Mauch, 2005). Elements of these pathways are known to play key roles in cross-talk between biotic and abiotic stress-signalling (Fujita *et al.*, 2006).

Plants are known to acquire tolerance to a particular stress after earlier periods of exposure in a process referred to as acclimation. Plant acclimation to stress triggers molecular, biochemical and physiological processes that are tailored for that specific stress (Mittler, 2006). There are challenges however when plants are acclimated under multiple stress situations. This is due to the fact that there are basic differences in acclimation between different abiotic stresses and plants may produce conflicting stress responses (Rizhsky *et al.*, 2004). For example, during high temperature stress plants open their stomata, thereby cooling leaves through transpiration. On the other hand when high temperature and drought stress are combined, plants will not open their stomata which will result in higher leaf temperature (Rizhsky *et al.*, 2002). Another scenario with conflicting responses include salinity stress combined with high temperature stress; because enhanced transpiration will increase uptake of salt (Mittler, 2006).

1.11.1 Drought Stress Response

Drought is a major limitation to crop production and a basic understanding of drought responses is crucial to the development of drought tolerant plants. In arid and semi-arid agro-climatic zones the periodic and unpredictable nature of drought experienced is a major challenge for agricultural production (FAO, 2009). The problem is exacerbated by breeding challenges of major crops for drought tolerance, mainly due to low heritability and the complex nature of drought traits (Nelson *et al.,* 2007). Exposure of plants to water limiting environment activates biochemical and molecular mechanisms for drought perception and tolerance (Valliyodan & Nguyen, 2006). Through functional genomics, the molecular regulators of drought stress-tolerance have been identified in *Arabidopsis* and have been used to improve drought stress-response in major crops such as maize and rice (Bruce *et al.,* 2002; Karaba *et al.,* 2007; Nelson *et al.,* 2007).

Plants often exhibit symptoms such as enhanced leaf senescence, cellular damage due to photo-oxidative stress, reduced leaf expansion and CO_2-fixation resulting in reduced plant yields during drought stress periods (Chapman & Edmeades, 1999). Plant resistance to drought can be classified as drought avoidance or tolerance. Drought avoidance mainly entails conserving water referred to as water use efficiency (WUE). The WUE is determined as biomass produced per unit transpiration (Karaba *et al.*, 2007). It therefore describes the relationship between water use and biomass production and varies between plants due to genetic variation (Condon *et al.,* 2004). In *Arabidopsis,* WUE has been associated with the HARDY (HRD) gene (an AP2/ERF-like transcriptional factor) which when expressed in rice improved WUE, by enhancing photosynthetic assimilation and reducing transpiration (Karaba *et al.,* 2007).

During drought stress there are biochemical and physiological responses that occur at the cellular level. These include loss of turgor, change in solute composition and concentration in the cell. Plants however can maintain turgor in tissues by avoiding or tolerating dehydration (Chaves & Oliveira, 2004) . Plants achieve these through morphological traits such as root size and depth. Physiological responses include reduction in photosynthetic activity due to

closure of stomata and reduction of photosynthetic enzymes (Tabaeizadeh & Kwang, 1998; Chaves *et al.*, 2009).

1.11.2 Temperature Stress Response

Plants are sessile organisms and therefore they frequently encounter detrimental conditions that make extreme temperature one of the factors that limits crop production world wide (Mittler, 2006). Temperature stress occurs when ambient temperature is elevated above the optimum resulting in metabolic and physiological malfunctions and consequently cell death (Sung *et al.*, 2003). Therefore temperature perception in plants is important for both survival and regulation of physiological and developmental events (Penfield, 2008). There is considerable evidence that plants can acquire tolerance to extreme temperature after previous exposure to non-lethal temperatures, in a phenomenon referred to as acclimation (Sung *et al.*, 2003; Chinnusamy *et al.*, 2007).

One notable response to heat stress in plants is the induction of heat shock proteins (HSPs). These HSPs are molecular chaperones that enable plant proteins to maintain their native configuration and function thereby protecting them from heat denaturation (Kregel, 2002). To counter the threat of heat-induced oxidative stress plants employ enzymatic and non-enzymatic systems to deal with the reactive oxygen species (Vittoria *et al.*, 2008). Plants have genetic capability to alleviate heat stress. In order to do this effectively they require effective heat stress transduction pathways. One of the known pathways involves heat stress factors (HSFs) signalling system. These HSFs bind to heat stress elements in the promoters of genes that encode HSPs to regulate their expression (Rizhsky *et al.*, 2004).

Cold stress can also be a threat to production of major crops such as wheat. It severely hampers reproductive developments of plants by damaging the cell membrane due to dehydration associated with freezing. The main phenotypic symptoms associated with cold stress in plants are; poor germination, stunted seedlings, leaf chlorosis, reduced leaf expansion and may lead to death of plant tissues (Yadav, 2009). Some cold stress signals may be transduced by cell membrane receptors thereby switching on genes for mediating cold stress

tolerance (Murphy *et al.*, 2011). In response to cold, it is well documented that C-repeat binding factors (CBFs) and dehydration-responsive elements (DRE) are central to activating cold stress-response genes (Fujita *et al.,* 2006; Yamaguchi-Shinozaki & Shinozaki, 2006).

1.11.3 Salt Stress Response

Salinization is one of the major factors that limit agricultural production in the world. It is a problem that affects 20% of the world's irrigated crop land and in lands categorized as Arid and Semi-arid lands (ASALs) and deserts too (Yamaguchi & Blumwald, 2005). Therefore loss of land due to salinity presents a major challenge to crop production as demand for food production increases to support the increasing world population (Yeo, 1998). Development of salt tolerant crops can contribute immensely in addressing salinization of arable lands (Wang *et al.,* 2003). Salinity stress is usually accompanied by other forms of stresses, such as altered nutrient uptake especially K^+ and Ca^+ ions, accumulation of Na^+ ions to toxic levels, oxidative stress and induction of low water potential (ψw) stress (Verslues *et al.,* 2006). In plants, three distinct adaptations to salinity have been recognized namely; osmotic stress tolerance (ψw), Na^+ and Cl^- exclusion, and tolerance of accumulated Na^+ and Cl^- (Quesada *et al.*, 2000). A plant's response to salinity stress can be rapid or prolonged; rapid response to salinity occurs within hours and is often associated with the effects of low water potential rather than accumulation of ions to toxic levels (Munns, 2002). On the other hand, plants tend to accumulate Na^+ and Cl^- ions to toxic levels when exposed to relatively high salt levels. The Na^+ and Cl^- ions toxicity may be experienced by plants after days or weeks of exposure (Munns & Tester, 2008).

Plants are also known to avoid salinity injury by maintaining ion homeostasis through exclusion of salt from the cytoplasm, reducing uptake by roots, activating salt export or compartmentalization of salts in the vacuoles (Munns, 2002). Since accumulation of salts in the vacuoles leads to dehydration, the mechanism for tolerating high salt concentration in the vacuole is thought to be similar to that of dehydration due to low water potential and freezing (Zhu, 2002). To counteract the effects of dehydration, plants accumulate compatible

solutes, proteins, and detoxifying reactive oxygen species (Verslues *et al.*, 2006).

1.12 Stress Response Translation Regulation

Gene expression in eukaryotes is regulated at several levels namely; alteration in the local chromatin state of the chromosome, transcription, and translation of mRNA. The ability of mRNA to be translated is depended on its association with the translation initiation complex. At the mRNA level the 5′- and 3′-UTR contain translation regulatory elements as shown in Figure 1.1 (Mignone *et al.*, 2002). Transcriptomics and proteomics studies indicate that the abundance of mRNA does not always correlate with protein levels (Branco-Price *et al.*, 2005). This can be attributed to selective translation of transcripts and is normally restricted to mRNAs that are post-transcriptionally regulated (Pierrat *et al.*, 2007). Change in the translation of most transcripts containing regulatory elements in their UTR region often occurs in response to stress cues (Hinnebusch, 2005; Carnevalli *et al.*, 2006).

Currently there is a greater understanding of genes involved in early stress signalling mechanisms in eukaryotes. One the remarkable mechanisms involved in early stress response entails translation regulation (Hinnebusch, 2005; Carnevalli *et al.*, 2006). Two modes of translation regulation mechanism have been illustrated in eukaryotes, namely; global translation control, in which a large amount of mRNAs in the cell is regulated, and mRNA-specific regulation where only distinct mRNAs with secondary structures are regulated without affecting general protein synthesis (Pesole *et al.*, 2001; Mignone *et al.*, 2002); regulatory structures are shown in Figure 1.1. Global translation regulation in yeast and mammalian systems can be mediated through phosphorylation of eIF2α-subunit (eIF2α-P) by eIF2α specific kinases such as GCN2, PKR, HRI and PERK (Lu *et al.*, 2004; Hinnebusch, 2005; Jiang & Wek, 2005), as shown in Figure 1.3. Phosphorylation of eIF2α results in translation of mRNAs containing upstream open reading frames (uORFs). These group of mRNAs code for important stress response transcription factors (TFs), such as yeast GCN4 and mammalian ATF4 (Hinnebusch, 2005; Carnevalli *et al.*, 2006). Phosphorylation of translation initiation complex proteins including initiation factors (eIFs),

elongation factors and poly(A)binding proteins (PABP) contributes significantly to global translation regulation (Browne & Proud, 2002; Proud, 2005).

Phosphorylation of eIF2α generally activates the stress-response mechanism involving a set of transcriptional factors which induce expression of downstream stress response genes (Fig.1.3). Phosphorylation of many eIFs is induced by abiotic and biotic stress signals. In plants and animals eIF2, eIF4E, eIF4A and eIF4B were found to be hyper-phosphorylated after nutrient depletion, hypoxia, heat, haeme depletion and viral infection (Clemens, 1997; Gallie *et al.*, 1997). In plants numerous changes in gene expression occurs and these changes are sometimes rapid and reversible especially during transient environmental stress cues such as temperature and light intensity (Bailey-Serres, 1999; Bray *et al.*, 2000; Szick-Miranda *et al.*, 2003).

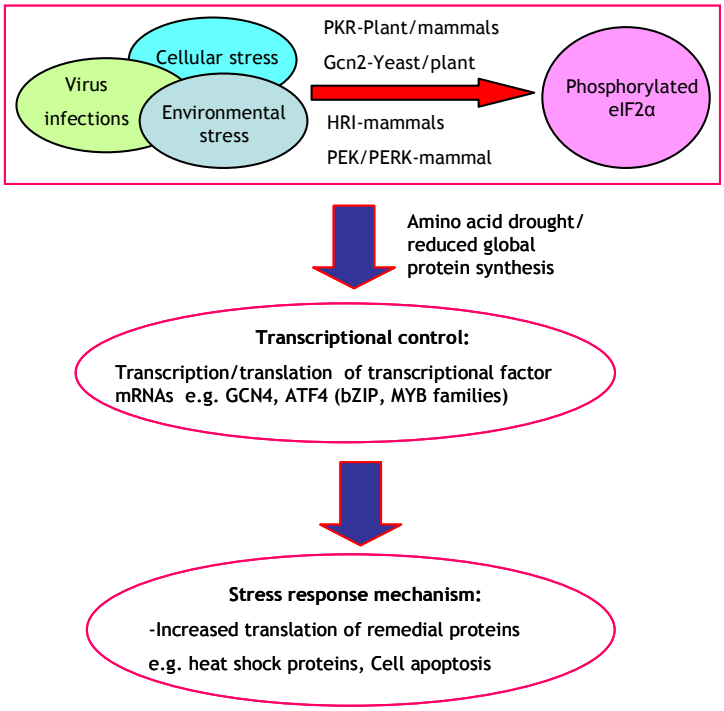

Figure 1.3. Schematic representation of eukaryotic stress response pathway mediated through phosphorylation of eIF2α subunit. Cellular, pathogen and environmental stress activates eIF2α-specific kinases that phosphorylate eIF2α. Stress induces amino acid starvation which triggers the translation of mORFs in mRNA containing uORFs which encode transcription factors that directly control the expression of down-stream stress-response genes.

1.13 General Amino Acid Control (GAAC)

Eukaryotic cells have well developed strategies to synthesize essential proteins during times of environmental stress or parasitism. These strategies mainly involve strict translational regulation and regeneration of new amino acids from existing proteins through autophagic pathways (Tallo'czy *et al.,* 2002). Phosphorylation of eIF2α impedes the exchange of GDP to GTP, which is required for subsequent rounds of translation initiation, thus unable to recruit Met-$tRNA_i^{Met}$ leading to reduction in global protein synthesis (Hinnebusch, 2005; Carnevalli *et al.,* 2006). Down-regulation of global translation due to phosphorylation of eIF2α is known to induce translation of key transcriptional activators such as general control non-derepressible 4 (GCN4) and ATF4 (activating transcriptional factor 4) in yeast and mammals, respectively (Asano *et al.*, 2000; Hinnebusch, 2005; Wek *et al.*, 2006); see Figure 1.4.

The transcriptional activators control the expression of transcripts encoding proteins required for alleviation of cellular damage due to stress or for induction of apoptosis (Zhang *et al.*, 2003). In mammals, ATF4 is known to enhance expression of other transcriptional factors such as ATF3, CHOP (CCAAT/enhancer binding protein homologues) or GADD153 (growth arrest and DNA-damage-inducible protein) that assist in regulation of genes in metabolism, redox status of cells and apoptosis (Wek *et al.,* 2006). In yeast, GCN4 is known to stimulate 12 different pathways through transcription of over 30 amino acid biosynthesis genes and those encoding various aminoacyl-tRNA synthetases (Hinnebusch, 2005). This regulatory response in yeast is known as General Amino Acid Control, GAAC (Hinnebusch & Natarajan, 2002), whereas in the *Neurospora* and *Aspergillus* fungi it is known as Cross-Pathway Control, CPC (Hoffmann *et al.*, 2001). A key *trans-acting* factor known as General Control Non-inducible 2 (GCN2 kinase) is required for steady state induction of the GAAC response, however transient induction of GAAC can also occurs when yeast cells are shifted from amino acid rich media to a minimal media(Hinnebusch, 1992). Proteins that are positive or negative regulators of GAAC have been identified in yeast through mutational analysis. In the study reported by Hinnebusch (1988), two groups of genes were identified based on their phenotypes, namely (i) recessive mutants that impair amino acid biosynthetic enzymes under conditions of amino

acid starvation referred to as General Control Non-derepressible (GCN) phenotypes, (ii) recessive mutants that have elevated levels of amino acid biosynthetic enzymes subject to GAAC under non-starvation conditions referred to as the General Control Derepressible phenotypes (GCD). A total of 9 GCN (GCN1-GCN9) genes were identified and recessive mutation of these GCN genes have been shown to impair enzyme derepression under conditions of amino acid starvation (Hinnebusch, 1988).

1.13.1 Phosphorylation of eIF2α-Subunit

During translation initiation, GTP bound to the eIF2 (eIF2.met-tRNA$_i^{Met}$) is usually hydrolyzed to GDP and eIF2.GDP is released. In order for another round of translation initiation to begin, GDP must be exchanged for GTP by eIF2B. However, phosphorylation of the eIF2α-subunit stabilizes eIF2.GDP complex and thus eIF2B is unable to convert GDP to GTP (Hinnebusch, 1996; Hinnebusch *et al.*, 2004) as depicted in Figure 1.4. Regulation of translation through the phosphorylation of the eIF2 α-subunit is a well-characterized mechanism and is a major mechanism for growth arrest when eukaryotic cells are stressed. eIF2α contains domains conserved across phyla including the SEL**S**RRRIRS domain containing serine 51 phosphorylation sites for yeast and mammals, however in *Arabidopsis* the phosphorylation site is serine 56 as shown in Figure 5.1. Furthermore, yeast GCN2 kinase phosphorylates wheat eIF2α (Chang *et al.*, 1999; Chang *et al.*, 2000) and expression of *Arabidopsis* GCN2 in yeast *Δgcn2* mutants complemented the mutation (Zhang *et al.*, 2003). Activation of the eIF2α-kinases and expression of genes such as *GCN4*, *ATF4* that encode for transcriptional activators under non-repressible conditions are usually induced by different stress cues (Carnevalli *et al.*, 2006). This is an indication that in both mammals and plants stress-response mechanisms through phosphorylation of eIF2α probably function in conjunction with other stress-response mechanisms such as those facilitated by mitogen-activated protein kinases (MAPK) cascades and jasmonate and salicylic acid pathways (Liang *et al.*, 2006; Wek *et al.*, 2006; Lageix *et al.*, 2008). Furthermore elements of these pathways namely ABA, ET, ROS, JA and SA acids are known to play a key role in cross-talk between stress signalling pathways (Fujita *et al.*, 2006).

1.13.2 GCN4 Translation

In yeast (*Saccharomyces cerevisiae*) transcription of mRNAs coding for amino acid biosynthetic enzymes is positively controlled by GCN4 transcriptional activator. GCN4 mRNA has three small uORFs that precede the GCN4 mORF. On the basis of scanning translation initiation mechanism, each of the three uORFs in the GCN4 mRNA could be selected as initiation site prior to the GCN4 mORF (Kozak, 1983; Hinnebusch, 2005). In the presence of sufficiently charged eIF2 (eIF2.GTP.met-tRNA$_i^{Met}$) i.e. under non-stress conditions, the uORFs 1, 2 and 3 are translated successively, however mORF (GCN4) is not translated (Fig. 1.4A). Re-initiation at mORF downstream following translation of uORFs 2 and 3 is generally inefficient (Kozak, 1983; Hinnebusch, 2005). However, under stress conditions (eIF2α-P) i.e. insufficient charged eIF2 (eIF2.GTP.met-tRNA$_i^{Met}$), uORFs 1, 2 and 3 are bypassed and the mORF (GCN4) is translated (Fig. 1.4B). In yeast, amino acid starvation induces phosphorylation of eIF2α by GCN2 kinase. This up-regulates the expression of the transcriptional activator GCN4, which in turn induces expression of up to 500 downstream genes (Yang *et al.*, 2000; Natarajan *et al.*, 2001; Hinnebusch, 2005). These include genes encoding key enzymes in every amino acid biosynthetic pathway except cysteine, vitamins, peroximal components, mitochondrial carrier proteins, autophagy proteins and many genes encoding protein kinases and transcriptional factors (Zhang *et al.*, 2002b). Indeed, GCN4 and regulation of its activity are so central to the survival of yeast, for this reason it is known as ‘the Master Regulator’ (Hinnebusch & Natarajan, 2002).

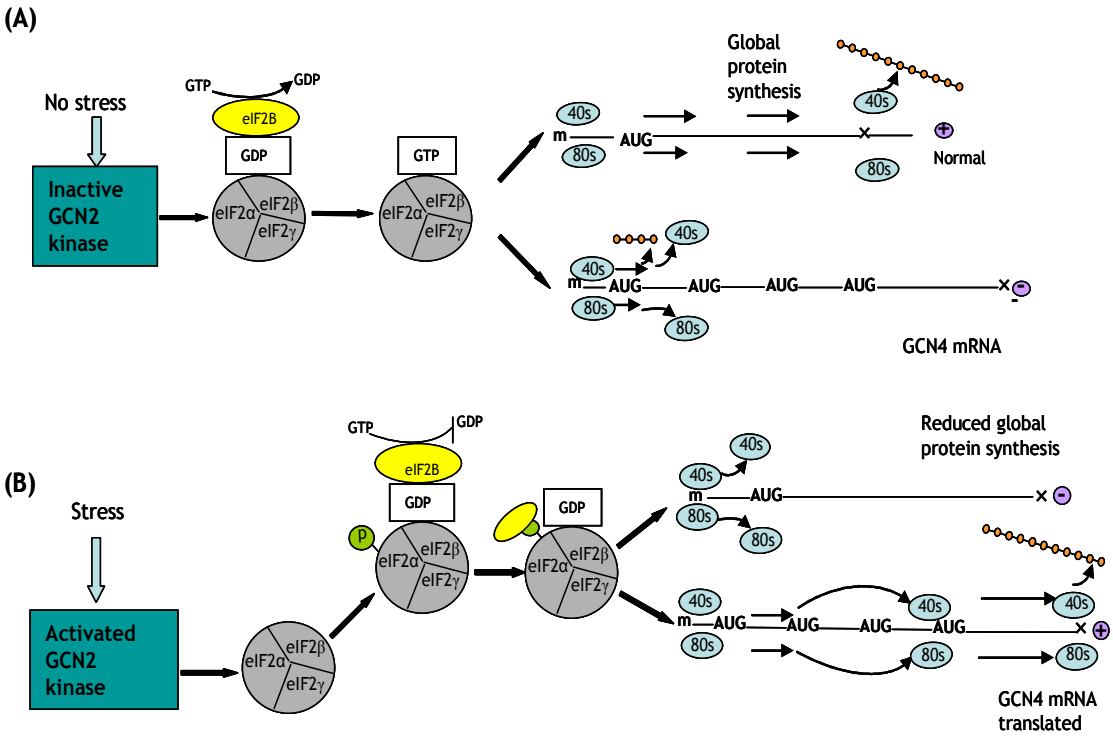

Figure 1.4. Stress response translation control in yeast (*Saccharomyces cerevisiae*). (A) Under non-stress conditions, there are sufficient charged tRNA (eIF2.GTP.met-tRNA$_i^{Met}$) complexes and as a result the uORFs repress translation of GCN4 mORF. **(B)** Under stress conditions there are insufficient charged tRNA complexes and this acts as a signal for stress; as a result uORFs 2 and 3 of GCN4 are by passed and GCN4 mORF is translated.

1.14 eIF2α-Kinases

There are four eIF2α protein kinases described namely; General Control Non-repressible kinase 2 (GCN2), RNA-depended protein kinase (PKR) and pancreatic eIF2-α kinase (PEK/PERK) (Lu *et al.*, 2001; Kaufman, 2004). Each of these protein kinases has unique regulatory regions that recognize different sets of stress cues. The mammalian (mainly mice and humans) and yeast eIF2α kinases are well described (Lu *et al.*, 2001; Kaufman, 2004; Hinnebusch, 2005). *Arabidopsis* has a homologue of yeast GCN2 (Zhang *et al.*, 2003), whereas a biochemical and immunological homologue of human PKR has been identified in wheat (Langland *et al.*, 1996). Activation of the eIF2α-kinases involves relief

from their distinct inhibitory domains to allow dimerization. This triggers an auto-phosphorylation event at the kinase activation loop, which facilitates recognition and phosphorylation of eIF2α (Dar *et al.*, 2005; Dey *et al.*, 2005). Although, each eIF2α-kinase activity is induced by different stress stimuli, there is evidence that more than one eIF2α kinase can function during a given stress condition, mediating either an additive or a compensatory mechanism (Carnevalli *et al.*, 2006). Multiple activation of eIF2α-kinases has been reported to occur during oxidative stress; which is dependent on cell type, dosage and duration of exposure (Lu *et al.*, 2001).

1.14.1 GCN2 Kinase

Yeast GCN2 kinase (ScGCN2) is relatively well characterized as compared to *Arabidopsis* GCN2 (AtGCN2). However, through inference AtGCN2 contains similar functional domains to ScGCN2 (Fig. 1.5). ScGCN2 is activated by amino acid and glucose starvation in yeast cells and is mediated by a GCN2 domain homologous to the histidyl-tRNA synthetase (HisRS) enzyme (Chang *et al.*, 2000; Hinnebusch, 2005). Similarly, AtGCN2 is activated by amino acid starvation, cold and UV light (Lageix *et al.*, 2008; Zhang *et al.*, 2008).

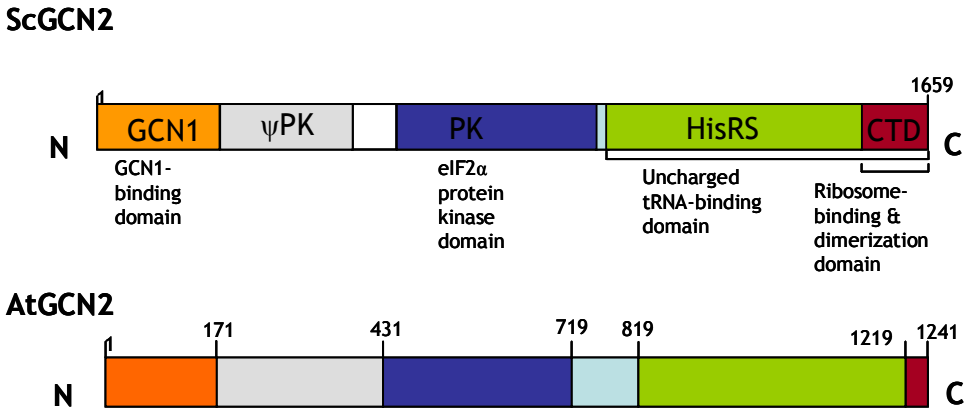

Figure 1.5 Schematic representation of the functional domains of yeast and *Arabidopsis* GCN2 kinases. Top image: functional domains of *S. cerevisiae* GCN2 kinase as described by Hinnebusch (2005). Below image; putative domains of *A. thaliana* inferred from yeast domains. The domains: GCN-1 binding domain, an N-terminal domain that binds to GCN1 protein during activation of GCN2 kinase: ψPK, a kinase domain domain of unknown function: PK, the protein kinase domain: HisRs and CTD domains, which bind uncharged tRNA producing conformational changes that activate the GCN2 kinase.

Uncharged tRNAs bind directly onto the HisRS related region and mutations in this region have been shown to block tRNA interaction hence eliminating kinase functions (Wek *et al.*, 1995; Yang *et al.*, 2000). Therefore the HisRs related domain of the GCN2 associates with uncharged tRNAs that accumulate in amino acid starved cells to activate its kinase activity (Yang *et al.*, 2000). Purine starvation in yeast also enhances activation of the GCN2 kinase, supporting the idea that there is a coordinated regulation of nucleotide and amino acid biosynthetic pathways (Rolfes & Hinnebusch, 1993). A second tRNA binding region is located at the carboxy terminus of GCN2 kinase (Ramirez *et al.*, 1991; Qiu *et al.*, 1998). The CTD domain is required by GCN2 kinase for association with ribosomes during GCN4 mediated translational control and may be involved in the monitoring of uncharged tRNA levels in cells (Yang *et al.*, 2000). Though not related to nutritional deprivation, the 26S proteosome is also reported to activate GCN2 kinase (Carnevalli *et al.*, 2006).

1.14.2 PKR Kinase

PKR is also referred to as interferon induced double stranded RNA activated protein kinase. It is among the 30 genes induced at the transcriptional level by type I interferons produced as the first line of defence against viral infection in mammals (Kaufman, 1999, 2000). In cells, PKR is expressed at low levels but hyper-activated by the presence of double stranded RNA (dsRNA) binding onto the dsRNA motif on its N-terminal domain, thus promoting its auto-phosphorylation (Meurs *et al.,* 1990; Kaufman, 2000; Matsui *et al.,* 2001). Activities of PKR consist of two distinguishable processes; (i) activation by dsRNA and auto-phosphorylation, and (ii) phosphorylation of eIF2α-subunit (Matsui *et al.,* 2001). Activation of PKR by dsRNA (an intermediary product of viral replication) leads to the shutting-off of viral and cellular protein synthesis of the virus-infected cells (Kaufman, 1999). However, viruses have developed strategies to defeat the PKR-mediated antiviral defence of mammalian host cells by inhibiting its auto-phosphorylation (Mathews & Shenk, 1991). The plant PKR (pPKR) is stimulated by virus and viroid infections, and is differentially regulated during plant development (Langland *et al.*, 1996). Auto-phosphorylation of pPKR *in vitro* is stimulated by dsRNA, selected poly-anions, or by base-paired single stranded RNAs of sufficient length, but not DNA or RNA-DNA hybrids (Chang *et al.,* 1999).

1.14.3 PERK and HRI Kinase

PERK/PEK is present in the endoplasmic reticulum (ER) as type I trans-membrane proteins. Among all the eIF2α kinases, PEK-kinase is the only one that is highly expressed in the pancreas of mammals (Zhang *et al.*, 2002a). It is activated by the accumulation of mis-folded proteins in the ER, and regulated by the ER as a resident protein chaperone referred to as BiP/GRP78 (Bertolotti *et al.,* 2000). Over-expression of viral glycoprotein has also been shown to activate PEK kinase (Kaufman, 1999). Phosphorylation of eIF2α due to mis-folded ER proteins leads to a reduction of mRNA translation, which in turn reduces protein substrate for ER folding and degradation mechanism (Yan *et al.,* 2002). In mammals, ER stress can be induced by drugs that impair N-linked glycosylation of proteins, block disulphide bond formation, or prevent ER calcium flux mediated by

sarcoplasmic/ endoplasmic-reticulum Ca^{2+}-ATPase (SERCA) (Kumar *et al.*, 2001). PEK kinase contains about 40% domain identity with PKR. However their stress signal-sensor domains are different and the two kinases are contained in different cell compartments; PEK- in the endoplasmic reticulum, and PKR- in the cytosol (Ron & Harding, 2000). PEK deficiency in humans and mice can result in postnatal exocrine pancreatic atrophy, causing severe growth deficiencies as well as metabolic anomalies in organs and tissues (Zhang *et al.*, 2002a; Iida *et al.*, 2007).

HRI is predominantly expressed in the reticulocytes, at low levels in the erythroid cells/tissues, and in the human parasite *Plasmodium falciparum* (Shi *et al.*, 1999). It is activated by haeme-deprivation, and oxidative, heat, and arsenite stress (Chen, 2000; Lu *et al.*, 2001). HRI activity is regulated by two heme-regulatory motifs, which mediate the inhibition of hemin (Clemens, 1996).

1.15 The JP-2 Activation Tagged Mutant

Previously in Dr. Peter Dominy's lab, the Weigel (Weigel *et al.*, 2000) *Arabidopsis* activation tagged collection containing 22,672 independent mutants was screened for a number of stress factors including salt tolerance. The activation tagged lines contain a T-DNA vector (pSKI015) that has four copies of enhancer elements of the 35S constitutive promoter (Fig. 1.6A). One mutant line that survived better under high salt (80 mM NaCl), low K^+ and Ca^{2+} concentrations was isolated, herein referred to as JP-2. Analysis of the JP-2 mutant using TAIL-PCR revealed that the enhancer was located between At3g59400 (AtGUN4) and At3g59410 (AtGCN2, protein kinase), at 270bp upstream of AtGCN2 kinase as shown in Figure 1.6B (Price, 2005) . As discussed earlier, in yeast the GCN2 kinase is involved in stress response translation regulation through phosphorylation of eIF2α. The JP-2 mutant demonstrated a strong salt tolerance phenotype when compared with wild type (Fig. 1.6C). Unfortunately the JP-2 line was unstable and the T-DNA insert was lost in the subsequent progenies and thus it was difficult to characterize.

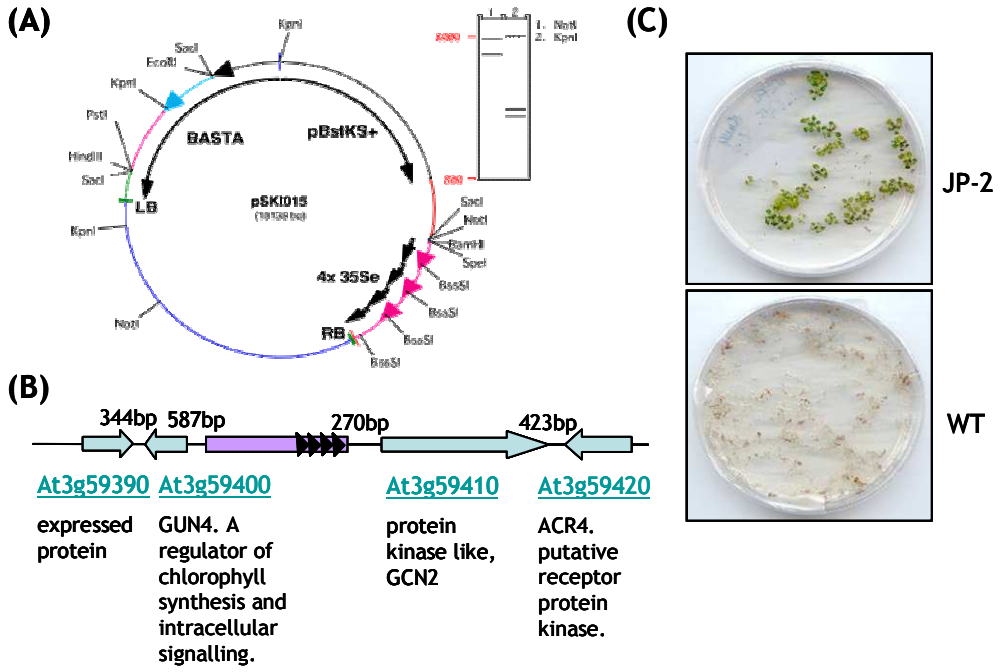

Figure 1.6. A gain-of-function screen of Weigel activation tagged *Arabidopsis* mutants (Price, 2005). **(A)** Map of pSKI015 T-DNA vector (diagram obtained from www.weigelworld.org), **(B)** TAIL-PCR of the mutant revealed that the T-DNA insert containing 35S enhancers was located 280bp upstream of AtGCN2, **(C)** Independent Weigel activation tagged mutants were screened for salt tolerance on 1/8 MS supplemented with 80 mM NaCl to isolate JP-2 mutant lines (Price, 2005).

1.16 The Objective of this Study

Translational control through phosphorylation of eIF2α by a group of eIF2α-specific kinases has recently generated a lot of interest, especially in plants. Unlike plants, the mechanism is well described in yeast and mammalian systems. In yeast and mammalian systems, the phosphorylation of eIF2α and uORFs-dependent activation of the GCN4 (see Figure 1.4) and ATF4 transcripts is well described. A number of eIF2-α kinases have been identified mainly in mammals, and the conditions at which they are activated are well reported in literature (Dey *et al.*, 2007; Toth *et al.*, 2009). Furthermore the downstream genes

induced after activation of yeast GCN4 and mammalian ATF4 have been identified (Hinnebusch & Natarajan, 2002; Wek *et al.*, 2006). For example in yeast, GCN4 translation during amino acid starvation directly affects the expression of up to 500 downstream genes and thus referred to as the Master Regulator (Hinnebusch, 2005). Components of this mechanism mainly GCN2 and pPKR kinases and the eIF2α sub-unit have been identified in plants and are said to be homologues of yeast and mammals. Contrasting the yeast and mammalian systems, the plant homologues of ScGCN4 and HsATF4, including the down stream genes induced by these transcriptional factors (TFs) that have not yet been identified. There are suggestions however indicating that plants may differ from other eukaryotes in some aspects of translational control mechanisms, since ScGCN4 and HsATF4 TFs which are translated when eIF2α is phosphorylated have not been identified (Browning, 2004; Halford *et al.*, 2004). Nonetheless eIF2α amino acid residues are highly conserved in most the eukaryotes including plants and AtGCN2 has been shown to functionally complement yeast *Δgcn2* null mutants (Zhang *et al.*, 2003). Furthermore studies by Zhang *et al*. (2008) and Lageix *et al*. (2008) have also demonstrated that activation of AtGCN2 kinase and *in planta* phosphorylation of *Arabidopsis* eIF2α is induced by abiotic stress. These reports therefore suggest that the mechanism is conserved and thus may be similar in plants as in the other eukaryotes, mainly yeast and mammalian systems.

Based on the previous work on the JP-2 mutant, one of the objectives of this study was to characterize the functions of AtGCN2 in *Arabidopsis* and identify phenotype(s) associated with 'gain-of-function' and 'loss-of-function' mutation of *Atgcn2* under stress and non-stress conditions. The 'gain-of-function' mutants used in this study were two 35S:*AtGCN2* expressing lines; (i) without a GFP tag (35S:AtGCN2) and (ii) with a 5′ GFP tag (35S:GFP.AtGCN2) generated using the pMDC32 (Curtis & Grossniklaus, 2003) and pH7WGF2.0 (Karimi *et al.*, 2002) binary vectors, respectively. The 'loss-of-function' mutant (*Atgcn2-1*) was isolated from *Arabidopsis* GABI-KAT T-DNA mutant lines obtained from European *Arabidopsis* Stock Centre, Nottingham, UK. The other objective of this study was to investigate the stress-response translation control mechanism mediated by phosphorylation of eIF2α in *Arabidopsis*. The first part of this objective was to demonstrate that *in planta* phosphorylation of AteIF2α inhibits protein

synthesis. The second part involved *in vitro* translation of *Arabidopsis* mRNA using Wheat Germ lysate to mimic translation under conditions of the de-phosphorylated (WGeIF2α) and phosphorylated (WGeIF2α-P) form of eIF2α, followed by attempts to identify translated ScGCN4/HsATF4-like transcripts. Finally the last objective was to isolate putative ScGCN4 and HsATF4 homologues of *Arabidopsis* using *in silico* approaches; identify transcripts which possess 5′ uORFs similar to ScGCN4 and HsTF4 which can be confirmed experimentally to be regulated through phosphorylation of eIF2α in *Arabidopsis*.

2 Chapter 2: Materials and Methods

2.1 Plant Materials and Growth Conditions

2.1.1 *Arabidopsis* Seed Stocks

The wild-type *Arabidopsis* seeds used in this study were Colombia ecotype (Col-0). The seeds were originally obtained from The European *Arabidopsis* Stock Centre (NASC), Nottingham, UK. The *Arabidopsis* null mutant line (*Atgcn2-1*) was isolated from seeds stocks of set N482670 also obtained from NASC. The set contained 6 GABI-KAT lines of Colombia background generated through T-DNA insertional mutation using pAC161 vector. The *Atgcn2-1* null mutant refers to a line that does not make functional copy of the AtGCN2 kinase.

2.1.2 Sterilization and Maintenance of *Arabidopsis*

Arabidopsis seeds were surface sterilized using chlorine gas. Seeds (~25 µl) were transferred to 1.5 ml microfuge tubes, and then opened tubes on a rack were placed inside a desicator. A 200 ml beaker containing 100 ml bleach solution (5% NaOCl) was also placed inside the desiccator in a fume hood and then 3 ml of concentrated HCl was added into the bleach solution. The desiccator was immediately closed and seeds sterilized for 5-6 h. The tubes containing seeds were then transferred into a laminar flow hood and left opened for 10-20 min to allow chlorine gas trapped inside the tubes to escape. Then 1 ml of sterile dH_2O was added and seeds stratified in dark at 4^oC for 3-4 days. The stratified seeds were spread on agar plates containing ½ MS media, 0.75% sucrose and 0.8% agar (w/v). Depending on the experiment conducted, the ½ MS was supplemented with stress or selective agents such as antibiotics, NaCl etc. Seed were germinated and maintained in a growth chamber set at 20/18^oC (day/night) temperatures, long day cycles 16/8 h (day/night) with a photosynthetic photon flux density (PPFD) of 20 µmol $m^{-1}s^{-1}$ provided by cool white fluorescent lamps. For compost-soil grown plants, seeds were spread on trays or pots containing sterile wet soil, then covered with cling film and stratified at 4^oC in dark for 4 days. The trays/pots were then transferred to the growth chamber, the cling

film removed and replaced with transparent try covers to maintain high humidity.

2.1.3 Isolation *Arabidopsis* GCN2 Null Mutant (*Atgcn2-1*)

Stratified seeds of set N482670 were spread on agar plates containing ½MS media supplemented with 7.5 µg/µl sulfadiazine. The seedlings were grown on sulfadiazine media for 14 days and the surviving seedlings, which were putative *Atgcn2-1* mutants, were rescued and transplanted to moistened compost soil. Genomic DNA was isolated from leaves of 30 days old *Atgcn2-1* plants and used for genotyping PCR (see section 2.4.1). Plants homozygous for pAC161 T-DNA insertion were grown to set seeds and these were then used for characterization experiments.

2.2 Molecular Biology Methods

2.2.1 Isolation of Genomic DNA

DNA was extracted from leaves or seedling using ~50 mg of pulverized plant material. Briefly, the harvested plant samples were immediately frozen and pulverized in liquid nitrogen using pre-chilled mortar and pestle. The powdered plants samples (~50 mg) were transferred to a pre-chilled 1.5 ml microfuge tubes, and temporarily stored in liquid nitrogen until all the samples were processed. DNA was extracted by adding 500 µl of the extraction buffer (200 mM Tris HCl pH 7.5, 250 mM NaCl, 25 mM EDTA, 0.5% SDS) to the frozen pulverized samples, mixed gently by pipetting up and down, then allowed to stand at room temperature until all the samples were processed(<1 h). The samples were then centrifuged (Eppendoff® micro-centrifuge) at 13000 rpm for 5 min at room temperature. Then 400 µl of the supernatant was transferred to a fresh microfuge tube, mixed with 400 µl of isopropanol and centrifuge at 13000 rpm for 2 min to pellet DNA. The isopropanol was removed and DNA pellets washed in 3 to 4 changes of ice cold 95% ethanol. After the last ethanol-wash, DNA was air dried by inverting microfuge tubes on clean paper towel for at least 8 h or overnight to remove residual ethanol. The DNA pellets were then re-suspended in 200 µl 1×TE buffer, pH 8.0 and stored at 4^{o}C.

2.2.2 Isolation of Total RNA

Total RNA was extracted using TRI-reagent (Sigma-Aldrich Chemical Co. Ltd., Dorset, UK). Approximately 100 mg fresh plant materials were pulverized in liquid nitrogen using pre-chilled pestle and mortar. The powdered frozen samples were transferred to pre-chilled 1.5 ml sterile microfuge tubes, and then 1 ml TRI-reagent was added and mixed, vortexed briefly, and incubated on ice for 5 min. Chloroform (200 µl) was added into the mixture, shaken vigorously for 15s and then incubated further on ice for 10 min. The samples were centrifuged at 13,000 rpm for 15 min at 4^{o}C and the top colourless supernatant containing RNA was transferred to a fresh 1.5 ml microfuge tubes and then mixed with 0.5 ml of Isopropanol. The samples were allowed to stand on ice for 10 min, centrifuged at 10,000 rpm for 10 min at 4^{o}C and the supernatant discarded. The RNA pellet was washed once with 1ml ice cold 75% ethanol. After all traces of ethanol had been removed, the pellets were re-suspended in 20 µl DEPC-treated dH_2O. The RNA samples were treated with Ambion DNase inactivation reagent (Cat No. AM1907 Lot No.0806013) following the manufacturer's protocol. The quantity and quality of RNA was validated using a spectrophotometer (Sambrook & Russell, 2001). The quantity of RNA was revealed by absorbance at A_{260} nm, where absorbance of 1 is equivalent to RNA concentration of 38 µg/ml. The quality (purity) of RNA was determined by the ratio of absorbance at A_{260} nm to A_{280} nm. An A_{260}/A_{280} ratio of between 1.8 and 2.0 indicates that the nucleic acid is generally free from protein contamination.

2.2.3 Denaturing Agarose Gel Electrophoresis of RNA

The quality of RNA isolated was further determined by agarose gel electrophoresis. Aliquots of RNA (1 µg) were separated on a 1.5% (w/v) agarose gel containing 10% formaldehyde and 1×MOPS buffer, pH 7.0 (20 mM MOPS, 5 mM sodium acetate, 1 mM EDTA (Sambrook & Russell, 2001). RNA was mixed with 1% (v/v) formaldehyde, 30% (v/v) formamide, 1×MOPS pH 8.0, and 0.1 volume of ethidium bromide. The mixtures were heated at 65^{o}C for 10 min, snap cooled on ice and then loaded on to the gel with 2 µl of loading dye (Promega UK Ltd, Southampton, UK). The gel was run for 2 h at 100 V in 1×MOPS buffer.

2.2.4 Complementary DNA (cDNA) Synthesis

For synthesis of cDNA, total RNA was incubated at 48°C for 15 min with oligo dT primers, in a 17.4 µl pre-reverse transcription reaction (pre-RT) mix containing, 2.8 µl of RNA (2.5 µg), 0.55 µl of oligo dT (0.25 µM) and 14.1 µl of DEPEC-treated dH_2O. The pre-RT (17.4 µl) mix was then used in a 25 µl reverse transcription PCR (RT-PCR) containing 5 µl AMV reverse transcriptase buffer (Promega, Southampton, UK), 1 mM dNTPs (Promega), 0.6 µl (1 U μl^{-1}) of RNase inhibitor (Promega) and 1 µl (0.4 U μl^{-1}) of AMV reverse transcriptase (Promega). The RT-PCR reaction was conducted using the following PCR programme cycle; 48°C for 45 min, 95°C for 5 min and 4°C for 5 min, and cDNA synthesized was stored at -20°C.

2.2.5 Polymerase Chain Reaction (PCR)

2.2.5.1 Oligonucleotides

PCR primers were designed either *de novo* or designed to coding sequence of the gene of interest using Primer3 software (www.justbio.com/primer/index.php). The primers were synthesized by Eurofin MWG Operon and were re-suspended in sterile dH_2O to achieve stock concentration of 100 pmol/µl. The working concentration of the primers was then prepared by diluting 25 µl of stock into 75 µl of sterile dH_2O to achieve a final concentration of 25 pmol/µl. In a typical 25 µl PCR reaction volume, 0.5 µl of each primer was added to a final concentration of 0.5 pmol/µl. The sequences of the primers used in this study are listed in Table 2.1 below.

Table 2.1. Primer description and sequences used for PCR reactions and sequencing.

PCR Experiment	Primer Combination	Primer Sequence*
Genotyping of *Atgcn2-1* T_3 plants	Gcn2Fw1 pAC161V1 Gcn2Fw1 Gcn2Rv1	5′-catattgatgttctgatgccacca-3′ 5′-gggctacactgaattggtagctc-3′ 5′-catattgatgttctgatgccacca-3′ 5′-agctccaaacagaggggtttc-3′
Semi-quantitative PCR of plants	Gcn2Fw2 Gcn2Rv1 GCN2Fw3 GCN2Rv2 Actin-2Fw Actin-2Rv	5′-gcatctagaggtcataccaatg-3′ 5′-agctccaaacagaggggtttc-3′ 5′-atgggtcgcagcagttcgaag-3′ 5′-aggaacactggttgaggcc-3′ 5′-cttacaatttcccgctctgc-3′ 5′-gttgggatgaaccagaagga-3′
Cloning (TOPO-TA) At2g40290.1	AteIF90Fw AteIF90Rv	5′-gcagtatcgaaatctacaatc-3′ 5′-catgtggtggagcaacatattc-3′
Cloning (TOPO-TA) At5g05470.1	AteIF70Fw AteIF70Rv	5′-caatcctcgcgctctctac-3′ 5′-ctgtttttgctcaaagggaaac-3′
Sub-cloning At2g40290.1(pENTR4)	P90NcoIFw P90NotIRv	5′-taa***ccatgg***cagcgagtcaaacaccgaatctc-3′ 5′-aata***gcggccgc***gattactcgatgattccggcacc-3′
Sub-cloning At5g05470.1(pENTR4)	P70NcoIFw P70NotIRv	5′-tat***ccatgg***cagcgaatcctgctccgaatctag-3′ 5′-aat***gcggccgc***gatcattcaattatcccgctacc-3′
Cloning (TOPO-TA) At3g59410	Atgcn2Fw Atgcn2Rv	5′-atgggtcgcagcagttcgaag-3′ 5′-ttagctccaaacagaggggtttc-3′
Sub-cloning At3g59410 (pENTR/D)	Atgcn2PDFw Atgcn2Rv	5′-**cacc**atgggtcgcagcagtt-3 5′-ttagctccaaacagaggggtttc-3′
Sequencing pENTR4 Clones	Pentr4U[#] Pentr4L[#]	5′-ctacaaactcttcctgttagttag-3′ 5′-aacatcagagattttgagacac-3′
Sequencing pDEST17 Clones	T7 universal primer[#] PDest17Rv[#]	5′-taatacgactcactataggg-3′ 5′-cttgtacaaagtggttgattc-3′

*Sequence with bold and italicized nucleotides indicates restriction enzyme sites. [#] Primer combination for sequencing

2.2.5.2 PCR Amplification of DNA

All PCRs were performed using a MJ Research DNA Engine PTC-200 Peltier Thermal Cycler (Genetic Research Instrumentation, Essex, UK). For general amplification of DNA, ReddyMix (Abgene, Epsom, UK) PCR master mix was used. In a typical reaction, 1×ReddyMix contains 1.25 units Thermoprime Plus DNA polymerase, 75 mM Tris-HCl pH 8.8, 20 mM $(NH_4)_2SO_4$, 1.5 mM $MgCl_2$, 0.01% (v/v) Tween 20, 0.2 mM each of dATP, dCTP, dGTP, and dTTP. In PCR reactions where Reddymix was used, the PCR products were directly loaded on to 1% agarose gel. The Reddymix PCR master mix was used in genotyping and colony PCR experiments. A typical 25 µl genotyping PCR reaction mix consisted of 12.5

µl of Reddymix, 0.5µl (25 pmol/µl) of forward and reverse primers, 1-2 ng of DNA/cDNA template and dH_2O added up to 25 µl. Cloning PCRs were conducted using Phusion™ High fidelity (Finnzymes) proof reading DNA polymerase. A typical cloning PCR reaction consisted of 4 µl of 5×HF Phusion buffer, 0.4 µl of 10 mM dNTPs mix, 0.5 µl (25 pmol/µl) of forward and reverse primers, 0.5 µl of cDNA template, 0.2 µl of Phusion HF polymerase and dH_2O added up to 25 µl. Prior to loading cloning PCR products to 1% agarose gel, they were mixed with 5×loading dye (Promega) to 1× final concentration. All the PCR products were resolved on 1% agarose gel melted in 1×TAE, containing 1:10000 SYBR safe (Invitrogen). A 1 kb ladder (Promega) was used as a DNA size marker and PCR products were resolved at a constant 100 V in 1×TAE and then visualized under UV.

2.2.5.3 Colony PCR

A sterile pipette tip was dabbed onto a bacterial colony then soaked in 20 µl dH_2O. The cells were re-suspended in dH_2O by gently pippeting up and down and then used as template to conduct a PCR. A typical 20 µl colony PCR reaction mix consisted of 10 µl of Reddymix, 0.5 µl (25 pmol/µl) of each primer pair and 9 µl of re-suspended cells. The following PCR programme used to conduct colony PCR; initial denaturing step at 96°C for 10 min. This was then followed by 25 cycles of a denaturing step at 96°C for 15s, an annealing step for 30s (temperature based on primer T_m) and an extension step at 72°C for 1 min (based on the expected size of PCR product). This was then followed by final extension step at 72°C for 5 min.

2.2.6 Restriction Digestion and DNA Gel Extraction

Restriction enzymes used in this study were purchased from either Roche or Promega and used following the manufacturer's instructions. Briefly, a 20 µl reaction was incubated from 3 hr up to overnight and contained ~0.7-1 µg of DNA, 5 units of restriction enzyme and the recommended buffer. The products of restriction digestion reaction were resolved on 1% agarose. DNA fragments of expected size were cut-out of the gel using a clean sharp razor blade under a UV trans-illuminator. The gel-extracted DNA fragments were purified using QIAquick® Gel extraction kit (Qiagen) following manufacturer's protocol. The

DNA was eluted using elution buffer (10 mM Tris-Cl, pH8.5) provided for in the kit and immediately used for subsequent reactions, especially cloning or ligation reactions.

2.2.7 Generation of Gateway Entry Clones

For Gateway directional cloning the forward primer sequences were designed to contain CACC sequence at the 5′ end. The Blunt-end PCR products were amplified using Phusion™ HF DNA polymerase and then cloned into Gateway entry vector using pENTR™/D-TOPO® Directional Cloning Kit (Invitrogen) following manufacturer's protocols. Briefly, 0.5-4 µl of gel extracted PCR product was mixed with 1 µl of salt solution and 1 µl of TOPO vector to a final volume of 6 µl. The mixture was incubated at room temperature for 5 min and then 2 µl of the reaction mix was used to transform TOP10 chemically competent *E. coli* cells (Invitrogen) or XL1-Blue *E. coli* cells (Stratagene). Gateway entry clones were also generated through restriction enzyme cloning using pENTR4 entry vector (Invitrogen). The gene of interest-specific primers (forward and reverse), were designed such that they contain appropriate restriction site to facilitate cloning. The entry clones were used to transfer the genes of interest (insert) into Gateway®-compatible gene expression vectors using the LR reaction protocol (Invitrogen). For LR reactions 150-200 ng of the entry clone was mixed with 1 µl of the destination vector and 2 µl of nuclease free sterile dH_2O, then 2 µl of LR clonase enzyme was added and the reaction incubated at room temperature (20-25^oC) for 1 h. The reaction was then inactivated by addition of 1 µl of proteinase K and incubated at 37^oC for 10 min. The LR recombination product (2 µl) was used to transform competent DH5α *E. coli* cells to maintain and amplify the clones. Mini-preps were prepared from the DH5α cells and clones were sequenced at Eurofin MWG Operon to confirm the orientation and sequence of the inserts.

2.2.8 Transformation of *E. coli* Cells

All *E. coli* cells used in this study were competent 50 µl aliquots. The competent *E. coli* cells stored at -80°C were thawed on ice, then 2 µl of ligation or LR product or 1 µl (5-10 ng) of plasmids mini-prep were added to the cells and incubated on ice for 20-30 min. After addition of the plasmid into the cells, the tubes were mixed briefly by gently tapping the tubes twice before incubation on ice. The cells were then heat-shocked at 42°C in a water bath for 30-45 s (depending on the cells used). The heat-shocked cells were then immediately incubated on ice for 2 min, then 250 µl of room temperature S.O.C media was added to the cells. The cells were then incubated in a shaker set at 37°C for 1 h with constant shaking at 200rpm. After incubation, 50-200 µl of the cells were spread on LB agar plates containing respective antibiotic and then incubated overnight at 37°C to allow colonies to form.

2.2.9 Plasmid Isolation from *E. coli*

Single discrete colonies of *E. coli* were inoculated into 5 ml of LB media containing appropriate antibiotics. The culture were grown overnight at 37°C with constant shaking at 200 rpm. The overnight cultures were centrifuged at 4000 rpm for 10 min at 4°C. The cell-pellets were re-suspended in plasmid extraction buffer provided for in the mini-prep kit. Plasmid extraction was conducted using QIAprep plasmid miniprep Kit (Qiagen) following manufacturer's protocols. The plasmids were eluted from the extraction column using 25 µl of elution buffer (10 mM Tris-Cl, pH8.5) provided for in the Kit. The concentration of plasmid DNA (µg DNA/ml) was determined using a spectrophotometer at OD_{260} using the formula A_{260}×50× dilution factor and then stored at -20°C.

2.3 Generation of *p35S:AtGCN2* and *p35S:GFP:AtGCN2* Lines

2.3.1 Cloning of *AtGCN2* Gene

Total RNA was extracted from 14 days old WT Col-0 seedlings grown on ½ MS media as described previously in section 2.2.2 and cDNA synthesized as described in section 2.2.4. The generated cDNA was used in cloning PCR reaction as template to amplify *AtGCN2* (AT3G59410.1) with gene specific primers Atgcn2Fw and Atgcn2Rv (Table 2.1) using Phusion® High Fidelity Polymerase as described in section 2.2.5.2. Cloning PCR was performed using the following 30 cycle programme; initial denaturisation at 98^{o}C for 30s, denaturisation at 98^{o}C for 10s, annealing at 62^{o}C for 30s, extension at 72^{o}C for 50s and final extension at 72^{o}C for 5 min. The PCR products were resolved on 1 % agarose gel and fragment corresponding to *AtGCN2* (3.7 Kb) was extracted using Qiaquick® gel extraction Kit (Qiagen). The *AtGCN2* fragment was immediately incubated with dATP to add 'A' overhang for TOPO-TA cloning (Invitrogen) in a 25 µl reaction mix consisting of 4 µl (Promega 5xGoTaq® DNA polymerase buffer), 1 µl (10 mM dATP), 0.1 µl (Promega GoTaq® polymerase) and 20 µl of extracted *AtGCN2* fragment. The reaction mix was incubated at 72^{o}C for 10 min using PCR block. The *AtGCN2* fragment with 'A' overhangs was immediately cloned to pCR4®-TOPO® sequencing vector (Invitrogen) and the construct used to transformed chemically competent XL1-Blue *E. coli* cells (Stratagene). The transformed cells (50-100 µl) were spread on on agar plates containing LB media supplemented with 50 µg/ml kanamycin and incubated overnight at 37^{o}C. Positive clones were confirmed by colony PCR as described in section 2.2.53 using Atgcn2Fw and Atgcn2Rv primers and the following 22 cycle programme; initial denature 98^{o}C for 10 min, denature 98^{o}C for 10s, annealing 62^{o}C for 30s, extension at 72^{o}C for 50s and final extension at 72^{o}C for 5 min. The positive clones were then sequenced to confirm authenticity and orientation of the *AtGCN2* inserts in pCR4®-TOPO® vector using T7 and T3 universal primers (Table 2.1).

.

2.3.2 Sub-cloning *AtGCN2* into pENTR/D Gateway Entry Vector

The *AtGCN2* fragment was sub-cloned from pCR4® TOPO TA vector on to pENTR™ /D-TOPO Gateway entry vector using primers Atgcn2PDFw and Atgcn2Rv (Table 2.1). The *pCR4.AtGCN2* plasmid construct (18 µg) was used as template. The plasmid were isolated from XL-1 Blue cells using Qiagen mini-prep Kit and diluted with EB (mini-prep kit elution buffer) to a final concentration of 0.35 µg/µl i.e. 0.5 µl (35 µg/µl) of plasmid was added to 49.5 µl of EB buffer. The 25 µl sub-cloning PCR reaction was set up as follows; 18.9 µl dH2O, 4 µl 5×HF Phusion Buffer, 0.4 µl 10 mM dNTPs, 0.5 µl of each primer, 0.5 µl diluted plasmid (pCR4.*AtGCN2)* and 0.2 µl Phusion HF polymerase. PCR amplification was conducted using Phusion® High Fidelity Polymerase and using the following 20 cycle programme; Initial denaturisation 98°C for 30s, denaturisation 98°C for 10s, annealing 62°C for 30s, extension 72°C for 50s and final extension 72°C for 5 min. The PCR products were resolved on 1% agarose gel and blunt end *AtGCN2* fragment was extracted using Qiaquick® gel extraction Kit (Qiagen) and immediately cloned to pENTR/D Gateway entry vector (Invitrogen) following manufacturer's protocol. Then 7 colonies growing on selective media were randomly picked to conducted colony PCR using the sub-cloning primers. Due to the size of full-length *AtGCN2* ORF (3.726Kb) insert, confirmation by sequencing was undertaken using three sets of primer pairs. The first set consisted of M13 forward and reverse universal primers, and gene specific primers; Atgcn2pDFw2: caagcatctcttcttttgactc and Atgcn2pDRv1: aggtaacttcaactcctgaagaag, and Atgcn2pDFw3: gacttatctatatattcaaat and Atgcn2pDRv2: tgcttcgcacaatgctgcc.

In order to characterise *Arabidopsis* mutant lines ectopically expressing AtGCN2 kinase, it was essential to place the *AtGCN2* ORF under the control of a strong promoter; a native *Arabidopsis* promoter would have been ideal. For this study however two Gateway™ compatible vectors that have been designed for *in planta* over expression of the gene of interest, containing the standard Gateway recombination cassette (attR1-ccdB-attR2) placed downstream of CaMV 35S promoter were selected. These were pMDC32 vector containing 2×35S promoter upstream of the recombination site with no fusion tag was chosen (Curtis & Grossniklaus, 2003) and pH7WGF2.0 containing 1×35S promoter with an N-terminal GFP fusion tag upstream of the recombination sites for localisation

experiments (Karimi *et al.*, 2002). The pH7WGF2.0 vector was chosen to investigate localization of AtGCN2 kinase because it has an N-terminal fusion tag. The CT-domain was earlier found to be crucial for *in planta* activation of AtGCN2 kinase, therefore use of N-terminal tag may be less disruptive to the CT-domain. The vector map of pMDC32 and pH7WGF2.0 are shown in Appendix 1. The binary expression construct namely, *pMDC32.AtGCN2* and *pH7WGF2.AtGCN2* were then generated using standard Gateway recombination protocol (LR). All positive clones were confirmed by colony PCR and the orientation of *AtGCN2* insert confirmed by restriction digest using *BamH I* and *Hind III* for, *pMDC32.AtGCN2* and *pH7WGF2.AtGCN2* constructs, respectively.

2.3.3 Transformation of *Agrobacterium* Cells

Electro-competent *Agrobacterium* strain GV3101 cells stored in 50 µl aliquots at -80^{o}C were thawed on ice. Then 1 µl of binary expression vector constructs (*pMDC32.AtGCN2* and *pH7WGF2.AtGCN2*) were added to separate aliquots and mixed by gently tapping the tubes twice. The cells were then transferred to electroporation cuvette (BIO-RAD) and pulsed with a MicroPulser^{TM} electroporator (BIO-RAD) and immediately 950 µl of ice chilled LB media was added into the cuvettes containing pulsed cells. Then cells were transferred to a sterile 1.5 ml microfuge tubes and incubated at 28^{o}C on 200 rpm shaker for 3 h. The cells were pelleted by brief centrifugation, re-suspended in 200 µl of LB medium and then 50 µl spread on LB agar plates containing gentamycin (30 ug/ml) and kanamycin (50 ug/ml) for selection of *pMDC32.AtGCN2* or spectinomycin (100 ug/ml) for selection of *pH7WGF2.AtGCN2* construct. The agar plates were incubated at 28^{o}C for 2 days for colonies to form. For control treatment, no plasmid clones were added to the *Agrobacterium* cells.

2.3.4 Floral-dip Solution

Agrobacterium floral dipping solution was prepared following an earlier described protocol (Zhang X *et al.*, 2006). Briefly, a 5 ml starter culture from single colonies of *Agrobacterium* strain GV3101 harbouring binary vectors pMDC32 and pH7WGF2.0 containing full-length *AtGCN2* gene were prepared. The 5 ml LB media was supplemented with 30 ug/ml gentamycin for selection of

Agrobacterium TI-plasmid. In addition the LB media also contained 50 ug/ml kanamycin and spectinomycin for selection of the binary vectors pMDC32 and pH7WGF2.0, respectively. The cultures were incubated at 28°C for 2 days on a 200 rpm shaker. The 5 ml starter cultures were then used to inoculate 500 ml of LB medium supplemented with appropriate antibiotics for selection of pMDC32 and pH7WGF2 constructs. The cultures were then grown at 28°C on a 200 rpm shaker at until an OD_{600}~1.5-2.0 (16-24 h) was obtained. The *Agrobacterium* cells were harvested by centrifugation at 4000 rpm for 10 min at room temperature and re-suspended in 500 ml of freshly made 5% (w/v) sucrose solution. Immediately before floral dip transformation, 100 µl of Silwett L-77 (0.02%) was added and mixed well into the solution. The floral dip solution was then transferred to a 1000 ml beaker and immediately used to transforming *Arabidopsis Atgcn2-1* plants.

2.3.5 Transformation of *Atgcn2-1 Arabidopsis* Plants

Arabidopsis Atgcn2-1 seeds were spread on compost soil packed in pots covered with a nylon mesh screen fastened with a rubber band. The seeds were stratified as described in section 2.1.2. The mesh screen was used for the purposes of securing the soil during the process transformation, which entails inversion of plants. The seeds were germinated and grown under short day conditions (8/16 h, light/dark) for three weeks, and then thinned to 5 plants per pot. The plants were then transferred to long day (16/8 h, light/dark) growth conditions to encourage induction of flowers. The plants were transformed when 10-30 inflorescence and a few maturing siliques had emerged. Transformation was achieved by inverting the plants and dipping the aerial parts of the plants in *Agrobacterium* cell suspension (section 2.3.4) with gentle agitation for 10-15s. The plants were removed and then excess solution drained off for 5-6s. The plants were immediately covered with a plastic bag and laid on their side in the lab (21-23°C) overnight. The transformed plants were taken back to long day growth chamber and grown until siliques started turning brown and then plants were dried gradually. The T_0 seeds were screened on ½ MS agar plates supplemented with 45 µg/ml hygromycin (Duchefa). The tolerant 21-day old seedling were rescued from the selective pressure and transplanted on to soil and grown to set T_1 seeds. The T_1 seeds obtained from independent

transgenic plants were also screen on media containing hygromycin B and surviving seedlings were transferred on to soil and allowed to set T_2 seeds. The putative AtGCN2 kinase mutants were grown on compost soil and at each level plants (T_1 and T_2 plants) were genotyped using PCR until T_3 seeds were obtained. The AtGCN2 kinase mutants are henceforth in this thesis referred to as *p35S:AtGCN2* for lines generated using *pMDC32.AtGCN2* construct and *p35S:GFP:AtGCN2* for those generated with *pH7WGF2.AtGCN2*. The basis of transforming *Atgcn2-1* mutant as opposed to wild type plants was to functionally complement the truncated GCN2 kinase synthesised by the *Arabidopsis* null-mutant. The phenotype produced would therefore be due to ectopic expression, rather than dual effects of the endogenous *AtGCN2* wild type expression and ectopic expression, if WT Col-0 plants were used.

2.4 Genotyping *Arabidopsis* Mutant Lines

2.4.1 Genotyping the *Atgcn2-1* Mutant

The *Arabidopsis* mutant lines in set N482670 were generated using pAC161 T-DNA binary vector (GABI-KAT). The T-DNA insertion is located on the second-last exon (3′) of the *AtGCN2* (At3g59410.1) gene and in the middle of the 1175 amino acid. Genotyping PCR reactions (25 µl reaction volume) was set up as described in section 2.2.5.2. The genotyping PCR was conducted to identify plants homozygous for pAC161 T-DNA insertion. The Gcn2Fw1 and Gcn2Rv1 primers (Table 2.1) were designed to hybridize *AtGCN2* sequence flanking the T-DNA insertion to detect wild-type allele with an expected product size of ~592bp. Therefore if a plant is heterozygous, a PCR product will be obtained because of the presence of wild-type version of *AtGCN2* gene. If the plant is homozygous for pAC161 T-DNA insert then it does not posses wild-type version of *AtGCN2*, hence no product is expected when PCR is conducted with Gcn2Fw1 and Gcn2Rv1 primer combination (Table 2.1). This is because the T-DNA insert would increase the distance between the two primer pairs by over 3.7kb. To distinguish heterozygous from wild-type plants, PCR was also conducted with one primer that specifically hybridized with pAC161 vector (pAC161V1) and the other hybridizing *AtGCN2* (Gcn2Fw1). A PCR product will only be obtained with heterozygous and homozygous plants. Genotyping PCR to isolate *Atgcn2-1* null

mutant was conducted using the following 30 cycle programme, initial denature 98°C for 30s, denature 98°C for 10s, annealing 56°C for 30s, extension 72°C for 40s and final extension 72°C for 5min. The PCR products were resolved on 1% agarose gel and homozygous *Atgcn2-1* plants were grown to set T_4 generation seeds which were used for characterization experiments.

2.4.2 Semi-quantitative PCR of the *Atgcn2-1* Mutant

A semi-quantitative PCR (SQRT-PCR) was conducted to ascertain the form of *AtGCN2* transcripts synthesized by the T_4 *Atgcn2-1* mutant line. Complementary DNA was generated from RNA isolated from 30 days old *Atgcn2-1* T_4 and WT Col-0 *Arabidopsis* plants as described in section 2.2.2 and 2.2.4, respectively. The cDNA generated was used to conduct SQRT-PCR to amplify two fragments; the first fragment representing full length *AtGCN2* gene (~3726bp) was amplified using primer pairs Gcn2Fw3 and Gcn2Rv1 (Table 2.1). The second fragment was amplified using primer pair Gcn2Fw3 and Gcn2Rv2 (Table 2.1), specific for *AtGCN2* ORF beginning with ATG start codon up to 1200bp position. The presence of the two fragments after conducting SQRT-PCR, suggests synthesis of full-length *AtGCN2* transcript. On the other hand presence of only the second fragment suggests synthesis of truncated transcript. SQRT-PCR reaction was conducted using ReddyMix PCR master mix and was set-up as described in section 2.2.5.2 and conducted using the following 30 cycle programme; initial denature 98°C for 30s, denature 98°C for 10s, annealing 55°C for 30s, extension 72°C for 30s and final extension 72°C for 5 min. The Actin-2 gene was used as a constitutive control and was amplified using Actin-2Fw and Actin-2Rv primers (Table 2.1).

2.4.3 Genotyping of *p35S:AtGCN2* and *p35S:GFP:AtGCN2* Lines

The *Arabidopsis p35S:AtGCN2* and *p35S:GFP:AtGCN2* lines were generated using *Atgcn2-1* mutant plants, which possess a non-functional truncated copy of AtGCN2 kinase. Transforming *Atgcn2-1* mutant by introducing a full-length *AtGCN2* ORF sequence was expected to functionally complement the truncated *AtGCN2* allele. Therefore genotyping PCR was conducted using genomic DNA with Gcn2Fw1 and Gcn2Rv1 primer combination that was also used earlier to

genotype *Atgcn2-1* mutant. Therefore like in the genotyping of *Atgcn2-1* mutant, a PCR product was expected on wild-type plants and the ectopically expressing AtGCN2 mutant lines. However the expected PCR product obtained with the wild-type allele should be bigger than that of the full-length insert present in the *p35S:AtGCN2* mutant lines generated. This is because the wild-type gene contains introns, while the inserted full length ORF lacks introns because it was amplified from cDNA. The *Atgcn2-1* plants have a truncated *AtGCN2* therefore no product was expected when PCR was conducted with Gcn2Fw1 and Gcn2Rv1 primer combination (Table 2.1).

2.5 Protein Methods

2.5.1 Extraction of Total Plant Proteins

Plant materials were harvested, quickly frozen and ground in liquid nitrogen using pre-chilled mortar and pestle. Then ~100 mg of ground plant samples were transferred to a pre-chilled 1.5 ml sterile microfuge tube. Protein was then extracted using a modified protocol described by Larkin (2007). Briefly, two volumes (w/v) of extraction buffer (25 mM Tris, 75 mM NaCl, 0.5 mM EDTA, 0.5 mM EGTA, 2 mM DTT, 5% Glycerol and 0.05% Nonidet NP 40) was added into frozen ground samples, mixed gently with micropipette tips and then incubated on ice until all the samples were processed. The extraction buffer contained protease (Complete, Mini protease inhibitor-EDTA free (Roche Cat No. 11836153001) and phosphatase inhibitors (Sigma, phosphatase inhibitor cocktail 1 P2850 and cocktail 2 P5726) at concentrations recommended by the manufacturers. The samples were briefly vortexed and then centrifuged at maximum speed (15,000 rpm) for 15 min at 4^{o}C. The supernatant containing crude protein extract was transferred to a fresh 1.5 ml sterile microfuge tube. Protein concentration was determined using Bradford Assay, and then samples were snap frozen in liquid nitrogen and stored at -80^{o}C.

2.5.2 Protein Quantification

The concentration of total protein extracted was determine using Bradford Assay (Bradford, 1976). Briefly, 2 µl of the extracted protein samples were diluted in 18µl of sterile dH_2O. The 20 µl of diluted protein samples were added to 980 µl of diluted Bradford reagent (Biorad) in a 1ml disposable cuvette, mixed thoroughly and incubated at room temperature for 5 min. Blank samples were prepared by diluting 2 µl of protein extraction buffer in 18 µl of dH_2O. After incubation the absorbance of each sample was determined at A_{595}. Then concentration of protein in each sample was estimated based on a standard curve generated using absorbance obtained by measuring the absorbance of a series of BSA concentrations (0, 0.25, 0.5, 0.75, 1.0, 1.25 and 1.5 mg/ml).

2.5.3 SDS-PAGE Protein Electrophoresis

Stored plant protein samples were thawed on ice, mixed with 3×SDS sample buffer and then denatured at 95^{o}C for 5 min. The samples were briefly centrifugation and the supernatant transferred to a fresh 1.5 ml microfuge tube. A pre-stained protein marker (NEB, catalogue No. P7703) and denatured samples were loaded onto 10% SDS-PAGE gel (10 µl per well~30 µg). The proteins were then resolved at a constant 130 V using BIO-RAD mini PROTEAN® gel tank. Equal loading of protein on SDS-PAGE gel was based on the basis of sample fresh weight (Larkin, 2007). To visualize resolved proteins the gel was stained with Coomassie® Brilliant Blue solution for 30 min at room temperature. The staining solution consisted of 50% (v/v) methanol, 10% (v/v) acetic acid and 0.05% Coomassie® Brilliant Blue R250. The gels were then distained in a solution consisting of 10% (v/v) acetic acid, 10% (v/v) methanol and 90% (v/v) dH_2O on a rocker overnight with gentle shaking.

2.5.4 Western Blotting and Membrane Hybridization

After resolving protein samples on SDS-PAGE gel, they were transferred on to nitrocellulose membrane (BIO-RAD) using BIO-RAD mini PROTEAN® blotting system (BIO-RAD). The transfer system was filled with cold 1×Towbins transfer buffer (25 mM Tris-HCl, 190 mM glycine, 20% methanol). The electro-transfer

was carried out at constant 100 V for 1 h and to ensure successful transfer of proteins, the membranes were lightly stained with Ponceau red (Sigma). The membranes were then washed gently with dH_2O and depending on the primary antibody used, the membranes were blocked with either 5% non-fat milk or 5% BSA dissolved in 1xTBS-T (15 mM Tris-HCl pH7.6, 150 mM NaCl, 0.1% tween20). The primary antibody hybridization was conducted based on manufacturer's protocol for each individual antibody. The membranes were washed in three changes of 1xTBS-T for 5 min each to remove unbound primary antibodies before hybridization with HRP secondary antibody (NEB Cat No. 70742) for 2 h and then washed in three changes of TBS-T for 5 min each. The membranes were then incubated with Horse Radish Peroxidase (HRP) enhanced-chemiluminescent detection substrates (Thermo Scientific) according to manufacturer's instructions. The films were exposed in a Kodak X-ray cassette and processed using Kodak X-OMAT developing system. For each western blot analysis equal loading was confirmed by running a preliminary gel and then stained with Coomassie® Brilliant Blue solution.

2.6 Characterization of the *Atgcn2-1 Arabidopsis* Line

2.6.1 Response to N-starvation Stress

A preliminary experiment to determine the effects of N-starvation on *in planta* phosphorylation of AteIF2α were conducted using soil-grown 30-days old WT Col-0 plants. The plants were sprayed with a solution of 150 µM glyphosate (Sigma), containing 0.01% (v/v) Silwet L-77 (Lehle Seeds) until the plants were drenched. Glyphosate is a herbicide that inhibits biosynthesis of aromatic amino acids (tryptophan, tyrosine and phenylalanine) thus inducing amino acid starvation. Leaves (~100mg fresh weight) were harvested after 0, 4, 8, 12, 24, 48 and 72 h after treatment with glyphosate and protein extracted as described in section 2.5.1. The objective of the preliminary experiment was to determine the exposure time required to achieve optimum *in planta* activation of AtGCN2 kinase for the plants treated with 150µM glyphosate. After treatment with 150µM gylphosate, total plant protein was extracted as described in section 2.5.1. The protein samples were resolved on 10% SDS-PAGE and blots probed with antibodies raised against phosphorylated form of eIF2α (eIF2α-P). Optimal

phosphorylation of eIF2α was detected at 24 h after treatment with glyphosate (see Fig.3.8A). In the subsequent experiments, WT Col-0 and *Atgcn2-1* seeds were germinated on agar plates containing ½ MS media. After 14 days of growth, seedlings were treated with 150 μM glyphosate solution following protocol described by Zhang *et al.* (2008). This was achieved by submerging the seedlings in 100 ml of filter sterilized glyphosate solution for 2-3 min. The solution was drained, plates sealed with parafilm and then returned to growth chamber for 24 h. Protein was then extracted from the seedlings and resolved on 10% SDS-PAGE gel and then transferred to nitrocellulose membrane. Western blots analysis was conducted using antibodies raised against phosphorylated (eIF2α-P) and de-phosphorylated (eIF2α) form of eIF2α.

To follow-up the result obtained with glyphosate, the effect of *in planta* phosphorylation of AteIF2α on general protein synthesis in *Arabidopsis* was investigated by monitoring the luciferase activity. Seedlings (14-day old, 35S-Luc seedlings) were treated with 150μM glyphosate for 6, 12, 24 and 48 h prior to supplying 5 mM luciferin substrate. The effect of AteIF2α phosphorylation on the luciferase activity was then assessed for up to 22 h. The luciferase activity was then used as an indicator of general protein synthesis in *Arabidopsis* seedlings when AteIF2α is in phosphorylated or de-phosphorylated form. The luciferase protein catalyses oxidative decarboxylation of lucifirin substrate in the presences of ATP and O_2 and as a result a yellow green light is emitted. The emitted light is used to estimate ATP, luciferase and luciferin substrate levels (Sharon *et al.*, 1996). Treatment with 150μM glyphosate was used to induce phosphorylation of AteIF2α; glyphosate herbicide interferes with synthesis of aromatic amino acids and thereby inducing an amino acid deficiency which in turn activates AtGCN2 kinase.

2.6.2 Response to Salinity Stress

The effects of NaCl-induced salinity stress on the activity of the truncated (*Atgcn2-1*) and wild-type (WT Col-0) alleles on germination, growth and *in planta* phosphorylation of AteIF2α were investigated. The effect of NaCl stress on germination and growth of the seedlings were assessed on agar plates containing ½ MS media supplemented with 0, 50, 100 and 150 mM NaCl. Germination was

assessed at 2, 3 and 4 days after transfer to the growth chamber. To assess germination, each plate was observed under a dissecting microscope and the presence of an emerging radical was scored as successful germination. In each treatment there were three replicate plates and each plate was split into two sectors containing WT Col-0 and *Atgcn2-1* seedlings. Since only germination differences were observed on *Atgcn2-1* and WT Col-0, follow up experiments to investigate the effect on NaCl-induced salinity stress on seedling growth were undertaken with plates incubated in vertical orientation. Seeds of WT Col-0 and *Atgcn2-1* were germinated on NaCl-free media for 4 days and transferred on to agar plates containing ½ Ms media supplemented with 0, 50, 100 and 200 mM NaCl. In each treatment there were three replicate plates and in each plate contained 4 or 5 seedlings per genotype. Root growth was assessed since it was the only growth parameter that was observed to be different in the two genotypes. For assessing germination and root growth, three independent replicate experiments were conducted.

The effect of NaCl stress on activation of AtGCN2 kinase and phosphorylation of AteIF2α was also investigated. To determine the effect of truncated and wild type AtGCN2 kinase on *in vivo* phosphorylation of AteIF2α, seeds of *Atgcn2-1* and WT Col-0 were germinated and grown on agar plates containing ½ MS supplemented with 0, 50 and 100 mM NaCl for 14 days. Protein was extracted from the 21 days old seedlings and resolved on 10% SDS-PAGE and western blot conducted using antibodies raised against eIF2α-P and eIF2α.

2.6.3 Characterization of *Atgcn2-1* under Temperature Stress

WT Col-0 and *Atgcn2-1* seeds were germinated on agar plates containing ½ MS media. After 14 days, seedlings were incubated at 4^{o} and 37^{o}C for 2 h in dark, for cold and heat acclimation, respectively. Both WT Col-0 and *Atgcn2-1* seeds were spread such that each seed type covers half of each plate. In each treatment (cold and heat acclimation) there were four replicate plates and the experiment was repeated twice. Acclimated seedlings were then returned to the growth chamber and activation of AtGCN2 kinase by extreme temperature acclimation and phosphorylation of eIF2α was assessed at 0, 2 and 4 h after cold and heat acclimation. Protein was extracted from the seedling as described in

section 2.5.1. The samples were resolved on 10% SDS-PAGE and blots hybridized with antibodies raised against eIF2α-P and eIF2α.

2.6.4 Characterization of *Atgcn2-1* under Biotic Stress

Arabidopsis jar1-1, *NahG*, *Atgcn2-1* mutants and WT Col-0 seeds were sown on 40 wells trays containing sterile compost soil. Plants were grown under conditions of 20/18^{o}C day/night temperature, photoperiod of 8/16 h day/night. Each tray contained 2 rows of each *Arabidopsis* genotype (~4 plants per well). After 14 days of growth, a set of trays were inoculated with Cauliflower Mosaic Virus (CaMV) and for the second set, 21 days old *Arabidopsis* plants were sprayed (using Atomizer) with *Pseudomonas syringae* DC3000 (1200 c.f.u per 1 ml) culture until plants were drenched. In the third set of trays, 30 days old plants were infiltrated with 6 µl of *Pseudomonas syringae* DC3000 (1200 c.f.u per 1 ml) culture using 1 ml syringe. In all the experiment negative control treatments consisted of a set of non-inoculated trays, whereas positive control plants were treated with 150 µM glyphosate herbicide. Plants inoculated with CaMV were assessed for disease severity at 7, 14 and 21 days post inoculation. Protein for assessment of AtGCN2 activation by CaMV infection was isolated from leaves of inoculated plants at 21-days post inoculation; when most leaves seem diseased. For plants sprayed with *P. syringae*, leaf samples (~100 mg) were harvested 2 days after treatment, then crude protein extracted and phosphorylation of AteIF2α analysed. Plants infiltrated with *P. syringae* were assessed for bacterial growth; the inoculated leaves were harvested at 1 and 3 days after inoculation. For each genotype, 7 leaves were harvested at each time point and placed in separate sterile microfuge tubes, ground in 1ml sterile 10 mM $MgCl_2$ and then 10^{-1} to 10^{-6} dilutions were prepared. Each of the dilution (40 µl) was placed on 9 cm square plates containing semi-solid King's Broth medium supplemented with 50 µg/ml rifampicin. The plates were allowed to dry in a laminar flow-hood followed by incubation at 28^{o} C for 24 h. The number of colonies in each dilution were counted and then used to estimate growth of *P. syringae* in leaves of each *Arabidopsis* genotype.

2.7 Characterization of *p35S:AtGCN2* and *p35S:GFP:AtGCN2* Lines

2.7.1 Segregation and Localisation Analysis

Putative mutants (T_2) seeds of *p35S:AtGCN2* and *p35S:GFP:AtGCN2* independent lines were spread on ½ MS plates containing the 30µg/ml hygromycin; the pMDC32 and pH7WGF2.0 vectors T-DNA carry a dominant hygromycin resistance gene as a plant selectable marker. This facilitated an indirect way of determining segregation of the integrated *AtGCN2* ORF. Seeds (96-115 per plate) were spread on ½ MS media supplemented with 45 µg/ml hygromycin. After 21 days of growth, sensitive seedlings were defined as those without secondary leaves, whereas resistant lines were defined as those seedlings with both cotyledonary and true leaves. There were three plates for each independent mutant line generated. The number of hygromycin resistant (H^R) and sensitive (H^S) seedlings was determined after 21 days of incubation. The segregation ratio (H^R:H^S) data was subjected to 'Goodness of fit' Chi-square test. The T_2 mutant seedlings that satisfied the 3:1 ratio were rescued, transplanted into soil and grown to produce T_3 seeds.

The ectopically expressing AtGCN2 lines were generated using *Atgcn2-1* plants, which lacked the capability of phosphorylating AteIF2α. Three independent *p35S:AtGCN2* (lines A, C and F) and *p35S:GFP:AtGCN2* lines, *Atgcn2-1* and WT Col-0 seeds were stratified and spread on ½ MS agar plates. After 14 days of growth, seedlings were treated with 150µM glyphosate as described in section 2.6.1. Protein was then extracted from the seedlings and resolved on 10% SDS-PAGE. Western blots analysis was also conducted and blots were then probed with eIF2α-P and eIF2α antibodies. However after the phosphorylation experiment (see Fig. 4.5) and preliminary germination analysis only *p35S:AtGCN2* (line A) and *p35S:GFP:AtGCN2* lines were used to conduct characterization and AtGCN2 localisation experiments, respectively (see section 4.2.4.).

GFP is one of the fluorescent proteins that have widely been used to investigate gene activity in living cells. It is a non-invasive technique that does not require substrate, chemical treatment or cofactors and hence its has widely been used to analyse protein abundance and intracellular dynamics of signalling processes *in planta* (Hennig *et al.*, 2010). The location of the GFP reporter protein as directed by a fused protein should provide additional evidence of the functional location of the product of gene of interest (Curtis & Grossniklaus, 2003). To investigate localisation of AtGCN2 kinase without targeting any sub-cellular cell structures or compartments, the binary vector pH7WGF2.0 was used to ectopically express GFP.AtGCN2 fusion protein. The *p35S:GFP:AtGCN2* T_2 seeds (~50 seeds) were spread of on ½ MS media and germinated under non-stress condition for 10 days. GFP activity on seedling tissues or whole plant was examined on randomly selected seedlings using fluorescence microscopy. Further analysis of AtGCN2 expression and subcellular localisation was investigated using *Arabidopsis* eFP browser (Winter *et al.*, 2007). For analysis of *AtGCN2* expression, the eFP browser was set on the 'relative' mode that displays the ratio of tissue's expression level to an appropriate control signal depending on the data set. The developmental map and tissue specific data sets the expression levels were relative to the median value, whereas for the abiotic and biotic data sets the expression values were relative to mock (control) treatment. Localisation of the AtGCN2 kinase was determined using the cell eFP browser (Winter *et al.*, 2007) and Subcellular Location of Proteins in *Arabidopsis* Database abbreviated as SUBA (Heazlewood *et al.*, 2005).

2.7.2 Salt Tolerance Assays

The effects of NaCl- and KCl-induced salinity stress on germination and growth of *p35S:AtGCN2* were investigated. For germination experiments stratified seeds of WT Col-0, *Atgcn2-1* and *p35S:AtGCN2* line A (*p35S:AtGCN2A*)were spread on ½ MS media supplemented with either NaCl (0, 100 and 150 mM NaCl) or KCl (0, 50, 100 and 150 mM) and assessed as described in section 2.6.2. Prior to conducting the experiment, germination kinetics of the three genotypes on NaCl-free ½ MS media was determined. For assessment of seedling growth, stratified seeds of WT Col-0, *Atgcn2-1* and *p35S:AtGCN2A* mutants were germinated on agar plates containing full-strength MS media (pH5.7) supplemented with 0.7% sucrose and

gelled with 8 g/l agar. Seedlings were allowed to grow for 6 days with plates in vertical orientation. To investigate sensitivity of *p35S:AtGCN2* mutant, seedlings were transferred to salt containing media (NaCl or KCl) using a fine forceps. The position of root tips were marked immediately after transfer and then agar plates placed in vertical orientation with roots facing downwards. For each genotype, four seedlings were placed per plate and then root growth was measured at 10 days after transplantation.

In the second experiment the effect of NaCl and KCl salinity on survival and general growth of *p35S:AtGCN2* plants was investigated. The 6 days old seedlings of WT Col-0, *Atgcn2-1* and *p35S:AtGCN2* (A&F) were transferred on to agar plates containing ½ MS media supplemented with NaCl or KCl. Each plate was separated into four sectors and two seedlings per genotype (WT Col-0, *Atgcn2-1* and two independent *p35S:AtGCN2* (A&F) mutant lines were placed in each plate. In all the NaCl or KCl treatments there were 4 plates per concentration and the experiment was repeated three times. The effect of NaCl and KCl on growth was assessed at 30 days after transplantation.

2.7.3 Seedling Exposure to Osmotic Stress

The influence of mannitol- and PEG6000-induced osmotic stress on germination and growth of *p35S:AtGCN2* seedlings were also investigated. For mannitol induced stress, ½ MS media containing 0.7% sucrose was supplemented with 0, 50,100, 200 and 300 mM mannitol and gelled with 0.8% agar. In the germination experiments stratified seeds of WT Col-0, *Atgcn2-1* and *p35S:AtGCN2* were spread on mannitol containing media and germination assesses after 2, 3 and 4 days. For root growth assay stratified seeds of WT Col-0, *Atgcn2-1* and *p35S:AtGCN2* were germinated on mannitol free ½ MS media and then transplanted onto mannitol supplemented media after 6 days, followed by assessment of root growth at 10 days after transplanting. For each mannitol treatment there were three replicate plates, and three independent replicate experiments were conducted for germination and root growth assay.

For PEG6000-induced osmotic stress, 20 ml plates of ½ MS media containing 0.7% sucrose and gelled with 8 g/l agar were infused with 0, 20 and 40% PEG6000 solution (w/v) corresponding to 0, -0.62 and -9.33 MPa. The calculation for osmotic potential of the PEG6000 were based on earlier described method (Michel & Kaufmann, 1973). In each plate 20 ml of the PEG solution were added per plate and allowed to infuse overnight and the excess solution was drained. Stratified seeds of WT Col-0, *Atgcn2-1* and *p35S:AtGCN2* were then spread on PEG6000 infused plates and germination assessed after 2, 3 and 4 days. For root growth experiment ½ MS plates were infused with 70% PEG6000 solution (-37.58 MPa), and after completely draining the excess solution. Seven day old seedlings previously grown on PEG free media were then transplanted and allowed to grow with plates in vertical orientation for 10 days before increased root growth was assessed.

2.7.4 Effect of Exogenous Application of ABA on Germination

Abscisic acid (ABA) is a key phytohormone that is involved in regulation of physiological processes in plants. It is implicated in regulating germination and seedling development as well in many abiotic stress responses (Price *et al.*, 2003; Fujii *et al.*, 2007). Germination kinetics was chosen as a parameter to determine the relationship between AtGCN2 kinase and exogenous application of ABA. The effects of wild type, knocking-out and ectopic expression of *AtGCN2* gene were evaluated. Germination experiment was therefore set up by spreading WT Col-0, *Atgcn2-1* and *p35S:AtGCN2A* seeds on ½ MS media supplemented with 0, 0.5, 1 and 2µM ABA.

2.7.5 Seedling Cold and Heat Shock Tests

Stratified seeds of WT Col-0, *Atgcn2-1* and *p35S:AtGCN2A* were spread on agar plates containing ½ MS media and grown for 7 days. The agar plates were divided into three sectors and at least 50 seeds were spread in each sector for each genotype. For cold shock tests, a set of seedlings were first cold acclimated by incubation at 4^{o}C in dark for 12 h, and then returned to the growth chamber for 3 days to recover. Then the acclimated and non-acclimated seedlings were cold shocked at -20^{o}C in dark for 25 min. The plates were

returned to the growth chamber and the number of surviving seedlings was assessed at 12 days after cold shock. For heat shock tests, a set of seedlings were first heat acclimated by incubation at 35±0.4°C in dark for 1 h, and then allowed to recover for 3 days. The acclimated and non-acclimated seedlings were then heat shocked at 42°C in dark for 2 h. The plates were returned to the growth chamber and the number of surviving seedlings scored at 12 days after heat shock. The cold and heat shock experiments were replicated twice and in each experiment there three plates per treatment.

2.8 Cloning and Expression of *Arabidopsis* eIF2α in *E.coli*

2.8.1 Cloning of *AteIF2a* Splice Variants

Total RNA was isolated from 3 weeks old WT Col-0 *Arabidopsis* seedling and cDNA synthesized as described in section 2.2.2 and 2.2.4, respectively. The cDNA generated was used as template conduct cloning PCR using primers specific for At2g40290.1 and At5g05470.1 eIF2α splice variants. The cloning PCR was conducted using the following primer combinations for At2g40290.1; AteIF90Fw and AteIF90Rev, and for At5g05470.1; AteIF70Fw and AteIF70Rev (Table 2.1). The amplification was conducted using Phusion™ High-Fidelity (FINNZYMES) DNA polymerase and the reaction setup was as described in section 2.2.5.2. The amplification were conducted using the following 30 cycles PCR programme; initial denature 98°C for 30s, denature 98°C for 10s, annealing 62°C for 30s, extension 72°C for 40s and final extension 72°C for 5 min. The PCR products were resolved on 1% agarose gel and *AteIF2a* fragments extracted using Qiaquick® gel extraction Kit (Qiagen) and 'A' overhangs added as described earlier (see 2.3.1).

The AteIF2α DNA fragments with 'A' overhangs were immediately cloned onto pCR4®-TOPO® sequencing vector (Invitrogen) and transformed into TOP10 *E. coli* cells (Invitrogen) following manufacturer's protocol. The transformed TOP10 cells were incubated overnight at 37°C on agar plates containing LB media supplemented with 50µg/ml kanamycin. Positive clones were confirmed by colony PCR using primer sets for At2g40290.1 and At5g05470.1, using the following 22 cycle programme; initial denature 98°C for 10 min, denature 98°C

for 10s, annealing 62°C for 30s, extension at 72°C for 40s and final extension at 72°C for 5 min. The clones were then sequenced to confirm the sequence authenticity and orientation of *AteIF2a* inserts in pCR4®-TOPO® vector using T7 and T3 universal primers.

The At2g40290.1 and At5g05470.1 fragments were then sub-cloned from pCR4®-TOPO® to pENTR4® Gateway entry (Invitrogen) vector via PCR using primers containing *NcoI* and *NotI* restriction sites for forward and reverse primers, respectively (Table 2.1). The inserts were finally sub-cloned from pENTR4® into pDEST17® expression vector (Invitrogen) containing N-Terminal 6× His tag via LR recombination reaction following manufacturer's protocol (Invitrogen). The *pENTR4:AteIF2* and *pDEST17:AteIF2* constructs were maintained in TOP10 and DH5α *E.coli* cells, respectively. The frame and sequence of the inserts in pENTR4® and pDEST17® vectors was confirmed by sequencing using Pentr4U and Pentr4L, T7 universal and PDest17Rv primers, respectively (Table 2.1).

2.8.2 Optimization of AteIF2α Expression in *E. coli*

Clones of *AteIF2a* splice variants At2g40290.1 and At5g05470.1 on pDEST17® expression vector were used to transform chemically competent BL21(DE3) *E. coli* expression cells (Novagen). The transformed cells were spread on agar plates containing LB media supplemented with 50 µg/ml carbenicillin and incubated overnight at 37°C. Single discrete colonies were used to prepare 20 ml cultures for optimization experiments of *pDEST17:eIF2a* fusion protein expression. Briefly single colonies harbouring *pDEST17:eIF2a* expression constructs (*pDEST17:AteIF90* and *pDEST17:AteIF70*) were inoculated into 5 ml of liquid LB media containing 50 µg/ml carbenicillin and grown overnight at 37°C in a 200 rpm shaker. Then 0.5 ml overnight cultures were then used to inoculate 20 ml LB media supplemented with carbenicillin and then grown at 37°C until an OD_{600} of 0.5-0.7 was achieved (6-7 h). To determine the optimum expression of eIF2α fusion proteins the cultures were induced using IPTG at 0, 0.3, 0.5 and 1 mM, and expression at 23 and 28°C for 1, 2 and 3 h, and overnight was evaluated. Following manufacturers' protocol (Invitrogen pDEST17® manual), the induced cells were pelleted by spinning at maximum speed (13 000 rpm) for 10 min and re-suspended in cell lysis buffer pH7.8 (50 mM K_2HPO4, 400 mM NaCl,

100 mM KCl, 10% glycerol, 0.5% triton X-100 and 10 mM imidazole). The cells were then lysed by 3 series of freeze and thaw cycles, followed by spinning at maximum speed for 15 min. The supernatant and pellet contained soluble and insoluble protein fractions, respectively. Soluble protein samples were then mixed with equal volume of 2×SDS-sample buffer, whereas insoluble protein sample were re-suspended in 1×SDS sample buffer. The samples were then denatured by heating at 95^{o}C for 5 min, centrifuged for 2 min at 13000 rpm and 10 µl resolved on 10% SDS-PAGE gel.

2.8.3 Analysis of His:AteIF2α Fusion Protein Expression in *E. coli*

Soluble proteins samples for induced and non induced cultures were resolved on 10% SDS-PAGE gel and then transferred onto nitrocellulose membrane. The membrane was then blocked with 10 ml of 5% non-fat milk powder in 1×TBS-T buffer for 1 h, this was immediately followed by washing in three changes of TBS-T for 5 min each and incubated with anti-histidine polyclonal primary antibody (Sigma cat. No. H102-2 ml) diluted in 5% (w/v) non-fat milk (1:10,000) for 1 h. The membrane was again washed in 3 changes of TBS-T to remove unbound primary antibody and then incubated with goat anti-mouse-HRP secondary anti-body (Sigma cat. No. A2304) diluted 1: 20,000 for 1 h. The membrane was finally washed in three changes of TBS-T, before incubating with HRP enhanced-chemiluminescent detection substrates (Thermo Scientific) according to manufacturer's protocol. The membrane was blocked and hybridized with antibodies at room temperature (22^{o}C) with gentle shaking on a rocker.

2.8.4 Purification of *AteIF2a* Splice Variant At2g40290.1

The *AteIF2a* fusion protein expressed by *pDEST17:AteIF90* construct was expressed and purified for further experimentation. This is because low yields were obtained with *pDEST17:AteIF70* during optimization experiment. A 5ml starter culture was used to inoculate 250 ml of LB liquid media supplemented with 50 µg/ml carbenicilin. The 250 ml cultures (induced and control) were grown to an OD_{600} 0.5-0.6 at 37^{o}C (6-7 h) and then transferred to a 23^{o}C shaker for 30 min to stabilize, prior to induction with 0.5 mM IPTG overnight. No IPTG

was added to non-induced control cultures. The cells for induced and control cultures were harvested by centrifugation at 4000 rpm for 10 min at 4°C using Sorvall® Legend RT bench top centrifuge. The cell pellets were then washed once with ice cold cell lysis buffer consisting of 50 mM NaH_2PO_4, 300 mM NaCl and 10 mM imidazole (pH 8.0), supplemented with complete mini EDTA-free protease cocktail tablets (ROCHE, 1 tablet per 10 ml of lysis buffer). The washed pellets were re-suspended in 5 ml ice cold cell lysis buffer pH8 (50 mM NaH_2PO_4 30 mM NaCl, 10 mM imidazole and 0.05% tween 20) and lysed three times using French press at 750 psi. Total cell lysate was then clarified by centrifugation at 30,000 rpm for 30 min at 4°C using Sorvall® Legend Centrifuge.

The supernatant was applied to the Ni-NTA agarose resin (Qiagen) column containing 4 ml bed volume of the nickel resin equilibrated with 5 column volume (20 ml) of the cell lysis buffer. The column was then washed with 10 bed volume (40 ml) of wash buffer pH 8.0 (50 mM NaH_2PO_4, 300 mM NaCl and 50 mM imidazole) and AteIF2α was eluted with 2 bed volumes (10 ml) of elution buffer (50 mM NaH_2PO_4, 300 mM NaCl and 250 mM imidazole) pH 8.0. Elutes were collected in 1 ml fraction and concentration of each fraction determined using Bradford Assay. The fractions were then pooled, concentrated and elution buffer exchanged with storage buffer pH7.9 (20 mM Tris-HCl, 50 mM NaCl and 40% glycerol) using Amicon Ultra 30 kDa column (Millipore) following manufacturer's protocol. The AteIF290 fusion protein was stored at -70°C in 50 µl aliquots (2 mg/ml concentration). During expression and purification of AteIF2α90 protein, 40 µl of each samples were collected, namely, total lysate (French press lysate) and supernatant samples for both induced and non-induced cultures after clarification. Similarly, 40 µl samples of column flow-through (supernatant passed through Ni-NTA agarose resins), column wash and 1 ml fraction with the highest protein concentration, for induced cells were analysed on 10% SDS-PAGE gel.

2.9 Expression of *Arabidopsis* GCN2 Kinase in *E. coli*

The pENTR/D:*AtGCN2* clone generated in section 2.3.2 were used to generated AtGCN2 kinase expression clone using pDEST17® expression vector via LR reaction following manufacturer's protocols (Invitrogen). The pDEST17:*AtGCN2* clone generated was used to transform chemically competent XL-1 Blue *E. coli* cells. The frame and sequence of the inserts in pDEST17® vector was confirmed by T7 universal and PDest17Rv primer (Table 2.1). The pDEST17:*AtGCN2* expression clone was used to transform Rosseta™ (DE3) BL21 cells and positive colonies were selected on LB media agar plates supplemented with 50 µg/ml carbenicillin and 34 µg/ml chloramphenical at 37°C overnight. A single distinct colony was then used to set up a 5ml overnight, then 0.5 ml was used to inoculate 20 ml LB media supplemented with carbenicillin and chloramphenical. The cultures were grown at 37°C until an OD_{600} of 0.5-0.7 was achieved (6-8 h). The optimum expression of AtGCN2 fusion protein using 0.5 mM IPTG at 20, 25 and 28°C overnight was assessed following manufacturers' protocol (Invitrogen pDEST17® manual). Total protein was separated on SDS-polyacrylamide gel and stained with Coomassie® Brilliant Blue as described in section 2.5.3. Due to extremely poor expression and partitioning in the insoluble protein fraction in *E. coli*, AtGCN2 kinase was substituted with mPKR kinase.

2.10 Expression of Mammalian PKR Kinase in *E. coli*

2.10.1 Induction of mPKR kinase

The expression vector construct pTYB2.PKR/PPase encoding non-phosphorylated form of mammalian PKR kinase (mPKR) was kindly provided by Dr Gramme Conn of The University of Manchester, Manchester, UK (Conn, 2003). The PKR expression construct was maintained in DH5α *E. coli* cells and plasmid prepared from 10 ml overnight cultures using Qiagen mini-prep kit. The plasmid were then used to transform chemical competent Rosseta™(DE3) BL21 protein expression cells (Novagen). The transformed Rosseta™ (DE3) BL21 cells were screened on LB medium plates supplemented with 50 µg/ml carbenicillin and 34 µg/ml chloramphenical at 37°C overnight. A single distinct colony was then used to set up a 50 ml overnight starter culture, from which 25 ml was used to

inoculate 250 ml LB media for induced culture and the remainder was used to inoculate control culture. The 250 ml LB media were supplemented with carbenicillin and chloramphenical. The cultures were then incubated at 37°C on a shaker at 200 rpm until they attained an OD_{600} of 0.5-0.7 (4-5 h) and then transferred to a 30°C shaker for 30 min to stabilize. The cultures were then induced by addition of IPTG to a final concentration of 0.3 mM for 6 h, whereas no IPTG was added to the control culture. Cells were then harvested by centrifugation at 4000 rpm for 10 min at 4°C. The cell-pellets were then washed twice and re-suspended in 4ml of ice cold cell lysis buffer pH 6.5 (20 mM Hepes, 1 M NaCl, 1 mM EDTA, 0.1% Triton® X-100, 10% glycerol). The re-suspended cells were lysed using French press, and clarified by centrifugation as described for purification of AteIF290 fusion protein (section 2.8.4).

2.10.2 Purification of mPKR Protein Kinase

Purification of mPKR was achieved following protocol described by the manufacturer of pTYB2 expression vector and Chitin Beads resins (NEB). Briefly, a 6 ml column was packed with 4 ml of chitin beads resins (NEB, Cat. No. S6651S). Prior to loading clarified supernatant containing soluble mPKR, the chitin beads were equilibrated with 5 bed volume (20 ml) of ice cold column buffer pH6.5 (20 mM HEPES, 1 M NaCl, 1 mM EDTA, 0.1% Triton® X-100 and 10% glycerol). The clarified supernatant from induced culture was then carefully loaded into a column to avoid air bubbles. The column was then washed with 10 bed volumes of column buffer and mPKR:CBD intein tag chimera cleaved from the column by flushing with 3 bed volume of freshly prepared column buffer (pH8.5) supplemented with 50 mM DTT (dithiothreitol). Unlike in the manufacturer's protocol, the flow-through after flushing the column contained mPKR and was therefore collected, and mPKR concentrated and exchanged into storage buffer pH7.5 (20 mM HEPES, 1 M NaCl, 10 mM B-mercaptoethanol, 10 % glycerol) using Amicon Ultra 30 kDa column (Millipore). All the purification steps for mPKR were conducted at 4°C. Analysis samples (100 µl) of the supernatant for induced and non-induced cultures, column flow-through and mPKR were collected and analysed on SDS-PAGE gel. The samples were first mixed with equal volume of 2×SDS sample buffer, denatured by heating at 95°C for 5 min

centrifuged for 1 min at 13000 rpm and 10 µl of each of the collected samples were resolved on 10% SDS-PAGE gel.

2.10.3 mPKR Activation and Phosphorylation of AteIF2α90

Prior to phosphorylation of AteIF290, mPKR was activated using double stranded RNA (poly I:C). The effect of poly I:C concentration (0, 0.5 and 10 µg/ml) on activation of mPKR was determined. The concentrations of poly I:C tested were chosen based on the reports in literature indicating that between 0.1-10 µg/ml of poly I:C activate mPKR kinase *in vitro* (Lamaire *et al.*, 2005). Activation of mPKR and phosphorylation of AteIF290 was conducted in a 30µl reaction volume consisting of 0.5 µl PKR (0.03 µg/µl), 3µl poly I:C (10 µg/ml) and 26.1 µl phosphorylation buffer (50 mM Tris pH7.8, 50 mM KCl, 2 mM $MnCl_2$, 2.5 mM DTT, 10 µM un-labelled ATP and 10% glycerol). The mPKR activation reaction mix was incubated at 26^{o}C for 5 min, before addition of 0.4 µl AteIF290 (0.04 µg/µl). The reaction mixture was further incubated at 26^{o}C for 10min and the reaction quenched by addition of 15 µl of 3×SDS sample buffer. The samples were denatured at 90^{o}C for 5 min and then 10 µl of each treatment resolved on 10% SDS-PAGE gel. Western blot analysis was conducted and nitrocellulose membrane probed with antibodies raised against eIF2α-P.

2.11 *In vitro* Translation Control of *Arabidopsis* mRNA

2.11.1 Extraction of *Arabidopsis* mRNA

Arabidopsis mRNA (AtmRNA) was extracted from actively growing leaves of 30 days old soil-grown WT Col-0 plants. The plants were grown under 8/16 h of light/darkness and 20/16^{o}C day/night temperatures. The leaves were harvested, immediately frozen in liquid nitrogen and ground into a fine powder using pre-chilled motor and pestle. Then mRNA was isolated directly from the ground leaves sample using Dynabeads® Oligo (dT) 25 Kit (Invitrogen, Cat. No. 610-02) following the manufacturer's protocol. The isolated mRNA was then quantified using spectrophotometer (Sambrook & Russell, 2001) and the purity of mRNA was determined by the ratio of A_{260} to A_{280}.

2.11.2 *In vitro* Translation of *Arabidopsis* mRNA

The *in vitro* translation experiments were conducted using Wheat Germ Extract lysate (Promega Cat. No. L4380). Prior to determining effect of the state of Wheat Germ Extract eIF2α (WGeIF2α) on translation of AtmRNA, there was need to optimize the translation efficiency of AtmRNA in this system. For optimization purpose, the concentrations of AtmRNA (0.01, 0.02, 0.03 and 0.04 µg/µl) on translation efficiency in a 12.5 µl reaction volume were evaluated. All the translation reaction experiments were assembled in PCR tubes, gently mixed and then incubated at 25^{o}C for 2 h on PCR block. After completion, the samples were mixed with 1×SDS sample buffer (1:3, sample: buffer) and denatured at 70^{o}C for 15 min. Then 10 µl of each sample was resolved 10% SDS-PAGE gel. Western blot analysis was conducted and membranes hybridized with Streptavidin-HRP antibody conjugate (Transcend™ Chemiluminescent system. Cat No: L5081, Promega) following manufacturer's protocol.

2.11.3 Translation of AtmRNA under Phosphorylated WGeIF2α

In vitro translation experiments to mimic eukaryotic stress-response translation control were undertaken. The effects of mPKR concentration on phosphorylation of WGeIF2α were tested in order to determine the optimal concentration required. Briefly, inactive mPKR was added into Wheat Germ Extract lysate to attain final concentrations of 0, 0.02, 0.04, 0.08, 0.1 and 0.2 µg/ml in a 12.5 µl reaction mix. The reaction was gently mixed, incubated at 26^{o}C for 10 min, and denatured samples were resolved on 10% SDS-PAGE gel and stained with Coomassie® Brilliant Blue. Western blot analysis was also conducted and nitrocellulose membranes were hybridized with eIF2α-P and eIF2α antibodies. Thereafter *in vitro* translation control of AtmRNA experiments were conducted using two lowest concentration of mPKR (0, 0.02 and 0.04 µg/ml) that induced optimal phosphorylation of WGeIF2α. The translation reactions were assembled in PCR tubes (Table 2.3) and then incubated at 25^{o} C for 2 h on a PCR block. Prior to undertaking translation experiments endogenous biotinylated proteins in the in Wheat Germ Extract were pulled down using Dynabeads®M-280 streptavidin beads following the manufacturer's protocol. Similarly after translation the biotinylated nascent proteins were pulled down

using Dynabeads®M-280 Streptavidin and then eluted using 1×SDS sample buffer. For each translation reaction, 10 µl were resolved on 10% SDS-PAGE gel, and then nitrocellulose blots were probed with antibody raised against Streptavidin-HRP antibody conjugate.

Table 2.2. *In vitro* translation control reaction set-up for AtmRNA translation using Wheat Germ Lysate system.

Component	Lysate Control	Lysate+ mPKR (0.02 µg/µl)	Lysate + AtmRNA (0.04 µg/µl)	Lysate + AtmRNA (0.04 µg/µl) + PKR (0.02 µg/µl)	Lysate + AtmRNA(0.04 µg/µl) + PKR (0.04 µg/µl)
Wheat Germ extract	6.25	6.25	6.25	6.25	6.25
Amino Acid mixture minus Methionine (1 mM)	0.5	0.5	0.5	0.5	0.5
Amino Acid mixture minus Leucine (1 mM)	0.5	0.5	0.5	0.5	0.5
RNasin Ribonuclease inhibitor (40 µ/µl)	0.25	0.25	0.25	0.25	0.25
Potassium Acetate (1 M)	0.96	0.96	0.96	0.96	0.96
PKR (~2.1 mg/ml)	-	0.125	-	0.125	0.25
mRNA substrate in TE buffer (0.04 µg/µl)	-	-	1.7	1.7	1.7
Nuclease-free water	3.54	3.415	1.84	1.72	1.59
Transcend™ tRNA	0.5	0.5	0.5	0.5	0.5
Total (µl)	**12.5**	**12.5**	**12.5**	**12.5**	**12.5**

2.12 *In silico* Analyses

2.12.1 Search for PKR and PERK Homologues in Plants

In *Arabidopsis*, a homologue of yeast GCN2 kinase has been cloned (Zhang *et al.*, 2003), however there are no reports of PKR, PERK or PEK homologues in plants. The possibility of the existence of mammalian PKR and PERK homologues in *Arabidopsis* and in other plants (Viridiplantae) was explored. Initially a BLASTP search was conducted using full-length yeast GCN2 (ScGCN2), human GCN2 (HsGCN2), human PKR (HsPKR) and human PERK (HsPERK) kinases against TAIR 10 (http://www.arabidopsis.org). Further analysis of the *Arabidopsis* BLASTP hits was conducted using a phylogenetic approach for the purpose of identifying *Arabidopsis* genes that cluster with the eIF2α kinases and to identify those with

the potential of phosphorylating AteIF2α. From each BLASTP search, 57 loci with highest e-value scores were selected and full-length protein sequences retrieved using the TAIR-Bulk sequence download tool. For genes with splice variants, only sequences that correspond to the representative gene model were retrieved. A total of 104 protein sequences were extracted and used to conduct phylogenetic analysis. The full-length protein sequences of ScGCN2, HsGCN2, HsPKR and HsPERK were compared with the 104 *Arabidopsis* loci. The sequences were aligned and phylogenetic analysis conducted using CLC Sequence Viewer version 6.5.1. To explore the possibility of kinase activity of the protein sequences that clustered with the eIF2α kinases, a search for conserved domains was performed using Conserved Domain Architecture Retrieval Tool (Geer *et al.*, 2002) referred herein as CDART, available on the National Centre for Biotechnology Information (NCBI) website (www.ncbi.nlm.nih.gov). A second BLASTP search was conducted using the full length protein sequences of the above mentioned eIF2α kinases against Viridiplantae (green plants and algae) non redundant protein sequences deposited at the National Centre for Biotechnology Information (NCBI) database (www.ncbi.nlm.nih.gov). This was followed by another BLASTP search against NCBI rice and maize genomic database. Full length Viridiplantae, rice and maize protein sequences were extracted and analysed as described for *Arabidopsis*.

2.12.2 Search for HsATF4 and ScGCN4 Homologues in Plants

To identify putative ScGCN4 and HsATF4 homologues in *Arabidopsis* a BLASTP search was conducted using full-length protein sequences of the two transcriptional factors against TAIR 10 (http://www.arabidopsis.org). Full-length protein sequences of the top hits obtained after the search, and ScGCN4, and HsATF4 as reference amino acid sequences of known functions were subjected to phylogenetic analysis. The protein sequences were retrieved using TAIR-Bulk sequence download tool, then aligned (Gap cost 10, and Gap extension costs 1) using CLC Sequence Viewer version 6.5.1. This was then followed by phylogenetic analysis (100 Bootstrap replicates) using Unweighted Pair Group Method (UPGMA) and Neighbour-Joining methods (N-J). The idea behind performing UPGMA (a divisive method) and the N-J analysis (an aggregative method), rather than N-J only, was to identify loci that consistently appear to

be closely related to ScGCN4 and HsATF4, thereby suggesting conserved function. The UPGMA method assumes that evolution of the amino acid sequences occurred at a constant rate in yeast, humans and *Arabidopsis*, while the N-J method assumes the evolutionary rates are different.

2.12.3 Search for ScGCN4 and HsATF4 Homologue Using FivePrime Viewer

Previously in Dr Peter Dominy's laboratory at the University of Glasgow, Shaun Webb (2008) developed FivePrime Viewer, a bioinformatics tool for identifying cDNAs containing UTRs with uORFs, and whose mORFs translation may be eIF2α-P or uORF-dependent. The program was designed to identify 5′ UTRs with regulatory uORFs that are likely to be regulated in a GCN4- or ATF4-like manner. The program utilizes three scoring methods, namely pair scoring, pathway scoring, and combined scoring methods. The pair scoring method is based on the model of eIF2α-p-dependent translation and compares pairs of uAUGs in the 5′ UTRs and scores on their regulatory potential. On the other hand the pathway method predicts the fate of ribosomes by estimating the stability of the leaky scanning translation initiation at each uORF and reinitiation at the mORF. The combined method encompasses the strengths of the two scoring methods, where the uORFs are compared and those with the highest scores identified. Using the FivePrime Viewer, a total of 99 *Arabidopsis* cDNAs that that may be regulated in a GCN4-/ATF4-like manner were identified (Webb, 2008). The *Arabidopsis* cDNAs were retrieved and analysed as described in section and for those that clustered with ScGCN4 and HsATF4, the 5′ UTRs were retrieved and analysed for presence of uORFs using CLC Sequence Viewer.

2.13 Statistical Analyses

The data generated were subjected to Analysis Of Variance (ANOVA) using General Analysis of Variance Design provided for by GenStat Discovery Edition 3 for everyday use (Buysse *et al.*, 2007). Data on % germination were log transformed prior to ANOVA. The data generated during assessment of the survival of the *p35S:AtGCN2* seedlings after cold shock, and the effect of various abiotic stresses on root growth were transformed using Arcsine prior to ANOVA.

The *p35S:AtGCN2* and *p35S:GFP:AtGCN2* mutant lines generated were subjected to 'Goodness-of-fit tests' to estimate the number of T-DNA insertion in the independent mutant lines. The calculations were performed using the Chi-test function for the observed and expect ratio for T_3 generation (3:1, hygromycin resistant: hygromycin sensitive).

3 Chapter 3: Characterization of AtGCN2 Null-Mutant (*Atgcn2-1*)

3.1 Introduction

Eukaryotes have generally well developed stress-response mechanisms that induce key metabolic events geared towards alleviation of stress. Successful stress alleviation is however highly dependent on the perception of environmental or cellular stress cues. For eukaryotes, response to stress cues can be immediate or may take weeks for example plant adaptation to temperature stress (Penfield, 2008). As discussed earlier (section 1.13), translation regulation is an important stress-response mechanism and there are several ways in which it is achieved in eukaryotes (Kozak, 1992; Muench *et al.*, 2012). Translation regulation mediated through phosphorylation of eIF2α by a group of eIF2α-specific kinases has been recognized as an important stress-response mechanism in eukaryotes (Dever *et al.*, 1992; Hey *et al.*, 2010). It is well demonstrated in yeast and mammalian systems, and it has been established that disrupting eIF2α kinases produces a distinctive phenotype. For example in yeast, knocking-out GCN2 kinase has been shown to impair growth under stress induced by amino acid starvation (Hinnebusch & Natarajan, 2002). On the other hand deletion of PERK kinase in mice, led to the development of diabetes mellitus, dysfunction of the pancreas and severe bone defects (Ron & Harding, 2000; Iida *et al.*, 2007). Although stress-response translational control is not well characterized in plants, it has been demonstrated that *Arabidopsis* GCN2 kinase functionally complements yeast *Δgcn2* (GCN2 null) mutants (Zhang *et al.*, 2003). Furthermore wheat eIF2α has also been shown to functionally complement yeast GCN2-mediated pathway (Chang *et al.*, 2000). These reports suggest that plant GCN2 kinase has a similar function as yeast GCN2 and thus may be involved in stress-response translation regulation mechanisms in plants.

Genetic mutation is one of the most effective ways to analyse genes. As discussed earlier (section 1.4 to 1.6), the most direct way of analysing function of a gene product is through 'gain-of-function' or loss-of-function' mutations. This is usually followed by examining and characterizing phenotypic changes

associated with the form of mutation. Since knocking-out eIF2α kinases produced distinct phenotypes in yeast (GCN2) and mammalian systems (PKR and PERK), it is expected that knocking-out AtGCN2 kinase or gene(s) involved in translation regulation mechanism in *Arabidopsis* should also produce an obvious phenotype. In order to investigate the function of AtGCN2 kinase, a forward genetics approach using a 'loss-of-function' mutation technique was undertaken. This consisted of isolating a T-DNA insertion mutant lines that give rise to *Atgcn2* null phenotype (see section 2.4.1). This chapter therefore reports on *in silico* search for homologues of mammalian PKR and PERK in plants, isolation and characterization of *Arabidopsis* GCN2 null lines (*Atgcn2-1*) and their response to salt, acclimation to extremes of temperature, and biotic stress.

3.2 *In silico* Search for ScGCN2, HsPKR and HsPERK Homologues in Plants

3.2.1 Search for Homologues of eIF2α Kinases in *Arabidopsis*

The *Arabidopsis* GCN2 homologue (At3g59410 splice variants 1 and 2) consistently emerged as the gene with the highest e-value scores in the BLASTP search conducted using ScGCN2, HsGCN2, HsPKR and HsPERK eIF2α kinases against TAIR 10 proteins; TAIR 10 protein search using ScGCN2, HsGCN2, HsPKR and HsPERK sequences, scored 7e-60, 5e-51, 3e-28 and 2e-24, respectively (Appendix 2-5). Phylogenetic analysis conducted using UPGMA and N-J methods revealed that apart from *Arabidopsis* GCN2 kinase (At3g59410), the At3g02760.1 gene also clustered with the eIF2α kinases (Fig. 3.1). The At3g02760.1 contains Class II tRNA aminoacyl synthetase and biotin synthetase functional domains which are involved in the histidine- and aminoacyl-tRNA ligase activities, and also in the nucleotide and ATP binding activities (www.arabidopsis.org). However the At3g02760.1 sequence seems to be evolutionary closer to the GCN2 kinases as opposed to the PKR and PERK kinase (Fig. 3.1). The At3g02760.1 protein also shares a number of functional domains with the GCN2 kinases; they all have domains associated with aminoacyl-tRNA ligase and ATP binding activities (www.arabidopsis.org).

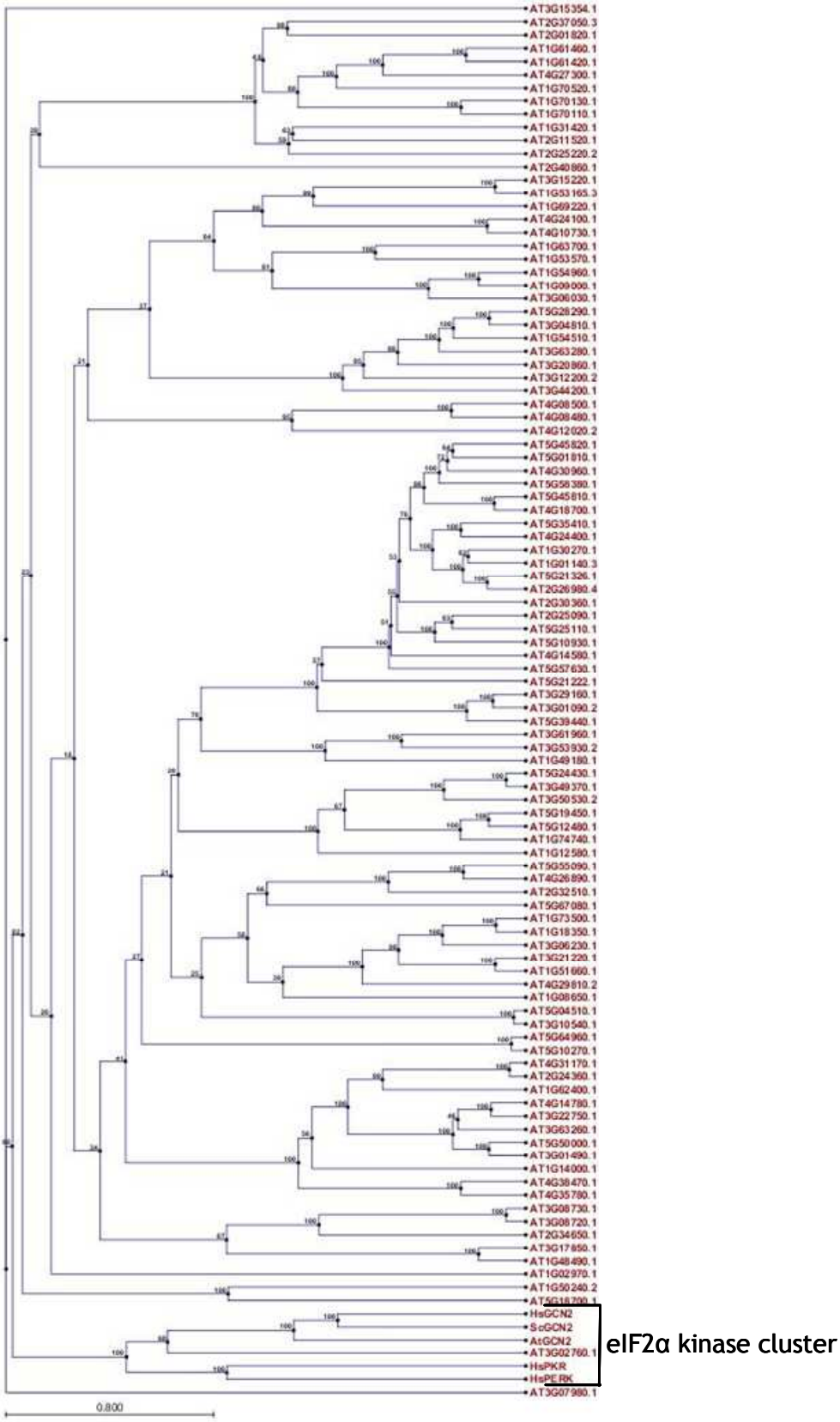

Figure 3.1. Phylogenetic analysis of *Arabidopsis* loci related to yeast and human eF2α kinases. Phylogeny of 104 *Arabidopsis* proteins inferred from alignment by CLC Sequence Viewer version 6.5.1 using UPGMA, an algorithm assuming the same rate of evolution. The branch lengths indicate relative evolution distance.

For At3g02760.1 to complement AtGCN2 it should possess all the functional domains as the eIF2α kinases. The results obtained with CDART analysis however show that At3g02760.1 shares only a conserved uncharged tRNA binding domain (HisRs-like core domain) with the AtGCN2 kinase but lacks kinase domains (Fig. 3.2).

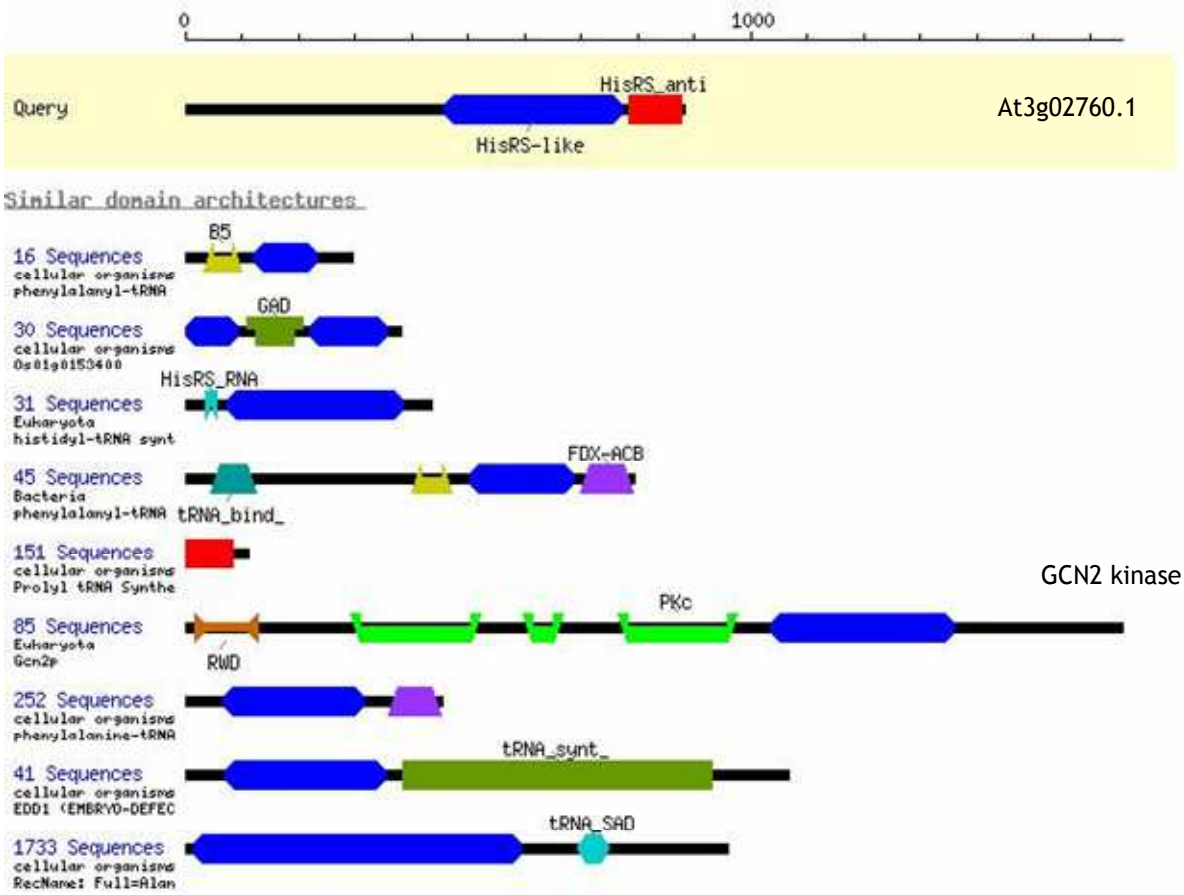

Figure 3.2. ***Arabidopsis*** **At3g02760.1 lacks a protein kinase domain.** Output of the Conserved Domain Architecture Retrieval tool (CDART-NCBI tools) showing the presence of conserved HisRs-like domains (blue) and absence of an RWD (functional domain that interact with GCN1 protein that mediates activation of the GCN2 kinase) and PKc (serine/threonine protein kinase) domains in At3g02760.1; suggesting that it cannot complement AtGCN2 kinase.

The identification of pPKR in barley by Langland *et al.* (1995), utilized monoclonal antibody raised against the conserved double stranded RNA binding domain (dsRBD) of human PKR. Their results suggested that the human PKR and the plant PKR dsRBD are conserved. The human PKR has two N-terminal dsRNA-binding domains generally annotated as dsRBM I and dsRBM II. These motifs are

70 amino acid residues long and are separated by a 20-22 amino acid residue linker(Jammi & Beal, 2001). The two dsRBMs are involved in dsRNA binding and PKR activation (Fig. 3.3). Failure to obtain a potential pPKR homologue using full-length HsPKR triggered further attempts to identify an equivalent of mPKR in *Arabidopsis* using the dsRBM domains. A BLASTP search was conducted on TAIR10 using the sequences of dsRBDs I and dsRNBD II of mPKR, including the linker sequence (Fig. 3.3). The BLASTP search returned only a single gene At1g09700.1. This gene codes for a nuclear dsRNA binding protein (DRB1), involved in mRNA cleavage during gene silencing by miRNA, production of miRNAs involved in gene silencing, production of transacting-small interfering RNA (ta-siRNAs) involved in RNA interference, response to abscisic acid, auxin and cytokinin stimulus (www.arabidopsis.org). Therefore At1g09700.1 contains dsRNA domain that is involved in RNAi-like pathway, as opposed to those present in eIF2α kinases.

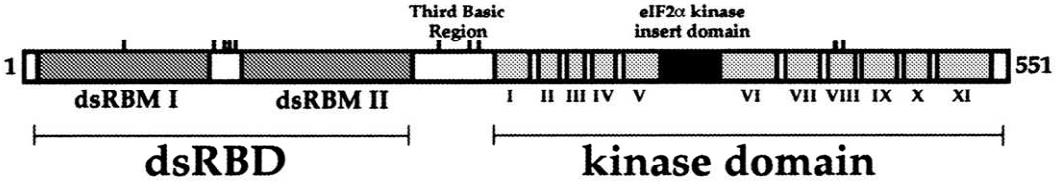

dsRBD I

MAGDLSAGFFMEELNTYRQKQGVVLKYQELPNSGPPHDRRFTFQVIIDGREFPEGEGRSKKEAKNAAAKLAVEILNKEKKAVSPLL

dsRBD II

LTTTNSSEGLSMGNYIGLINRIAQKKRLTVNYEQCASGVHGPEGFHYKCKMGQKEYSIGTGSTKQEAKQLAAKLAYLQILSEETSV
KSDYLSSGSFATTCESQSNSLVTSTLASESSSEGDFSADTSEINSNSDSLNSSSLLMNGLRNNQRKAKRSLAPRFDLPDMKETKYT

Kinase I-XI domains

VDKRFGMDFKEIELIGSGGFGQVFKAKHRIDGKTYVIKRVKYNNEKAEREVKALAKLDHVNIVHYNGCWDGFDYDPETSDDSLESS
DYDPENSKNSSRSKTKCLFIQMEFCDKGTLEQWIEKRRGEKLDKVLALELFEQITKGVDYIHSKKLIHRDLKPSNIFLVDTKQVKI
GDFGLVTSLKNDGKRTRSKGTLRYMSPEQISSQDYGKEVDLYALGLILAELLHVCDTAFETSKFFTDLRDGIISDIFDKKEKTLLQ
KLLSKKPEDRPNTSEILRTLTVWKKSPEKNERHTC

Figure 3.3. The domain make-up of human PKR kinase (Jammi & Beal, 2001). Depiction of double stranded RNA-binding domain (dsRBD) and the kinase domains of human PKR. Modified image adapted from Jammi V.N., Beal P.A. Nucleic Acids Research, 2001, 29, 3020-3029.

3.2.2 Search for Homologues of eIF2α Kinases in Viridiplantae, Rice and Maize Genome Database

Phylogenetic analysis of the protein sequences obtained after BLASTP search was conducted against NCBI Viridiplantae non-redundant protein sequences produced AtGCN2, HsPKR and HsGCN2/ScGCN2/PERK Clusters (Table 3.1). Nearly all protein sequences that were in the AtGCN2 and HsGCN2/ScGCN2/PERK clusters possessed RWD (domain that interacts with GCN1 protein during activation of GCN2 kinase), PKc (protein kinase catalytic domain specific for serine/threonine and tyrosine kinase) and HGTP_anticodon (anticodon binding domain/HisRS-related) functional domains, and Class_II_aaRS (Class II tRNA amino-acyl synthetase catalytic domain) domains, as opposed to those in the HsPKR cluster that had only the PKc domain (Table 3.1). There were 4 *Arabidopsis* genes namely gi|7801691, gi|30694992, gi|297817238 and gi|334186129 that clustered with AtGCN2 and CDART analysis revealed that they have similar functional domains (Table 3.1), further analysis of these *Arabidopsis* protein sequences through alignment using CLC sequence viewer suggest that they are splice variants of the same gene (data not shown). AtGCN2 kinase has a single RWD, PKc and HGTP, and two Class_II_aaRS functional domains as shown in Table 3.1 CDART analysis of the Viridiplantae sequences revealed that gi|356544520 and gi|359478149 proteins of *Glycine max* (soya bean) and *Vitis vinifera* (common grape vine), respectively have exactly similar functional domains as AtGCN2 kinase (Table 3.1). Another *V. vinifera* protein namely gi|297743778 was similar to gi|356544520 but lacked the RWD domain (Table 3.1). On the other hand *Ricinus communis* (Castor oil plant) protein sequence had similar domain as AtGCN2 except for a single Class_II_aaRS domain as opposed to two in AtGCN2 kinase (Table 3.1). CDART analysis of the Viridiplantae sequences that clustered with the eIF2α kinase also revealed that the single celled green algae of Chlorella and Micromonas spps possessed protein sequences with functional domains similar to AtGCN2 as was the case for soya bean, common grape and castor oil plants. However these micro-algae sequences possessed 2 PKc domains as opposed to 1 in the higher plants (Table 3.1).

Table 3.1 Functional domains of Viridiplantae protein sequences (N to C terminal) that clustered with AtGCN2, HsPKR and HsGCN2/ScGCN2/HsPERK kinases after Phylogenetic (UPGMA and NJ) analysis using CLC sequence viewer.

Kinase Cluster	Sequence ID (NCBI)	Domains (N to C terminal)*	Species
AtGCN2	gi|7801691	RWD, PKc, Class_II_aaRS (2#), HGTP	*A. thaliana*
	gi|30694992	RWD, PKc, Class_II_aaRS (2), HGTP	*A. thaliana*
	gi|255585505	RWD, PKc, Class_II_aaRS, HGTP	*R. communis*
	gi|297817238	RWD, PKc, Class_II_aaRS (2), HGTP	*A. lyrata*
	gi|334186129	RWD, PKc, Class_II_aaRS (2), HGTP	*A. thaliana*
	gi|356544520	RWD, PKc, Class_II_aaRS (2), HGTP	*G. max*
	gi|359478149	RWD, PKc, Class_II_aaRS (2), HGTP	*V. vinifera*
	gi|297743778	PKc, Class_II_aaRS (2), HGTP	*V. vinifera*
HsPKR	gi|38345934	PKc	*O. Sativa*
	gi|116309697	PKc	*O. Sativa*
	gi|224104109	PKc	*P. trichocarpa*
	gi|224105789	PKc	*P. trichocarpa*
HsGCN2/ScGCN2/ HsPERK	gi|303276522	RWD,PKc (2), Class-II-aaRS, HGTP	*M. pusilla*
	gi|255077416	RWD,PKc (2), Class_II_aaRS, HGTP	*Micromonas spp*
	gi|307105988	RWD, PKc (2), Class_II_aaRS, HGTP	*C. variabilis*
Reference sequences	HsPKR	DRSM, DRSM, PKc	*H.sapiens*
	AtGCN2	RWD, PKc, Class_II_aaRS (2), HGTP	
	ScGCN2	RWD, PKc(3), Class_II_aaRS (2), HGTP	*S. cerevisiae*

*Functional domains from N to C- terminal as revealed by CDART analysis. RWD domain, interacts with GCN1; PKc, protein kinase catalytic domain specific for serine/threonine and tyrosine kinase; Class_II_aaRS, Class II tRNA amino-acyl synthetase catalytic domain; HGTP, anticodon binding domain. #The value in parenthesis indicate the number of domain present.

Unlike *Arabidopsis* the phylogenetic (UPGMA and NJ) analysis of rice and maize sequences did not produce distinct eIF2α kinase clusters, but all the kinases were in the same cluster (data not shown). For rice and maize, 4 and 3 sequences, respectively clustered with the eIF2α kinases, and these were gi|115459156, gi|115462139, gi|1154559154 and gi|115472015 for rice, and gi|226509340, gi|195652767 and gi|5821717 for maize. CDART analysis of the rice sequences that clustered with the eIF2α kinases revealed that they did not possess a kinase domain except for gi|115472015, whose protein sequence is similar to that of the inositol-requiring enzyme 1 (IRE1) protein that possess the luminal dimerization, type I transmembrane serine/threonine protein kinase (STK), PKc and RNase L (Ribonuclease L) functional domains. For maize, the gi|195652767 and gi|58217172 sequences possessed only a kinase domain whereas gi|226509340 had Class_II_aaRS and the HGTP, but with no kinase domain.

3.3 Isolation of AtGCN2 Null-mutant (*Atgcn2-1*)

3.3.1 PCR Screening of *Atgcn2-1* Mutant

Following the results obtained in section 3.2 which suggested the presence of only one eIF2α kinase in *Arabidopsis* (AtGCN2), as is in the case for yeast, prompted the search for AtGCN2 null-mutant lines available in The European *Arabidopsis* Stock Centre (NASC), Nottingham, UK. The *Arabidopsis* null-mutants lines ordered from NASC were generated through insertional mutation using pAC161 T-DNA vector (Fig. 3.4A). The insertion is located on the second last exon on the 3′ end of AtGCN2 (At3g59410.1) gene, disrupting the codon for amino acid 1175, and hence CT-domain (Fig. 3.4B). The lines in set N482670 were ordered based on the fact that disruption of CT-domain has been shown to impair dimerisation of yeast GCN2 kinase *in vivo* and hence its kinase activity; CT-domain is the most potent dimerization domain of yeast GCN2 kinase and its crucial for its function (Qiu *et al.*, 1998). After screening for seedlings with T-DNA insertions on ½ MS supplemented with 7.5μg/μl of sulfadiazine, genotyping PCR was conducted to differentiate homozygous from heterozygous insertions.

To isolate homozygous *Atgcn2-1* mutants (T_3 plants), two fragments were PCR amplified. The first fragment (~1090bp) was amplified using primer pair hybridizing wild-type *AtGCN2* (Gcn2Fw1) and left border of T-DNA (pAC161V1) insert (Fig. 3.4). This fragment is present in the both homozygous and heterozygous *Atgcn2-1* mutants but not in the wild-type plants (Fig. 3.5). The second fragment (~592bp) was amplified using primer pair (Gcn2Fw1 and Gcn2Rv1) hybridizing wild-type *AtGCN2* sequences flanking the T-DNA insert (Fig. 3.4). This fragment is present in both heterozygous and wild-type plants and but absent in homozygous plants (Fig. 3.5). This is because the T-DNA insert is >2500bp and since the PCR programme used was designed to amplify only the fragment of expected size (~592bp); the T-DNA insert present in homozygous plants increases the size of the expected product thus no amplification will be achieved. A total of 4 homozygous *Atgcn2-1* mutant plants were isolated from the 30 plants rescued from the sulfadiazine screen.

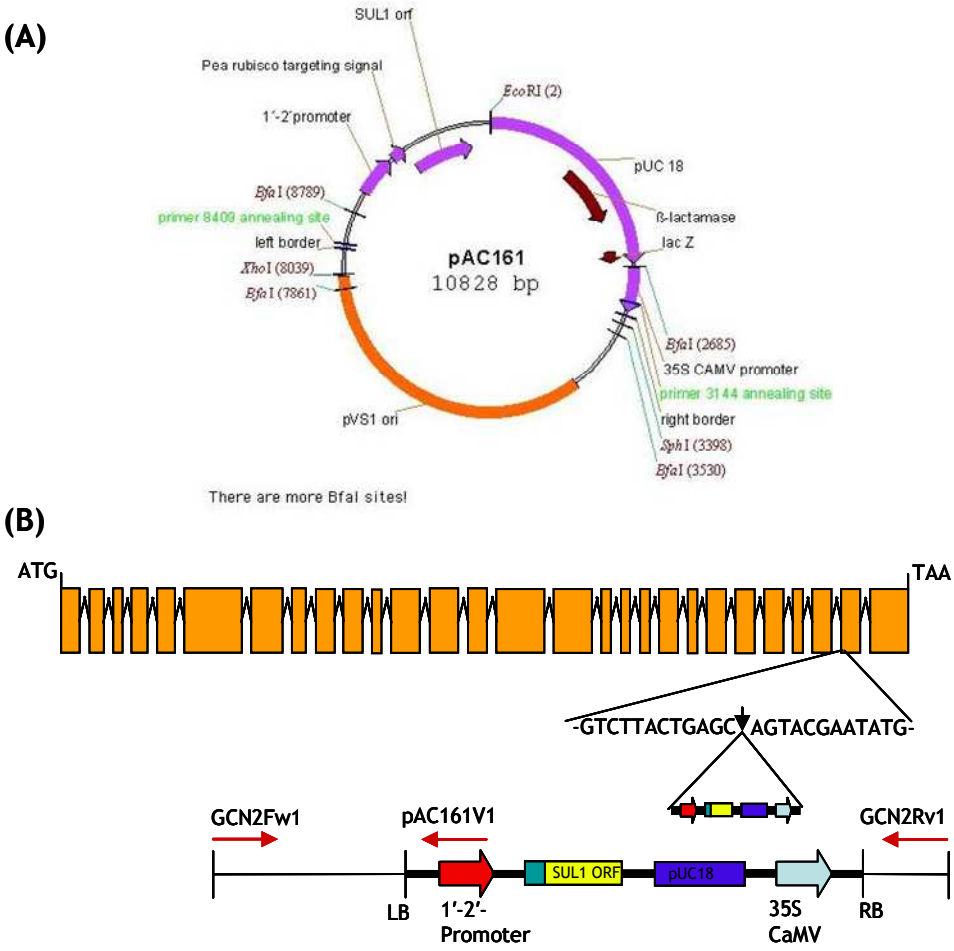

Figure 3.4. Isolation of *Arabidopsis Atgcn2-1* homozygous mutant line. (A) Map of pAC161 T-DNA vector used to generate AtGCN2 loss-of-function mutant seeds of set N482676. **(B)** Schematic representation of the position of T-DNA insert in *Atgcn2-1* mutant and position of genotyping primers. The pAC161 vector construct and T-DNA position were obtained from www.gabi.kat.de.

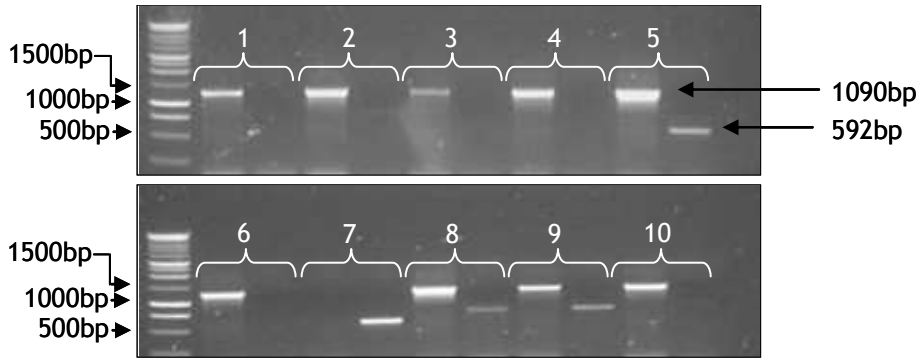

Figure 3.5. Genotyping of *Atgcn2-1* mutant lines using PCR. Isolation of homozygous *Atgcn2-1* mutant plants (T_3) previously screened on ½ MS containing 7.5µg/µl sulfadiazine. Lanes 1, 2, 3, 4 and 6 show homozygous *Atgcn2-1* mutants, lanes 2, 5, 8, 9 and 10 indicate heterozygous *Atgcn2-1* mutants and lane 7 is control WT Col-0.

3.3.2 Phenotype of *Atgcn2-1* Mutant under Optimal Conditions

To determine the form of *AtGCN2* transcripts synthesized by homozygous *Atgcn2-1* plants, Semi-Quantitative PCR (SQRT-PCR) was conducted. The SQRT-PCR experiment was conducted using cDNA synthesized as described earlier (section 2.2.4). The SQRT-PCR results obtained revealed that *Atgcn2-1* plants were synthesizing a truncated *AtGCN2* transcript when compared with WT Col-0 plants (Fig. 3.6A). The homozygous *Atgcn2-1* and WT Col-0 plants were grown on compost soil to investigate whether disruption of AtGCN2 kinase CT-domain produced a phenotype under optimum growth conditions. However there was no strong *Atgcn2-1* phenotype observed compared with WT Col-0 plants grown on compost soil under short-day conditions. A similar trend was observed on seedlings grown on ½ MS media (Fig. 3.6A&C).

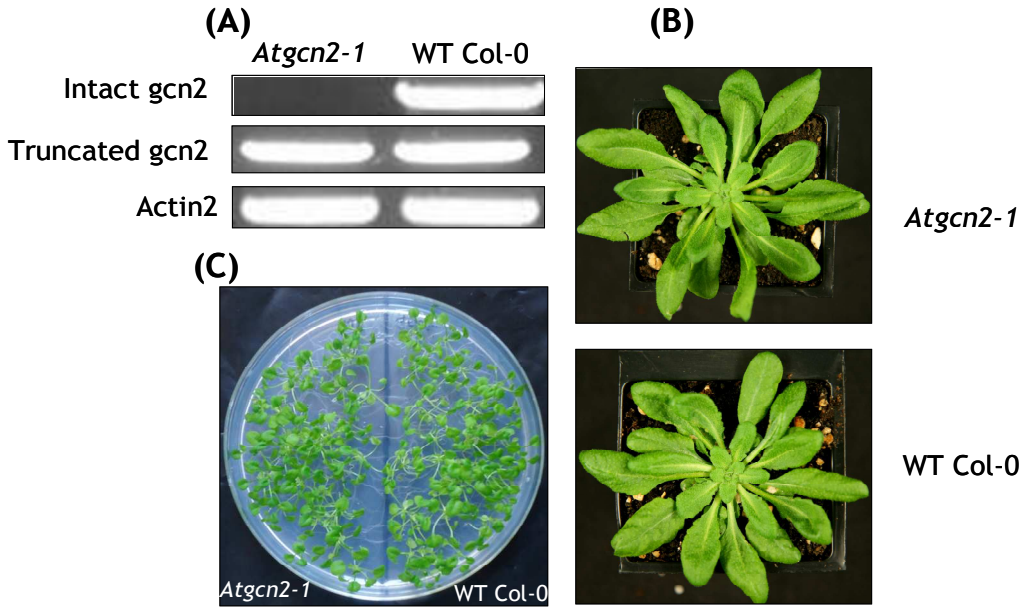

Figure 3.6. Confirmation of *Atgcn2*-1 mutant using Semi-quantitative PCR. **(A)** Semi-quantitative PCR using cDNA generated from total RNA isolated from homozygous *Atgcn2-1* and WT Col-0 plants. Intact gcn2 refers to PCR products using a primer pair that amplify full-length *AtGCN2* transcript (ATG to TAA), whereas truncated gcn2, refers to a primer pair amplifying truncated *AtGCN2* fragment from ATG up 1200bp excluding T-DNA insertion region. Presence of the two fragments (WT Col-0), suggests intact CT-domain as opposed to truncated (*Atgcn2-1*). Actin2 refers to loading control using Actin2 gene primers. **(B&C)** Phenotype of 6 and 3-week old *Atgcn2-1* and WT Col-0 plants grown on soil and ½ MS media, respectively.

3.4 Assessment of Truncated Kinase in *Atgcn2-1* Seedlings

Lack of a strong *Atgcn2-1* mutant phenotype under optimal growth condition prompted investigation on the activity of the truncated AtGCN2 kinase synthesized by the *Atgcn2-1* null-mutants. To study the activity of the truncated AtGCN2 kinase, the null mutants were subjected to different stress conditions. These include treatment with 150 µM glyphosate herbicide to induce amino acid starvation, extreme temperature acclimation (heat and cold) and prolonged exposure to NaCl stress. In these experiments the activity of AtGCN2 kinase was

determined by assessing the phosphorylation state of AteIF2α using western blot analysis. The substrate for activated AtGCN2 kinase is AteIF2α serine 56, therefore assessing the state of eIF2α provided an insight into the activities of AtGCN2 kinase *in planta*. Although the antibodies used in this study to determine the state of AteIF2a were raised against serine 51 of mammalian eIF2α, preliminary experiments conducted revealed that it is capable of hybridizing with *Arabidopsis* eIF2α serine 56; *Arabidopsis* and mammalian eIF2α have a conserved SELS domain, which contain the target serine at position 56 and 51 for *Arabidopsis* and mammalian, respectively (Fig. 3.7).

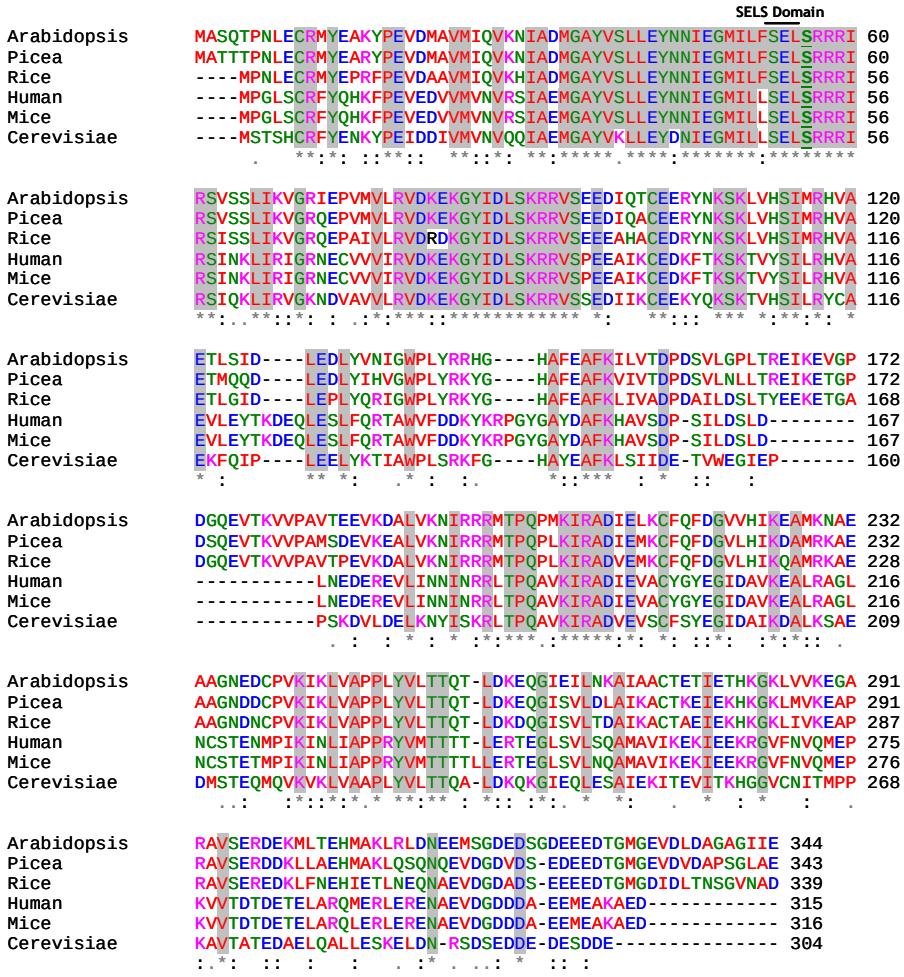

Figure 3.7. ClustalW2 alignment of plant, mammalian and yeast eIF2α subunit. Phosphorylation sites are serine 51(S51) for rice, human, mice and yeast, and S56 for *Arabidopsis* and Picea, however all sites are located on a conserved SELS domain. Regions highlighted in 25% grey indicate highly conserved amino acid residues.

3.4.1 Response of *Atgcn2-1* to N-Deficiency Stress

In the preliminary *in planta* phosphorylation of AteIF2α experiment, western blot analysis revealed that phosphorylation of eIF2α was detectable 4 h after glyphosate treatment and peaked after 24 h. Thereafter lower signals were obtained up to 72 h after treatment (Fig. 3.8A). The results also show that optimal activation and phosphorylation of AteIF2α was achieved at 24 h after treatment with 150 µM glyphosate (Fig. 3.8A). After the preliminary experiment, a second amino acid starvation experiment was conducted using 14 days old seedlings to investigate the effect of truncated CT-domain on *in planta* activation of AtGCN2 kinase. Only AteIF2α in the WT Col-0 seedlings was phosphorylated at 24 h after treatment with 150 µM glyphosate (Fig. 3.8B).

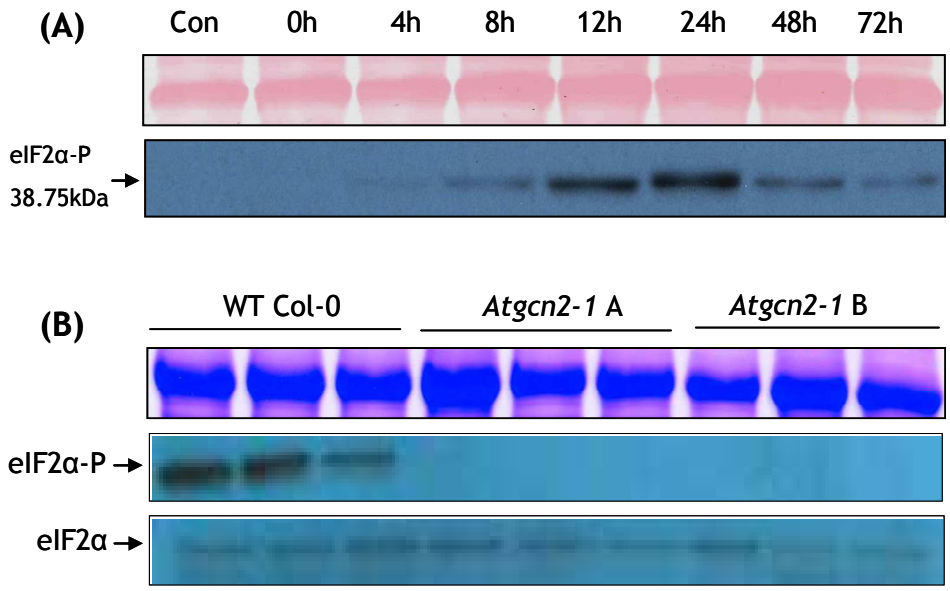

Figure 3.8. Disruption of CT-domain impairs activation AtGCN2 kinase *in vivo*. **(A)** Effect of exposure time on activation of AtGCN2 kinase after treatment of WT Col-0 plants with 150 µM glyphosate. **(B)** Treatment of 14 days old seedlings for 24 h with 150 µM glyphosate failed to activate AtGCN2 kinase in *Atgcn2-1* independent mutant lines A and B. Each lane is an independent mutant line. Top panels, nitrocellulose membrane and SDS-PAGE gel stained with Ponceau and Coomassie® Brilliant Blue stain, respectively indicating equal loading. Lower panels, western blot probed with eIF2α-P and eIF2α antibodies.

3.4.2 *In planta* Translation Regulation in *Arabidopsis* Seedlings

The effects of AtGCN2 activation on *de novo* protein synthesis was investigated using a *p35S:LUC* (luciferase) reporter line in a WT (Col-0) background. Under normal conditions this line should synthesize the luciferase protein and emit luminescence when treated with the substrate luciferin. Four hours after treatment with glyphosate AtGCN2 is activated and has phosphorylated its target AteIF2α (section 3.4.2) and this should lead to a suppression of translation. Figure 3.9 shows a time course experiment for luminescence from *p35S:LUC* seedlings with up to 48 hours prior treatment with glyphosate. The results show a characteristic decline in luminescence reaching a pseudo-steady state level after approximately 12 hours reflecting steady-state *de novo* protein synthesis. Treatment with glyphosate 24 and 48 hours prior to the start of the experiment does appear to suppress protein synthesis and this is consistent with a role for AteIF2α phosphorylation in controlling protein synthesis. An alternative explanation, however, is that glyphosate treatment reduced the endogenous pools of amino acids and this suppressed protein synthesis. A better approach would have been to compare the luminescence signals after glyphosate treatment from lines expressing p35S:LUC in a WT and At*gcn2-1* background. This would have separated the effects of amino acid depletion and phosphoAteIF2α–mediated suppression on translation. A *p35S:LUC* x *Atgcn2-1* line was generated in this study but there was insufficient time to assess its phenotype.

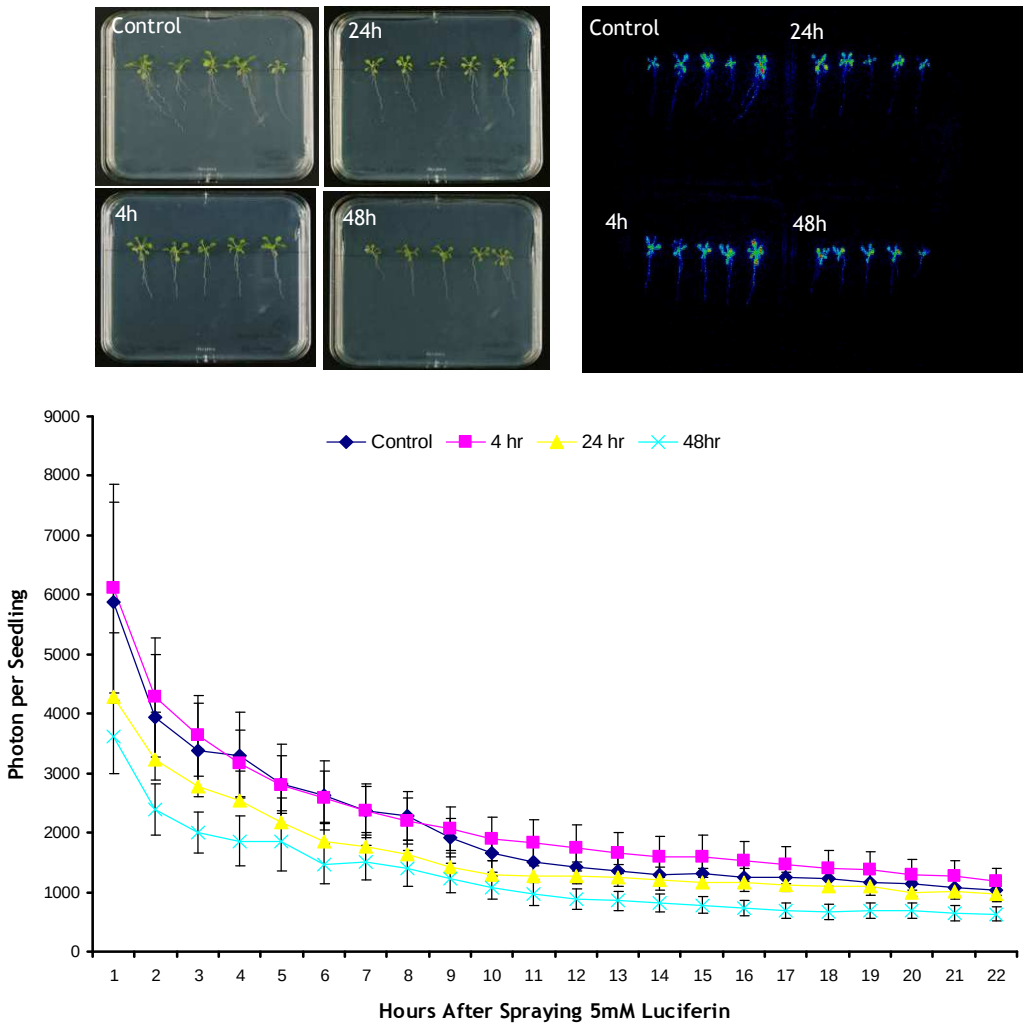

Figure 3.9. The effect of *in planta* phosphorylation of AteIF2α on the synthesis of luciferase protein. Fourteen days old 35S-Luc *Arabidopsis* seedling grown on ½ MS were treated with 150 µM glyphosate to induce phosphorylation of eIF2α at 48, 24, and 4 h prior to spraying luciferin. Control seedlings were not treated with glyphosate. Values are means of photon counts for 5 seedlings per plate and bars on the graphs are S.E.M.

3.4.3 Effect of NaCl and Temperature Acclimation on AtGCN2

Western blot analysis of the 14 days old *Arabidopsis* seedlings grown on ½ MS supplemented with 50 and 100 mM revealed that only samples from WT Col-0 seedlings produced a signal when probed with eIF2α-P antibody. For the control treatments (0 mM NaCl) there were no signal obtained in either of the two genotypes. However when were probed with eIF2α antibody signals were obtained for samples from both *Atgcn2-1* and WT Col-0 seedlings in all the NaCl treatments (Fig. 3.10 A&B). The strength of eIF2α-P signal in the WT Col-0 seedling seems to increase with the concentration of NaCl, 100 mM producing the strongest signal (Fig. 3.10 A&B).

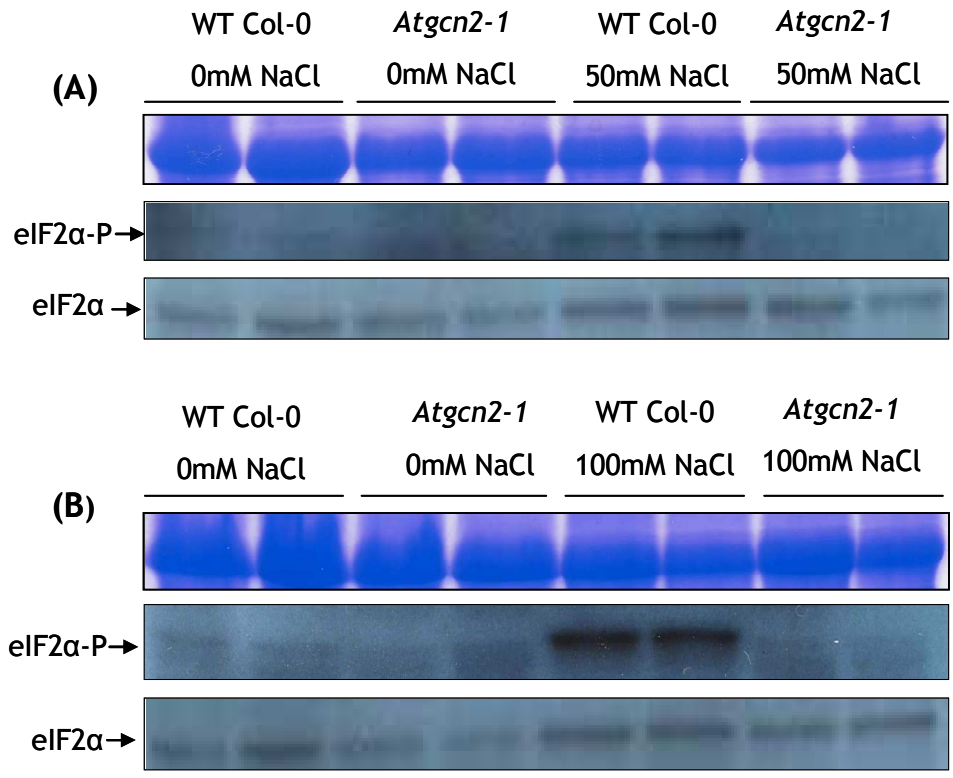

Figure 3.10. NaCl stress induces *in vivo* activation of AtGCN2 kinase. (A) and **(B)** *Atgcn2-1* and WT Col-0 seedlings were germinated and grown on ½ MS media supplemented with 0, 50 and 100 mM NaCl and phosphorylation of AteIF2α after 14-days of growth was assessed. Top panels, SDS gel stained with Coomassie Brilliant® Blue stained bands of large subunit RuBisCO indicating similar loading and lower panels, nitrocellulose membranes hybridized to eIF2α-P and eIF2α antibodies. Each lane is a biological replicate.

For temperature acclimation experiments there were no eIF2α-P signal obtained with *Atgcn2-1* and WT Col-0 seedlings harvested immediately (0 h) after heat (37°C) and cold (4°C) acclimation. However eIF2α-P signals were obtained only with protein samples prepared from WT Col-0 seedlings harvested at 2 and 4 h after heat and cold acclimation, with a higher signal achieved on seedlings assessed at 4 h after acclimation. On the other hand, similar to the NaCl experiments the eIF2α signal was observed in samples from all temperature treatments and genotypes (Fig. 3.11 A&B).

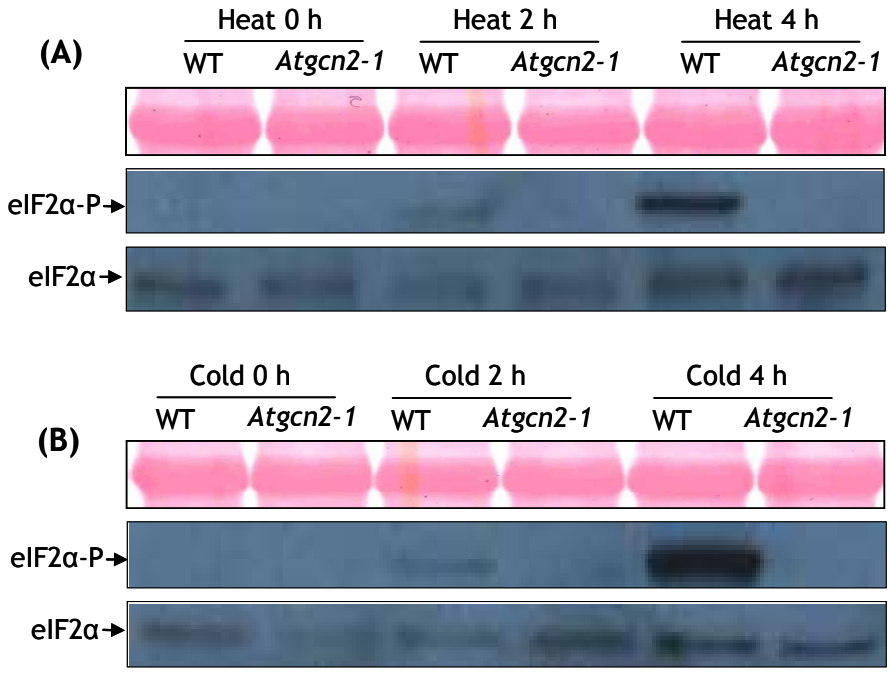

Figure 3.11. Cold (4°C) and heat (37°C) acclimation induces phosphorylation of *Arabidopsis* eIF2α. Assessment of extreme temperature acclimation on the phosphorylation state of AteIF2α 0-4 h after treatment; **(A)** heat acclimation, and **(B)** cold acclimation. Top panels; ponceau stained nitrocellulose membranes showing bands of large subunit RuBisCO indicating similar loadings. Lower panels; membranes probed with eIF2α-P and eIF2α antibodies, respectively.

3.5 Response of *Atgcn2-1* to NaCl Stress

3.5.1 Effect of NaCl on Germination of *Atgcn2-1* Seeds

The germination rates of *Atgcn2-1* and WT Col-0 seeds generally decreased with an increase in NaCl concentration. This was expected as increase in the concentration of NaCl may be directly proportional to the level of salinity stress experienced by the germinating seeds (Fig. 3.12). Relatively higher rates of germination were achieved on *Atgcn2-1* seeds compared with WT Col-0 seeds on all the NaCl concentrations tested at 3, 4 and 5 days after transfer to salt. At 3 days after transfer, clear differences in the rate of germination between *Atgcn2-1* and Wt Col-0 were observed on 50 and 100 mM NaCl treatments. Though higher germination rates were obtained on 0 and 50 mM NaCl and no germination was obtained on 150 mM NaCl (Fig. 3.12). Increasing the assessment time to 4 and 5 days resulted in an increase in the germination rates irrespective of the genotype, however ANOVA tests showed significant ($p<0.05$) differences between the *Atgcn2-1* and Wt Col-0 was obtained on 150 mM NaCl (Fig. 3.12). After 4 and 5 days treatment with 0 and 50 mM NaCl, *Atgcn2-1* seeds generally had longer radicals with visible root hairs. In contrast, irrespective of the genotype, seeds germinated on 100 and 150 mM NaCl had extremely short radicals protruding from the seed coat. The effect of delayed germination was observed on all NaCl treatments, however, it was significant ($p<0.05$) only on seeds germinated on 100 and 150 mM NaCl media (Fig. 3.12). These results clearly demonstrated that there was delay in germination as a result of NaCl treatment in both *Atgcn2-1* and Wt Col-0 seeds. However, compared with WT Col-0, there was less suppression in the *Atgcn2-1* seeds. To compare the effects of NaCl on seed germination at each period, data collected were subjected to analysis of variance (ANOVA) using GenStat Discovery Edition 3. Seed genotype, NaCl treatment and interaction (genotype×NaCl) significantly ($p<0.05$) influenced the germination rates assessed at 3 days after incubation. The means were further compared using least significant difference value (LSD) and significant ($p<0.05$) differences in germination rates between WT Col-0 and *Atgcn2-1* were obtained at 50 and 100 mM NaCl treatments at 3 days after incubation. However at 4 and 5 days after incubation, only seeds spread on 150 mM NaCl were significantly ($p<0.05$) different.

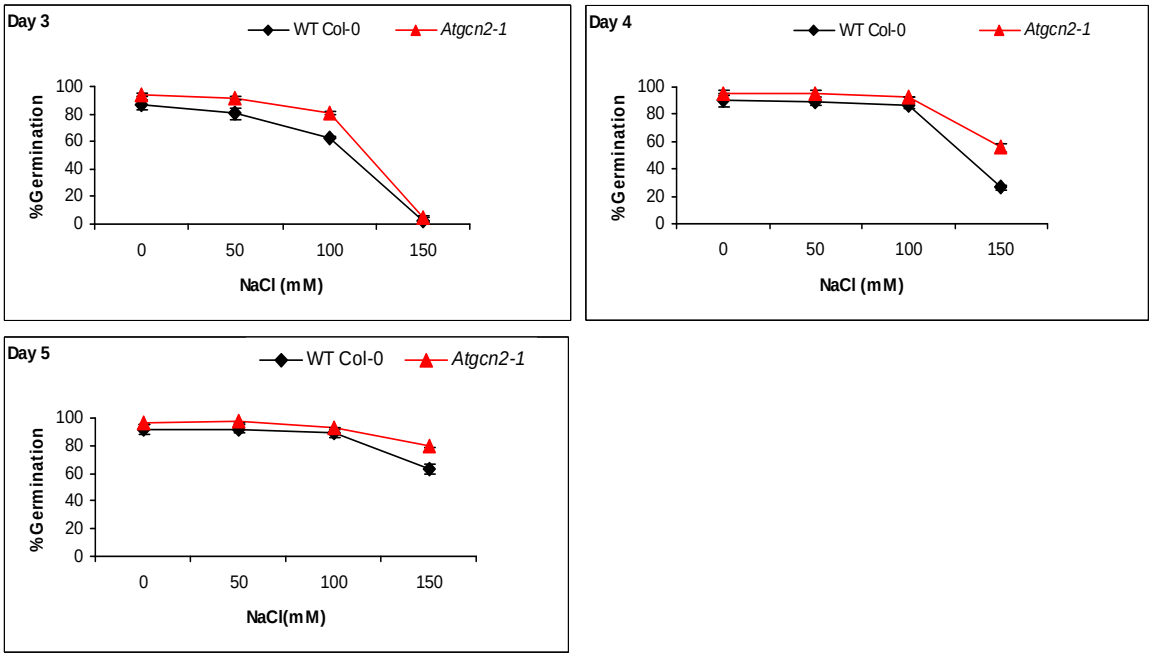

Figure 3.12. The effect of NaCl concentration on germination of WT Col-0 and *Atgcn2-1* seeds. *Arabidopsis* seeds were germinated and allowed to grow on ½ MS media supplemented with 0-150 mM NaCl and the rate of germination assessed at 3-, 4- and 5-days after incubation. Values are means of 3 replicate experiments and bars on the graphs represent S.E.M.

3.5.2 Effect of NaCl on Growth of *Atgcn2-1* Seedlings

Since no strong phenotypic differences between *Atgcn2-1* and WT Col-0 seedlings were observed on ½ MS media supplemented with NaCl, a further experiment was conducted using 15 cm square plates. This experiment was designed to investigate the effects of NaCl on general growth of *Arabidopsis*. The WT Col-0, *Atgcn2-1* and heterozygous *Atgcn2-1* seeds were germinated on NaCl-free MS media for 6 days and then transplanted on to 15 cm plates containing MS media supplemented with NaCl (0-200 mM). The effects of NaCl on growth of the seedlings were assessed at 20 days after transplanting. There were no strong phenotypic differences between the three genotypes in terms of shoot growth in all NaCl concentrations (Fig. 3.13A). Unlike shoot growth, *Atgcn2-1* had significantly ($p<0.05$) shorter primary roots compared with WT Col-0 and heterozygous *Atgcn2-1* seedlings on all NaCl treatments (Fig. 3.13 A&B).

Furthermore, irrespective of the genotype, 200 mM NaCl significantly suppressed growth of seedlings (Fig. 3.13A). The ANOVA results confirmed that primary root growth was significantly ($p<0.05$) influenced by NaCl concentration and seedling genotype. There was no significant interaction ($p>0.05$) between genotype and NaCl concentration on root growth, although increasing the concentration of NaCl did reduced root growth (Fig. 3.13B).

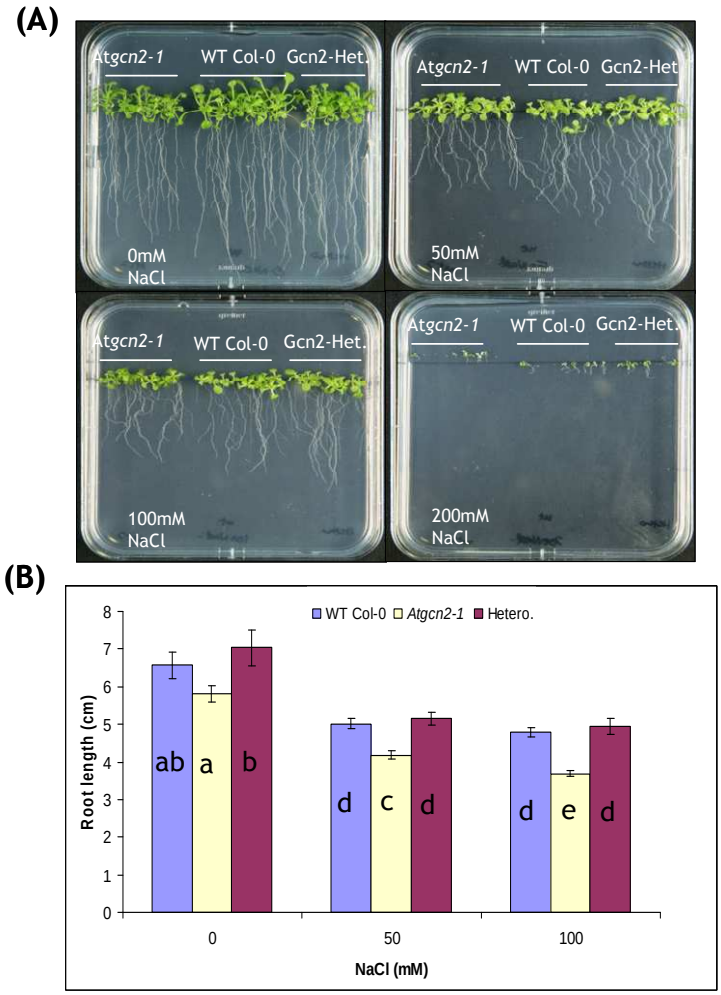

Figure 3.13. Phenotypic characterization of WT Col-0 and *Atgcn2-1* seedlings on ½ MS media supplemented with 0-200 mM NaCl. Effects of NaCl concentration on growth of *Arabidopsis* WT, and heterozygous and homozygous lines of the *Atgcn2-1* null mutant. Values on the graph are means of 3 replicate experiments and bars represent S.E.M of means. Graphs with different letters are significantly different ($p<0.05$) based on LSD tests.

3.6 Response of *Atgcn2-1* to Biotic Stress

3.6.1 Effect of CaMV and *P. Syringae* Inoculation on Activation of AtGCN2 Kinase

To investigate the role of JA and SA in activation of AtGCN2 kinase, a JA-insensitive mutant line (*jar1-1*), a mutant with defective SA signalling pathway (*NahG*), *Atgcn2-1* and WT Col-0 seedlings were inoculated with CaMV and an avirulent strain of *Pseudomonas syringae* pv. *tomato* DC3000 (*Pst* DC3000), a phytopathogenic bacterium. The positive controls consisted of plants treated with 150 μM glyphosate, 24h prior to assessment of the phosphorylation state of AteIF2α. All *Arabidopsis* seedlings (*jar1-1*, *NahG*, *Atgcn2-1* and WT Col-0) inoculated with CaMV showed symptoms of disease at 7 days post inoculation. Disease severity progressed with time and at 21 days, some leaf senescence was observed in all seedlings (Fig. 3.14A). There were no apparent differences observed between the four genotypes, in terms of the rate of disease progression and severity at each assessment time (7, 14 and 21 days post inoculation). This observation implied that knocking-out AtGCN2 kinase did not increase susceptibility of *Arabidopsis* to CaMV compared with WT Col-0 and other mutants. Furthermore analysis by western blotting on the state of AteIF2α revealed that challenging the four *Arabidopsis* genotypes with CaMV did not activate AtGCN2 kinase as opposed to 150 μM glyphosate control treatment (Fig. 3.14B). Similar results were obtained on seedlings inoculated by spraying *Pst* DC3000 when analysis of AteIF2α phosphorylation was undertaken at two days after inoculation (data not presented).

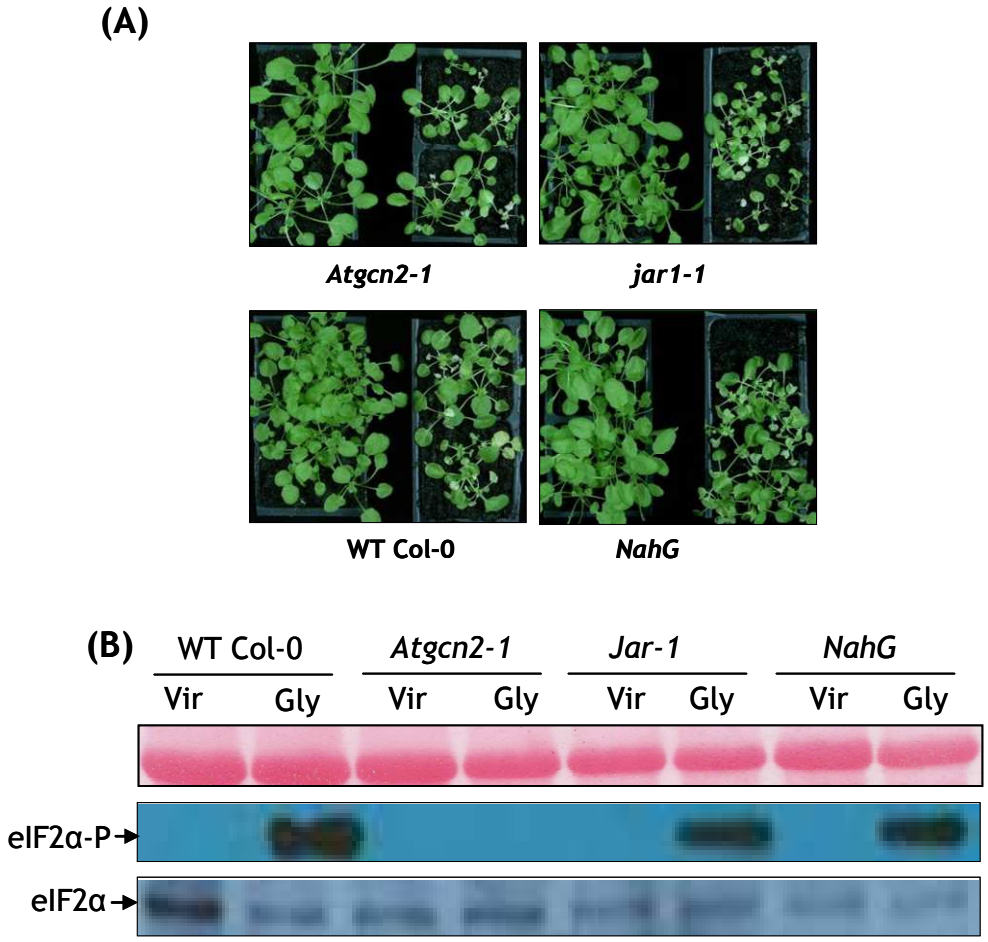

Figure 3.14. Activation of AtGCN2 kinase is independent of salicylic and jasmonate pathways. **(A)** *Arabidopsis* mutant lines *Atgcn2-1*, *jar1-1*, WT Col-0 and *NahG* with non-infected (left) and infected (right) at 21 days after inoculation with CaMV, **(B)** Immunoblot analysis of *Atgcn2-1*, *jar1-1*, *NahG* and WT Col-0 plants at 21-days after inoculation with CaMv (vir) and 150 µM glyphosate (Gly) positive control. Top panel, Ponceau stained nitrocellose membrane showing equal loading and below blots were probed with eIF2α-P and eIF2α antibodies.

3.6.2 Growth of *Pst* DC3000 in *Atgcn2*-1 Leaves

Failure of *Pst* DC3000 to induce phosphorylation AteIF2α prompted further investigation on the effects of knocking-out AtGCN2 kinase on the intercellular multiplication of the phytopathogenic bacteria. *P. syringae* DC3000 strain was originally identified as a tomato pathogen and was also found to cause disease in *Arabidopsis* (Dong *et al.*, 1991; Crute *et al.*, 1994). The bacteria usually enter

plant leaves through stomata or wound and then multiply in the intercellular spaces (Beattie & Lindow, 1995). However during infection of the *Arabidopsis* plants in this study, the inoculation of *Pst* DC3000 was conducted by infiltrating the bacteria into the intercellular spaces using a syringe. This is for the purposes of circumventing the initial stages of plant defence against *Pst* DC3000 (Zipfel *et al.*, 2004). To study the effect of knocking-out AtGCN2 kinase on bacterial growth, the leaves of *Atgcn2-1* plants were infiltrated with *Pst* DC3000. The leaves of *Jar1-1, NahG*, and WT Col-0 plants were also infiltrated in order to compare bacterial growth in *Atgcn2-1* mutant and in these genotypes. After infiltration *Pst* DC3000 growth in infiltrated leaves was assessed at 1 and 3 days after inoculation. During the two assessment periods the highest numbers of colony forming units (c.f.u) were obtained on leaves of *NahG* plants, although notably higher counts were obtained at 3 days after inoculation. A nearly similar trend was observed on the number of c.f.u obtained on WT Col-0 leaves (Fig. 3.15). Compared to *NahG* and WT Col-0, relatively lower counts of c.f.u were obtained on *Atgcn2-1* leaves, whereas *jar1-1* leaves recorded the least number of c.f.u (Fig. 3.15). The number of c.f.u obtained at 3 days post inoculation was subjected to one-way ANOVA and results obtained show that the number of c.f.u obtained was significantly ($p<0.05$) influenced by *Arabidopsis* genotype. Further discrimination using LSD value suggests that all the means were significantly different. However based on the accepted threshold, where c.f.u should be at least 5 folds higher, revealed that only *NahG* plants had significantly higher c.f.u.

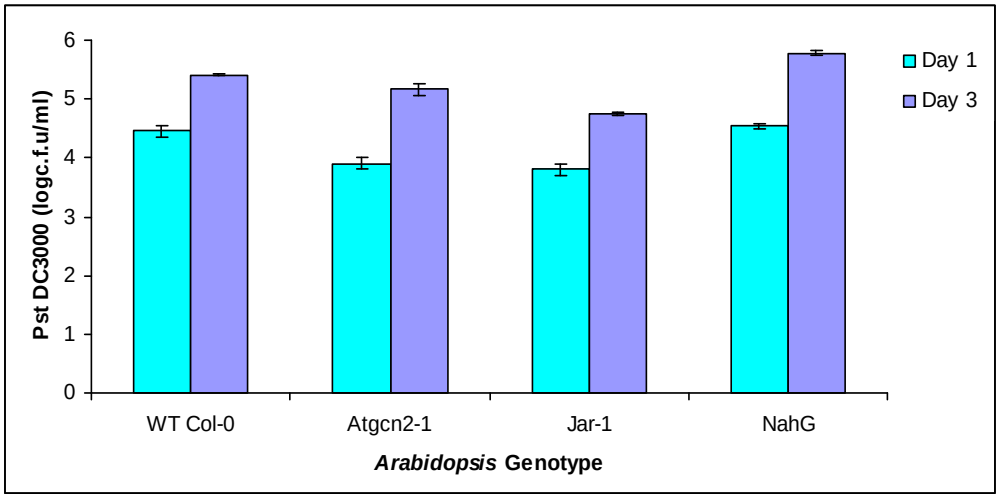

Figure 3.15. Disrupting AtGCN2 CT-domain does not increase *Arabidopsis* susceptibility to *P. syringae* DC3000. WT Col-0, *Atgcn2-1*, *jar1-1* and *NahG* *Arabidopsis* mutants were sown on sterile composed soil grown under photoperiod of 8/16hrs light/dark and 20^{o}C for 21 days. The abaxial side of leaves were then infiltrated with 6µl of 1/500 diluted culture with an OD_{600} 0.2 using a 1ml syringe. The experiment consisted of 5 replicates and bars on the graphs indicated S.E.M.

3.7 Discussion

3.7.1 Plants Lack Mammalian PKR and PERK Homologues

Mammals possess several eIF2α-kinases namely, GCN2, PKR, PEK/PERK and HRI. These kinases are differently activated and therefore they have unique regulatory regions that respond to different stress stimuli. Although activated differently, there is evidence that more than one kinase can be activated simultaneously and hence a stress-response is mediated in an additive or concerted manner (Carnevalli *et al.*, 2006). Unlike mammalian systems, yeast has only one eIF2α kinase, namely GCN2 (Wek *et al.*, 1990; Ramirez *et al.*, 1991; Hinnebusch, 1997). The limited available literature on eIF2α phosphorylation in plants suggests that there may be more than one eIF2α-kinase, namely plant PKR (pPKR) and GCN2 (Langland *et al.*, 1995). It is further reported that pPKR is activated by virus and viroid infections and auto-phosphorylated *in vitro* by dsRNA, selected poly-anions, or by base-paired single stranded RNAs of sufficient

length (Langland *et al.*, 1996; Chang *et al.*, 1999). The results of *in silico* searches for plants homologues of ScGCN2, HsGCN2, HsPERK and HsPKR eIF2α kinases reported in section 3.2, provided evidence for the presence of only one AtGCN2 kinase in *Arabidopsis,* as is the case for yeast. Although the At3g02760.1 sequence clustered with the eIF2α kinases (Fig. 3.1), further analysis (Fig. 3.2) clearly indicated that it lacks a kinase domain confirming that it cannot phosphorylate AteIF2α and hence cannot complement the AtGCN2 kinase. Similarly the gene (At1g09700.1) identified after BLASTP searches using the HsPKR dsRBD as a query sequence does not contain a dsRNA domain that is involved in an RNAi-like pathway, and this suggests that *Arabidopsis* also lacks a HsPKR homologue.

The function of uncharacterized proteins can be inferred from homology using algorithms that rely on known functional domains (Geer *et al.*, 2002). Protein sequences containing similar functional domains to GCN2 kinases were found in soya bean, common grape, castor oil plant, and in the photosynthetic micro-algae of *Micromonas* and *Chlorella* species (Table 3.1). Although no putative plant homologue of HsPERK was identified in the *in silico* search one rice protein sequence (gi|115472015) has functional domains similar to those of the IRE1 protein. The IRE1 protein is essential in the endoplasmic reticulum (ER) unfolded protein response (UPR) in mammalian, yeast, and metazoans systems (Cox & Walter, 1996; Ron & Walter, 2007). In the mammalian system apart from the IRE1 pathway there are two other mechanisms that facilitate the UPR namely PERK and the ATF6 pathways (Ron & Walter, 2007). PERK mediates the UPR by repression of protein synthesis through phosphorylation of eIF2α (Ron & Harding, 2000). Unlike PERK, the IRE1 pathway has been identified in *Arabidopsis* where two homologues of IRE1 namely IRE1A (At2g175200) and ARE1B (At5g24360) have been implicated, although IRE1B is said to be the functional homologue of IRE1 in plants (Chen & Brandizzi, 2012). A PERK homologue has not been identified in plants and since both PERK and IRE1 are involved in UPR, it would be interesting to investigate if IRE1 is indeed the homologue of PERK in plants.

3.7.2 *Atgcn2-1* Mutant Lacks a Strong Growth Phenotype

Characterization of the *Atgcn2-1* mutant seedlings revealed that null mutation of AtGCN2 kinase does not produce a strong phenotype on media supplement with or without NaCl, although they had relatively shorter roots compared with WT Col-0 and heterozygous null mutant seedlings. Similarly no phenotype was observed under optimal conditions for soil-grown *Atcgn2-1* mutant plants (Fig. 3.6). The apparent lack of a strong *gcn2-1* mutant phenotype has also been reported in mice and nematodes (*Caenohabditis elegans*), even when the GCN2 kinase null mutants ($GCN2^{-/-}$) were given a diet that was deficient in essential amino acids (Zhang *et al.*, 2002b; Ron & Harding, 2007). Although not a strong phenotype, there are reports indicating that $GCN2^{-/-}$ mice are unable to conserve muscle mass (Anthony *et al.*, 2004). Lack of a strong *Atgcn2-1* phenotype, as reported in this thesis and reports on $GCN2^{-/-}$ mice, suggests that translational control mediated by GCN2 kinase may be partially redundant in plant and mammalian systems. Functional redundancy of the GCN2 kinase may arise in mammalian systems, since other eIF2α kinases (PKR, PERK and HRI) which are activated differently from GCN2 are present which could complement (Koumenis *et al.*, 2002; Jiang & Wek, 2005; Carnevalli *et al.*, 2006). This is further supported by reports indicating that in contrast to GCN2 knockouts deletions of PKR, PERK and HRI in mice produced strong phenotypes (Chen, 2000; Zhang *et al.*, 2002a; Ron & Harding, 2007). Similar to *Arabidopsis*, yeast has only one eIF2α kinase but unlike mice and nematodes null mutation of ScGCN2 kinase produces a strong phenotype (Goossens *et al.*, 2001; Zhan *et al.*, 2004). Although speculative, lack of a strong *Atgcn2-1* mutant phenotype raises the possibility of the presence of a not-yet-identified mechanism that acts redundantly with the AtGCN2 kinase.

On the other hand it may be argued that lack of a strong phenotype observed with *Atgcn2-1* as describe herein is due to the compensatory effects of a truncated AtGCN2 kinase since only the CT-domain that interacts with uncharged tRNAs was disrupted (see Fig. 3.4). This suggestion may not be true since in previous studies on the *Arabidopsis* GCN2 kinase conducted using a different null-mutant generated by insertion of a transposable element in the first 5′

intron also failed to produce a strong phenotype (Lageix *et al.*, 2008; Zhang *et al.*, 2008).

3.7.3 Disruption of CT-Domain Impairs AtGCN2 Kinase *In planta*

The AtGCN2 kinase has been reported to be activated by cold stress, amino acid starvation, UV, wounding JA and SA (Lageix *et al.*, 2008; Zhang *et al.*, 2008). In this study NaCl and heat stress were also shown to be effective (see Fig. 3.11). The inability to activate the AtGCN2 kinase *in planta*, after exposure of *Atgcn2-1* seedlings to N-starvation, salinity and temperature stress (4^{o}C cold and 37^{o}C heat acclimation), demonstrated that the CT-domain is critical for its activation *in planta*. Failure of the CT-truncated AtGCN2 kinase to induce phosphorylation of AteIF2α is reported for the first time in this thesis. However these results are consistent with *in vitro* studies conducted using ScGCN2 kinase, where the CT-domain (~160 residues) was demonstrated to be required for tRNA binding and hence activation of the kinase (Wek *et al.*, 1995; Zhu *et al.*, 1996). Furthermore the HisRs-like and CT-domains physically interact with the kinase domain thereby causing conformational changes that autoactivate the GCN2 kinase (Hinnebusch, 2005). Therefore mutation or deletion of the CT-domain disrupts dimerization of the full-length ScGCN2 kinase *in vivo*; CT-domain is the most potent dimerization domain and thus crucial for kinase function (Zhu *et al.*, 1996; Qiu *et al.*, 1998). The *Atgcn2-1* mutant used in the experiments reported herein, has a T-DNA insert located near the end of the HisRs domain, completely disrupting the CT-domain and hence *in planta* activation of AtGCN2 kinase. In that regard the inability of truncated AtGCN2 kinase to phosphorylate AteIF2α also confirmed that the isolated *Atgcn2-1* mutant line reported in this thesis was indeed a true functional null-mutant.

3.7.4 NaCl, Heat and Cold Acclimation Activate AtGCN2 Kinase

The detrimental effects of NaCl stress on plants shoot growth is usually reported to arise from osmotic stress and/or Na^{+} toxicity. Therefore for plants to tolerate high levels of NaCl, they have to be able to utilize ions for osmotic adjustments and keep Na^{+} ions away from metabolic sites (Munns, 2002). Exposure of *Arabidopsis* seedlings to NaCl has been reported not to induce the activation of

AtGCN2 kinase (Lageix *et al.*, 2008), this contradicts results reported in this thesis where prolonged exposure of WT (but not *Atgcn2*-1) seedlings to 50 and 100 mM NaCl induced the phosphorylation of eIF2α (Fig. 3.10). The contradictory results may have been due to experimental procedures, since in their experiments, Lageix *et al*. 2008 exposed *Arabidopsis* seedlings to 250 mM NaCl stress for 4 h; this may have been a short time-period enough to cause accumulation Na^+ or Cl^-, thereby testing only the aspect of osmotic stress elicited by NaCl. Although using 'Electronic Fluorescent Pictographs' (*Arabidopsis* eFP) browser (Winter *et al.*, 2007), with *Arabidopsis* α-tubulin (At1g04820) as the secondary gene revealed that expression of AtGCN2 started at 3 h after exposure to 150 mM NaCl, and mainly in the roots. In the study reported herein, however, germination and growth of seedlings was conducted on media supplemented with NaCl for 14 days to allow accumulation Na^+/Cl^+ ions and hence assess their effects on activation of AtGCN2 kinase. Therefore results obtained clearly demonstrate that AtGCN2 kinase is indeed activated by prolonged exposure to NaCl stress and Na^+/Cl^- toxicity may be responsible for its activation rather than NaCl-induced osmotic stress.

Apart from salinity, extreme temperature is recognised as an important limiting factor on plant growth and development and its effects are usually exacerbated by prolonged exposure. Furthermore just like salinity stress, response to extreme temperature can be rapid or extended over a period of time, mainly days or weeks (Penfield, 2008). The results of temperature acclimation clearly show that exposure to 4 and 37^oC activated AtGCN2 (Fig. 3.11). On the other hand, failure to detect eIF2α-P in protein samples obtained immediately after acclimation suggested that the AtGCN2 kinase may be temperature sensitive or may not be involve in immediate alleviation of extreme temperature stress. The effects of temperature on function of other *Arabidopsis* kinases involved in translation regulation have been reported. For example in mammalian cells, mitogen-induced phosphorylation of ribosomal protein S6 by p70s6k kinase has been implicated in the selective translational up-regulation of mRNA transcripts with oligopyrimidine tract at their transcriptional start site, referred to as 5′ TOP mRNAs (Kakigi *et al.*, 2011). A homologue of this kinase (AtS6k2) has been isolated in *Arabidopsis* and its function has been shown to be temperature dependent; when *Arabidopsis* cell suspensions are moved from 25 to 37^oC the

kinase is rapidly inactivated. This change is consistent with the observations on *Arabidopsis* plants subjected to heat shock treatment (Turck *et al.*, 1998). Therefore, failure of AtGCN2 to phosphorylate AteIF2α for up to one hour post temperature (4 and 37^{o}C) acclimation (Fig. 3.11) may be attributed to the kinase undergoing thermally-induced conformational changes that rendering it inactive. This assumption is supported by data in *Arabidopsis* eFP browser as reported in chapter 4 of this thesis; indicating that no AtGCN2 kinase activity was observed at 0 and 1 h after heat acclimation at 38^{o}C for 3 h (see section 4.2.4).

The activation of AtGCN2 kinase and phosphorylation of AteIF2α in WT Col-0 seedlings achieved through amino acid starvation and cold acclimation are in agreement with earlier reports (Lageix *et al.*, 2008; Zhang *et al.*, 2008), however activation by prolonged exposure to NaCl stress and heat acclimation are reported for the first time in this thesis. Exploring AtGCN2 gene using *Arabidopsis* eFP browser (Data source-Abiotic stress) with *Arabidopsis* α-tubulin as secondary reference gene, revealed that expression of AtGCN2 expression is generally detected after 3 h of exposure to cold, heat, NaCl and Osmotic stress. In addition, results reported in this thesis on activation of AtGCN2 using glyphosate (Fig. 3.8), cold and heat acclimation clearly suggest that *in planta* activation AtGCN2is relatively slow.

3.7.5 Is GCN2 Kinase Differentially Activated in *Arabidopsis*

Temperature acclimation, NaCl and amino acid starvation induced phosphorylation of AteIF2α *in planta*. Since only GCN2 eIF2α kinase homologue is present in *Arabidopsis*, these results clearly imply that these stress factors activated AtGCN2 kinase. Activation of AtGCN2 kinase by different stress factors is not surprising and a similar response has been reported in yeast where a wide spectrum of nutrient deprivation (amino acids, purines, glucose), salinity and heat stress have been shown to activate ScGCN2 (Yang *et al.*, 2000; Goossens *et al.*, 2001; Hinnebusch & Natarajan, 2002). Therefore phosphorylation of AteIF2α by different stress factors suggests that the AtGCN2 activation mechanism during amino acid starvation seems to be conserved with those operating during extreme temperature and NaCl-induced salinity stress in *Arabidopsis*. In other studies on yeast have shown that the mechanism for activation of ScGNCN2

during amino acid deprivation differs from NaCl stress and glucose starvation (Goossens *et al.*, 2001). For ScGCN2 kinase to be activated, the HisRs related region interacts with uncharged tRNA during amino acid starvation, whereas accumulation of Na^+ interfere with normal synthesis of tRNA thus creating defective tRNAs. The defective tRNAs interact with the HisRs region to activate ScGCN2, in the absence of amino acid starvation (Norbeck & Blomberg, 2000; Goossens *et al.*, 2001; Pascual-Ahuir *et al.*, 2001). Based on these reports, it is appropriate to speculate that activation of AtGCN2 by temperature acclimation and salinity stress may be different from that of amino acid starvation. However there is need to investigate how each of these stress factors activates *Arabidopsis* GCN2 kinase *in planta*.

3.7.6 *P. syringae* and CaMv do not Activate AtGCN2 Kinase

Plants have well developed pathogen inducible defence mechanisms such as those that trigger systemic acquired resistance (SAR). Salicylic acid (SA) is one of the key molecules in SAR and also plays an important role in biotic and abiotic stress response mechanisms (Westernack, 2007). SA has been shown to confer resistance to a broad spectrum of micro-organisms (Durrant & Dong, 2004). On the other hand jasmonic acid (JA) is one of the members of the jasmonate family that controls the expression of genes that mediate plant response to wounding, pathogen infection and UV damage (Xiao-Yi Shan, 2007). For JA, there are three loci in *Arabidopsis*, namely JAR1, COL1 and JIN1, that are involved in the Jasmonate signalling pathway. Analysis of JAR1 locus using *jar1-1* knock-out mutants has shown that this locus is involved in protection against a variety of plant stresses, including pathogens (Clarke *et al.*, 2000; Laurie-Berry *et al.*, 2006).

The results obtained on growth of *Pst* DC3000 clearly demonstrated that *NahG* plants supported more bacterial growth than WT Col-0, *jar1-1*, and *Atgcn2-1* plants. Higher counts were expected on *NahG* leaves, since the SA pathway has been abolished in this mutant, therefore rendering *NahG* mutants more susceptible to *Pst* DC3000. The *Pst* DC3000 growth results also demonstrate that disruption of AtGCN2 kinase did not increase susceptibility of *Atgcn2-1* *Arabidopsis* plants to *Pst* DC3000 compared with WT Col-0 and *NahG* plants (Fig.

3.15). Furthermore, the activation of AtGCN2 kinase by glyphosate and failure of pathogens (*P. syringae* and CaMv) to induce phosphorylation of AteIF2α *in planta* clearly supports the suggestion that activation of AtGCN2 kinase may be independent of the SA and JA signalling pathways. These results however are in contrast with those reported by Lageix *et al*. (2008) in which exogenous application of JA (25 μM) and SA (0.6 mM) activated AtGCN2 kinase. This can be attributed to the concentrations of the JA and SA applied on to seedlings and may have been physiologically high compared to levels induced by pathogens. This is because treatment of *Arabidopsis* seedlings with 10 μM of JA and SA induced low expression of AtGCN2 as revealed by analysis conducted using *Arabidopsis* eFP browser. Similarly no increase in AtGCN2 expression was obtained with inoculation of *Arabidopsis* leaves with *P. syringae* (see section 4.2.4).

Mammalian systems have PKR kinase that is activated by binding double-stranded RNA (dsRNA) in response to virus infection (Kaufman, 2000). The mammalian PKR has been shown to phosphorylate wheat eIF2α (Langland *et al.*, 1996) and *Arabidopsis* eIF2α as reported in 5.4 of this thesis. Failure of CaMV inoculation to induce phosphorylation of AteIF2α (Fig. 3.14) support the results of genome search that *Arabidopsis* lacks a PKR homologue as reported herein section 3.1, and also demonstrates that CaMV does not activate AtGCN2 kinase *in planta*. These results are in agreement with those obtained by Zhang *et al*. (2008), using *Turnip crincle virus* (TCV) and *Turnip yellow mosaic virus* (TYMV) to inoculate *Arabidopsis* plants. These two viruses infect *Arabidopsis* and produce double stranded DNA (dsDNA) molecules as reproductive intermediates. Although CaMV has a dsDNA genome and its replication may be different from the TCV and TYMV. CaMV however replicates in plant cytoplasm through reverse transcriptase generating RNA as reproductive intermediates.

3.7.7 Does Phosphorylation of AteIF2α Reduce Global Protein Synthesis

The molecular cloning of *Arabidopsis* homologue of yeast GCN2 by Zhang et al. (2003) partly confirmed that plants possess a stress-response translation control mechanism similar that of yeast and mammalian systems. This is supported further by reports in the literature indicating that some elements of amino acid control are present in plants. For example amino acid starvation in *Arabidopsis* results in the induction of genes encoding enzymes involved in tryptophan biosynthesis pathway (Guyer *et al.*, 1995; Zhao *et al.*, 1998). In addition it is well documented that phosphorylation of eIF2α plays a key role in the regulation of protein synthesis in response to nutrient, cellular, and environmental stresses in mammalian and yeast systems (Dever *et al.*, 1992; Natarajan *et al.*, 2001; Carnevalli *et al.*, 2006).

Reporter gene assays have been widely used to study mechanisms that control cellular processes. Luciferase is one of the reporter genes that has widely been utilized to investigate rates of *de novo* transcription as it is a non-invasive and highly sensitive assay (Birch *et al.*, 2010). This has been achieved by isolation of RNA from transfected cells and subsequent use as template in *in vitro* translation systems and quantification of luciferase activity from the nascent proteins synthesized (Birch *et al.*, 2010). Lower levels of luciferase activity indicate weaker promoter or enhancer, similarly higher level would indicate a stronger promoter (Ruediger & Walter, 1997). As an ideal non-invasive reporter marker, luciferase has been successfully used to analyze cellular processes such as abundance of protein *in planta* in response to external stimuli (Hennig *et al.*, 2010).

Usually after reacting with its substrate, regeneration of luciferase is extremely slow and for this reason it can be considered in-active. This is because after application of substrate, the luciferase molecules undergo a single catalytic cycle and thereafter it is unable to produce any detectable signal (Hennig *et al.*, 2010). Therefore, when under the control of a strong constitutive promoter such as the p35S, luciferase signals can be used over a period of time to estimate *de novo* rates of protein synthesis. The luminescence signals between

one and seven hours reported here (Fig. 3.9), therefore, can be used as an estimate of the *in vivo* rates of translation. The results presented in this thesis suggest that addition of glyphosate activates AtGCN2 which subsequently phosphorylates eIF2α resulting in a 50% decrease in protein synthesis. Caution should be exercised here, however, as the observed decline in translation may arise from a decline in key amino acid levels. Measurements of luminescence signals from p35S:LUC constructs in a WT and *Atgcn2-1* background should resolve this.

4 Chapter 4: Characterization of *p35S:AtGCN2* Mutant Lines

4.1 Introduction

In yeast and mammalian systems, it is well established that GCN2, PERK and PKR kinase are critical in stress response translation control mechanisms mediated through phosphorylation of the eIF2α-subunit (Dever *et al.*, 1992; Hinnebusch *et al.*, 2004; Zhan *et al.*, 2004; Carnevalli *et al.*, 2006; Nayak & Pintel, 2007). Disruption of genes encoding the eIF2α kinases should therefore negatively influence stress response translation control mechanism. In the preceding chapter, however, null-mutation of *AtGCN2* did not produce an obvious stress-phenotype. Lack of a strong *Atgcn2-1* abiotic and biotic stress-phenotype suggested that loss-of-function mutation strategy was insufficient to elucidate the functions of AtGCN2 kinase and hence translation control mechanism in *Arabidopsis*. As discussed earlier herein (section 1.4), lack of an obvious stress-phenotype using loss-of-function mutation approach has been attributed to gene redundancy, duplication or gene families, and for genes that are required during multiple stages of cell cycles (Weigel *et al.*, 2000; Wielopolska *et al.*, 2005; Weigel & Glazebrook, 2006; Kuromori *et al.*, 2009). Nonetheless, gain-of-function approach can be used to complement or as an alternative to loss-of-function mutation analysis, as well as to investigate novel genes (Weigel *et al.*, 2000; Kuromori *et al.*, 2009; Kondou *et al.*, 2010). For example, in *Arabidopsis* the mechanism that perceives ethylene is composed of five genes encoding for ETR1, ETR2, EIN4, ERS1 and ERS2 proteins. Loss-of-function mutation of either *etr2*, *ein4 or ers2* individually does not produce a phenotype with altered ethylene response, contrasting triple null-mutation of *etr2ein4ers2* (Hall *et al.*, 2000). Unlike loss-of-function, gain-of-function mutation of individual ethylene response genes has been shown to produce strong phenotypes (Hua & Meyerowitz, 1998).

On the other hand, analysis of genes can be facilitated by expressing proteins encoded by a cloned gene of interest either in homologous or non-homologous biological systems (Early *et al.*, 2006). For example, *in planta* expression of a protein of interest with an epitope tag can facilitate affinity purification of the protein of interest and associated proteins. Purification then provides a means of isolating the expressed proteins for purposes of identifying and biochemical characterisation of the multi-protein complexes associated with the protein of interest and hence its function (Jarvik & Telmer, 1998; Early *et al.*, 2006). Furthermore, fusing a gene of interest with a fluorescent protein such as GFP, YFP, RFP or CYP can also be very useful for determining the localisation of the protein of interest within living cell, organ or whole plant (Fritze & Anderson, 2000; Hanson & Kohler, 2001). Lack of a strong phenotype associated with *Atgcn2-1* prompted the need to identify phenotypes associated with the gain-of-function mutation through *in planta* expression of AtGCN2 kinase under the control of a 35S promoter. This chapter therefore focuses on the generation and characterisation of *p35S:AtGCN2* mutant line under salinity, osmotic and temperature stress, and localisation of AtGCN2 using *p35S:GFP:AtGCN2* line.

4.2 Cloning and *In Planta* Expression of AtGCN2 Kinase

4.2.1 Generation of *AtGCN2* Gateway™ Entry Clone

The *AtGCN2* cloning PCR conducted using cDNA produced an expected product of 3.726Kb (Fig. 4.1A), which was gel extracted and cloned on to pCR®4 sequencing vector. The pCR®4.*AtGCN2* constructed was then used to transform XL1-Blue *E. coli* cells. A total of 7 colonies growing on selective media were randomly picked and after colony PCR only 4 colonies were positive for *AtGCN2* fragment (Fig. 4.1B). Out of the 4, one colony (colony 1, on Fig. 4.1B) was then picked from which plasmid mini-prep for sequencing was prepared. The sequencing results of the cloned *AtGCN2* fragment were aligned to the sequence deposited in the TAIR database and was found to be a 100% match (Data not shown). Previous attempts to transform TOP10 (invitrogen) and DH5α cell (Stratagene) using pCR®4.*AtGCN2* construct were unsuccessful, since only cells containing inserts confirmed by sequencing to contain deletions survived on the selection media unlike for XL1-Blue cells.

The *AtGCN2* fragment on the pCR®4 sequencing vector was sub-cloned on to pENTR™ /D-TOPO Gateway entry vector. The *pENTR/D:AtGCN2* construct was used to transform XL1-Blue (Stratagene) *E. coli* cells and only 1 colony was positive for *AtGCN2* insert out of the 7 that were randomly picked for colony PCR (Fig. 4.1C). To confirm that the positive colony was indeed harbouring *pENTR/D:AtGCN2* construct, the colony was streaked on a fresh plate containing selective media and mini preps prepared from four distinct colonies. A PCR was then used to confirm the authenticity and orientation of the insert in the *pENTR/D:AtGCN2* using T7 vector specific primer (forward) and *AtGCN2* specific primer (Gcn2Rv3; tcataacccgaccttcacgag) hybridizing at 400bp downstream of ATG start codon. The PCR produced an expected product of ~572bp, thus confirming that the single colony obtained indeed harboured *pENTR/D:AtGCN2* construct and was not a false positive (Fig. 4.1D). Reconstruction of *Atgcn2* fragment in *pENTR/D:AtGCN2* construct after sequencing was found to be 100% match with the *AtGCN2* sequence deposited in TAIR database (Appendix 6).

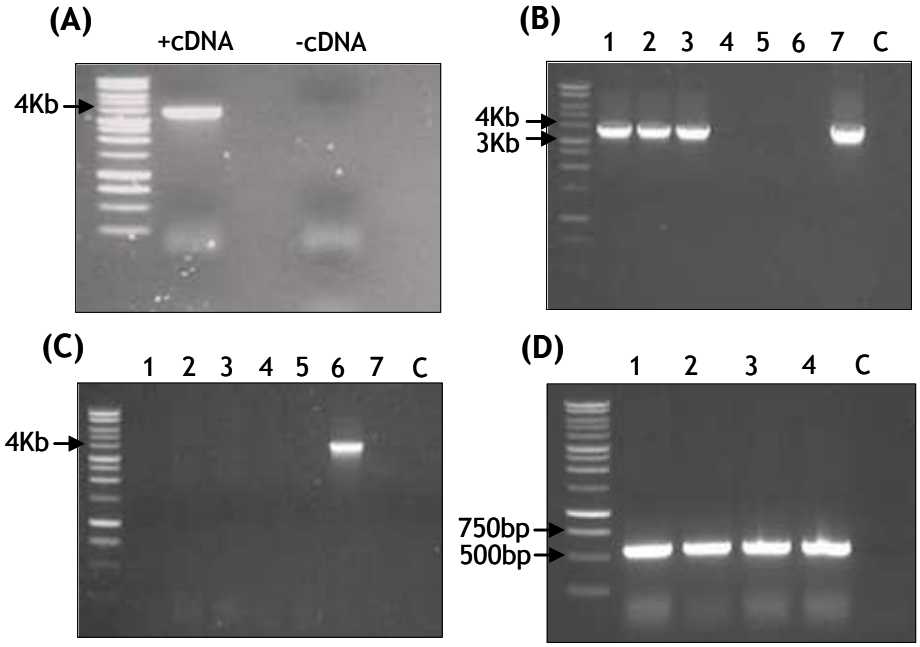

Figure 4.1. Cloning of *AtGCN2* into pENTR/D Gateway entry vector. (A) PCR amplification of *AtGCN2* using cDNA as template, **(B)** Colony PCR of XL1-Blue cells harbouring *pCR4:AtGCN2* construct, **(C)** Colony PCR of XL1-Blue cells harbouring *pENTR/D:AtGCN2* construct, **(D)** Confirmation PCR of *AtGCN2* insert orientation in *pENTR/D* vector, using T7 primer and *AtGCN2* specific primer hybridizing at 400bp downstream of ATG start codon.

4.2.2 .Generation of AtGCN2 Binary Expression Construct

The *AtGCN2* insert in *pENTR/D* Gateway™ entry vector was sub-cloned onto *pMDC32* and *pH7WGF2.0* binary vectors through the LR reaction to generate *pMDC32:AtGCN2* and *pH7WGF2:AtGCN2 in planta* expression constructs (Fig. 4.2). The generated constructs were used to transform XL1-Blue *E. coli* cells and single distinct colonies growing on selective media were used to prepare plasmid mini preps. The presence and orientation of the *AtGCN2* insert in the two constructs was confirmed by restriction enzyme digestion using BamH1 and Hind III for *pMDC32:AtGCN2* and *pH7WGF2:AtGCN2*, respectively. The restriction digestion reaction produced expected fragments of ~2.5 and 3Kb, respectively, confirming the presence and correct orientation of the *AtGCN2* insert (Fig. 4.3).

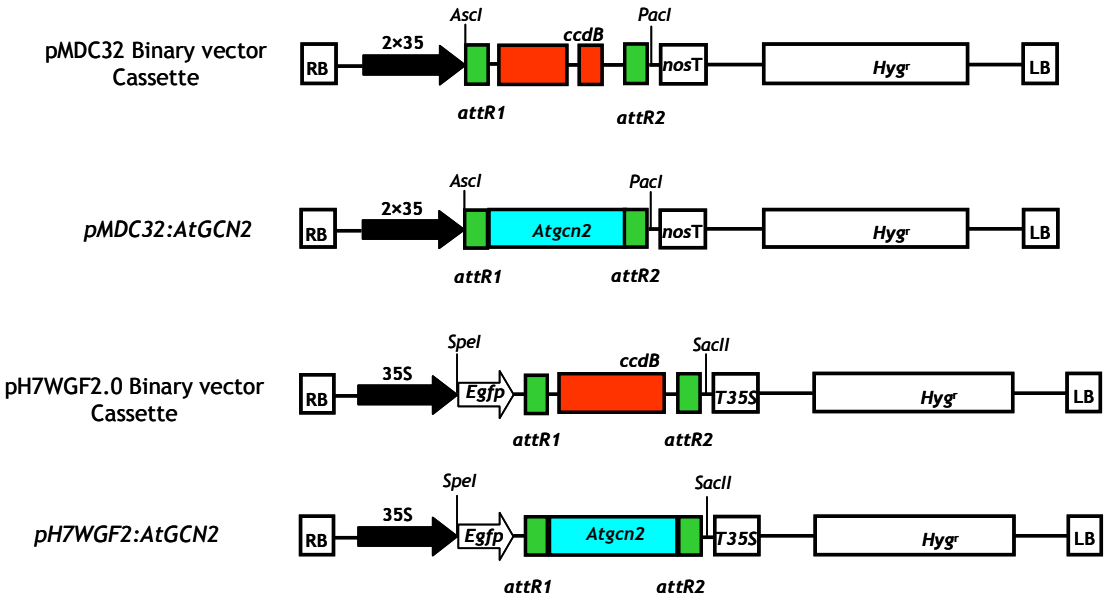

Figure 4.2. Schematic representation of the generated *pMDC32:AtGCN2* and *pH7WGF2:AtGCN2 in planta* expression constructs.

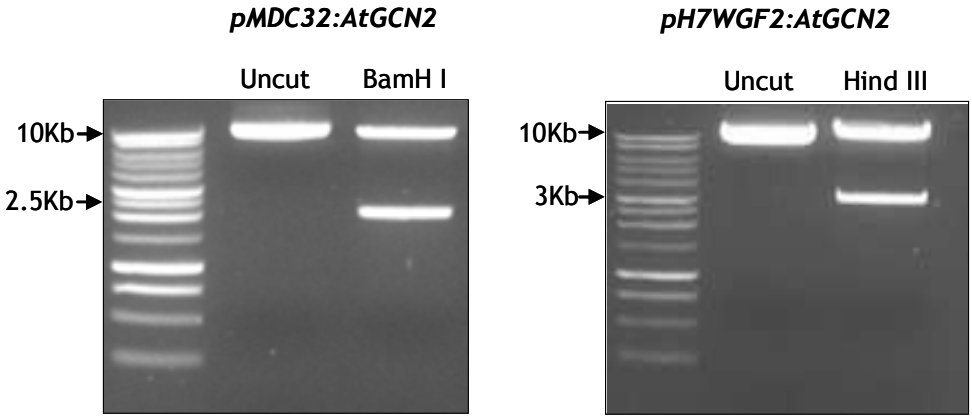

Figure 4.3. Confirmation of *AtGCN2* inserts and orientation in pMDC32 and pH7WGF2.0 binary vectors constructs via restriction digestion. The *pMDC32:AtGCN2* and *pH7WGF2:AtGCN2* constructs generated after recombination reaction with *pENTR/D:AtGCN2* were digested using *BamH I* and *Hind III* using enzyme, producing expected ~2.5 and 3.0 Kb fragments, respectively.

4.2.3 Transformation of *Arabidopsis Atgcn2-1* Plants

Both the non- and transgenic seeds germinated on the hygromycin B selection media, however, after 21 days of growth transgenic seedlings were identified as the actively growing seedlings with true green leaves and with roots penetrating the selection media (Fig. 4.4A). Non-transgenic seedlings were identified as those with stunted growth and yellowing or browning cotyledons (Fig. 4.4A). Transformation efficiency of up to 1.2% was achieved when *Agrobacterium* cultures harbouring *pMDC32:AtGCN2* and *pH7WGF2:AtGCN2* constructs were used to transform *Atgcn2-1* plants. For genotyping purposes, 7 and 8 independent *p35S:AtGCN2* and *p35S:GFP:AtGCN2* T_2 plants, respectively, were randomly selected and the presence of full-length *AtGCN2* determined. To achieve this, genomic DNA was isolated and PCR conducted using Gcn2Fw1and Gcn2Rv1 primers that hybridize to the intact CT-domain of the AtGCN2 kinase gene (Table 2.1). This primer pair had initially been used for genotyping of *AtGCN2-1* plants; where lack of a PCR product indicated presence of a truncated *AtGCN2* CT-domain (see section 3.3.2). The genotyping PCR produced an expected PCR product of ~592bp with genomic DNA obtained from *p35S:AtGCN2* and *p35S:GFP:AtGCN2* plants, and none for the *Atgcn2-1* plants (Fig. 4.4B). On the other hand a product of ~1050bp was obtained with genomic DNA obtained from WT Col-0 plants (Fig. 4.4B). A bigger fragment was obtained in WT Col-0 seedling because of the presence of introns within its genomic DNA as opposed to mutants ectopically expressing the cDNA encoding the *AtGCN2* ORF. These results suggested the presence of an intact CT-terminal domain in the *p35S:AtGCN2* and *p35S:GFP:AtGCN2* lines but not the *Atgcn2-1* mutant line.

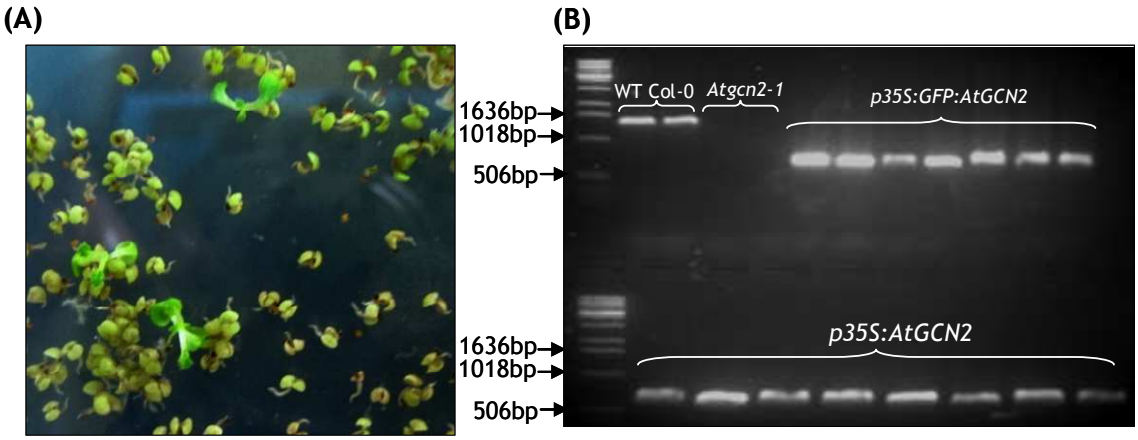

Figure 4.4. Isolation and genotyping of *p35S:AtGCN2* and *p35S:GFP:AtGCN2* mutant lines. (A) Screening of T_1 seeds of ectopic AtGCN2 expressing mutants on ½ MS supplemented with 45 µg/ml hygromycin B at 21 days after incubation, **(B)** Genotyping PCR of soil grown T_2 *p35S:AtGCN2* and *p35S:GFP:AtGCN2* plants, 4 weeks after transplanting. A PCR product of ~592bp and ~1050 was expected using genomic DNA from ectopic AtGCN2 expressing mutants and WT Col-0 plants, respectively.

4.2.4 Segregation and Functional Analysis of *p35S:AtGCN2* and *p35S:GFP:AtGCN2* Lines

Screening and isolation of ectopic AtGCN2 expressing mutant lines after transformation of the *Arabidopsis Atgcn2-1* null-mutant plants suggested successful insertion of the full-length *AtGCN2* ORF. However it was essential to analyse the integrated ORF to determine its segregation and it's *in planta* kinase activities. For *p35S:AtGCN2* seedlings, 3 lines satisfied the 3:1 (resistant: sensitive) Mendelian ratio (Table 4.1), as opposed to *p35S:GFP:AtGCN2* seedlings, where only a single line satisfied this ratio (x^2 = 0.89, P = 0.30). The *p35S:AtGCN2* and *p35S:GFP:AtGCN2* lines were generated in the *Atgcn2-1* mutant background, hence it was important to confirm whether the integrated full-length *AtGCN2* ORF complemented the null mutation. For this purpose T_2 *p35S:AtGCN2* A, C and F seeds described in Table 4.1 and the *p35S:GFP:AtGCN2* line that satisfied the 3:1 ratio, WT Col-0 and *Atgcn2-1* were spread on ½ MS media and grown for 14 days.

Table 4.1. Segregation analysis of 6 independent *p35S:AtGCN2* T_2 seedlings. Segregation analysis was conducted on ½ MS media supplemented with 45 µg/ml of hygromycin B antibiotic. The number of resistant and sensitive seedling was determined and data were subjected to 'Goodness of fit test'.

Mutant	H^R:H^S seeds	Chi square statistic (x^2)	P value	*Goodness of fit (p>0.05)
*p35S:AtGCN2*A	23:7	0.18	0.70	Yes
*p35S:AtGCN2*B	10:9	30.42	>0.001	No
*p35S:AtGCN2*C	21:8	0.41	0.50	Yes
*p35S:AtGCN2*D	59:47	21.14	>0.001	No
*p35S:AtGCN2*E	12:9	64.08	>0.001	No
*p35S:AtGCN2*F	23:12	1.07	0.30	yes

*Yes and No; segregation of the dominant characteristic (hygromycin B resistant gene in T_2 seeds conforms and does not conform to a 3:1 segregation ratio, respectively.

To assess the activity of AtGCN2 kinase and hence the integrated *AtGCN2* ORF, the 14-day old seedlings were treated with 150 µM glyphosate to activate the AtGCN2 kinase. The phosphorylation state of AteIF2α after treatment with glyphosate revealed that the integrated *AtGCN2* ORF, indeed complemented the *Atgcn2-1* mutant (Fig. 4.5). The AtGCN2 kinase activity was present in *p35S:AtGCN2* lines A and F, the *p35S:GFP:AtGCN2* and WT Col-0 seedlings, whereas no kinase activity was observed on *Atgcn2-1* seedlings and all genotypes for control treatment (Fig. 4.5). However high phosphorylation signals were obtained with the *p35S:AtGCN2* line A (*p35S:AtGCN2*A) and *p35S:GFP:AtGCN2* (Fig. 4.5) and these lines were then used to conduct further characterization and localisation experiments. Localisation experiments showed higher GFP activity on primary roots, particularly on the root apical meristem region (Fig. 4.6A), on emerging leaves and sections of cotyledonary leaves (Fig. 4.6B & C). High GFP activity was also observed on the apical shoot tip meristem (Fig. 4.6D).

Exploring the developmental map data in the *Arabidopsis* eFP browser revealed that *AtGCN2* is generally expressed (up to 1.37 fold) in the whole plant except for the stage 6-10 siliques. However highest expressions are present in the cauline (1.66 fold) and senescent (1.79 fold) leaves. For tissue specific data set, *AtGCN2* is expressed in the meristematic zone of root tips (*ca.*2 fold) and on all stages of zygotic embryo development (globular, heart and torpedo). For

globular, heart and torpedo stages, up to 2.48 fold expression are present in the apical, basal, root and meristem zones. The highest expression (17.25 fold) however is present on the root zone of embryos at torpedo stage; in contrast expression is masked in the basal zone. In the biotic stress data, infiltration of leaves with avirulent *P. syringae* elicited no expression of *AtGCN2* at 16 up to 24 h after infiltration. On the other hand exogenous application of methyl jasmonate (10 µM) and salicylic acid (10 µM) also induced low expressions of 1.22 and 1.33 folds, respectively at 3 h after treatment. On the abiotic stress data, low expressions of 1.09 fold were present mainly on the shoots of seedlings of seedlings exposed to cold (4^{o}C continuous exposure) and osmotic (300 mM mannitol) stress for 12 h. Expression of 1.21 and 1.15 folds were observed on shoots of seedlings exposed to 150 mM NaCl for 6 up to 24 h and no expression for seedling recovering at 25^{o}C, after heat shock at 38^{o}C for 3 h. Both the cell eFP and SUBA browsers prediction based on the protein sequence indicated the AtGCN2 kinase is localised in the nucleus.

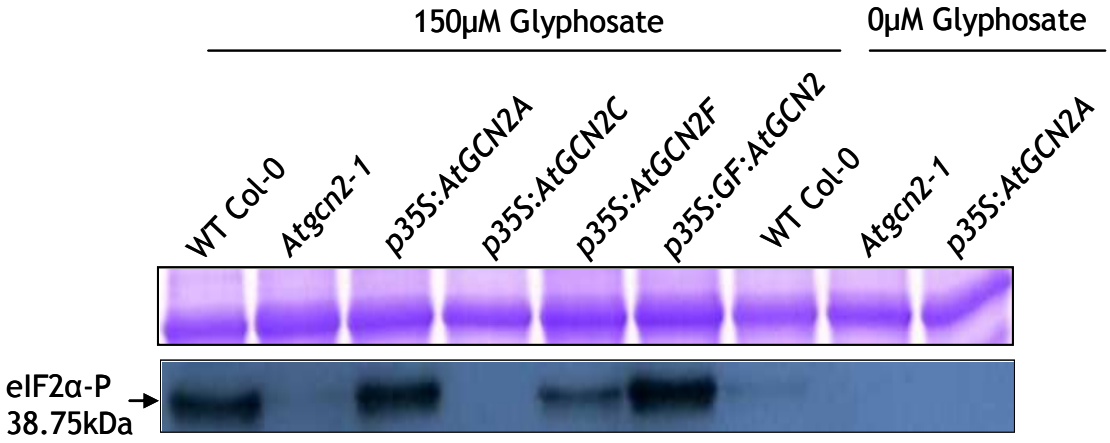

Figure 4.5. Ectopic expression of *AtGCN2* ORF complemented *Atgcn2-1* *Arabidopsis* mutants. The 14 days old seedling of WT Col-0, *Atgcn2-1*, *p35S:AtGCN2* A, C and F, and *p35S:GFP:AtGCN2* T_2 seedlings were treated with 150 µM glyphosate. Total protein was extracted, resolved on 10% SDS-PAGE, transferred on to nitrocellulose membrane and probed with eIF2α-p antibody. Top panel Coomassie® brilliant blue stained SDS-PAGE indicating equal loading.

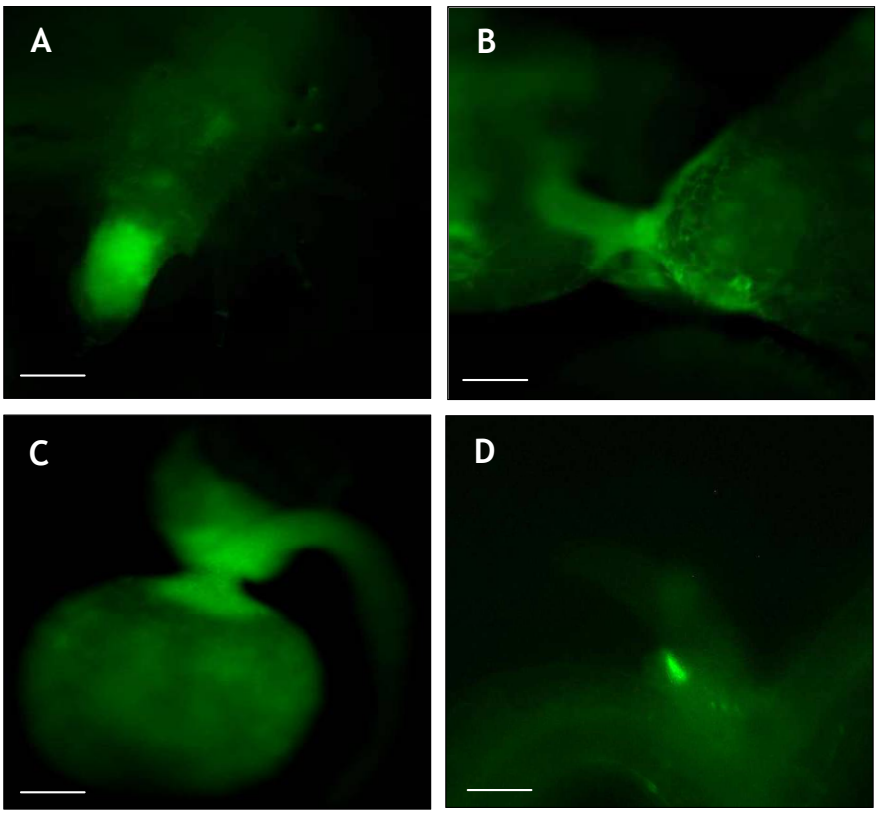

Figure 4.6. Localisation of constitutively expressed *GFP:AtGCN2* fusion protein on 10-day old *p35S:GFP:AtGCN2 Arabidopsis* seedlings. **(A)** GFP activity localised on primary root tip meristem, **(B & C)** GFP activity localised on shoot tip and on adjacent regions on cotyledonary leaves, **(D)** GFP activity on shoot apical meristem. Bars on the pictures represent 1 mm.

4.3 Response of *p35S:AtGCN2* Line to Salinity Stress

4.3.1 Germination on NaCl-supplemented Media

Seed germination was assessed at 2, 3 and 4 days after of incubation, and increasing the assessment period increased germination rates obtained. Over 80% germination was achieved on the three genotypes (WT Col-0, *Atgcn2-1* and *p35S:AtGCN2*A) after 3 and 4 days incubation on media supplemented with or without NaCl (Fig. 4.7). Although lower germination rates were obtained on WT Col-0 seeds, ANOVA tests revealed that only the assessment period had a significant ($p<0.05$) influence on germination. For media supplemented with NaCl, germination rates decreased with an increase in the concentration of NaCl (Fig. 4.7). A germination trend similar to that obtained on NaCl-free media was also observed; consistently lower germination rates were obtained on WT Col-0

seeds (Fig. 4.7). Furthermore, ANOVA tests also revealed that assessment period had significant ($p<0.05$) influence on germination. To determine the influence of genotype and NaCl concentration on germination, the data generated in each assessment period were subjected to separate ANOVA tests. Only NaCl concentration had a significant ($p<0.05$) influence on germination at 2, 3 and 4 days after incubation, but genotype and the interaction (genotype×NaCl concentration) did not(Appendix 7). Post-ANOVA tests were conducted using LSD at the $p<0.05$ level to compare the effect of NaCl and genotype on germination during each assessment period. Analysis using LSD values revealed that *p35S:AtGCN2*A and *Atgcn2-1* had significantly ($p<0.05$) higher germination rates than WT Col-0, for seeds spread on 0 mM NaCl at 2 days after incubation, unlike for 3 and 4 days (Table 4.2). For 2 and 3 days, significantly ($p<0.05$) higher germination rates were obtained with *p35S:AtGCN2*A seeds spread on 100 mM NaCl than for the other two lines. At day 4, higher germination rate were obtained were again observed with *p35S:AtGCN2*A seeds spread on 100 and 150 mM NaCl, but the germination rates were not significantly different ($p<0.05$) from those obtained on WT Col-0 seeds (Table 4.2).

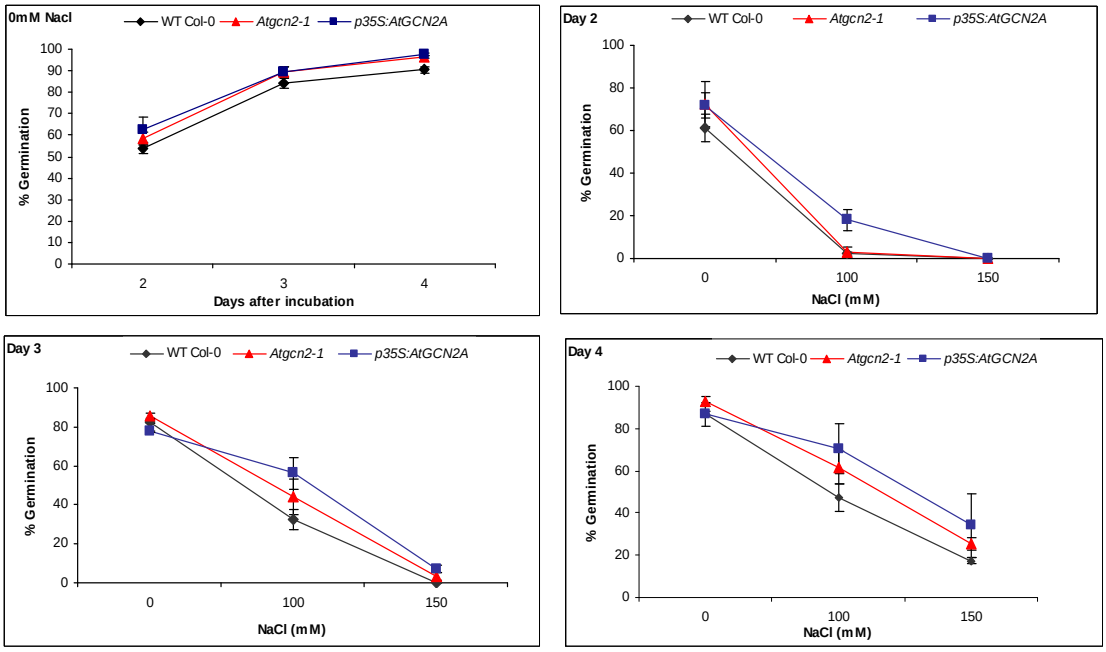

Figure 4.7. The effect of increasing NaCl concentration on germination of *p35S:AtGCN2*A *Arabidopsis* line. (A) Germination rate of *Atgcn2-1*, WT Col-0 and *p35S:AtGCN2*A seeds on NaCl-free ½ MS media at 2, 3 and 4 days after incubation. **(B, C and D).** Germination rates of *Atgcn2-1*, WT Col-0 and *p35S:AtGCN2*A seeds on ½ MS media supplemented with 0, 100 and 150 mM NaCl at 2, 3 and 4 days after incubation. Bars are S.E.M of 3 independent replicate experiments.

Table 4.2. Variation in germination of WT Col-0, *Atgcn2-1* and *p35S:AtGCN2*A seeds under NaCl stress. *Arabidopsis* seeds were spread on ½ MS supplemented with 0,100 and 150 mM NaCl and germination assessed at 2, 3 and 4 days after incubation.

NaCl	Genotype	% Germination*		
		Day 2	Day 3	Day 4
0 mM	WT Col-0	61.3**c**	82.7**e**	87.9**d**
	Atgcn2-1	73.3**d**	86.0**e**	93.3**d**
	*p35S:AtGCN2*A	72.0**d**	77.7**e**	86.7**d**
100 mM	WT Col-0	2.1**a**	32.3**b**	47.3**b**
	Atgcn2-1	3.0**a**	44.3**c**	61.3**c**
	*p35S:AtGCN2*A	18.0**b**	56.3**d**	70.3**c**
150 mM	WT Col-0	0.0**a**	0.0**a**	17.3**a**
	Atgcn2-1	0.0**a**	3.3**a**	25.0**ab**
	*p35S:AtGCN2*A	0.0**a**	7.3**a**	34.0**b**
LSD value		**7.4**	**7.9**	**13.0**

***LSD tests showed value in the column with the same letter are not statistically ($p<0.05$) different.

4.3.2 Growth of Seedlings under NaCl-induced Stress

There were no obvious phenotypic differences observed in terms of shoot growth between the three genotypes (WT Col-0, *Atgcn2-1* and *p35S:AtGCN2*A) grown on media with or without NaCl. On the other hand, it was clear that *p35S:AtGCN2*A seedlings had longer primary roots and were relatively bigger compared with WT Col-0 and *Atgcn2-1* seedlings on all NaCl treatments (Fig. 4.8A). Increasing NaCl concentration generally reduced root growth in all the genotypes with the lowest obtained on 100 mM NaCl treatment (Fig. 4.8A & B). Nonetheless, *p35S:AtGCN2*A seedlings still had the highest root growth, whereas the lowest was obtained with *Atgcn2-1* seedlings (Fig. 4.8B). Root growth data were subjected to ANOVA tests, and genotype and NaCl concentration were found to have had significant ($p<0.05$) influence on root growth (Appendix 8). Analysis of the means using LSD value indicated that irrespective of the genotype, significant ($p<0.05$) reduction in root growth was obtained on seedlings transplanted on to 100 mM NaCl media (Fig. 4.8B). Furthermore LSD analysis revealed that there were no significant ($p>0.05$) decrease in root growth for any genotype induced by 50 mM when compared with that 0 mM NaCl (Fig. 4.8B).

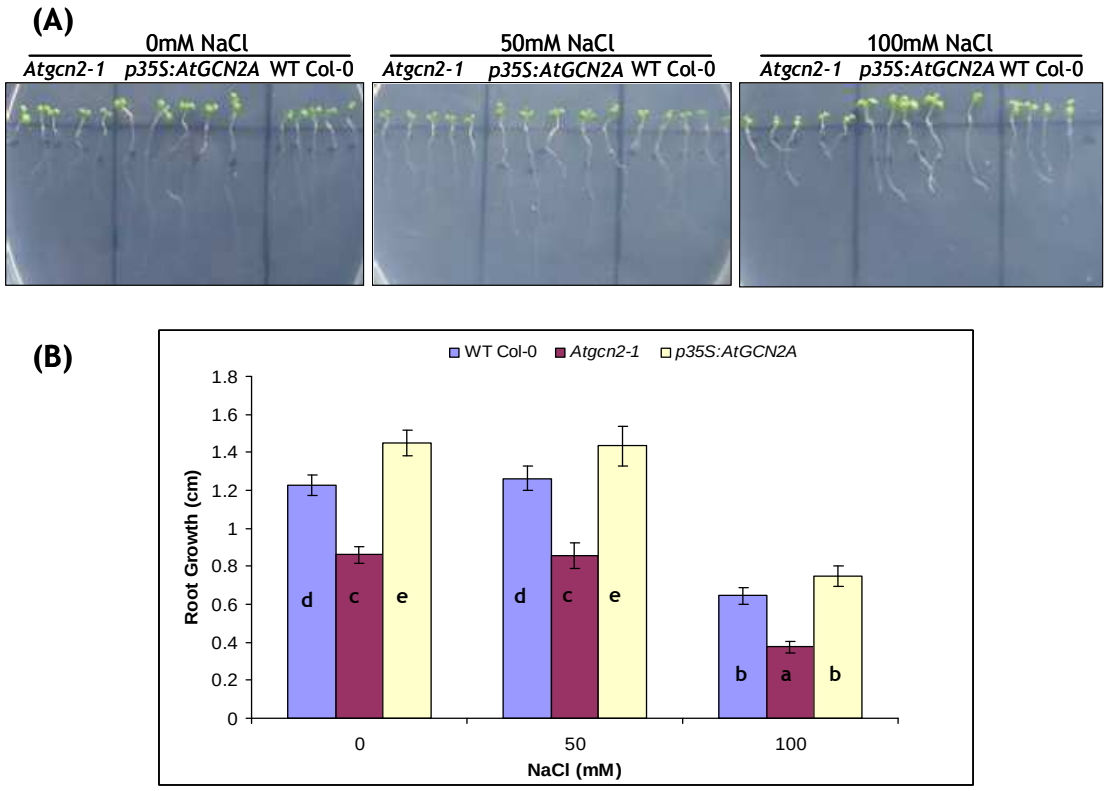

Figure 4.8. The *p35S:AtGCN2*A seedlings have longer primary roots on MS media supplemented with 0-100 mM NaCl. (A) Root phenotype of 14-day old WT Col-0, *Atgcn2-1* and *p35S:AtGCN2*A seedlings, **(B)** Increase in root growth on MS media supplemented with 0-100 mM is genotype dependent. Bars on the graph represent S.E.M of 3 independent replicate experiments and graphs with the same letters are not significantly ($p>0.05$) different based on LSD value (0.17).

The *p35S:AtGCN2*A mutant showed increased root growth compared with WT Col-0 and *Atgcn2-1* seedlings on MS media supplemented with or without NaCl. A follow-up experiment was then conducted to determine whether the increased root growth observed with *p35S:AtGCN2*A seedlings translated into NaCl tolerance. For this purpose 6 days old WT Col-0, *Atgcn2-1* and *p35S:AtGCN2* line A and F (Table 4.1 & Fig. 4.5) seedlings grown on ½ MS devoid of NaCl were transferred on to ½ MS supplemented with 0, 50 and 100 mM NaCl and grown for 30 days. There were no obvious phenotypic differences observed in all the NaCl concentrations tested, however increased NaCl concentration generally suppressed seedling growth irrespective of the genotype (Fig. 4.9).

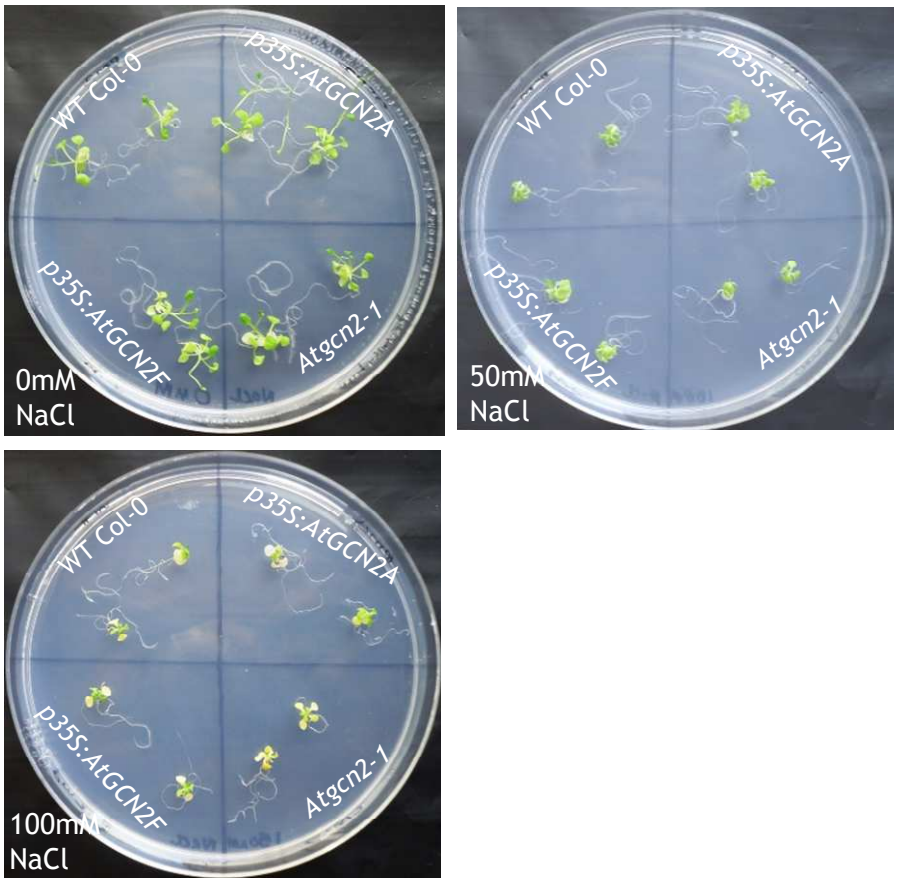

Figure 4.9. Increased primary root growth in *p35S:AtGCN2* mutants does not confer tolerance to NaCl-induced stress. *Arabidopsis* seeds of WT Col-0, *Atgcn2-1*, *p35S:AtGCN2* lines A & F were germinated on MS media devoid of NaCl for 6 days. Seedlings were then transplanted on to MS media supplemented with 0, 50 and 100 mM NaCl and allowed to grow for 30 days under continuous light conditions.

4.3.3 Germination and Growth of Seedlings under KCl-induced Stress

Plants experience salinity stress mainly due to the accumulation of ions to toxic levels. KCl among other salts such as CsCl have commonly been used in conjunction with NaCl to determine initial effects of ion specificity in salt stress experiments (Verslues *et al.*, 2006). To establish ion specificity effects on germination, seeds of WT Col-0, *Atgcn2-1* and *p35S:AtGCN2*A were subjected to increasing concentrations of KCl. After 2 days increasing KCl concentration

caused a marked initial reduction in germination (day 2) irrespective of genotype (Fig. 4.10). By day 3 and 4, however, the effects of KCl concentration were less apparent. ANOVA tests on the factors KCl concentration, genotype and their interaction (KCl concentration x genotype) were all significant ($p<0.05$; Appendix 9). Further analysis of the means using LSD values indicated that germination at day 3 and 4 on all KCl concentrations were not significantly ($p>0.05$) different (Fig. 4.10; Appendix 9).

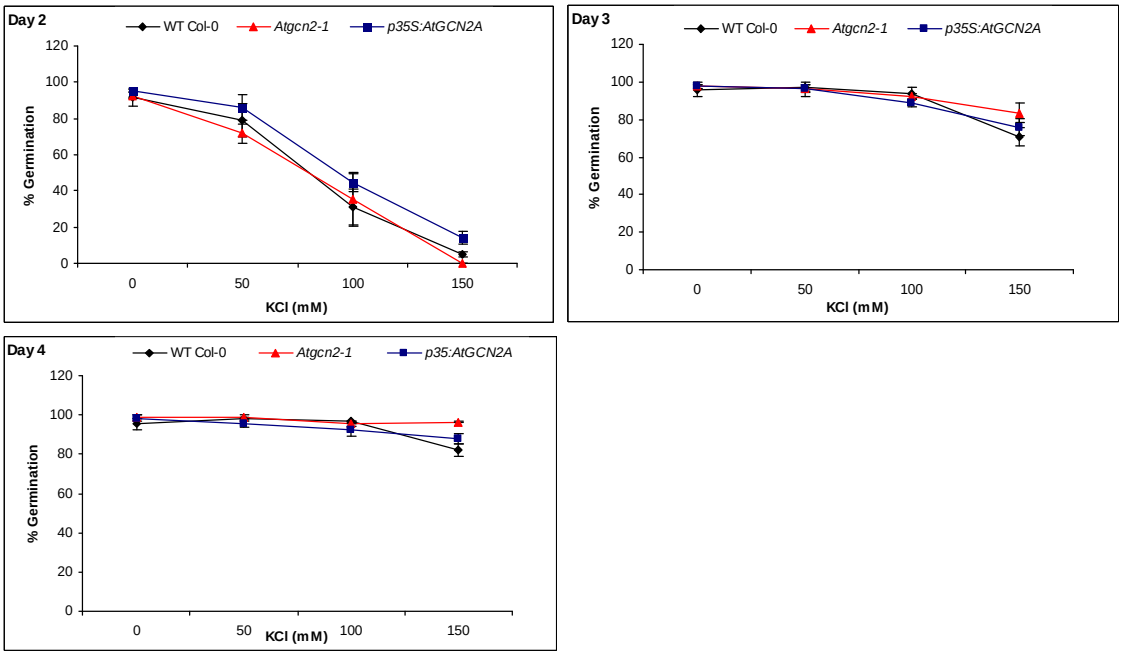

Figure 4.10. The effects of increasing KCl concentration on germination of *Atgcn2-1*, WT Col-0 and *p35S:AtGCN2*A seeds. Germination of *Atgcn2-1*, WT Col-0 and *p35S:AtGCN2*A seeds were assessed on ½ MS media supplemented with 0, 100 and 150 mM KCl at 2, 3 and 4 days after incubation. Bars on the graphs are S.E.M of 3 independent replicate experiments.

Similar to the root growth response obtained on media supplemented with NaCl, increasing the KCl concentration resulted in reduced primary root growth for all the genotypes. The lowest root growth was obtained on seedlings transplanted onto MS supplemented with 150 mM KCl (Fig. 4.11). Furthermore, just like in the NaCl experiment (Fig. 4.7), *p35S:AtGCN2*A seedlings had the highest root growth, whereas the lowest was obtained with *Atgcn2-1* seedlings, irrespective

of the KCl treatment (Fig. 4.11). Root growth data were subjected to ANOVA tests which revealed factors genotype and KCl concentration had a significant ($p<0.05$) influence on root growth but the interaction (KCl concentration x genotype) was not (Appendix 10). Analysis of the treatment means using LSD tests revealed on all KCl treatments except 150 mM, the *p35S:AtGCN2*A seedlings had significantly ($p<0.05$) longer roots than WT Col-0 and *Atgcn2-1* seedlings (Fig. 4.11).

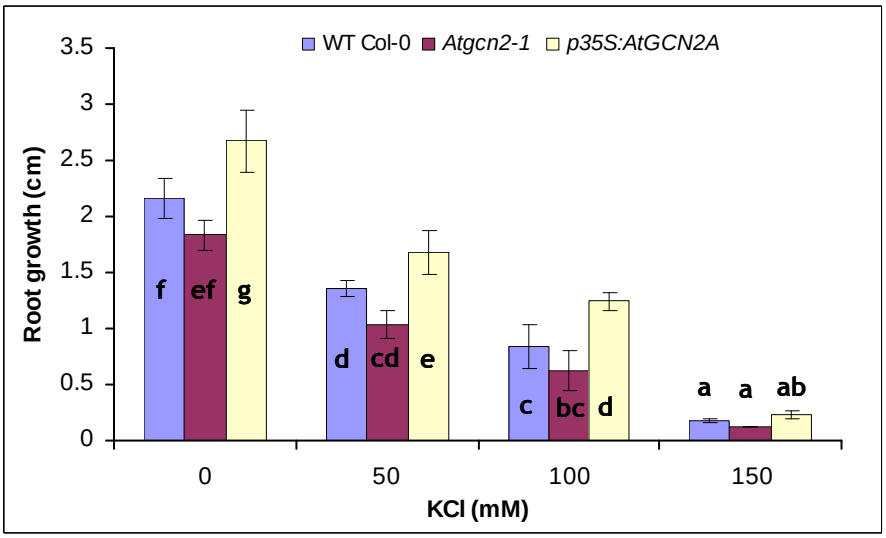

Figure 4.11. Increased root growth of *Arabidopsis* on KCl-supplemented media is genotype dependent. Seedlings of WT Col-0, *Atgcn2-1* and *p35S:AtGCN2*A germinated for 6 days on MS media were transplanted onto MS media supplemented with 0-150 mM KCl. Root growth was assessed at 10 days after transplanting. Bars on the graph represent S.E.M of 3 independent replicate experiments and graphs with the same letters are not significantly ($p>0.05$) different based on the calculated LSD value (0.44).

The general growth and survival of WT Col-0, *Atgcn2-1* and *p35S:AtGCN2*A seedlings on ½ MS media supplemented with KCl (0-150 mM) was also evaluated. The results obtained show that increasing the concentration of KCl inhibited the growth of seedlings with severe inhibition observed on 150 mM KCl (Fig. 4.12). Although higher germination rates were obtained with *p35S:AtGCN2*A seeds,

there were no clear phenotypic differences observed on survival and growth of seedlings for all the genotypes after 30 days (Fig. 4.12).

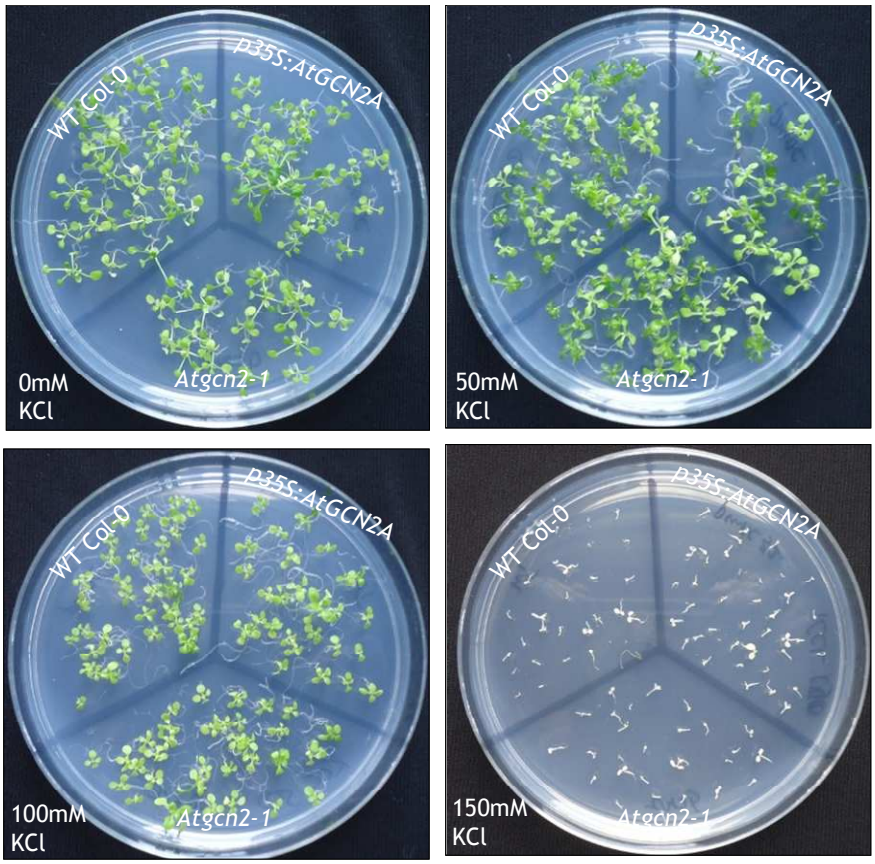

Figure 4.12. Effects of KCl-induced salinity stress on growth of *Atgcn2-1*, *p35S:AtGCN2*A and WT Col-0 seedlings. *Arabidopsis* seeds were spread on ½ MS media supplemented with 0-150 mM KCl and allowed to grow for 30 days under long day growth conditions.

4.4 Response of *p35S:AtGCN2* Line to Osmotic Stress

4.4.1 Mannitol-Induced Osmotic Stress

Mannitol is one of the solutes that have been used in experiments investigating the effect of low water potential on plant growth and development. However it is known to have toxic effects like other solutes that have been used to impose low water potential particularly melibiose (Verslues *et al.*, 2006). Nonetheless

the effect of mannitol-induced osmotic stress on germination and growth of *p35S:AtGCN2*A seedlings were investigated. For germination experiments, WT Col-0, *Atgcn2-1* and *p35S:AtGCN2*A seeds were spread on ½ MS supplemented with 0, 50, 100, 200 and 300 mM mannitol and similar to earlier experiments, germination was assessed at 2, 3 and 4 days after incubation. Higher germination rates were obtained with *p35S:AtGCN2*A seeds at day 2 and 3 on 0, 50 100 and 200 mM mannitol, but not on day 4 (Fig. 4.13). However the initial germination rates obtained in this experiment were low and unexpected (Fig. 4.13) and are probably associated with the tropical glass house growth conditions (Day/night 28/18^{o}C) and the loam soil used. None-the-less ANOVA tests revealed that factors genotype, mannitol concentration and their interaction exerted a significant ($p<0.05$) influence on germination at 2 and 3 days after incubation. At day 4 ANOVA tests revealed only mannitol concentration had significant ($p<0.05$) influence on germination rates (Appendix 11). Further analysis between treatment means using LSD values, revealed that at day 2 and 3, *p35S:AtGCN2*A showed a significantly ($p<0.05$) higher germination compared with WT Col-0 and *Atgcn2-1* on 0-100 and 0-200 mM mannitol, respectively, unlike on day 4 (Table 4.3).

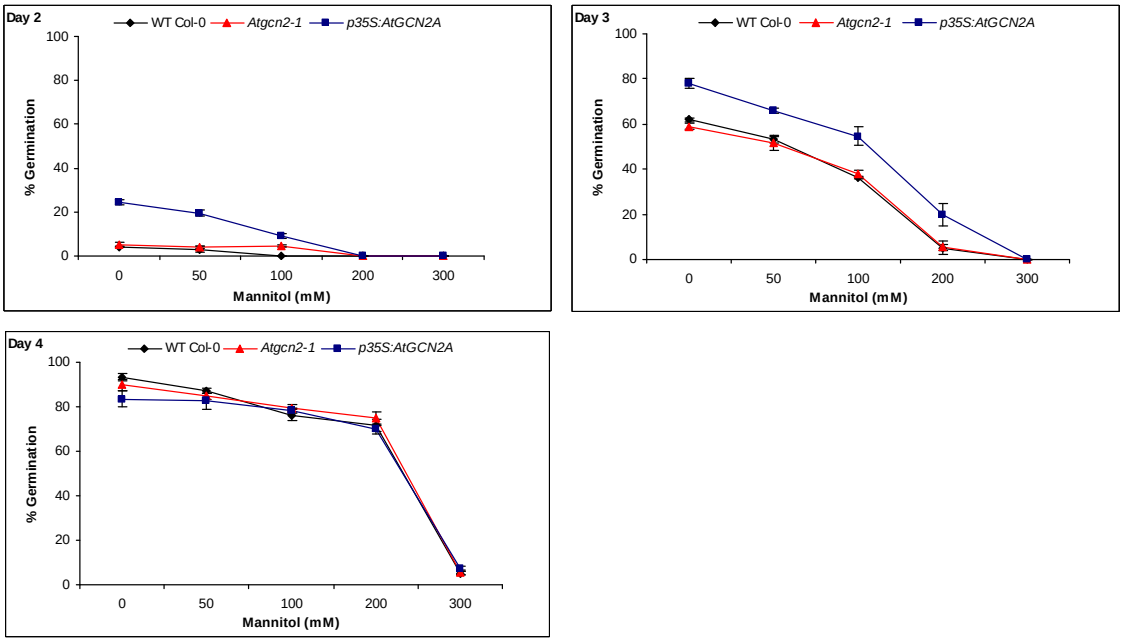

Figure 4.13. Germination of *Atgcn2-1*, WT Col-0 and *p35S:AtGCN2*A *Arabidopsis* seeds in response to increasing mannitol concentration. *Arabidopsis* seeds of *Atgcn2-1*, WT Col-0 and *p35S:AtGCN2*A were spread on ½ MS media containing 0.7% sucrose supplemented with 0, 50, 100, 200 and 300 mM mannitol. Germination was assessed at 2, 3 and 4 days after incubation. Bars are S.E.M of 3 independent replicate experiments.

Table 4.3. Variation in germination of WT Col-0, *Atgcn2-1* and *p35S:AtGCN2*A seeds under mannitol-induced osmotic stress. Seeds were spread on ½ MS supplemented with 0, 50, 100, 200 and 300 mM mannitol and germination assessed at 2, 3 and 4 days after incubation.

Mannitol	Genotype	% Germination*		
		Day 2	Day 3	Day 4
0 mM	WT Col-0	3.97**b**	61.30**e**	93.33**e**
	Atgcn2-1	5.10**b**	58.97**e**	89.77**de**
	*p35S:AtGCN2*A	24.53**e**	77.90**f**	83.53**d**
50 mM	WT Col-0	3.10**b**	53.27**d**	87.20**d**
	Atgcn2-1	4.07**b**	51.40**d**	84.83**d**
	*p35S:AtGCN2*A	19.53**d**	65.85**e**	82.63**cd**
100 mM	WT Col-0	0.0**a**	36.53**c**	76.33**c**
	Atgcn2-1	4.50**b**	37.73**c**	79.50**c**
	*p35S:AtGCN2*A	9.17**c**	54.70**d**	78.37**c**
200 mM	WT Col-0	0.0**a**	5.03**a**	71.77**b**
	Atgcn2-1	0.0**a**	5.47**a**	74.73**b**
	*p35S:AtGCN2*A	0.0**a**	19.77**b**	69.90**b**
300 mM	WT Col-0	0.0**a**	0.0**a**	5.07**a**
	Atgcn2-1	0.0**a**	0.0**a**	5.57**a**
	*p35S:AtGCN2*A	0.0**a**	0.0**a**	7.17**a**
LSD value		**2.43**	**6.44**	**6.36**

***Values in columns with the same letter are not statistically ($p>0.05$) different as distinguished using LSD values.

After assessing germination, the effects mannitol-induced osmotic stress on seedling growth was also evaluated. Seeds were spread on ½ MS media containing 0.7% sucrose, supplemented with mannitol (0-200 mM) and grown for 28 days. There were no obvious survival and growth differences observed between any of the genotypes, but increasing mannitol concentration inhibited seedling growth (Fig. 4.14). Root growth after 28 days under mannitol-induced stress followed a similar trend as reported for NaCl and KCl; the highest and lowest growth was obtained on *p35S:AtGCN2*A and *Atgcn2-1* seedlings, respectively. ANOVA tests indicated that factors mannitol concentration and genotype had significant ($p<0.05$) influence on root growth (Appendix 12). Although the highest root growth was obtained with *p35S:AtGCN2*A, analysis of treatment means using the LSD (0.49) revealed that the increase was not significantly ($p<0.05$) different from the WT Col-0 seedlings (Fig. 4.15).

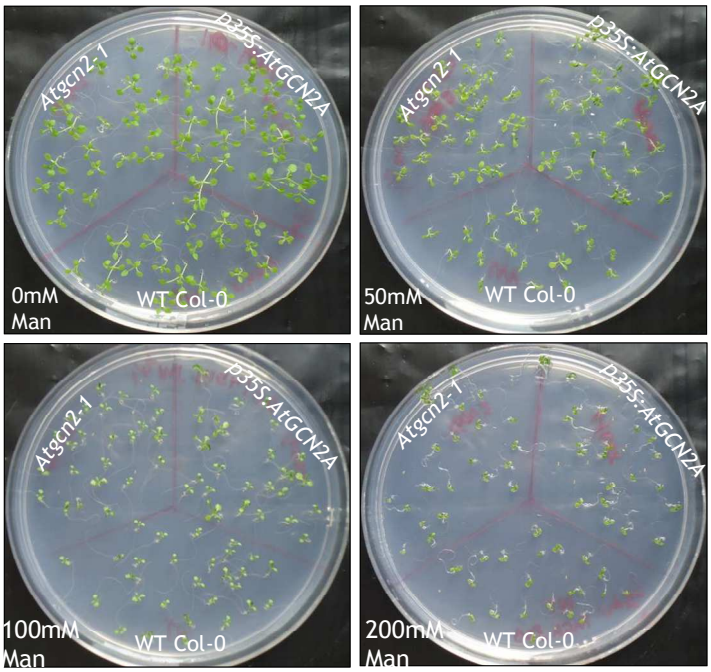

Figure 4.14. Growth of WT Col-0, *Atgcn2-1* and *p35S:AtGCN2*A seedlings on ½ MS containing 0.7% sucrose and supplemented with 0-200 mM mannitol. *Arabidopsis* seeds were spread on ½ MS media supplemented with 0-200 mM KCl and allowed to grow for 28 days under long day growth conditions.

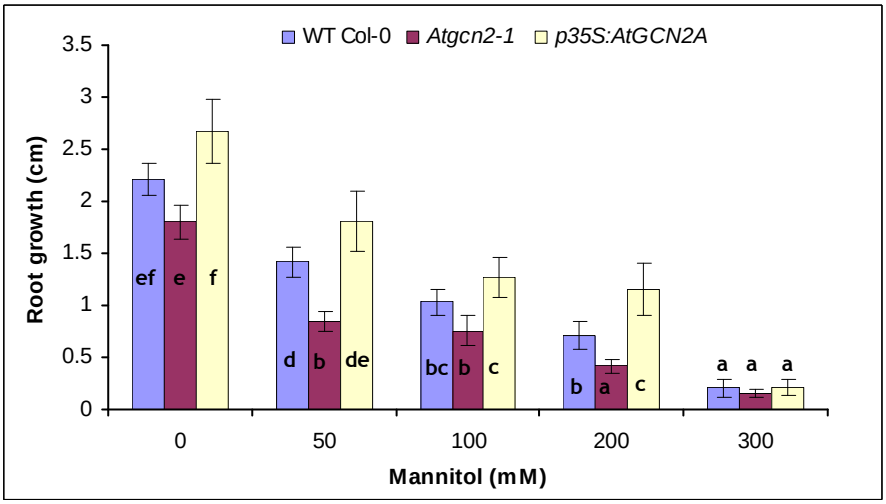

Figure 4.15. Mannitol-induced osmotic stress inhibits root growth of WT Col-0, *Atgcn2-1* and *p35S:AtGCN2*A seedlings. WT Col-0, *Atgcn2-1* and *p35S:AtGCN2*A 7-day old seedlings were transplanted onto MS media supplemented with 0-300 mM mannitol. Root growth was assessed at 10 days after transplanting. Bars on the graph represent S.E.M of 3 replicate experiments and graphs with the same letters are not significantly ($p<0.05$) different based on LSD value (0.44).

4.4.2 PEG6000-Induced Osmotic Stress

High molecular weight solutes have been used to impose low water potential in experiments to investigate the effects of osmotic stress on plant growth. The use of high molecular weight solutes such as PEG has been preferred to mannitol for such experiments. This is mainly because mannitol is usually taken up by plants and metabolic perturbations rather than osmotic stress are more often than not observed (Verslues *et al.*, 2006). The effects of PEG 6000-induced osmotic stress on germination and root growth of *p35S:AtGCN2*A seedlings were therefore investigated. For germination experiments seeds were spread on ½ MS media containing 0.7% sucrose infused with 0, 20 and 40% PEG6000 solutions (w/v) with calculated osmotic potentials of ca. 0, -0.62 and -9.33 MPa. Germination was then assessed 2, 3 and 4 days after incubation. Increased PEG concentration reduced germination rates. Unlike NaCl, KCl and mannitol supplemented media, lower germination rates were consistently obtained on *p35S:AtGCN2*A seeds on 20 and 40% PEG6000-infused media (Fig. 4.16).

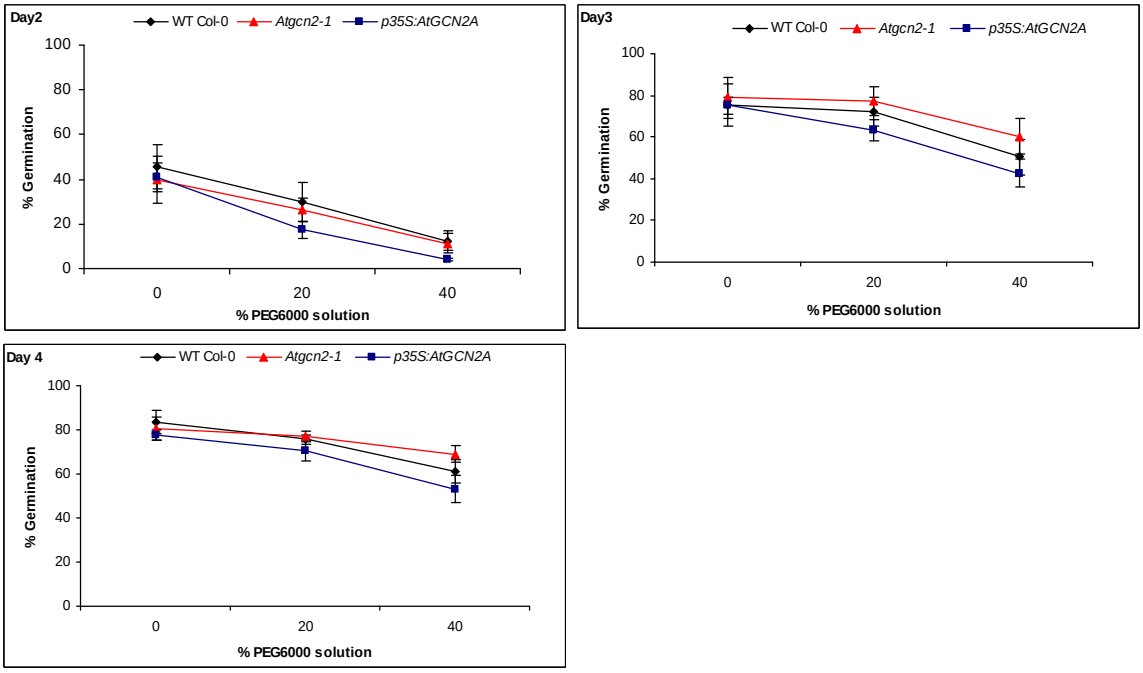

Figure 4.16. Effects of PEG concentrations on germination of *Atgcn2-1*, WT Col-0 and *p35S:AtGCN2*A *Arabidopsis* seeds. *Arabidopsis* seeds were spread on 20 and 40% PEG6000-infused ½ MS media containing 0.7% sucrose. Germination was assessed at 2, 3 and 4 days after incubation. Bars are S.E.M of 3 replicate experiments.

ANOVA tests on germination on PEG infused media indicated that only the factor PEG concentration had a significant ($p<0.05$) influence on germination (Appendix 13). Further analysis using LSD revealed no significant ($p<0.05$) differences in germination rates between the genotypes on all PEG levels at 2 days after incubation. A similar trend was obtained on day 3 and 4, except for media infused with 40% PEG. On 40% PEG infused media, lowest and highest germination rates were obtained on *p35S:AtGCN2*A and *Atgcn2-1* seeds, respectively, and these were significantly ($p<0.05$) different (Table 4). However WT Col-0 germination rates were not significantly ($p>0.05$) different from those of *p35S:AtGCN2*A and *Atgcn2-1* seeds (Table 4.4).

Table 4.4. Variation in germination of WT Col-0, *Atgcn2-1* and *p35S:AtGCN2*A seeds under PEG6000-induced osmotic stress. Seeds were spread on ½ MS containing 0.7% sucrose infused with 0, 20 and 40% PEG6000 solution and germination assessed at 2, 3 and 4 days after incubation.

PEG6000	Genotype	% Germination*		
		Day 2	Day 3	Day 4
0%	WT Col-0	45.7**d**	73.5**c**	83.6**d**
	Atgcn2-1	39.9**d**	78.9**c**	80.8**cd**
	*p35S:AtGCN2*A	40.8**d**	70.1**c**	77.5**cd**
20%	WT Col-0	30.1**cd**	72.4**c**	75.6**cd**
	Atgcn2-1	26.2**bc**	76.4**c**	77.2**cd**
	*p35S:AtGCN2*A	17.3**abc**	63.3**bc**	70.6**bc**
40%	WT Col-0	12.5**ab**	54.5**ab**	61.3**a**
	Atgcn2-1	11.3**ab**	67.7**bc**	69.1**bc**
	*p35S:AtGCN2*A	4.1**a**	42.7**a**	53.2**a**
LSD value		**16.97**	**18.19**	**11.03**

*****Values in columns with the same letter are not statistically ($p<0.05$) different as distinguished using LSD values. Values are means of 3 replicate experiments.

The effect PEG-induced osmotic stress on primary root growth on MS media infused with 70% PEG (ca.-37.58MPa) solution was also evaluated. As described in earlier experiments evaluating root growth, 6 day old *Arabidopsis* seedlings were transferred on PEG infused plates and root growth assessed after 10 days. Root growth on media infused with 0% PEG was highest and lowest with *p35S:AtGCN2*A and *Atgcn2-1* seedlings, respectively (Fig. 4.17A & B). Unlike 0% PEG, root growth on media infused with 70% PEG, the highest and lowest root growth was obtained with *Atgcn2-1* and WT Col-0 seedlings, respectively (Fig. 4.17A & B). ANOVA tests revealed that factors PEG treatment and interaction (PEG×Genotype) had significant ($p<0.05$) influence on root growth, but factor genotype alone did not (Appendix 14). Further analysis of root growth using LSD values also revealed that *Atgcn2-1* root growth on media infused with 70% PEG was significantly different from that achieved on WT Col-0 seedlings (Fig. 4.17B).

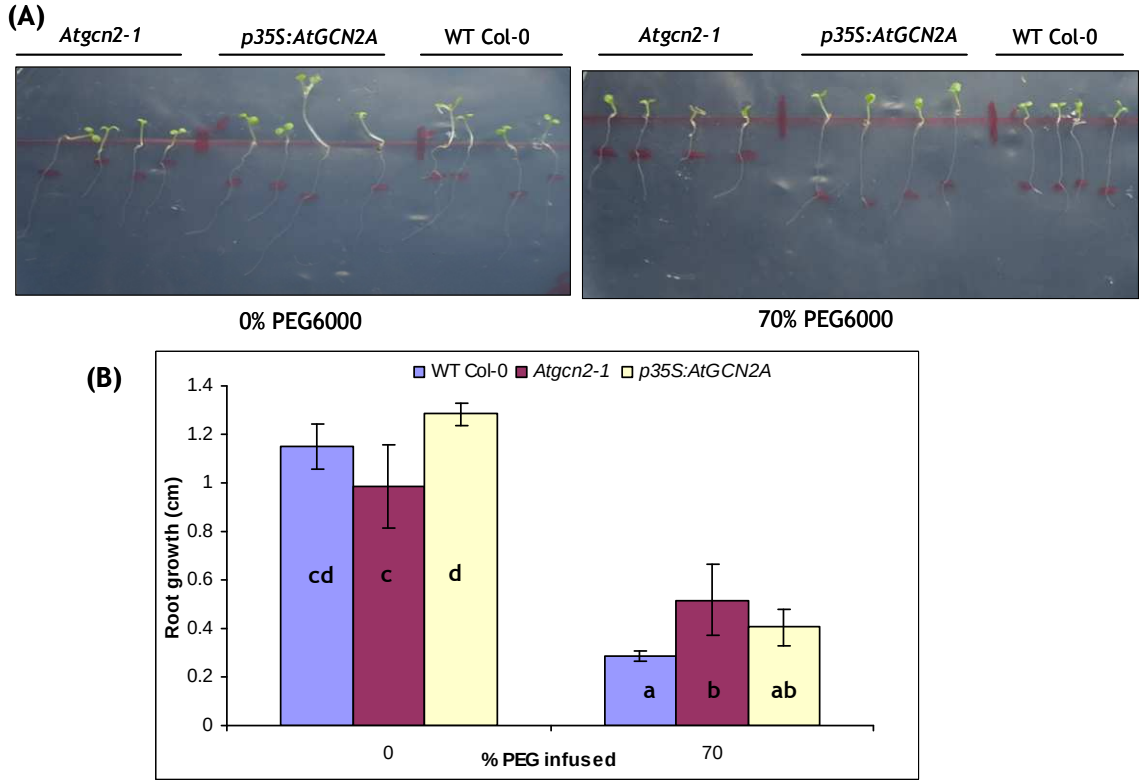

Figure 4.17. Effects of PEG-induced osmotic stress on root growth of WT Col-0, *Atgcn2-1* and *p35S:AtGCN2*A seedlings. Six day-old seedlings of WT Col-0, *Atgcn2-1* and AtGCN2 over expressing lines were transplanted onto MS media containing 0.7% sucrose infused with 0 and 70% PEG solution. Root growth was assessed after 10 days. Bars on the graph represent S.E.M of 3 replicate experiments and graphs with the same letters are not significantly ($p<0.05$) different based on LSD value (0.20).

4.5 Germination of *p35S:AtGCN2* Line on Media Containing ABA

Over 80% germination was obtained with seeds spread on media devoid of ABA (0 µM) at 2, 3 and 4 days after incubation, however, only up to 12%, 17% and 18%, respectively was achieved on *p35S:AtGCN2*A seeds spread on 0.5 µM. Increasing ABA concentration reduced germination drastically with the lowest rates achieved on 2 µM ABA (Appendix 15). On the other hand increasing the assessment period to 7, 14 and 21 days increased germination with over 70% achieved on all seed genotypes spread on media containing 0.5 and 1.0 µM ABA

(Fig. 4.18A). Lower germination rates were scored between 2-7 days after incubation; however most seeds had ruptured testa, but with radicle covered by micropylar endosperm hence scored as non-germinated (Fig. 4.18B). Only seeds which had protruding radicle that had ruptured the micropylar endosperm were scored as germinated (Fig. 4.18B). Although increasing assessment period up to 21 days resulted in increased germination, seedling growth was significantly inhibited in all the genotypes and no greening of the cotyledons was observed at any ABA treatment.

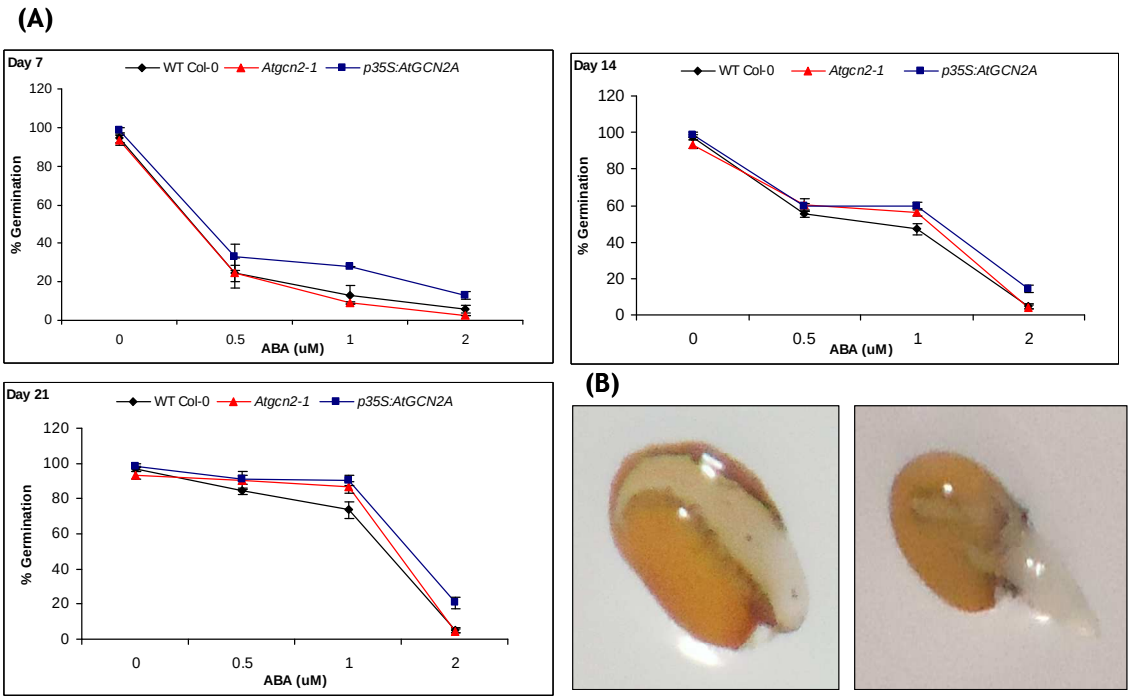

Figure 4.18. Effects of ABA concentrations on germination of *Atgcn2-1*, WT Col-0 and *p35S:AtGCN2*A *Arabidopsis* seeds. **(A)** Germination of *Atgcn2-1*, WT Col-0 and *p35S:AtGCN2*A ½ MS media containing 0, 0.5, 1.0 and 2.0 µM ABA after 7, 14 and 21 days. **(B)** Left: non-germinated seeds with ruptured testa and radicle covered with microplar endosperm, right: germinated seed with radicle protruding from the micropylar endosperm. Bars on the graph represent S.E.M of 3 replicate experiments.

4.6 Response of *p35S:AtGCN2* Line to Temperature Shock

4.6.1 Cold Shock Treatment

Temperature acclimation of WT Col-0 seedling at 4^{o}C activates the AtGCN2 kinase (section 3.4.4), for this reason the response of *p35S:AtGCN2*A to cold tolerance was investigated. To induce cold shock, 14-day old WT Col-0, *Atgcn2-1* and *p35S:AtGCN2*A seedlings were incubated at -20^{o}C in dark for 25 min as acclimated or non-acclimated seedlings. The survival of seedlings was assessed at 12-days after cold shock, and irrespective of genotype, acclimation increased seedling tolerance to cold shock as opposed to non-acclimated seedlings. The WT Col-0 and *p35S:AtGCN2*A seedlings whether acclimated or not, were generally tolerant to cold shock compared with *Atgcn2-1* seedlings (Fig. 4.19A). A higher survival rate was achieved with cold acclimated WT Col-0 seedlings after a cold stress, whereas the lowest survival rate was obtained on *Atgcn2-1* seedlings (Fig. 4.19B). ANOVA tests revealed that factor genotype significantly ($p<0.05$) influenced seedling survival after cold shock (Appendix 16). On the other hand WT Col-0 seedlings had the highest survival rate but their survival was not significantly ($p<0.05$) different from *p35S:AtGCN2*A seedlings (Fig. 4.19B).

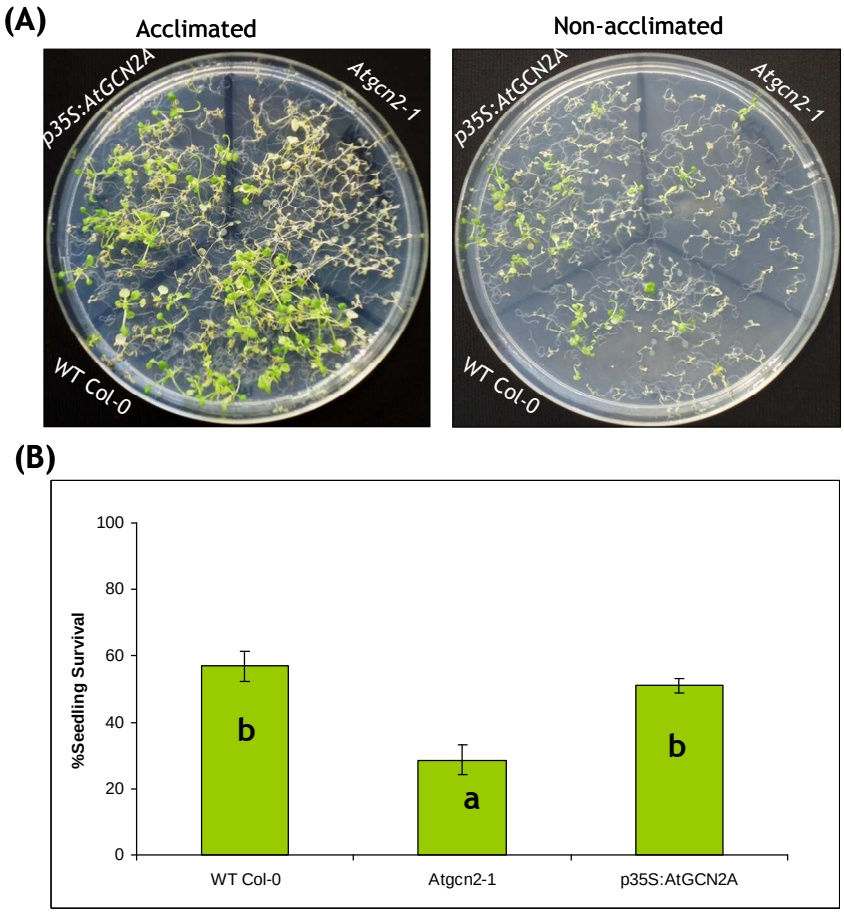

Figure 4.19. Survival of *p35S:AtGCN2*A seedlings after cold shock treatment. **(A)** Images of seedlings observed at 12 days after cold shock for acclimated and non-acclimated seedlings. **(B)** Graph showing the survival of acclimated WT Col-0, *Atgcn2-1* and *p35S:AtGCN2*A seedlings after cold shock treatment. Bars on the graphs are S.E.M of 3 replicate experiments. Graphs with the same letters are not different based on LSD value (12.4).

4.6.2 Heat Shock Treatment

Heat acclimation (37^{o}C) also activated AtGCN2 kinase (section 3.4.4). To induce heat shock, 14-day old non- and acclimated seedlings were exposed to 44^{o}C for 1, 2 and 3h in dark and then immediately transferred back to the growth chamber. Initial preliminary experiments were conducted using 7- and 14-day old seedling to determine the effect of time on survival of seedlings after heat shock. Heat shocking the 7 and 14-day old seedlings for 2 and 3 hour killed all

seedlings irrespective of the genotype (Fig. 4.20A & B), unlike when seedlings were shocked for 1 h. Heat shock experiment for non- and acclimated seedlings was therefore conducted by subjecting 7-day old seedlings to heat shock for 1 h and survival assessed at 7 days after heat shock treatment. Significant damage was observed mainly on the leaves especially for the non-acclimated seedlings compared with the acclimated seedlings, where actual leaf damage was minimal. At 12 days after heat shock new leaves were observed emerging from non- and acclimated seedlings (Fig. 4.20C & D), suggesting seedling recovery after heat shock. Unlike in the cold shock experiment, there were no obvious survival differences with respect to genotype observed after heat shock for non- and acclimated seedlings.

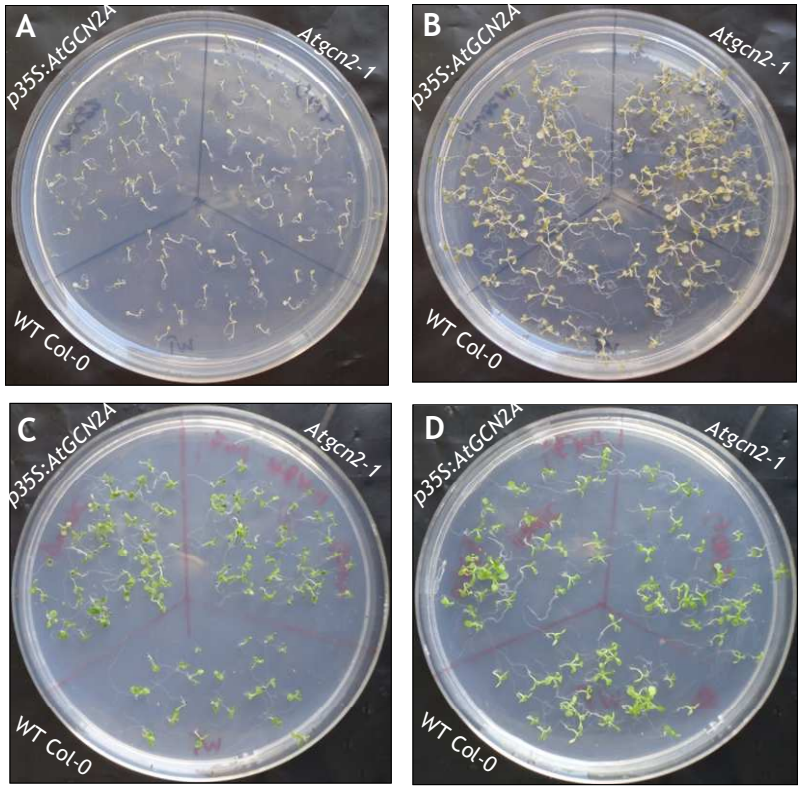

Figure 4.20. Ectopic expression of *AtGCN2* does not confer heat-shock tolerance in *Arabidopsis*. (A & B) Images of 7 and 14 days old acclimated WT Col-0, *Atgcn2-1* and *p35S:AtGCN2*A seedlings observed at 14 days after 2 h of 44^{o}C heat shock. **(C & D)** Survival of non- and acclimated 14-day old seedlings at 12 days after heat shock treatment for 1 h at 44^{o}C.

4.7 Discussion

4.7.1 Ectopic Expression of AtGCN2 Kinase Increases Primary Root Growth

The ectopic AtGCN2 expressing lines were generated by transforming *Atgcn2-1* mutant line possessing non-functional truncated AtGCN2 kinase. Therefore *in planta* phosphorylation of AteIF2α when the *p35S:AtGCN2* (A and F) and *p35S:GFP:AtGCN2* seedlings were treated with 150 µM glyphosate confirmed the presence of a functional AtGCN2 kinase in the null mutant line (Fig. 4.5). Furthermore the phosphorylation results demonstrated that ectopic expression of AtGCN2 under the control of 35S promoter successfully complemented the null mutation (truncated AtGCN2 kinase). Apart from complementing the null-mutation, ectopic expression of AtGCN2 kinase also produced a phenotype with increased primary root growth compared with WT Col-0 and *Atgcn2-1* seedlings. The effect of AtGCN2 ectopic expression on root growth was consistent in all MS media with or without NaCl, KCl and mannitol, except for PEG6000-infused media (Fig. 4.8, 4.11, 4.15 & 4.17). Plant growth is generally localised in regions with intense cell division (mitosis and cytokinesis) known as meristems. Active meristems are located at the tips of the stems and roots known as shoot and root apical meristems, respectively. Primary growth occurs as a result of the activities in the apical meristems, where cell division is followed by remarkable increase in length and width of cells (Sharp *et al.*, 2004). This is more often followed by differentiation into specialised cells from which elaborate shoot and root systems are formed (Leibfried *et al.*, 2005). Maintenance of these stem cells in *Arabidopsis* root meristem is therefore required for its indeterminate growth, and hence mutation or interference of genes involved in the maintenance of stem cells can lead to cessation of root growth (Dhondt *et al.*, 2010; Hernandez-Barrera *et al.*, 2011). Therefore increased primary root growth observed in the *p35S:AtGCN2*A line and reduced primary root growth in the *Atgcn2-1* seedlings suggested that AtGCN2 kinase may be involved in *Arabidopsis* primary root growth. There are reports suggesting that kinases in *Arabidopsis* seem to influence seed germination, seedling growth and even root growth. The kinases reported to regulate such growth activities are SNF1-RELATED PROTEIN KINASE 2.2 and 2.3 (SnRK2.2 and 2.3). Although

SnRK2.2 and 2.3 act redundantly, studies on double knock-out have shown that the two kinase seem to control root growth by mediating ABA signalling (Fujii *et al.*, 2007). On the other hand, localisation of GFP:AtGCN2 fusion protein in the root and shoot apical meristematic regions of the *Arabidopsis* seedlings (Fig. 4.6) supports the idea that AtGCN2 kinase may be involved in regulation of cell proliferation and differentiation in the root and shoot apical meristems. This is further supported by the results obtained from the analysis conducted using the *Arabidopsis* eFP browser, where significantly higher AtGCN2 expression was observed on the root zone of the zygotic embryo torpedo stage (section 4.2.4), both zygotic embryos and the meristems are usually characterised by highly ordered rapid cell divisions and elongation. The subcellular localisation of AtGCN2 kinase is predicted to be in the nucleus (section 4.2.4), this prediction is based on its protein sequence (Heazlewood *et al.*, 2005; Winter *et al.*, 2007). The nucleus consists mainly of the nucleolus and the chromatin and in most cells the nucleus contains all of the cell's chromosomes except the organellar chromosomes (Albert *et al.*, 2002). In most eukaryotes proteins are encoded in the nuclear genome and synthesized in the cytoplasm and they need to be localised at the right subcellular compartment for them to carry out their desired function (Grefen *et al.*, 2008). The nucleus coordinates cell activity such as growth, protein synthesis and cell division and therefore subcellular localisation of AtGCN2 in the nucleus suggests that it may be involved in either one or all the nucleus activities; most probably regulation of protein synthesis.

4.7.2 PEG-induced Osmotic Stress Reduced Root Growth

Increased root growth due to ectopic AtGCN2 expression did not confer tolerance to NaCl-, KCl- or mannitol-induced stress when compared with WT Col-0 and *Atgcn2-1* seedlings. This possibility is demonstrated by lack of a strong *p35S:AtGCN2*A growth phenotype compared with WT Col-0 and *Atgcn2-1* seedlings. However ectopic expression of AtGCN2 kinase increased sensitivity of *Arabidopsis* seedlings to PEG6000-induced osmotic stress compared with mannitol as demonstrated by germination and primary root growth results (Table 4.3 & 4.4; Fig. 4.15 & 4.17). Plants have evolved mechanisms that allow perception of stress cues and direct modifications in growth and development patterns that channel resources from growth related processes to stress-

alleviation mechanism (Baena-Gonzalez, 2009). Under PEG-induced osmotic stress root growth was significantly reduced in *p35S:AtGCN2* and WT Col-0 compared with *Atgcn2-1* seedlings (Fig. 4.17). These results suggested that presence of a functional AtGCN2 kinase inhibited root growth under PEG stress. As discussed in the preceding section (4.7.1), key to root growth is cell division in the root apical meristem and cessation or reduction in cell division negatively influences root growth. In addition, proliferation of meristematic cells and further differentiation is influenced by environmental, developmental or hormonal cues (Gutierrez, 2005; Petricka *et al.*, 2012). Furthermore localisation of GFP:AtGCN2 fusion protein and expression of AtGCN2 (*Arabidopsis* eFP tissue specific data) in the apical/ meristematic region of the root, which is known to be the most water permeable region of roots where salinity or osmotic stress is experienced first hand may imply that AtGCN2 kinase is involved in stress response mechanism. Although PEG6000 was not tested and reported on phosphorylation of AteIF2α in this thesis, but reduction in root growth due to PEG-induced osmotic stress suggest that AtGCN2 kinase may have been activated. Activation of the AtGCN2 pathway may have lead to reduced protein synthesis in the actively dividing meristematic cells, hence reduced cell division and root growth. Although the expression of *AtGCN2* was relatively low, the eFP browser indicated that *AtGCN2* expression in response to abiotic stress begins is first observed in root tissues during heat and drought conditions (section 4.2.4), supports the suggestion that the AtGCN2 kinase is involved in stress responses.

4.7.3 Tolerance of *p35S:AtGCN2*A Line to Temperature Shock

Plants can acquire freezing tolerance after exposure to low non freezing temperatures through a process referred to as acclimation. Cold acclimation induces cellular and physiological changes, and alteration in gene expression (Sakai & Larcher, 1987). Cold regulated genes are highly expressed during acclimation and substantially contribute to acquisition of freezing tolerance (Yadav, 2009). Proteins such as the C-REPEAT–BINDING FACTORS (CBFs) and DEHYDRATION RESPONSIVE ELEMENT-BINDING PROTEIN 1(DREB1) have been identified as transcriptional activators for expression of COLD RESPONSIVE (COR) genes (Zhu *et al.*, 2005). Furthermore ectopic expression of CBF in plants conferred tolerance against freezing even in the absence of acclimation (Jaglo-

Ottosen *et al.*, 1998). Apart from the CBF–dependent pathway, CBF-independent pathways have also been recognised as necessary for cold acclimation, and hence their elucidation is required to understand cold tolerance mechanism in plants (Kim *et al.*, 2009). The cold shock results described in this thesis, confirmed that acclimation conferred cold tolerance to *Arabidopsis* seedlings irrespective of the genotype. In addition, the results also suggested that the level of tolerance for the three genotype tested was influenced by the presence of a full-length functional AtGCN2 kinase (WT Col-0 and *p35S:AtGCN2*A seedlings) as opposed to a truncated one (*Atgcn2-1*). Therefore, whether participation of AtGCN2 kinase is crucial for cold tolerance in *Arabidopsis* needs to be investigated further. The results obtained in section 3.4.4 of this thesis however clearly demonstrate that AtGCN2 kinase is activated by cold acclimation, just like the expression of cold regulated genes. Similarly prolonged exposure to 4^{o}C also induced expression of *AtGCN2* albeit at a low level over a 12 h period (section 4.2.4).

Heat-stress occurs when ambient temperature is raised above optimum level, leading to damage of cellular component, and followed by metabolic malfunctions and cell death (Wang *et al.*, 2003). Sustained heat-stress or shock can have devastating effects on cell function, and leads to production of reactive oxygen species (Suzuki & Mittler, 2006; Volkov *et al.*, 2006). The primary defence to heat stress is induction of heat shock proteins that maintain the native configuration and function of cellular proteins, and hence protect them from heat denaturisation (Kregel, 2002). In the heat shock recovery experiment reported herein results obtained indicated that there were no differences in survival rates of the three genotypes tested whether acclimated or non-acclimated for seedling subjected to 44^{o}C for 1 h. These results suggest that the AtGCN2 mutants are not sensitive or tolerant to heat shock relative to WT Col-0 seedlings; suggesting that AtGCN2 kinase may not be directly involved in *Arabidopsis* heat stress tolerance. This is further confirmed by extremely low expression level (1.11 fold) obtained only on the roots obtained AtGCN2 was analysed with *Arabidopsis* eFP browser (section 4.2.4).

4.7.4 Germination and Growth of *p35S:AtGCN2*A Seedlings

Successful germination and seedling establishment are the most critical early stages of plant growth and development. However, under field conditions germination is generally limited by salinity and drought, which elicit osmotic and ionic stress (Mittler, 2006). Both salinity and drought elicit osmotic stress, however they induce divergent signalling components to alleviate low water potential stress (Vallejo *et al.*, 2010). Nonetheless there are reports suggesting that in seeds some of the osmotic and ionic response pathways are shared while others are specific (Zhu, 2002). Germination results reported herein revealed that both null-mutation and ectopic expression of AtGCN2 kinase generally increased seed germination compared with wild type under non- and salinity-stress conditions. Furthermore germination of WT Col-0 seeds was sensitive to NaCl induced-stress than KCl, when compared with *Atgcn2-1* and *p35S:AtGCN2*A seeds. Rapid response to salinity stress by plants usually occurs within hours of exposure, which resembles osmotic-stress induced by non-ionic solutes, whereas ionic stress occurs after days or weeks of exposure (Munns, 2002). In this study, germination was assessed at between 2-4 days after exposure to salinity stress, therefore results reported herein suggests that germination was influenced by ionic rather than osmotic stress, apart from the influence of seed genotype.

Germination rates obtained on WT Col-0, *Atcgn2-1* and *p35S:AtGCN2*A increased with assessment period on media supplemented with either NaCl or KCl, suggesting delayed germination, however presence of Na^+ significantly delayed germination compared with K^+ ions. Various molecules have been reported to play key roles in plant-response to abiotic stress. One of these key molecules that has been reported to partly mediate salinity stress is ABA (Munns & Tester, 2008). Delayed germination and early seedlings growth has been associated with ABA adaptive responses, that allow plants to delay start of growth until conditions are favourable (Verslues *et al.*, 2006; Holdsworth *et al.*, 2008). However exogenous application of ABA significantly inhibited germination and establishment of WT Col-0, *Atgcn2-1* and *p35S:AtGCN2*A seedlings, suggesting that ectopic expressing and null *Arabidopsis* mutants were sensitive to ABA, similar to the wild type. Despite early germination of *Atgcn2-1* and *p35S:AtGCN2*A seeds, there were no significant advantage for seedling growth

and establishment on NaCl, KCl and mannitol supplemented media. This observation is in agreement with reports indicating that high rate of germination under salt stress is not correlated with salinity tolerance at later developmental stages (Almansouri *et al.*, 2001). Furthermore on media with high sucrose seed germination and growth can occur in the presence of relatively high salt, which is normally blocked by ABA (Ruggiero *et al.*, 2004). Therefore higher rate of germination for *Atgcn2-1* and *p35S:AtGCN2*A seeds on NaCl and KCl media cannot be associated with salinity tolerance.

5 Chapter 5: *In vitro* Translation Control of AtmRNA

5.1 Introduction

As discussed earlier in section 1.13 and 1.14, there are several steps involved in translation initiation process. These include recruitment of the Met-tRNA$_i^{Met}$ and mRNA to the 40S ribosomal subunit containing the ternary complex, and after several steps, the hydrolysis of the GTP bound to eIF2α and subsequent release of GDP and eIF2α from the 40S subunit (Albert *et al.*, 2002). To participate in further rounds of initiation and translation the GDP bound to eIF2α must be exchanged for GTP. However when eIF2α is phosphorylated the exchange of GDP to GTP is inefficient and thus translation initiation is inhibited (Asano *et al.*, 2000).

Regulation of translation mediated by phosphorylation of eIF2α is an essential mechanism by which eukaryotic cells adjust their gene expression in response to cellular or environmental stress (Wek *et al.*, 2006). In mammals, the mechanism entails induction of a transcriptional activator ATF4 (a bZIP transcription factor; a basic leucine zipper), among other regulatory proteins such as ATF6 (Lu *et al.*, 2004; Vattem & Wek, 2004). In yeast it is involved in the induction of GCN4, also a regulatory bZIP transcriptional activator (Hinnebusch, 1997; Hinnebusch, 2005). In both yeast and mammals the induction of GCN4 and ATF4 transcriptional activators is dependent on eIF2α phosphorylation state and controlled by upstream open reading frames (uORFs) in their 5′ UTRs (Hinnebusch, 1997; Lu *et al.*, 2004). Although not well described, components of this mechanism have already been identified in plants (Zhang *et al.*, 2003; Zhang *et al.*, 2008). In addition ClustalW2 analysis reported herein also revealed conserved amino acid residues in *Arabidopsis* eIF2α, yeast and mammals (see Fig. 3.7). Furthermore a biochemical and immunological homologue of human PKR kinase has been reported in wheat (Langland *et al.* 1996). Although a homologue of this kinase was not found in *Arabidopsis*, as reported in section 3.2 of this thesis, there are however reports suggesting the existence of a plant ortholog of mPKR kinase inhibitor referred to as P58^{IPK} in *Arabidopsis* and

Nicotiana benthamiana, but its biological significance in mammalian and plant systems is different (Bilgin *et al.*, 2003).

There are no plant homologues of ATF4 or GCN4 reported in literature, however *Arabidopsis* bZIP28 is reported to be structurally similar to mammalian ATF6 and implicated in the mitigation of unfolded protein-stress in the endoplasmic reticulum (Liu & Howell, 2010). In mammalian systems endoplasmic reticulum stress due to mis-folding of proteins activates PERK kinase which then phosphorylates eIF2α leading to reduced mRNA translation and hence protein substrate for folding or degradation in the endoplasmic reticulum (Yan *et al.*, 2002); however there are no reports of PERK kinase homologue in plants. Based on the available evidence thus far, this chapter reports on the use of an *in vitro* translation system to demonstrate that phosphorylation of eIF2α inhibits translation of *Arabidopsis* mRNA. It also focuses on the use of a bioinformatics approach to identify putative ScGCN4 or HsATF4 homologues in *Arabidopsis*.

5.2 Cloning and Expression of *Arabidopsis* eIF2α-subunit

5.2.1 The *Arabidopsis* eIF2α Loci

Eukaryotic initiation factor 2 (eIF2) is a trimeric GTP/GDP-binding protein consisting of the three subunits namely; α (35kDa), ß (38kDa) and γ (52kDa). In this study the α-subunit was of interest and as discussed earlier its primary function is to recruit Met-tRNA$_i^{Met}$ in a GTP/GDP-dependent manner. It is also involved in the identification of the initiation AUG codon as well as recruiting charged tRNAs (aminoacylated-tRNA) to the P-site during protein synthesis (Merrick, 1992). In order to investigate *in vitro* phosphorylation of the α-subunit and down regulation of protein synthesis, *Arabidopsis* eIF2α-subunits were cloned and expressed in an *E. coli* system.

Arabidopsis has two eIF2α loci annotated in TAIR (www.arabidopsis.org) database as At2g40290 and At5g05470. The At2g40290 locus has three splice variants (At2g40290.1, At2g40290.2 and At2g40290.3), whereas At5g05470 has none. Due to the presence of At2g40290 splice variants there was need to identify a representative sequence for the At2g40290 locus. This was achieved

by conducting ClustalW2 analysis of amino acid sequences of the three splice variants. The results obtained revealed that the amino acid sequence for the splice variants At2g40290.2 and At2g40290.3 were similar and that the two seem to be truncated versions of At2g40290.1. The splice variant At2g40290.1 was therefore selected as a representative of the At2g40290 locus. Another ClustalW2 analysis was also conducted to compare similarities between the two eIF2α loci (At2g40290 and At5g05470) using amino acid sequences for At2g40290.1, At2g40290.2 and At5g05470.1. The results obtained clearly illustrate that the two loci are similar except for a few amino acid residues (Fig. 5.1A). Furthermore, they both possess highly conserved amino acid residues flanking the SEL**S** domain (Fig. 5.1A). Although the alignment results show that At2g40290.1 (*AteIF2*90) and At5g05470.1 (*AteIF270*) were not different, because the two contain 7 exons (Fig. 5.1B). However, the gene structure of the two loci appears to be different, especially the length of exons 3, 4, 5 and 6, and an intron between exon 5 and 6 (Fig. 5.1B). For these reasons the two *AteIF2a* (*AteIF290* and *AteIF270*) genes were cloned for expression using the *E. coli* system.

(A)

```
At2G40290.1     MASQTPNLECRMYEAKYPEVDMAVMIQVKNIADMGAYVSLLEYNNIEGMILFSELSRRRI 60
At2G40290.2     MASQTPNLECRMYEAKYPEVDMAVMIQVKNIADMGAYVSLLEYNNIEGMILFSELSRRRI 60
AT5G05470.1     MANPAPNLECRMYESRYPDVDMAVMIQVKTIADMGAYVSLLEYNNIEGMILFSELSRRRI 60
                **. :*********::**:**********.****************************

At2G40290.1     RSVSSLIKVGRIEPVMVLRVDKEKGYIDLSKRRVSEEDIQTCEERYNKSKLVHSIMRHVA 120
At2G40290.2     RSVSSLIKVGRIEPVMVLRVDKEKGYIDLSKRRVSEEDIQTCEERYNKSKLVHSIMRHVA 120
AT5G05470.1     RSISSLIKVGRTEPVMVLRVDRERGYIDLSKRRVSDEDKEACEERYNKSKLVHSIMRHVA 120
                **:******** *********:*:**********:** ::******************

At2G40290.1     ETLSIDLEDLYVNIGWPLYRRHGHAFEAFKILVTDPDSVLGPLTREIKEVGPDGQEVTKV 180
At2G40290.2     ETLSIDLEDLYVNIGWPLYRRHGHAFEAFKILVTDPDSVLGPLTREIKEVGPDGQEVTKV 180
AT5G05470.1     ETVGVDLEELYVNIGWPLYKKHGHAFEAFKIVVTDPDSVFDALTREVKETGPDGVEVTKV 180
                **:.:***:**********::**********:*******:..****:**.**** *****

At2G40290.1     VPAVTEEVKDALVKNIRRRMTPQPMKIRADIELKCFQFDGVVHIKEAMKNAEAAGNEDCP 240
At2G40290.2     VPAVTEEVKDALVKNIRRRMTPQPMKIRADIELKCFQFDGVVHIK-------------- 225
AT5G05470.1     VPAVSEELKDAFLKDIRRRMTPQPMKIRADIELKCFQFDGVLHIKEAMKKAEAVGTDDCP 240
                ****:**:****::*:*************************:***

At2G40290.1     VKIKLVAPPLYVLTTQTLDKEQGIEILNKAIAACTETIETHKGKLVVKEGARAVSERDEK 300
At2G40290.2     ----------VVSLIRLS---------------------------------------- 233
AT5G05470.1     VKIKLVAPPLYVLTTHTHYKEKGIVTLNKAIEACITAIEEHKGKLVVKEGARAVSERDDK 300
                          *::

At2G40290.1     MLTEHMAKLRLDNEEMSGDEDSGDEEEDTGMGEVDLDAGAGIIE 344
At2G40290.2     -LTCEMNTL------------------------------------ 241
AT5G05470.1     LLAEHMAKLRMDNEEMSGDEGSEDEEEDTGMGEVDIDGGSGIIE 344
                   *:.*.*
```

(B)

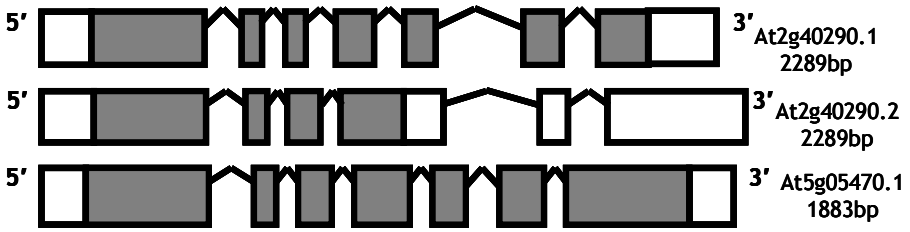

Figure 5.1. ***Arabidopsis thaliana*** **has two eIF2α loci.** **(A)** ClustalW2 alignment of *AteIF2a* full-length protein sequences. The phosphorylation site serine 56 (S56) is located on a conserved SEL**S** domain highlighted in turquoise. **(B)** Illustrations of *Arabidopsis* full-length gDNA sequences of At2g40290.1, At2g40290.2 and At5g05470.1 genes. The schematic representations of the genes are drawn to scale using annotations obtained from TAIR (www.Arabidopsis.org). Regions shaded in grey represent exons, un-shaded regions represent non-coding sequence and lines represent the introns.

5.2.2 Cloning of *Arabidopsis eIF2a* Splice Variants

To clone the two AteIF2α genes (*AteIF290* and *AteIF270*), a PCR was conducted with cDNA as template and the amplified *AteIF290* and *AteIF270* fragments (Fig. 5.2A) were extracted from an agarose gel and cloned into pCR4-TOPO sequencing vector. The *AteIF2a* fragments were then subcloned from *pCR4-TOP:eIF2a* constructs into the pENTR4 Gateway entry vector after restriction

with *Nco I* and *Not I* enzymes (Fig. 5.2B). The *pENTR4:eIF2a* constructs were maintained in TOP10 *E. coli* and results of colony PCR performed to select positive clones show that out of the 6 colonies tested only 3 produced distinct PCR products, two of which were from cells transformed using the *pENTR4:eIF270* construct (Fig. 5.2C). Plasmid mini preps were set up using the positive colonies showing the presence of *AteIF2a* inserts was confirmed by restriction digestion using *Nco I* and *Nde I* enzymes (Fig. 5.2D). The *AteIF2a* fragments in the pENTR4 vector were then sub-cloned into pDEST17 Gateway expression vector through LR reaction and maintained in DH5α *E. coli* cells. The protein expression vector pDEST17 has a 6×Histidine N-terminal tag, thus fusion protein expressed using this vector contain an N-terminal 6×His tag.

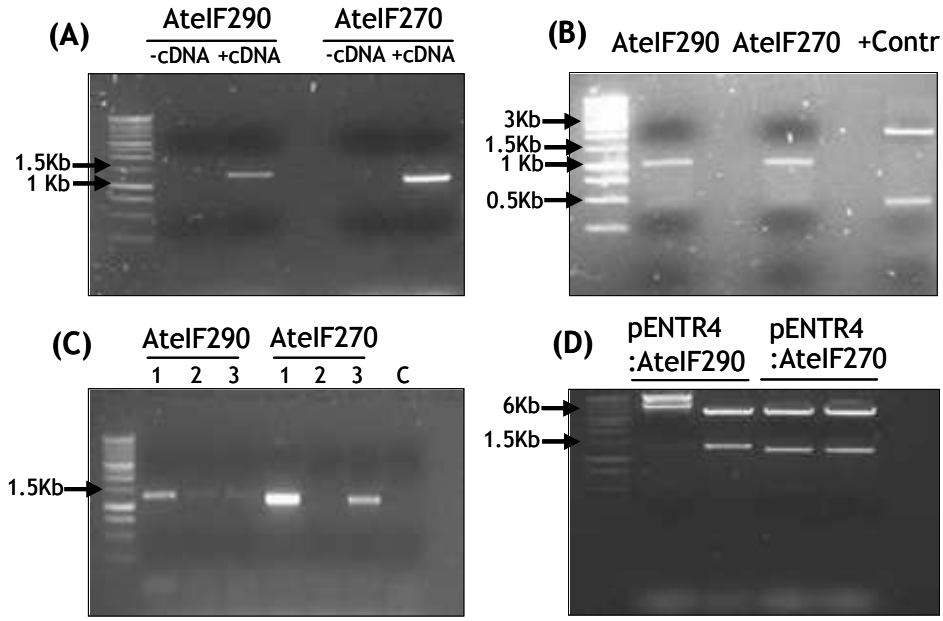

Figure 5.2. Cloning of Atg40290.1 (*AteIF290*) and At5g05470.1 (*AteIF270*) sequences into pENTR4 Gateway® entry vector. **(A)** PCR amplification of *AteIF290* and *AteIF270* using cDNA template, **(B)** Restriction digestion of PCR amplified *AteIF290* and *AteIF270* fragments containing *NcoI* and *NdeI* sites, **(C)** Colony PCR of *E. coli* cells transformed with *pENTR4:eIF2a* constructs, **(D)** Restriction digestion of the isolated *pENTR4:AteIF290* and *pENTR4:AteIF270* vector constructs using *NcoI* and *NdeI* enzymes.

The authenticity of *AteIF2a* inserts in pCR4®-TOPO (Fig. 5.3A) was confirmed by sequencing using T7 and T3 universal primers (Table 2.1) and the nucleic acid sequences of the cloned *AteIF2a* fragments were aligned with sequences deposited in TAIR and were found to be a 100% match (Appendix 17). Similarly confirmation by sequencing of the *AteIF2a* inserts in pENTR4 and pDEST17 vectors (Fig. 5.3B) was conducted using Pentr4U and Pentr4L, T7 universal and PDest17Rv primers, respectively (Table 2.1).

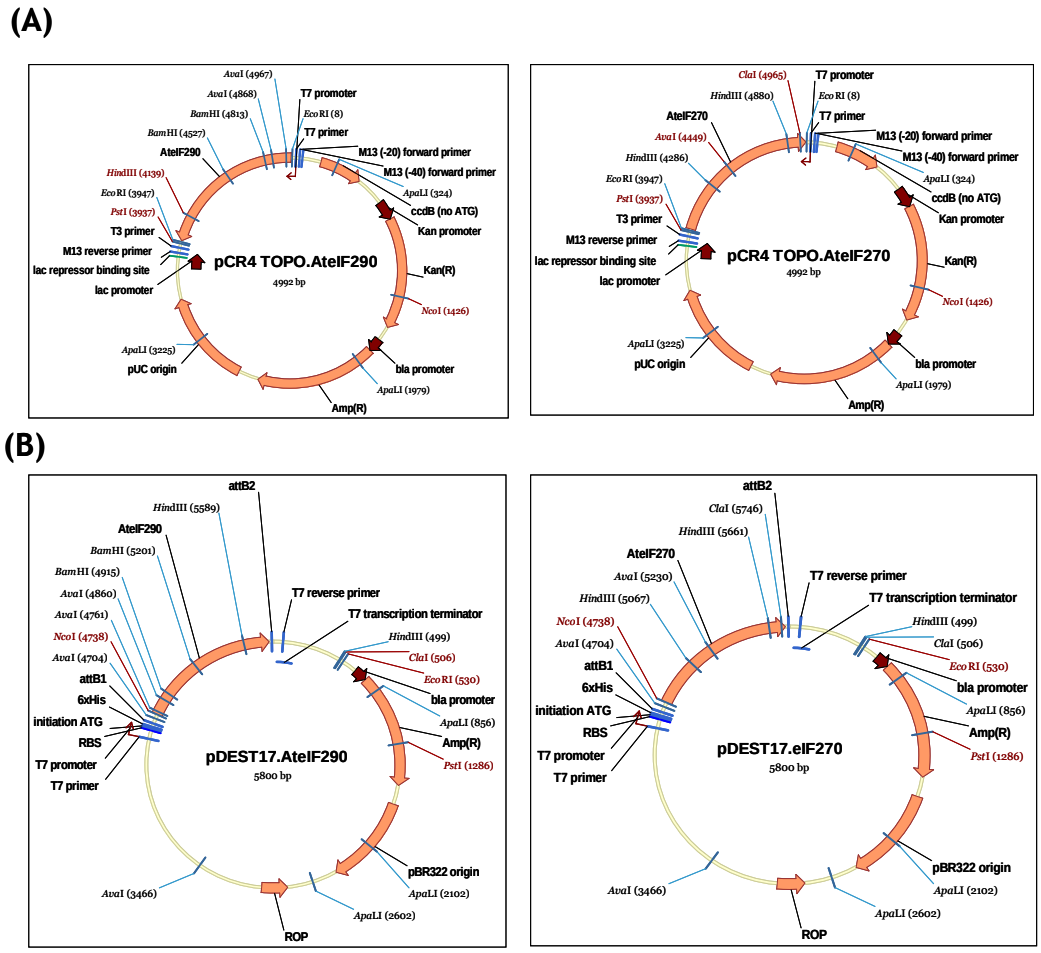

Figure 5.3. Sequencing and expression construct of *AteIF290* and *AteIF270* fragments. **(A)** *pCR4:AteIF2a* sequencing constructs, **(B)** *pDEST17:AteIF2a* expression constructs.

5.2.3 Expression and Purification of AteIF2α-subunits

5.2.3.1 Optimization of AteIF2α Expression in *E. coli*

The generated *pDEST17:AteIF2α* expression constructs were used to transform chemically competent BL21(DE3) *E. coli* expression cells. Then expression of 6×His.AteIF2α fusion protein at 23^{o} and 28^{o}C after induction with 0, 0.3, 0.5 and 1 mM IPTG was tested. SDS-PAGE analysis of the total cell lysate revealed that there was basal expression in control treatments irrespective of the construct used (Fig. 5.4A). Nonetheless substantial expression of AteIF2α fusion protein was achieved from overnight cultures incubated at 23^{o}C after induction with 0.3 and 0.5 mM IPTG. This was especially true for cells transformed with the *pDEST17:AteIF290* construct although optimal expression was achieved after induction with 0.5 mM IPTG (Fig. 5.4A). For cells transformed with *pDEST17:AteIF270* induction using 0.3 and 0.5 mM IPTG did not result in significant expression of fusion protein (Fig. 5.4A). During the course of conducting expression experiments, relatively slower growth rates were observed in pDEST17.*AteIF270* cultures compared with *pDEST17:AteIF290*. Further optimization experiments were conducted to assess the partitioning of AteIF2α fusion protein (6×His.eIF2α) expressed using *pDEST17:AteIF290* and *pDEST17:AteIF270* constructs. The cell cultures were induced with 0.5 mM IPTG and grown overnight at 23^{o}C, and denatured soluble protein fraction resolved by 10% SDS-PAGE and then analysed using western blots. The results obtained confirmed that substantial amount of induced fusion protein was in the soluble fraction for cells transformed with *pDEST17:AteIF290*. They also confirmed poor expression of fusion protein in cells transformed with the *pDEST17:AteIF270* construct and also basal expressions in control treatments (Fig. 5.4B). The presence of substantial amount of fusion protein in cells harbouring *pDEST17:AteIF290* after induction with 0.5 mM IPTG appeared to optimal and hence amenable for column purification.

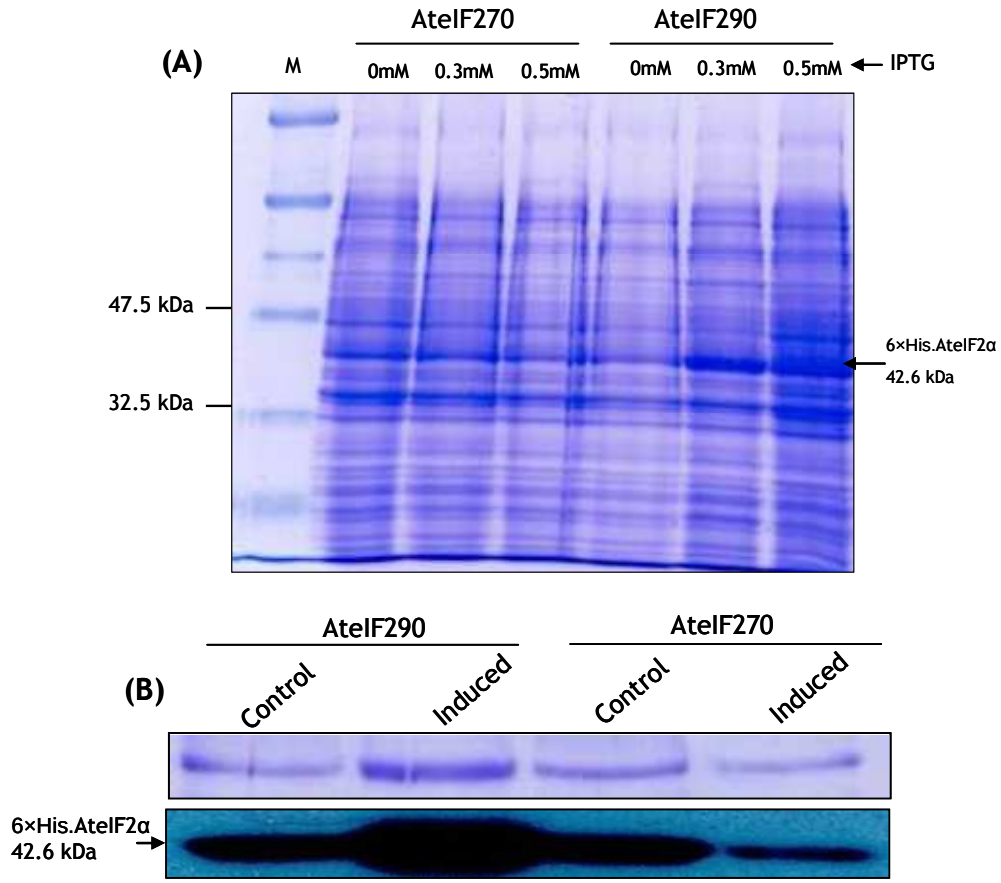

Figure 5.4. Expression of 6×His.AteIF2α fusion protein in BL21(DE3) *E. coli* cells. **(A)** SDS-PAGE analysis of 6×His.AteIF2α fusion protein in total cell lysate induced overnight at 23°C and induced by 0.3 and 0.5 mM IPTG. **(B)** Analysis of soluble fractions of 6×His.AteIF2α fusion proteins induced at 23°C overnight with 0.5 mM IPTG. Lower panel is nitrocellulose membrane probed with 6×His specific antibody.

5.2.3.2 Purification of AteIF2α Splice Variant At2g40290.1

The colony harbouring *pDEST17:AteIF90* used for the optimization experiment reported in section 5.2.3.1 was also used to set up expression cultures for purification of 6×His.eIF2α fusion protein. No IPTG was added to non-induced control cultures, whereas 0.5 mM IPTG was used to induce cultures grown overnight at 23°C. The cells for induced and control cultures were harvested, lysed using a French press and the clarified lysate was applied to the Ni-NTA agarose resin (Qiagen) column. Fusion protein elutes were collected in 1 ml fractions and concentrations of each fraction determined using the Bradford

method (Bradford, 1976). Purified AteIF290 protein fractions containing up to 1.2 mg/ml were obtained (Fig. 5.5). All fractions were pooled, concentrated and elution buffer exchanged with storage buffer to a final concentration of 2 mg/ml and samples then stored at -70°C in 50 µl aliquots. During expression and purification of AteIF290, at each step 40 µl samples were collected and then analysed on 10% SDS-PAGE. The analysis confirmed successful purification of 6×His.AteIF290 fusion protein (Fig. 5.5).

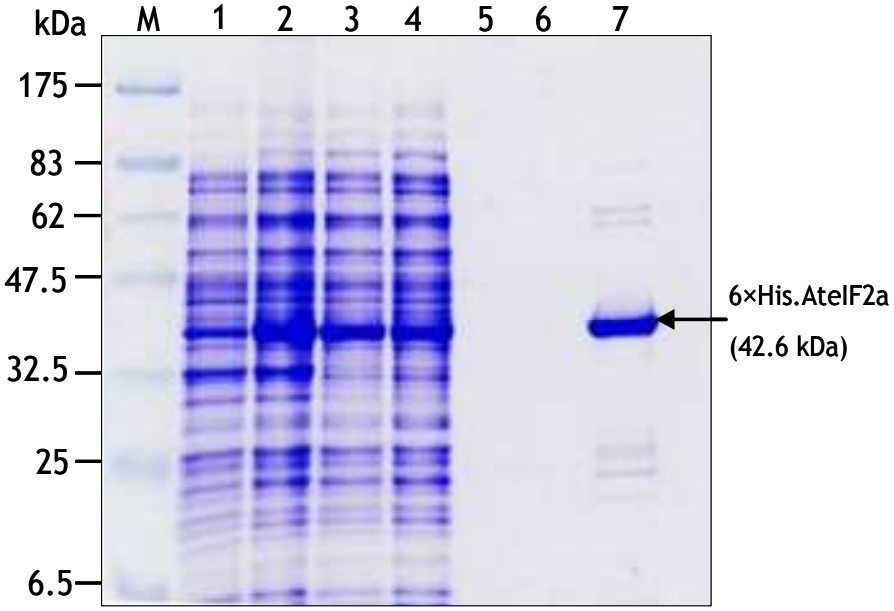

Figure 5.5. Analysis of *E. coli* expression and purification of 6×His.AteIF290 fusion protein on 10% SDS-PAGE. **M**, Protein Maker: **1**, No-induced total cell lysate: **2**, induced lysate: **3**, clarified lysate: **4**, induced column flow through: **5**, first column wash: **6**, last column wash: **7**, 1 ml fraction with highest protein concentration (1.2 mg/ml).

5.3 Expression of eIF2α Kinases in *E. coli*

5.3.1 Expression of AtGCN2 Kinase

In order to facilitate *in vitro* phosphorylation experiments there was a need to express and purify the AtGCN2 kinase. For this purpose an expression construct for the AtGCN2 kinase was generated using the *pENTR/D:AtGCN2* entry clone described in section 4.2 and pDEST17 expression vector via the LR reaction. The

resultant expression construct *pDEST17*:*AtGCN2* was used to transform competent Rosseta™ (DE3) BL21 expression cells. Repeated earlier attempts to express AtGCN2 kinase using BL21 (DE3) expression cells were unsuccessful suggesting that AtGCN2 protein was toxic. Therefore Rosseta™ (DE3) BL21 (Novagen) expression cells containing rare tRNA codons that allow expression of eukaryotic proteins that are toxic to *E. coli* cells was used. The expression of 6×His.AtGCN2 fusion protein was evaluated after induction with 0.5 mM IPTG overnight at 20, 25 and 28°C. The initial induction was assessed by 10% SDS-PAGE gels using total cell lysate shows that there was expression at all temperatures tested (Fig. 5.6A). Follow-up experiments to determine the solubility of 6×His.AtGCN2 fusion protein expressed at 20 and 28°C were conducted. This was done because the expression of recombinant protein in *E. coli* under relatively high temperatures induces increased misfolding when compared with lower temperatures (Vera *et al.*, 2007). Therefore 20 ml cultures were set up to assess the solubility of recombinant 6×His.AtGCN2 fusion protein induced at 20 and 28°C. The cultures were also induced with 0.5 mM IPTG overnight, then the soluble and insoluble fractions were analysed on 10% SDS-PAGE. The results obtained show that irrespective of the temperature used the expressed recombinant AtGCN2 kinase was present in the insoluble fraction and undetectable level in the soluble fraction (Fig. 5.6B). Due to problem associated with refolding of proteins isolated from the insoluble fraction, further purification of the AtGCN2 kinase was not pursued.

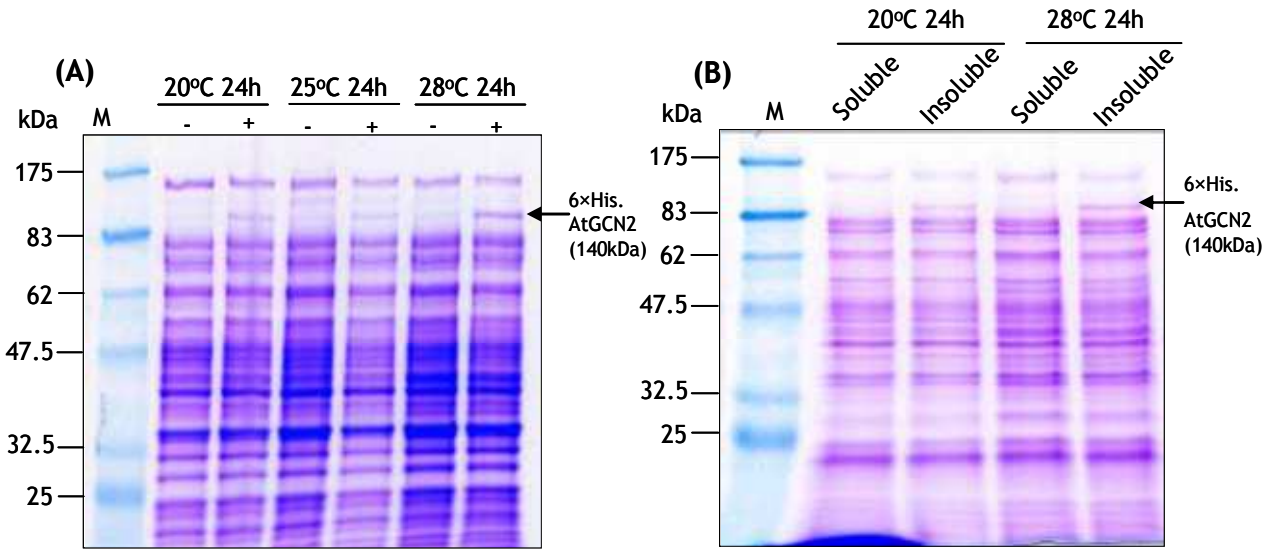

Figure 5.6. Expression of 6×His.AtGCN2 fusion protein in Rosseta™ (DE3) BL21 *E. coli* cells. (A) *E. coli* cells were transformed with pDEST17:*AtGCN2* and then expression of recombinant fusion proteins induced using 0.5 mM IPTG at 20, 25 and 28°C overnight was evaluated. (-) indicate control non-induced culture and (+) indicate culture induced with 0.5 mM IPTG. **(B)** Determination of the fraction in which recombinant 6×His.AtGCN2 fusion protein was present after induction at 20 and 28°C overnight with 0.5 mM IPTG.

5.3.2 Expression and Purification of mPKR Kinase

Although AtGCN2 kinase was successfully cloned and expressed in *E. coli*, the insoluble form induced required denaturing and refolding may not have been suitable for *in vitro* assay. Instead, expression and purification of mPKR was pursued since an optimized protocol has previously been described (Conn, 2003). The two eIF2α kinases (ScGCN2 and mPKR) have been shown to phosphorylate eIF2α-subunit *in vitro* (Cherkasova & Hinnebusch, 2003; Carnevalli *et al.*, 2006; Iida *et al.*, 2007). Furthermore dimerization of the regulatory and kinase domains is a common feature in the activation of both ScGCN2 and mPKR (Zhu *et al.*, 1996; Taylor *et al.*, 2005). Although the X-ray crystallographic structure of mPKR and ScGCN2 show distinct dimeric configuration of the kinase domain, their activation requires a conserved salt bridge; hence the proposition that mPKR and ScGCN2 structures represent active and inactive state of eIF2α kinase domains, respectively (Dey *et al.*, 2007). These reports on ScGCN2 and mPKR kinase and the conserved nature of the SEL**S** domain in the eIF2α substrate (see

Fig. 3.7) across eukaryotes guided the decision to substitute AtGCN2 with mPKR kinase to facilitate *in vitro* eIF2α phosphorylation experiments.

5.3.2.1 Expression Optimization of mPKR in Rosseta^{TM}(DE3) BL21 *E. coli* Cells

An expression vector construct *pTYB2:PKR/PPase* (Fig. 5.7) encoding the inactive form (dephophorylated) of mPKR kinase was maintained in DH5α *E. coli* cells. The *pTYB2:PKR/PPase* plasmid mini preps were prepared from 10 ml overnight cultures and used to transform Rosseta^{TM}(DE3) BL21 expression cells. The transformed cells were screened on LB medium plates supplemented with appropriate antibiotics at 37^{o}C overnight. A single distinct colony was used to set up cultures for optimizing the expression of mPKR kinase. Although there is an established mPKR expression and purification protocol using *pTYB2.PKR/PPase* construct (Conn, 2003), there was need to optimize its expression in Rosseta^{TM}(DE3) BL21 cells. This is because the protocol established earlier by Conn (2003) utilized different expression cells namely, BL21 (DE3)-CodonPlus-RIL cells (Stratagene Europe).

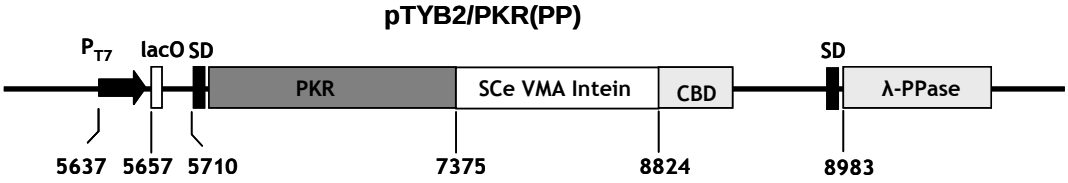

Figure 5.7. Illustration of *pTYB2/PKR(PP)* expression construct based on the IMPACT-CN vector for expression of mPKR kinase in *E. coli* (Conn, 2003). In order to obtain inactive (non-phosphorylated) form of mPKR kinase in *E. coli* a second Shine-Dalgarno region (SD) followed by the λ-protein phosphatase (λ-PP) gene were included after the intein/CBD coding region. Co-expression of mPKR with λ-PP allows expression and purification of inactive (non-phosphorylated) kinase in *E. coli* cells.

The effects of different concentrations of IPTG (0, 0.3, 0.5 and 1 mM) on the induction of mPKR at 23 and 28°C for 2, 4 and 6 h were tested. The results obtained indicated that optimum expression of mPKR was obtained in cultures induced by 0.3 mM IPTG for 6 h at 28°C. Further experimentation was conducted to assess the fractions with the highest mPKR levels. To achieve this, 100 ml cultures were induced with 0.3 mM IPTG for 6 h at 28°C. The insoluble and soluble fractions were then analysed by 10% SDS-PAGE gels. The results obtained indicate that lower levels of mPKR were present in the soluble as opposed to the insoluble fraction (Fig. 5.8).

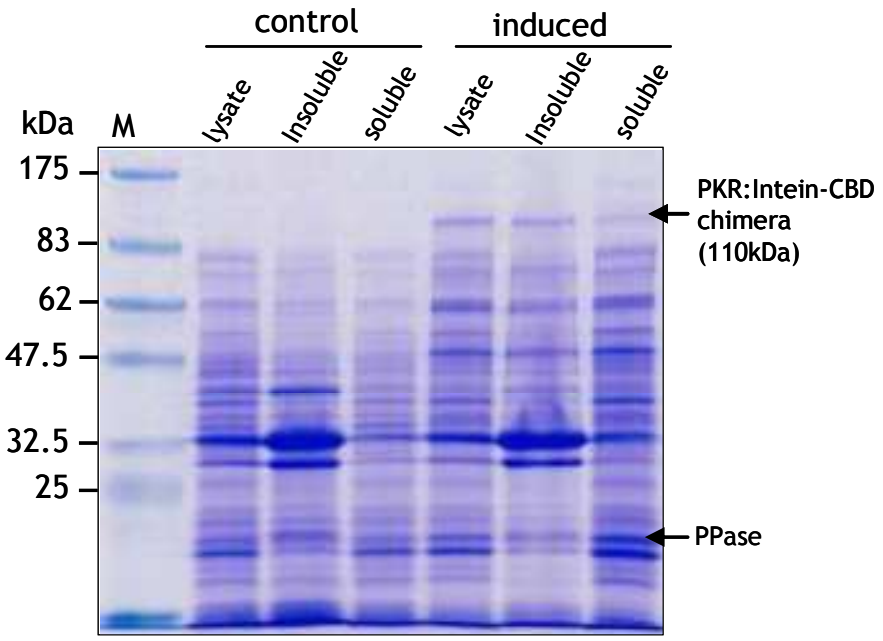

Figure 5.8. Analysis of mPKR expression in Rosseta™ (DE3) BL21 *E. coli* cells after induction with 0.3 mM IPTG at 28°C for 6 h. Total cell lysate, insoluble fraction and soluble fraction were analysed by 10% SDS-PAGE.

5.3.2.2 Purification of mPKR

A 250 ml culture of Rosseta™ (DE3) BL21 *E. coli* cells harbouring the *pTYB2/PKR(PP)* expression construct was induced with 0.3 mM IPTG for 6 h at 28°C. After induction, cells were harvested, lysed and the clarified lysate was applied to a column packed with Chitin Bead resin for purification of mPKR. After each purification step, 40 µl aliquots were collected and analysed on 10% SDS-PAGE gel. Analysis of the samples collected revealed that in spite of

relatively low expression of mPKR in *E. coli*, there was sufficient mPKR in the soluble fraction to be purified (Fig. 5.9). However the purified mPKR was co-eluted with the intein CBD (Chitin Binding Domain) tag, whereas the column flush buffer prior to elution of mPKR contained only mPKR (Fig. 5.9). For this reason, mPKR in the column flush buffer was collected in 1 ml fractions unlike in the protocol recommended by the manufacturer of the chitin resins. The mPKR in 1 ml fractions were quantified using the Bradford assay (1976) and fractions with the highest concentration contained 0.2 mg/ml of mPKR. All the protein fractions containing mPKR were pooled, column flush buffer containing mPKR was exchanged with storage buffer, and the sample then concentrated to 2.1 mg/ml and aliquots of 50 µl stored at -70^{o}C.

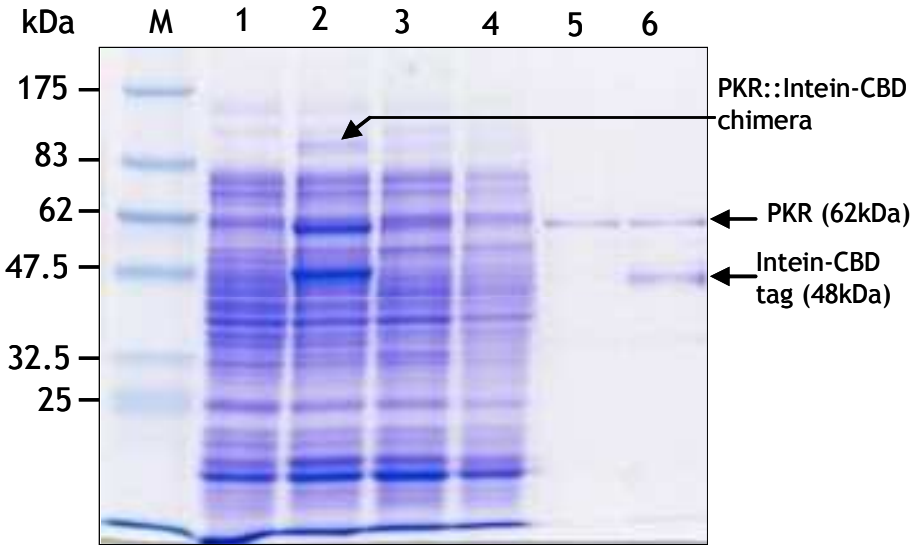

Figure 5.9. Expression and purification of mPKR using Rosseta^{TM} (DE3) BL21 *E. coli* cells. Purification of mPKR kinase using a 4 ml column packed with Chitin resin. Lanes **M**, protein marker: **1**, induced French press lysate: **2**, induced soluble fraction: **3**, column flow-through: **4**, column wash flow-through: **5**, column flush before mPKR elution: **6**, eluted mPKR fraction. Expression using pTYB2/PKR(PP) vector yielded mPKR fused with Intein-Chitin Binding Domain tag (intein-CBD) which facilitated affinity purification of the mPKR::Intein-CBD protein chimera. The mPKR is then cleaved from the intein-CBD tag and eluted.

5.4 *In vitro* Phosphorylation of AteIF2α and WGeIF2α

The purified AteIF290 and mPKR recombinant proteins were tested for their ability to act as substrate and kinase, respectively. The purified mPKR was inactive (non-phosphorylated) and therefore needed to be activated (phosphorylated) prior to use in phosphorylation experiments. The effect of double stranded RNA (poly I:C) concentrations (0, 5 and 10 µg/ml) on activation (auto-phosphorylation) of mPKR was tested. The concentrations of poly I:C tested were chosen based on reports in the literature which indicated that between 0.1-10 µg/ml of poly I:C is effective in activating mPKR *in vitro* (Langland *et al.*, 1996; Lamaire *et al.*, 2005). Activation of mPKR was achieved by both 5 and 10 µg/ml poly I:C, and this was demonstrated by the ability of the inactive mPKR kinase incubated with poly I:C to successfully induce *in vitro* phosphorylation of AteIF290 (Fig. 5.10A). The inability of inactive mPKR to induce phosphorylation of AteIF290 was also confirmed in treatments where only mPKR was added into the reaction mix (Fig. 5.10A).

As discussed earlier, phosphorylation of eIF2α by ScGCN2 and mPKR kinases induced the translation of ScGCN4 and HsATF4 mORFs by bypassing the uORFs. However the ratio of eIF2α:eIF2α-P which triggers translation of GCN4 and ATF4 mRNA has not yet been reported. Attempts to investigate the effect of mPKR concentration on phosphorylation of Wheat Germ Lysate eIF2α (WGeIF2α) and to determine the ratio of eIF2α:eIF2α-P was undertaken. To investigate *in vitro* phosphorylation and translation, Wheat Germ Lysate (WG) was chosen because it is a plant based translation system. Therefore different concentrations of inactive mPKR (0-0.2 µg/µl) were added into the WG lysate and then phosphorylation of WGeIF2α evaluated. The addition of inactive mPKR induced phosphorylation of WGeIF2α (Fig. 5.10B). Furthermore increasing the concentration of inactive mPKR resulted in increased WGeIF2α-P signal (Fig. 5.10B). However the absolute de-phosphorylation and phosphorylation status of the WGeIF2α hence WGeIF2α:WGeIF2α-P ratio could not be determined in this experiment. This was due to background signal detected by both eIF2α-P and eIF2α antibodies in the negative control (0 µg/µl mPKR) treatment (Fig. 5.10B). The results however suggested that the ratio WGeIF2α:WGeIF2α-P was inversely proportional to the increase in mPKR concentration. However authentic

quantification of WGeIF2α:WGeIF2α-P ratio may be undertaken using radioactive isotope techniques rather than immunoassays.

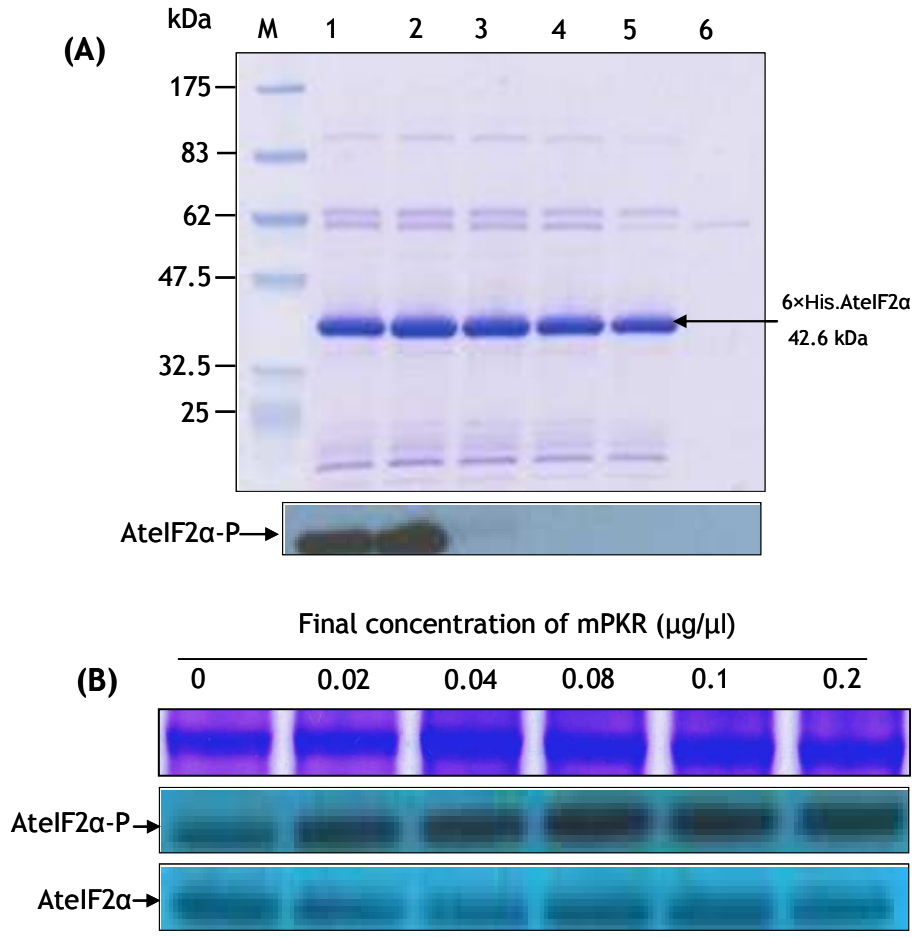

Figure 5.10. ***In vitro*** **phosphorylation of AteIF2α90 and WGeIF2α by mPKR.** SDS-PAGE and western blot analysis of, **(A)** *in vitro* phosphorylation of AteIF2α by poly I:C activated mPKR. Lanes: **M**, Protein Maker (NEB cat No.P7708S): **1**, eIF2α (1.5 ug) + PKR (1 µg) + poly I:C (5 µg/ml): **2**, eIF2α (1.5 ug) + PKR (1 µg) + poly I:C (10 µg/ml): **3**, eIF2α (1.5 ug) + poly I:C (5 µg/ml): **4**, eIF2α (1.5 ug) + PKR(1 µg): **5**, eIF2α (1.5 ug): 6, PKR (1 µg). **(B)** *In vitro* phosphorylation of WGeIF2α using inactivated (dephosphorylated) mPKR. Upper panel: protein loading controls, Coomassie ®Brilliant Blue stained 10% SDS-PAGE of RuBisCO Large subunit: lower panels, nitrocellulose membranes probed with eIF2α-P and eIF2α antibodies.

5.5 *In vitro* Translation of AtmRNA under Conditions of Phosphorylated and dephosphorylated WGeIF2α

5.5.1 Optimization of *In vitro* Translation of AtmRNA

Following successful *in vitro* phosphorylation of AteIF2α and WGeIF2α by mPKR, experiments were set up to investigate the effects of WGeIF2α phosphorylation on *in vitro* translation of total *Arabidopsis* mRNA (AtmRNA). Although WG lysate was the best plant based system for *in vitro* assessment of the role of phosphorylation of plant eIF2α on translation, there were technical challenges, because of the presence of endogenous WGeIF2α. A perfect system for evaluating the phosphorylation state of eIF2α on translation efficiency would have been devoid of endogenous eIF2α to facilitate addition of exogenous phosphorylated or de-phosphorylated eIF2α. Nonetheless prior to determining the effects of WGeIF2α phosphorylation on translation, the translation efficiency of extracted AtmRNA in WG lysate system was evaluated. For optimization experiments, the effects of AtmRNA at a final concentration of 0.01, 0.02, 0.03 and 0.04 µg/µl in a 12.5 µl reaction volume on translation efficiency was evaluated. Western blot analysis of the optimization experiments revealed that optimum translation was achieved using a final concentration of 0.03 and 0.04 µg/µl AtmRNA and 130 mM potassium acetate. The optimized translation reaction setup is shown in Table 5.1.

Table 5.1. Optimized Wheat Germ lysate setup for translation of *Arabidopsis* mRNA. Total mRNA was isolated from WT Col-0 seedlings incubated under 20°C/16°C day/night temperature, photoperiod of 8/16 day/night with a photosynthetic photon flux density (PPFD) of 20µmol $m^{-1}s^{-1}$, provided by cool white fluorescent lamps.

Component	Volume (µl)*
Wheat Germ extract	6.25
Amino Acid mixture minus Methionine (1 mM	0.5
Amino Acid mixture minus Leucine (1 mM)	0.25
RNasin Ribonuclease inhibitor (40 U/µl)	0.96
Potassium Acetate (1 M)	1.7
mRNA substrate in TE buffer (0.294 µg/µl)	1.84
Nuclease-free water	
Transcend™ tRNA	0.5
Total	12.5

*Volume of components optimized for non-radioactive detection using Transcend™ tRNA translation detection system (Promega Cat. No. L5070).

5.5.2 *In vitro* Translational Control of AtmRNA using WG Lysate

The effect of WGeIF2α phosphorylation on translation efficiency of AtmRNA was investigated. As discussed in section 5.4, inactive mPKR was added into the translation reaction mix to induce phosphorylation of WGeIF2α. The effect of mPKR at final concentrations of 0, 0.02 and 0.04 µg/ml on translation of 0.04 µg/ml AtmRNA in a 12.5 µl reaction volume was tested. The translation control experiment was setup as indicated in Table 5.2 below. Translation of AtmRNA using the de-phosphorylated form of WGeIF2α (WG+AtmRNA) was efficient and provided an estimate of plant protein synthesis under non-stress conditions (Fig. 5.11A). On the other hand addition of mPKR to a final concentration of 0.02 µg/ml (WG + AtmRNA + mPKR1) or 0.04 µg/ml (WG + AtmRNA + mPKR2) into the translation mix resulted in dramatic reduction of protein synthesis; however it did not result in complete shutdown of the *in vitro* translation machinery (Fig.5.11A).

Table 5.2. Setup of in vitro experiment for investigating translation of AtmRNA under **WGeIF2α and WGeIF2α-P.** The components were added and mixed gently in PCR tubes in the order indicated in the Table. mPKR was added into translation mix to induce phosphorylation of WGeIF2α and hence mimic translation of AtmRNA under stress conditions.

Component	**Lysate Control**	**Lysate + mPKR (0.02µg/µl) Control**	**Lysate + AtmRNA (0.04µg/µl)**	**Lysate + AtmRNA (0.04µg/µl) + PKR (0.02µg/µl)**	**Lysate + AtmRNA(0.04µg/µl) + PKR (0.04µg/µl)**
Wheat Germ extract	6.25	6.25	6.25	6.25	6.25
Amino Acid mixture minus Methionine (1 mM)	0.5	0.5	0.5	0.5	0.5
Amino Acid mixture minus Leucine (1 mM)	0.5	0.5	0.5	0.5	0.5
RNasin Ribonuclease inhibitor (40 U/µl)	0.25	0.25	0.25	0.25	0.25
Potassium Acetate (1 M)	0.96	0.96	0.96	0.96	0.96
PKR (~2.1 mg/ml)	-	0.125	-	0.125	0.25
mRNA substrate in TE* buffer (0.04 µg/µl)	-	-	1.7	1.7	1.7
Nuclease-free water	3.54	3.415	1.84	1.72	1.59
Transcend^{TM} tRNA	0.5	0.5	0.5	0.5	0.5
Total (µl)	**12.5**	**12.5**	**12.5**	**12.5**	**12.5**

*mRNA in elution buffer (TE) provided for in the mRNA extraction kit (Dynabeads® Oligo(dT) 25 Kit, Invitrogen, Cat. No. 610-02)

Since phosphorylation of WGeIF2α significantly reduced translation of AtmRNA, an attempt to identify the nascent protein synthesized in the presence of WGeIF2α-P was conducted using a pull-down assay. Several nascent proteins were obtained with the pull-down assay using Dynabeads®M-280 streptavidin beads as shown on lanes 4 and 6 marked with an asterix (Fig. 5.11B). On the other hand, there were several bands observed in control treatment lane 1(lysate) and on lane 3 and 5 i.e. remainder of lysate after pull-down of nascent proteins (Fig. 5.11B). These are remnants of endogenous biotinylated proteins after the initial pull-down conducted before a translation experiment was undertaken. Further attempts to identify the pulled-down nascent proteins synthesized under WGeIF2α-P conditions were not successful. This was due to low protein yields obtained and hence not visible on a Coomassie® Brilliant Blue

stained SDS-PAGE gel, but only on nitrocellulose membrane hybridized with extremely sensitive Streptavidin-HRP antibody conjugate (Fig. 5.11B).

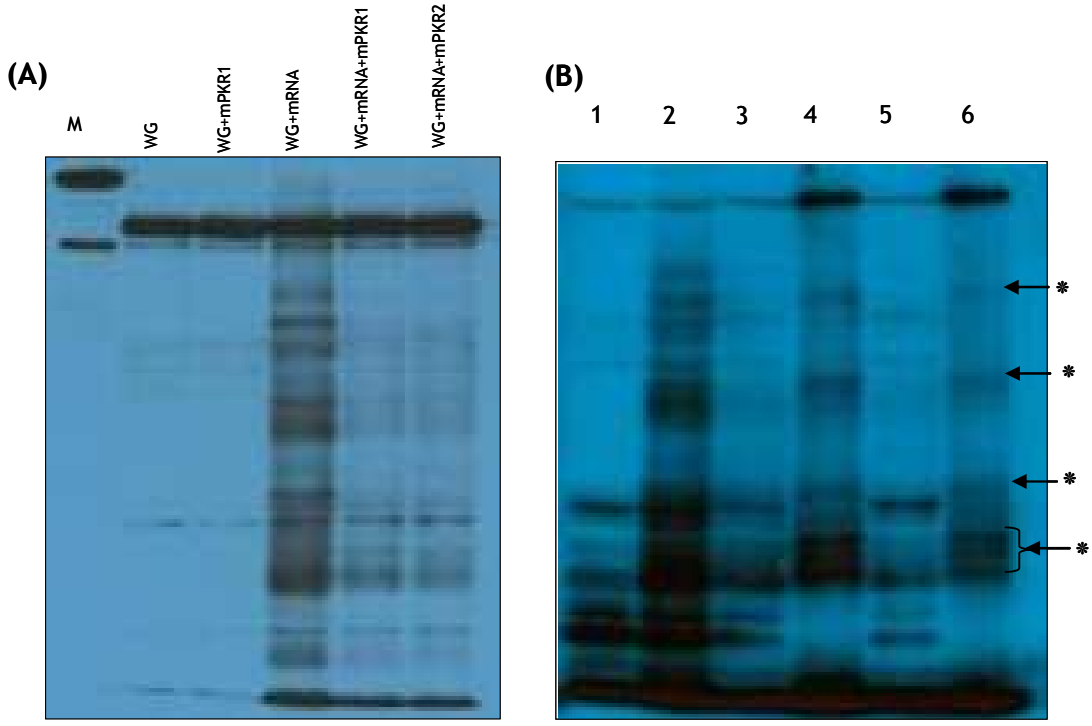

Figure 5.11. Phosphorylation of WGeIF2α inhibits *in vitro* translation of AtmRNA. **(A)** *In vitro* translation of AtmRNA under dephosphorylated (without mPKR) and phosphorylated (with mPKR) WGeIF2α status. Phosphorylation was achieved by addition of inactive mPKR1 (0.02 µg/µl) and mPKR2 (0.04 µg/µl) in a 12.5 µl reaction volume. **(B)** Streptavidin pull-down of nascent protein after *in vitro* translation reactions. Lanes, **1**, WG lysate; **2**, WG + AtmRNA: **3**, remainder of WG + AtmRNA + mPKR2 after pull-down: **4**, WG + AtmRNA + mPKR1 pull-down: **5**, remainder of WG + AtmRNA + mPKR2 after pull-down: **6**, WG + AtmRNA + mPKR2 pull-down. The two panels are nitrocellulose membranes probed with Streptavadin-HRP antibody. Asterix (∗) indicate unique nascent proteins on lane 4 and 6 after pull-down conducted using translation reaction under conditions of phosphorylated WGeIF2α.

5.6 *In silico* Search for *Arabidopsis* Stress Response Translationally Regulated Proteins

5.6.1 Search for *Arabidopsis* HsATF4 and ScGCN4 Homologues Using BLASTP

The results of *in vitro* phosphorylation experiments demonstrated that a number of mRNAs were translated in the presence of excess phosphorylated WGeIF2α (see Fig. 5.11). It was, however, difficult to determine which transcripts were translated when WGeIF2α was phosphorylated, i.e. the AtmRNA translated only when WGeIF2α is phosphorylated as is the case for ScGCN4 and HsATF4 transcripts when eIF2α is phosphorylated in yeast and mammalian systems, respectively. Therefore further attempts to identify putative ScGCN4 and HsATF4 homologues in *Arabidopsis* were conducted using a bioinformatics approach as described in section 2.12.2. The BLASTP search for *Arabidopsis* ScGCN4 and HsATF4 homologues returned 4 candidates for HsATF4 (AT4G24480.1, AT5G03730.1, AT5G03730.2 and AT5G11850.1), whereas for ScGCN4 there were over 60. Further analysis of the putative ScGCN2 *Arabidopsis* homologues was conducted using N-J and UPGMA phylogenetic analysis (see section 2.12.2). For the N-J method ScGCN4 and HsATF4 clustered with AT5G37340.2, AT1G20132.15 and AT3G15190.1, AT5G35210.1 and AT5G18160.1 genes (Fig. 5.12A), whereas for the UPGMA analysis ScGCN4 and HsATF4 clustered with two *Arabidopsis* genes namely, AT5G37340.2 and AT1G20132.1 (Fig. 5.12B). These results suggest that these genes may be associated to *ScGCN4* and *HsATF4*. However further analysis on the presence of shared functional domains or regulatory structures such as uORFs were necessary to ascertain their functional relationship with ScGCN4 and HsATF4 transcriptional activators.

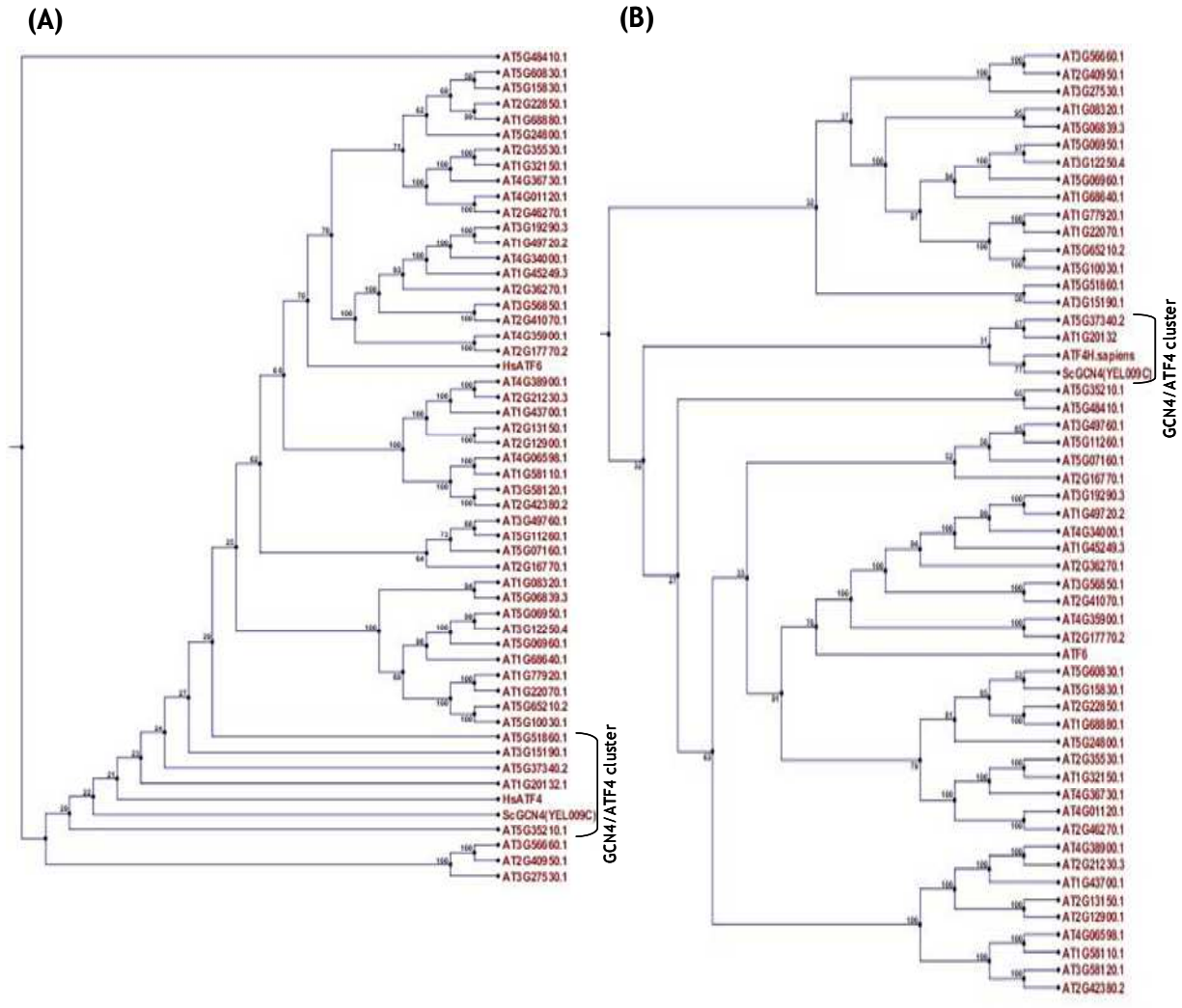

Figure 5.12. Phylogenetic analysis of 54 *Arabidopsis* hits obtained after ScGCN4 BLASTP search against TAIR 10. *Arabidopsis* loci representing amino acid sequences that clustered with ScGCN4, HsATF4 and HsATF4 after phylogenetic analysis using, **(A)** Neighbour-Joining method (N-J) and **(B)** Unweighted Pair Group Method (UPGMA).

The 5′ UTRs of the 5 *Arabidopsis* genes clustering with ScGCN4 and HsATF4 were retrieved from TAIR and the presence of uORFs with a minimum of 2 codons was analysed using CLC Sequence Viewer. The analysis revealed that AT1G20132.1 and AT3G15190.1 had single uORFs, whereas AT5G35210.1 had four uORFs, and AT5G37340.2 and AT5G51860.1 genes completely lacked them (Fig. 5.13A). The 5′ UTRs of eukaryotic mRNAs possess features that play a very important role in the translation initiation efficiency (Pesole *et al.*, 2001; Mignone *et al.*, 2002). One of the UTRs features that is well demonstrated is the nucleotide sequence or context sequences surrounding the AUG codon (Kozak, 1987a; Pesole *et al.*,

2000). According to the Scanning model, the efficiency of translation initiation is determined by the sequence context surrounding the AUG start codon; GCCRCC**AUG**G (Kozak, 1987b). For mammalian mRNAs the most important nucleotides are a purine at position -3 (A/G), where adenine is favoured over guanine. At position +4 (G) guanine is well conserved, however uracil (U) at position +5 appears to be important especially in the absence of A at position -3 (Kozak, 1987b). The positions of the nucleotides are with respect to the A (+1) in the **AUG** start codon. In plants the agreed consensus sequence context is AACA**AUG**GCU (Lutcke *et al.*, 1987) and in *Arabidopsis* it has been suggested to be AA(A/G)AA**ATG**GCUGCU (Rangan *et al.*, 2008; Shashikanth *et al.*, 2008). Therefore like in the mammalian system for efficient translation initiation to occur either A or G should be at -3 position and G at +4. The AT1G20132.1 and AT3G15190.1 genes possessed a single uORFs, they therefore did not conform to the number of uORFs similar to either ScGCN4 or HsATF4 uORFs and hence they were regarded as not potential candidates. Further analysis of AT5G35210.1 uORFs indicated that they lacked the prerequisite nucleotides at position -3 and +4 and only the second uORF had G at position +4. This observation suggests that translation initiation efficiency for these uORFs may not be optimal (Fig. 5.13B). The AT5G35210.1 gene encodes a DNA binding, metalloendopeptidase and zinc ion binding protein that is involved in proteolysis and regulation of transcription activity.

(A)

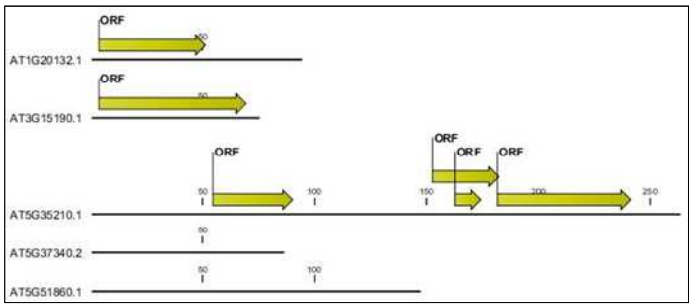

(B)

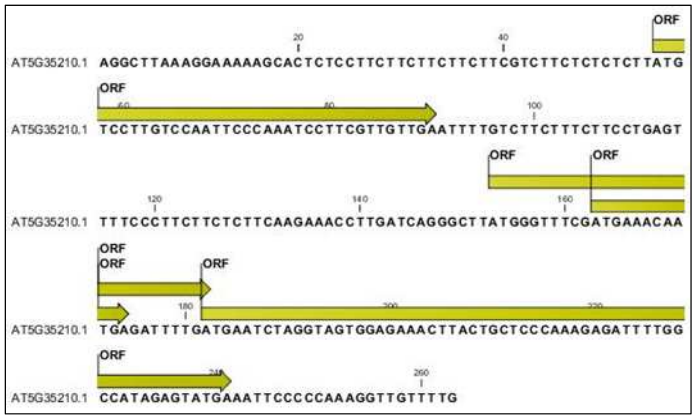

Figure 5.13. The 5′ UTRs region of the selected *Arabidopsis* genes clustering with ScGCN4 and HsATF4 after phylogenetic analysis. **(A)** Schematic representation of uORFs present on 5′ UTRs region of 5 *Arabidopsis* genes clustering with ScGCN4 and HsATF4. **(B)** Illustration of the leader sequence of AT5G35210.1 showing the length of 4 uORFs (12, 10, 4 and 20 codons) and sequences flanking upstream AUG/ATG (uAUG/uATG).

5.6.2 Search for *Arabidopsis* HsATF4 and ScGCN4 Homologues Using FivePrime Viewer

Using FivePrime Viewer, a bioinformatics tool developed at Glasgow University, a total of 99 *Arabidopsis* cDNAs deposited in TAIR database that may be regulated in a GCN4-/ATF4-like manner were identified (Webb, 2008). The list generated was used as the starting point for searching for *Arabidopsis* ScGCN4 and HsATF4 homologues. Arabidopsis cDNAs were assessed using four search criteria (groups): (1), cDNAs that encoded proteins with a high similarity score (98-99): (2), cDNAs that have physical resemblance to the HsATF4 5′ UTR sequence: (3), cDNAs that have physical resemblance to the ScGCN4 5′ UTR

sequence: (4), cDNAs coding for transcription factor (Appendix 18). Phylogenetic analysis was conducted to identify putative ScGCN4 and HsATF4 homologues in the cDNAs using each of the four search criteria (groups). As described earlier, full-length protein sequences corresponding to representative gene model were retrieved from TAIR10. The retrieved sequences, and ScGCN4 and HsATF4 full-length protein sequences were aligned and subjected to phylogenetic analysis. The UPGMA and N-J analysis methods produced phylogenetic trees containing either a single or two distinct clusters containing either one or both ScGCN4 and HsATF4. The clusters formed using the criteria of groups 1, 2 and 3 cDNAs are summarized in Table 5.3 below.

Table 5.3. Summary of ScGCN4 and HsATF4 clusters formed when protein sequences of representative cDNAs were subjected to phylogenetic analysis.

cDNAs	Analysis Method	Cluster 1	Cluster 2
Group 1	UPGMA	AT1G58120.1	-
		AT3G53670.1	-
		AT5G18940.1	-
		AT5G08120.1	-
		ScGCN4	-
		HsATF4	-
	N-J	AT3G53670.1	AT1G58120.1
		AT5G18940.1	HsATF4
		AT5G08120.1	-
		ScGCN4	-
Group 2	UPGMA	ScGCN4	AT3G26750.1
		HsATF4	AT2G02620.1
		-	AT3G54350.1
		-	AT3G54090.1
		-	AT4G28600.1
	N-J	AT2G05510.1	AT3G26750.1
		-	AT2G02620.1
		-	AT3G54350.1
		-	AT3G54090.1
		-	AT4G28600.1
		-	ScGCN4
		-	HsATF4
Group 3	UPGMA	ScGCN4	AT3G20870.1
		AT3G54120.1	HsATF4
	N-J	ScGCN4	AT3G20870.1
		AT3G54120.1	HsATF4
		AT2G39870.1	-

For group 4 cDNAs, the N-J method produced a single cluster that included ScGCN4 and HsATF4 (Fig. 5.14A), whereas in the UPGMA analysis there were two clusters of ScGCN4 and HsATF4, and AT3G54390.1 and AT5G67480.2 (Fig. 5.14B).

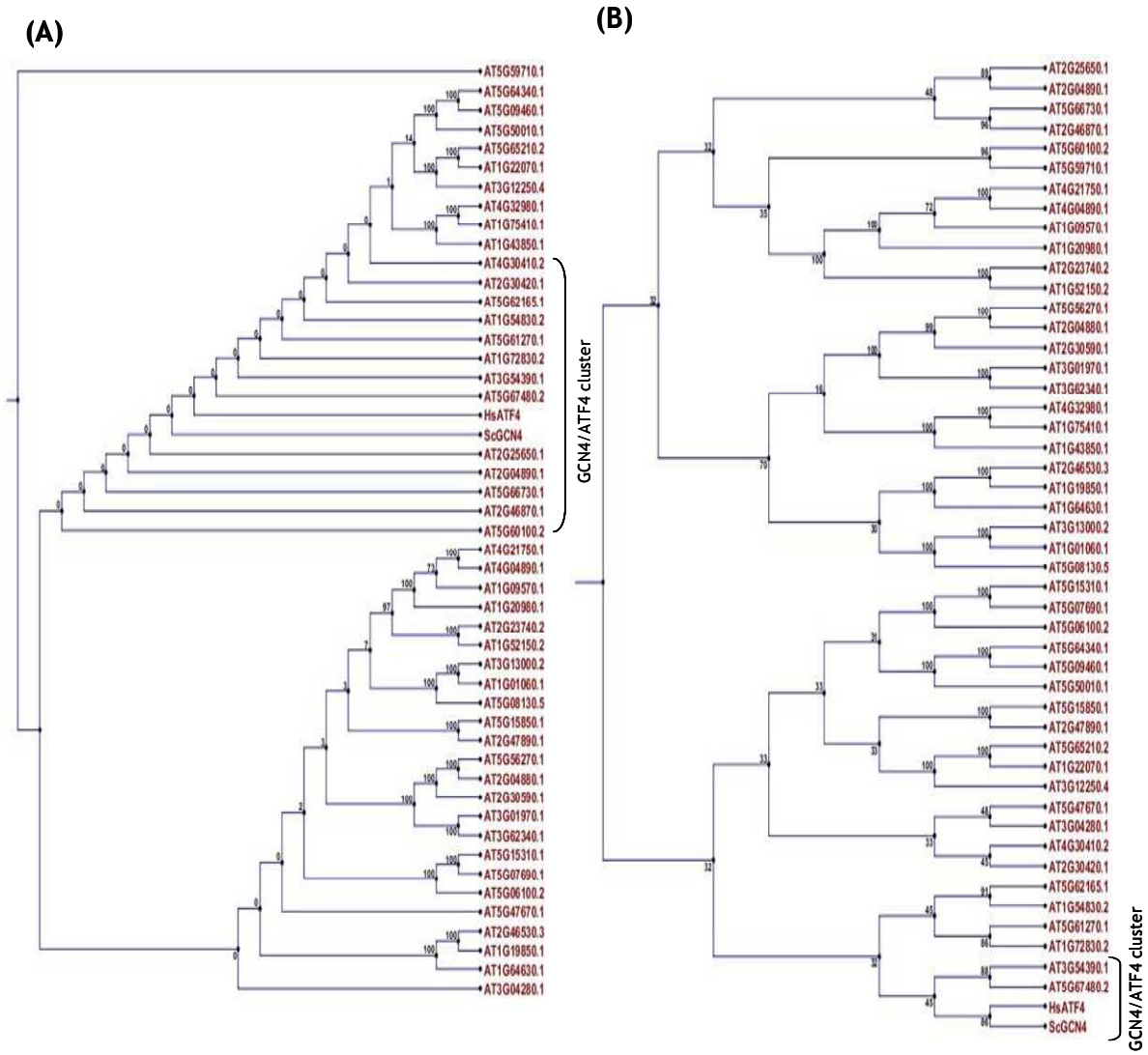

Figure 5.14. Phylogenetic analysis of protein sequences representing group 4 cDNAs. *Arabidopsis* loci encoding amino acid sequences that clustered with ScGCN4 and HsATF4 amino acid sequences after analysis using, **(A)** Neighbour-Joining method (N-J) and **(B)** Unweighted Pair Group Method (UPGMA).

The *Arabidopsis* cDNAs clustering with ScGCN4 and HsATF4 were further analyzed for presence of functional uORFs in their 5′ UTR. To achieve this, the 5' UTRs were retrieved from TAIR10 and the nucleotide sequences analyzed for the presence of uORFs as described earlier. The conditions for identifying a uORF were: presence of an AUG start codon: uORF must contain a minimum of 2 codons and a stop codon: uORFs should posses consensus nucleotides at position

-3 (A/G) and +4 (G). The conditions set for identifying uORFs were based on the models of ScGCN4 and HsATF4. Therefore, to qualify as a putative ScGCN4 homologue, the UTRs of the *Arabidopsis* genes should possess 4 uORFs, whereas for HsATF4 it should have 2 uORFs, and the second uORF should overlap the mORF (Fig. 5.15). Although size of uORFs and the distance between uORFs are believed to be important they were not considered at this stage of the analysis.

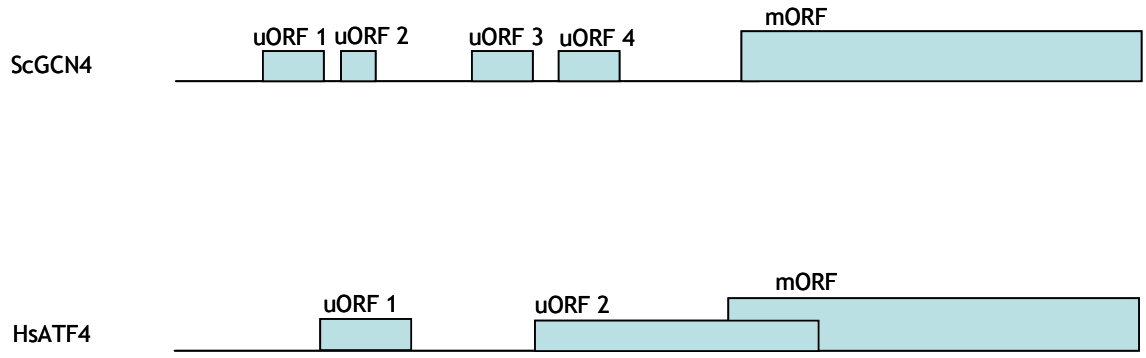

Figure 5.15. Schematic representations of regulatory uORF present in the 5' UTRs of ScGCN4 and HsATF4 model genes. The images are not drawn to scale.

The UTRs possessing 2 or 4 uORFs containing part of the context sequence at -3 (A/G) and +4 (G) or at either position were identified (Table 5.4). There were no uORFs with a perfect match for HsATF4 observed in any of the cDNAs that clustered with ScGCN4 and HsATF4 using either UPGMA or N-J analysis. On the other hand six cDNAs (At1G58120.1, At2G02620.1, At5G66730.1, At4G31590.1, At5G60100.2 and At2G04890.1) possessed at least two uORFs containing consensus sequence at -3 and +4 (Fig. 5.16). In addition the gene structures of At1G58120.1 and At4G31590.1 resemble those of ScGCN4, and *cpc-1* and *cpcA* genes, respectively (Fig. 5.16). The *cpc-1* and *cpcA* genes are found in the filamentous fungi, *Neurospora crassa* (Paluh *et al.*, 1988) and *Neurospora nidulans* (Hoffman *et al.*, 2001). In TAIR the At4G31590.1 gene is reported to encode a protein involved in the cellulose synthase and gylcosyltransferase activity. As for the At1G58120.1 gene is annotated in TAIR10 as encoding a proteins involved in methyltransferase activity. However using the NCBI Conserved Domain Search tool, the two *Arabidopsis* genes lack bZIP domains, a key component of ScGCN4.

Table 5.4. List of gene possessing 2 or 4 uORFs and conserved nucleotides critical for translation initiation efficiency at position -3 (A/G) and +4 (G).

TAIR Annotation	uORF	Nucleotide position -3 of ATG	Nucleotide position +4 of ATG	consensus position
AT2G25650.1	1	-	A	-,
	2	A	A	-3
AT2G46870.1	1	G	A	-3
	2	A	A	-3
	3	T	T	-
AT5G62165.1	1	A	A	-3
	2	T	A	-
AT5G67480.2	1	T	A	-
	2	G	A	-3
AT2G04890.1	1	C	T	-
	2	G	T	-3
	3	G	T	-3
	4	G	A	-3
AT2G60100.2	1	T	A	-
	2	T	C	-
	3	C	G	+4
	4	T	G	+4
	5	G	T	-3
	6	G	T	-3
	7	T	G	+4
AT5G66730.1	1	A	C	-3
	2	T	A	-
	3	G	A	-3
	4	A	A	-3
AT1G58120.1	1	C	T	-
	2	A	G	-3, +4
	3	T	A	-
	4	A	G	-3, +4
AT3G53670.1	1	G	T	-3
	2	A	C	-3
AT1G55920.1	1	-	G	+4
	2	A	T	-3
AT2G02620.1	1	A	G	-3, +4
	2	C	A	-3
	3	C	C	-3
AT3G54120.1	1	-	A	-
	2	A	A	-3
AT4G31590.1	1	A	G	-3, +4
	2	A	G	-3, +4

(A)

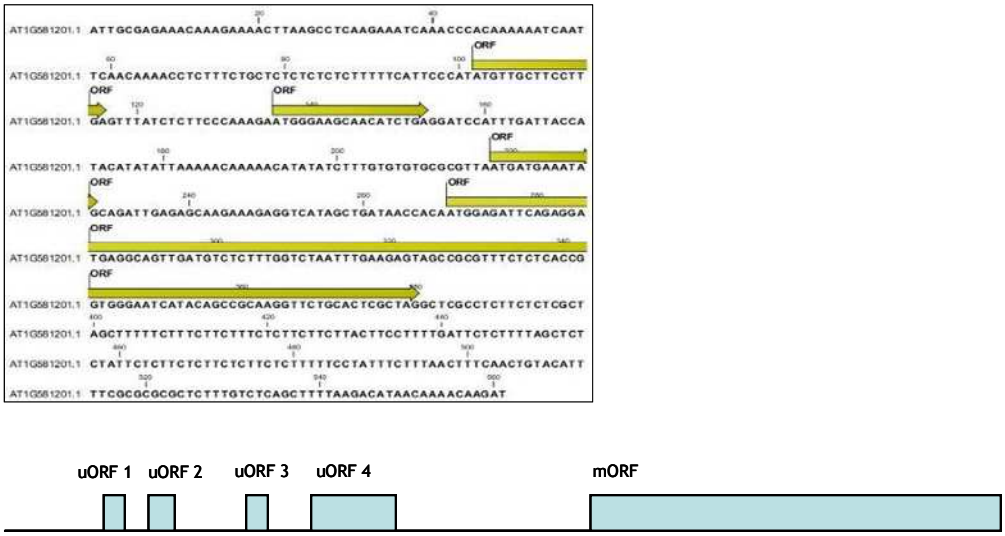

(B)

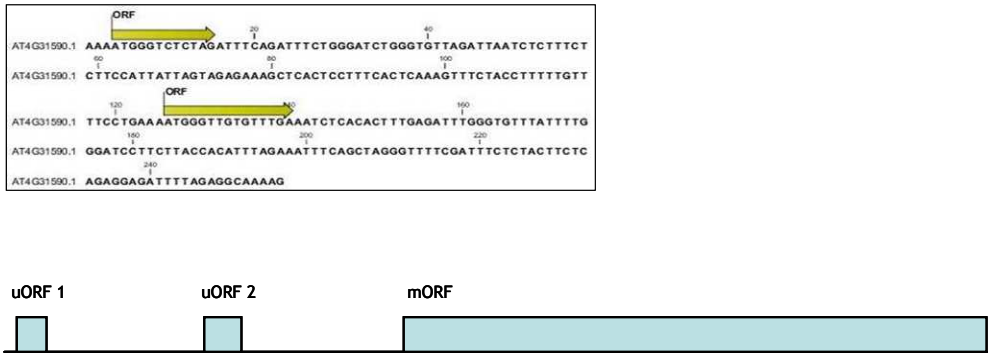

Figure 5.16. Schematic representation of 5′ UTRs region of putative *Arabidopsis* homologues of ScGCN4. **(A)** The leader sequence containing 4 uORFs of 5, 4, 3 and 36 codons long, respectively, present in AT1G58120.1. **(B)** The leader sequence of AT4G31590.1 containing 2 uORFs of 3 and 4 codons long. The schematic representations of the uORFs are drawn to scale.

5.6.3 Analysis of At1g58120 and At4g31590.1 Expression

Investigation using the on-line tool eFP Browser revealed that the At1g58120.1 protein is localised in the plastid, mitochondrion, and endoplasmic reticulum, whereas At4g31590.1 is localised in the mitochondrion, cytosol and plasma membrane. Further analysis with *Arabidopsis* eFP Browser indicated that At1g58120.1 is expressed in seeds (up to 23-fold), and highly expressed in

flowers mainly the stamens (264-fold), and mature pollen (1925-fold). It is also expressed at all the stages of the zygotic embryo, however the highest expression is found in the root zone of embryos at the torpedo stage (18-fold). Exposure to cold, osmotic stress and NaCl induced low expression of At1g58120.1 (up to 2.3-fold) after 0.5 h to 3 h exposure, thereafter no differential expression was present. Treatment with SA induced low expression (up to 1.9-fold) of At1g58120.1 as opposed to JA which did not activate it. At4g31590.1 expression was found to be increased by up to 11.6-fold but only in stage 6-10 seeds. It is also expressed at all stages of the zygotic embryos although highest expression at 2.6-fold is present in the root zone of embryos and at the torpedo stage. Similar to At1g58120.1 cold, osmotic, heat and NaCl stress induced low expressions (up to 2.3 fold) of At4g31590.1 after 0.5 to 24 h of exposure. Treatment with JA induce low expression (1.11 fold), whereas treatments with SA and inoculation with *P. syringae* does not activate At4g31590.1.

5.7 Discussions

5.7.1 Expression of AteIF2α, AtGCN2 and mPKR in *E. coli*

The relatively slow growth of cells harbouring pDEST17.*AteIF270* construct suggested that expression of 6×His.AteIF270 fusion protein was active and also toxic to *E. coli* cells. Furthermore the 6×His.AteIF270 protein was poorly expressed compared with 6×His.AteIF290 (Fig. 5.4). This was unexpected considering that ClustalW2 alignment revealed the splice variants are highly conserved except for a few amino acids (~25 amino acid residues) as shown in Fig. 5.1. Although speculative, poor expression of AteIF270 in *E. coli* may have been due to the differences in the amino acid residues. This is because the effect of primary sequence features such as amino acid composition and rare codons have been cited as some of the biochemical factors that influence expression levels and solubility of heterologous proteins in *E. coli* (Price *et al.*, 2011). To overcome these problems, several approaches have been described including targeted mutagenesis to remove rare codon and addition of rare codon tRNA to expression cell lines (Burgess-Brown *et al.*, 2008). Since all the splice variants possessed the conserved SEL**S** domain containing the Ser56 phosphorylation target site, only AteIF290 was expressed and used in subsequent

phosphorylation experiments. Although the experiments reported in this chapter show AteIF2α expression in *E. coli*, there are reports on expression of mammalian and yeast eIF2 (α, ß and γ) subunits using a baculovirus vector system and Sf21 and Sf9 cells (Kimball *et al.*, 1998; Suragani *et al.*, 2006) and it may be this is a more suitable protein expression system for these proteins.

Expression of the AtGCN2 kinase using Rosseta™ (DE3) BL21 *E. coli* was successful although the protein was found mainly in the insoluble fraction (Fig. 5.6). The formation of insoluble inactive protein aggregates usually occurs when a eukaryotic protein is expressed in a heterologous host such as *E. coli*. It is associated with misfolded proteins, which are stored in inclusion bodies (Trimpin & Brizzard, 2009). These proteins can be purified from the inclusion bodies under denaturing conditions, however, attempts to refold the denatured proteins to re-activate have met with limited success (Mihic & Harris, 1996). Unlike insoluble protein, the soluble recombinant proteins are usually correctly folded and fully functional (Vera *et al.*, 2007). Attempts to prepare large quantities of active, soluble AtGCN2 protein in *E. coli* lines containing rare codon tRNAs were disappointing. Perhaps this is not surprising since there are reports that expression of heterologous protein in codon adjusted cells can be detrimental to their solubility (Rosano & Ceccarelli, 2009).

Due to problems associated with the expression of soluble AtGCN2 kinase in *E. coli*, the mPKR kinase was used as a substitute in *in vitro* phosphorylation experiments. mPKR expression in *E. coli* and its subsequent purification protocols are well established (Conn, 2003), and mPKR has been shown to phosphorylate plant eIF2α (Langland *et al.*, 1995; Conn, 2003). Although mPKR has been reported to express poorly in *E. coli*, this poor expression has been associated mainly with codon bias (Lamaire *et al.*, 2005). For this reason expression of the inactive mPKR in this study was conducted using Rosseta™ (DE3) BL21 expression cells. These cells host extra plasmids that contain mammalian sequences codons that are rare in *E. coli*, hence making it possible to express recombinant protein that may be toxic to *E. coli* cells.

5.7.2 mPKR Phosphorylates AteIF2α and WGeIF2α *In vitro*

In vitro phosphorylation of AteIF290 and WGeIF2α was achieved using mPKR (Fig. 5. 10A&B). Despite the differences in the position of the target serine (Ser 51 for mammalian eIF2α and Ser 56 for *Arabidopsis*) and differences in the activation mechanism of mPKR and AtGCN2, phosphorylation of AteIF2α and WGeIF2α demonstrated that eIF2α phosphorylation is conserved across eukaryotes. This assumption is supported further by reports on functional complementation of yeast eIF2α by wheat eIF2α (Chang *et al.*, 2000) and *Arabidopsis* GCN2 kinase functionally complementing yeast *Δgcn2* mutants (Zhang *et al.*, 2003). On the other hand phosphorylation of AteIF2α by mPKR also confirmed that the recombinant α-subunit and inactive mPKR expressed in *E. coli* cell systems could subsequently be activated. The addition of inactive mPKR to the *in vitro* AteIF90 phosphorylation mix failed to phosphorylate AteIF2α, unlike when added to WG lysate (Fig. 5.10A&B). These results clearly demonstrated that mPKR must have undergone auto-phosphorylation in the WG lysate to become active. Furthermore, there are reports on *in vitro* activation of mPKR by auto-phosphorylation in the presence of over 3 mM ATP (Lamaire *et al.*, 2005). The WG lysate (Promega, Cat. No. L4380) used in this study contains 1.2 mM ATP per reaction mix set-up, hence these results suggests that mPKR can undergo auto-phosphorylation in the presence of less than 3 mM ATP.

The purpose of addition of mPKR into the translation mixture was to induce phosphorylation of WGeIF2α and therefore mimicking translation control under stress conditions. Indeed addition of mPKR dramatically reduced translation of AtmRNA compared with control treatment (Fig. 5.11A). This reduction demonstrated that *in vitro* translation of AtmRNA was inefficient when WGeIF2α was phosphorylated. These results are consistent with reduction of protein synthesis *in planta*, when WT Col-0 *Arabidopsis* seedlings were subjected to amino acid (purine) starvation (Lageix *et al.*, 2008). Although AtGCN2 kinase was not tested in the experiments reported herein, the ability of mPKR to suppress translation of AtmRNA suggests that plant eIF2α kinases may also regulate protein synthesis through this mechanism. On the other hand there are reports indicating that plant PKR (pPKR) is constitutively present in WG lysate (Langland *et al.*, 1996), however, in the translation experiment reported herein

there was no significant suppression of AtmRNA translation observed in non-mPKR treatment (see Fig.5.11A, WG + mRNA lane). These results clearly demonstrate that presence of any endogenous pPKR in the lysate did not induce significant phosphorylation of WGeIF2α or inhibit protein synthesis.

5.7.3 Does *Arabidopsis* Possess ScGCN4 and HsATF4 Homologues?

It has been suggested that up to 20% of the plant genes possess a 5′ UTR containing uORFs (Neafsey & Galagan, 2007; Saul *et al.*, 2009). However only a few plant genes possessing regulatory uORFs have been identified; for example Arabidopsis bZIP11 that is translationally repressed in presence of sucrose (Rahmani *et al.*, 2009), among others. On the other hand the most direct way of verifying functional uORFs has been through experimentation where the amount of mRNA containing uORF and the abundance of protein produced by the mORF with and without mutation of the uORFs is determined. This method has successfully been used to determine the functional uORFs in ScGCN4 and bZIP11, in yeast and Arabidopsis, respectively (Hinnebusch, 2005; Rahmani *et al.*, 2009). Although successful, this method is time consuming and costly, especially when it involves investigating a large number of sequences. For this reason, bioinformatics tools were employed to narrow down putative candidate genes of ScGCN4, HsATF4 and HsATF6 *Arabidopsis* homologues and to determine the presence of any regulatory uORFs in the 5' UTR sequences.

Multiple sequence alignment has been widely used to compare biological sequences using bioinformatics tools such as BLAST, PSI-BlAST among others (Altschul *et al.*, 1997; Katoh & Toh, 2008). It has also been used in deducing the functions of unknown protein in one organism from that of a known related protein in another organism. The idea behind this assumption is that conserved structural motifs, mainly in amino acid sequences suggest functional similarity (Conesa *et al.*, 2005). Although BLASTP searches provide a fast and concise analysis of many gene sequences simultaneously, identified sequences are often not closely related (Liisa & Brian, 2001). In contrast, phylogenetic trees provide information on the evolutionary relationship between the sequences and have proved to be a valuable tool for determining the functional relationship between the different proteins (Zufall, 2008). Therefore in this thesis, phylogenetic

analysis was used to refine the relationship between sequences identified by BLASTP in an attempt to establish a sound basis for inferring functional similarity to ScGCN4 and HsATF4.

In eukaryotes uORFs are a common feature of many transcripts, and unlike the well studied ScGCN4 and ATF4 transcripts, some of the uORFs are thought to play no significant regulatory role (Selpi *et al.*, 2006). None-the-less uORF-mediated regulation of translation clearly illustrates the potential of uORFs to function as *cis* regulators of protein expression, especially for mORF encoding transcriptional factors that may themselves control the expression of regulons (Hayden & Jorgensen, 2007). It has been established that a minimum of two uORFs is required for the translation regulation mechanism to be functional where an 'inhibitory' uORF is preceded by a 're-initiation friendly' uORF (Grant *et al.*, 1995).

It is conceivable that the *Arabidopsis homologue* of ScGCN4 homologue has two uORFs rather than four, as is the case for *cpcA* the homologue from the filamentous fungi *Aspergillus nidulans* (Hoffman *et al.*, 2001; Hood *et al.*, 2009), and *cpc-1* the equivalent sequence in *Neurospora crassa* (Luo *et al.*, 1995). The *cpcA* and *cpc-1* genes have been shown to fulfil roles similar to ScGCN4 and they encode transcriptional activators for cross-pathway control of amino acid biosynthesis. In filamentous fungi, cross-pathway control is a phenomenon in which starvation of one amino acid results in the induction of all amino acid biosynthesis pathways (Hoffman *et al.*, 2001; Elliott *et al.*, 2011). In *S. cerevisiae* (yeast) cross-pathway control is referred to as general control of amino acid biosynthesis (Hinnebusch, 1992). Furthermore, the *cpcA* gene encodes a bZIP transcription factor that has been shown to functionally complement yeast *Δgcn4* mutants (Wanke *et al.*, 1997). Similarly *cpc-1* also encodes a bZIP transcription factor that act as a positive activator of amino acid biosynthesis (Paluh *et al.*, 1988). However, the *cpcA* transcript has 14 and 58 codons in uORFs 1 and 2, respectively (Elliott *et al.*, 2011). On the other hand *cpc-1* has also two uORFs which have some sequence similarities to the ScGCN4 uORFs 1 and 4, that have been established as necessary for translation control of ScGCN4 transcript (Hinnebusch, 1992; Hinnebusch, 2005). The *Arabidopsis* At4g31590.1 gene has two uORFs with 3 (ATGGGTCTCTAG) and 4 (ATGGGTTGTGTTTGA) codons (Fig. 5.16), which are as short as the ScGCN4

uORFs 1 (ATGGCTTGCTAA) and 4 (ATGTTTCCGTAA). On the other hand, uORF1 of AT1G58120.1 has 5 codons (Fig. 5.16) whereas uORF 4 has 36 codons, twelve-fold more than for ScGCN4 uORF 4. Generally higher reinitiation efficiency is possible after a short uORF whereas longer uORFs significantly inhibit mORF translation (Wang & Wessler, 1998). The length of AT1G58120.1 uORF 4 (36 codons) suggests that it is highly inhibitory; studies have demonstrated that re-initiation becomes virtually undetectable when a uORF is greater than ~35 codons (Luukkonen *et al.*, 1995; Wang & Wessler, 1998). However the length of AT1G58120.1 uORF 4 (36 codons) does not disqualify it from being a putative ScGCN4 homologue, since the *cpcA* has been established to complement yeast *Δgcn4* mutants, does not conform to the length of ScGCN4 uORF 1 and 4 either (14 and 58 codons).

In eukaryotes most of the transcripts that are regulated by uORFs are those of important genes that play a critical role in growth and development. One such gene in plants is AdoMetDC, that is implicated in the synthesis of polyamines (Walden *et al.*, 1997). These molecules are key in important plant functions including cell division, embryogenesis, flower development and stress-response (Evans & Malmberg, 1989; Walden *et al.*, 1997). Annotations in TAIR10 indicate that AT1G58120.1 and At4g31590.1 are involved in methylation and cellulose synthase/glycosyltransferase activities, respectively. DNA methylation in plants is tissue-, organelle- and even age-specific, and it is implicated in the control of transcription, replication, DNA repair and cell differentiation (Vanyushin & Ashapkin, 2011). On the other hand, cellulose synthase and gylcosyl transferase are key enzymes in cellulose synthesis, one of the main components of the plant cell wall (Lerouxel *et al.*, 2006; Liepman *et al.*, 2007). Among many other functions, plant cell wall defines the shape of cells, act as barriers against pathogens, and are directly involved in growth and development signals, and responses to variable environmental conditions (Crute *et al.*, 1994 ; Freshour *et al.*, 2003). The significance of methylation and cellulose synthesis in plants underscores the importance of these two *Arabidopsis* genes (AT1G58120.1 and At4g31590.1) that possess putative regulatory uORFs. Their importance in plant reproduction, growth and developement is supported further by their expression in seeds, embryos, pollen and stamens as revealed by *Arabidopsis* eFP browser (Section 5.6.3). However there is need to experimentally verify the importance

of these genes in growth and development, and meristematic cell division, and whether the uORFs are regulatory and phosphorylation of AteIF2α is involved in translation regulation of these transcripts.

6 Chapter 6: General Discussion

6.1 Introduction

The underlying mechanisms of tolerance and adaptation to environmental stresses has for a long time been the focus of many plant scientists, with the ultimate aim of developing stress tolerant crops (Bray *et al.*, 2000). An enormous amount of research work has been conducted to investigate how plants respond to various stresses, and these can be categorised as specific and general responses. The specific responses are those that are induced by factors unique to that particular stress, whereas the general responses are those triggered by signals and signalling components that are shared by multiple pathways (Bowler & Fluhr, 2000; Swindell *et al.*, 2007; Saibo *et al.*, 2009). Recently it has become clear that multiple signalling pathways interact to form networks (Bostock, 2005; Swindell *et al.*, 2007). These networks are linked by key protein kinases, phophatases and transcription factors that play very important roles as nodes where pathways either converge or diverge, thereby facilitating cross-talk between networks (Halford *et al.*, 2004; Fujita *et al.*, 2006; Hey *et al.*, 2010).

Some ancient stress signalling pathways controlling fundamental responses in eukaryotes are highly conserved (Halford *et al.*, 2004). One of the mechanisms that is conserved across all eukaryotes is the control of protein synthesis at the global or sequence-specific level. In the recent past, plant scientists have become interested in translational control mechanisms mediated by phosphorylation of eIF2α, a major component of the 40S ribosomal subunit (Zhang *et al.*, 2003; Lageix *et al.*, 2008; Zhang *et al.*, 2008). As discussed earlier in the preceding sections of this thesis, in yeast and mammals this mechanism activates key transcription factors that control the expression of regulons that are geared towards stress mitigation (Szick-Miranda *et al.*, 2003; Hinnebusch *et al.*, 2004). In higher eukaryotes this pathway plays an important role in regulating protein synthesis in response to cellular and environmental stresses (Jiang & Wek, 2005; Wek *et al.*, 2006; Toth *et al.*, 2009; Muench *et al.*, 2012). Although not well characterized in plants, in *Arabidopsis* this pathway seems to be regulated by only one eIF2α (ser56) specific kinase, namely GCN2,

and results are presented in this thesis to support this contention (Section 3.7.1 and 3.7.2). In principle this mechanism is amenable to manipulation in plants (even if plants possess other eIF2α kinases apart from GCN2) and the kinase(s) can be potential target(s) for development of stress tolerant crops. In mammalian systems, the eIF2α (ser51) kinases have already been targeted for the development of drugs for treatment of a variety of common human disorders (Ron & Harding, 2007).

Being sessile organisms, plants have evolved a wide range of mechanisms to cope with biotic and abiotic stresses. Although it is important to understand how different stress response pathways converge, it is equally important to understand how each of the pathways function. This is especially important for newly or not well characterised pathways such as the GCN2/GCN4 pathway in plants. Characterization of global translational regulation mechanisms through phosphorylation of eIF2α in plants is therefore important for the purpose of evaluating its role in stress mitigation and possible interaction with other metabolic or stress response pathways. This was the main objective of the work presented in thesis, the elucidation of stress response translation regulation mechanism in plants using *Arabidopsis* as model species.

6.2 The Kinase AtGCN2 is Solely Responsible for Abiotic Stress-Induced eIF2α Phosphorylation

Isolation of a functional AtGCN2 null (*Atgcn2*-1) line allowed a detailed comparison of the effects of different stress factors on the activation of endogenous GCN2 kinase and its role in the phosphorylation of eIF2α. These experiments were facilitated by the availability of commercial antibody that was specific for eIF2α and for phosphorylated eIF2α (eIF2α-P). Several abiotic stress factors were applied to WT and a functional AtGCN2 null mutant (*Atgcn2-1*) lines including extremes of temperature, salinity, drought, and amino acid depletion. In all cases eIF2α was strongly phosphorylated within hours of exposure to stress in the WT line but not in the *Atgcn2-1* line. Exposure to biotic stress factors failed to induce eIF2α phosphorylation in either the WT or *Atgcn2-1* lines. These results strongly indicate that in *Arabidopsis* abiotic stress factors activate endogenous AtGCN2 kinase which subsequently phosphorylates eIF2α and that

this is the only kinase in *Arabidopsis* that can perform this task. There may be other kinases that can also phosphorylate eIF2α but the results presented in this thesis indicate these are not activated by the abiotic or biotic stress factors investigated here.

Yeast (*S. cerevisiae*) also has only one eIF2α kinase (ScGCN2) that is activated by glucose, amino acid and purine starvation, but unlike the *Arabidopsis* null mutation produces a strong phenotype (Yang *et al.*, 2000; Goossens *et al.*, 2001). High salinity also induces ScGCN2-mediated phosphorylation of eIF2α thereby activating translational control of the bZip transcription factor ScGCN4 which in turn negatively affect salt tolerance; ScGCN2 null mutants are hypertolerant of salinity stress (Goossens *et al.*, 2001). In contrast, seedlings of *Arabidopsis* GCN2 functional null (*Atgcn2-1*) and those of p35S:AtGCN2 lines did not show a strong phenotype and were equally sensitive as WT Col-0 to NaCl-induced stress even through the AtGCN2 kinase was activated and eIF2α was phosphorylated under these conditions (Section 3.4.3 and 4.3.2). Yeast stress-response translation regulation mechanism under NaCl-induced stress appears to be different from those operating under amino acid stress conditions (Pascual-Ahuir *et al.*, 2001). Furthermore there are reports of the presence of an alternative pathway activated by various stress conditions that induce ScGCN4 mRNA translation without the requirement of a functional ScGCN2 (Qiu *et al.*, 2000). Lack of clear phenotype for AtGCN2 null and p35S:AtGCN2 expressing lines (apart from root growth) under NaCl, KCl and mannitol stress, suggests the possibility of such an alternative pathway in *Arabidopsis*.

One of the potential alternative pathways has been reported in yeast, where studies on eIF2α have revealed that it is constitutively phosphorylated at multiple sites by the protein kinase Casein Kinase II (CK2). Phosphorylation occurred through a GCN2-independent mechanism and the process is required for optimal function of yeast eIF2α-P dependent responses (Feng *et al.*, 1994). This mechanism is reported to be essential for cell proliferation, transcription and translational control, cell cycle progression, and apoptosis and is also involved in cross-talk between CK2 and eIF2β (Bibby & Litchfield, 2005; Llorens *et al.*, 2005). Recently, putative CK2 protein kinases (holoenzymes) have been identified in *Arabidopsis* and various isoforms of plant CK2 are reported to be involved in the phosphorylation of translational machinery components including

eIF2α and hence regulate translation initiation amongst other physiological processes in plants (Dennis *et al.*, 2009).

There are also some major differences in the mechanism of translation in eukaryotes. For example eIF4E-binding protein is a key regulator of translation in most eukaryotes but is absent, there is a poorly conserved eIF4B and there are two isoforms of eIF4F; this suggests the mechanisms for control of translation may be different in plants (Browning, 2004). Although speculative, these reports support the idea that there may be an alternative pathway that regulates translation of putative *Arabidopsis* ScGCN4 homologues or other stress response transcription factors which are independent of AtGCN2. As sessile photoautotrophic organisms, plants are required to perform unique biological processes that other eukaryotes do not (e.g. photosynthesis, cellulose biosynthesis, etc.) and it would not be surprising, therefore, for them to have unique mechanisms for stress-induced regulation of translation in addition to some features that are conserved across all eukaryotes (Browning, 2004).

6.3 eIF2α Phosphorylation is Induced by Abiotic Stress and Strongly Suppresses Protein Synthesis

Experiments using a commercial wheat germ *in vitro* translation system and *Arabidopsis* mRNA as template confirmed that phosphorylation of eIF2α (eIF2α-P) with the human PKR kinase significantly suppresses protein synthesis although the abundance of a few major proteins was not affected. It was not possible to demonstrate an AtGCN2-dependent phosphorylation of eIF2α and commensurate suppression of protein synthesis in the wheat germ *in vitro* translation system due to difficulties associated with the expression of AtGCN2 in *E. coli*. None-the-less, these findings are consistent with reports in other eukaryotes, phosphorylation of eIF2α greatly suppresses protein synthesis and is probably the major mechanism that accounts for the rapid cessation in translation that accompanies the imposition of stress that has been widely reported (Hinnebusch *et al.*, 2004).

Attempts to demonstrate stress-induced suppression of protein synthesis *in planta* by monitoring the effects of stress on the expression of transgenic luciferase were equivocal. In these experiments the strong constitutive *p35S* promoter was used to drive the expression of luciferase and stress was imposed by treatment of these transgenic plants with the herbicide glyphosate to mimic nitrogen starvation. Whilst the results confirmed eIF2α was phosphorylated under these conditions and a commensurate decline in luciferase activity was observed, the possibility that the luminescence signal declined due to low abundance of amino acids rather than a suppression of translation cannot be discounted. Further experiments are required to confirm this point. Crosses between the relevant *Arabidopsis* lines have been made to generate *p35S:LUC* reporter lines in an *Atgcn2-1* (GCN2 null) and WT background and this will allow a comparison of the effects of a range of abiotic stress factors on translation *in vivo*. Unfortunately, due to time constraints, it was not possible to conduct these experiments with the duration of the project.

Taken together, the work presented in this thesis is consistent with a central role for *AtGCN2* in shutting down protein synthesis in response to abiotic stress factors. In contrast, there was no evidence to confirm reports that *AtGCN2* acts in a similar way to suppress translation in response to biotic stress factors. These findings are not entirely consistent with reports that were published during the term of this project (Zhang *et al*. 2008; Lageix *et al*. 2008).

6.4 Manipulation of the AtGCN2 Kinase Influences Root Morphology

Although null mutation is a direct way of studying gene function, sometimes null mutants lack readily identifiable phenotypes unless the mutant is subjected to specific growth conditions (Thorneycroft *et al.*, 2001). Characterisation of the *Atgcn2-1* mutant revealed that null mutation of AtGCN2 kinase did not produce a strong growth phenotype either under the non-stress or stress growth conditions used here. None-the-less it was clear that seedlings of the *Atgcn2-1* line had reduced primary root growth compared with the wild type and the *p35S:AtGCN2* seedlings under all growth conditions (Section 3.7.2 and 4.3). Lack of a clear phenotype with null lines has long been attributed to 'functional redundancy'

where a protein is encoded by two or more genes each of which is *de facto* redundant (Krysan *et al.*, 1999; Weigel *et al.*, 2000). Furthermore evaluation of gene function using null mutations, also fails to produce phenotypes for genes that are required at multiple stages of the life cycle and whose mutation can lead to early embrogenic or gametophytic lethality (Ichikawa *et al.*, 2003). The successful isolation of a homozygous *Atgcn2-1* mutant outlined in this study and reported by others (Zhang *et al*. 2008; Lageix *et al*. 2008) clearly suggests that AtGCN2 is not an essential protein that is required for survival under normal growth conditions but that does not preclude the possibility that it does improve survival under a certain set of environmental conditions. Rather than attempt to identify hypersensitive null mutants in stress response screens an alternative is to look for hypertolerant lines amongst a population of lines showing ectopic activation of genes; if these activated genes regulate key stress responses survival should be enhanced (Weigel *et al.*, 2000). Screening of the *p35S:AtGCN2* seedlings on media with or without NaCl, KCl and mannitol, however, did not produce strong phenotypes (Section 4.3 and 4.4) except for increased root growth and relatively bigger seedlings compared with wild type and null mutant seedlings (Fig. 4.8A). Furthermore, the reduced root growth of the *p35S:AtGCN2* seedlings under PEG-induced osmotic stress conditions unlike *Atgcn2-1* (Section 4.4.2), localisation of GFP:AtGCN2 kinase in the root apical meristem, and high AtGCN2 expression on the root zone of torpedo stage zygotic embryos (as revealed by *Arabidopsis* eFP Browser, Section 4.2.4) clearly suggests that AtGCN2 kinase may be involved in root growth and development. This is supported further by the observation that functional complementation of *Atgcn2-1* mutants through ectopic expression of *Atgcn2* increased primary root growth in the *p35S:AtGCN2* seedlings.

6.5 Manipulation of the AtGCN2 Kinase Augments Cold Stress Responses

Acclimation of seedlings to low and high temperatures by incubation for a few hours at 4° or 36°C induced the phosphorylation of eIF2α suggesting a role for GCN2 in adaptation to extremes of temperature. In addition, interrogation of the on-line resource *Arabidopsis* eFP browser for *AtGCN2* transcription rates (4.2.4) revealed a modest activation by conditions that induce cold acclimation

(3.4.3) again suggesting the AtGCN2 kinase may play a role in cold stress responses.

Due to time constraints the role of AtGCN2 in acclimation to low temperature was not fully investigated, but its role in the survival of seedlings to cold and heat shock was. Higher survival rates were observed from seedlings expressing the WT AtGCN2 protein (WT Col-0 and *p35S:AtGCN2*) compared with the functionally null truncated form (*Atgcn2-1*) twelve days after exposure to a brief but deep cold shock (Section 4.6.1). After completion of the practical work described in this thesis further experiments were undertaken by others on the effects of cold stress on cold acclimated and non-acclimated plants grown in soil and grown on agarose plates. The germplasm generated during this project (*Atgcn2-1* and lines over expressing AtGCN2 in an *Atgcn2-1* background) and WT Col-0 were cold acclimated (4°C) or not for 12 hours, allowed to recover at 22°C for 12 hours, and then exposed to freezing temperatures for a further 12 hours. The injury of these plants was assessed after a further 7 days recovery in normal growth conditions. These experiments demonstrated clearly that AtGCN2 is required for full acclimation to freezing temperatures in both seedlings and mature plants (Dr P Dominy and L Haarfeldt, University of Glasgow, per. comm.). These finding add further support to the conclusions from the experiments reported in this thesis; AtGCN2 is activated by low temperatures and mediates responses that improves survival of freezing temperatures.

In contrast, there was no evidence for a role of AtGCN2 in the survival of non-acclimated or acclimated seedlings to high temperatures (Section 4.6.2). These observations were somewhat surprising given the rapid and extensive phosphorylation of eIF2α that accompanies heat acclimation. Failure to establish a role for AtGCN2 in heat stress responses, however, may be attributable to the experimental difficulties associated with imposing a uniform and precise heat stress on shoot tissue, rather than reflecting its true function. One reason for this is that the transition from full survival to near complete death occurs over a narrow range of temperature, just 3° or 4°C. Another reason is the difficulty associated with controlling air temperature, even in sealed petri dishes to ±1°C of the set temperature, and this is further compounded by between and within leaf differences in the rates of transpiration that lead to local differences in the severity of heat stress. The effects of

transpiration can be minimised by performing these experiments in the dark (to induce stomatal closure and reduce the heating effect of irradiance), but unpublished experiments have shown stomata open widely when leaf temperature exceeds 36°C (Dr Peter Dominy, University of Glasgow; per. comm.). When grown on sealed plates it might be assumed seedlings are exposed to an atmosphere with 100% relative humidity thereby minimizing transpiration, but theoretically small cyclical changes in air temperature associated with an incubator's thermostat are sufficient to decrease relative humidity by a few percent which would allow transpiration to resume. For these reasons, it is not a trivial task to impose a constant heat stress uniformly across all exposed leaf tissue, and therefore with variability in the extent of damage between individual leaves of the same genotype, it is difficult to assess differences between genotype responses.

6.6 Are Stress Responses in *Arabidopsis* Activated by eIF2α Phosphorylation?

Translational control of stress responses in mammalian and yeast systems is manifest as a suppression of general protein synthesis and the synthesis of transcription factors (e.g. GCN2 and ATF4) that activate stress response regulons. Work presented in this thesis has provided compelling evidence that in plants abiotic stress triggers a GCN2/eIF2α suppression of protein synthesis, but no evidence has been provided to show the activation of regulons through the translation of key transcription factors by a uORF/mORF mechanisms comparable to that found in other eukaryotes, particularly yeast and mammals.

It was hoped that comparison of the *in vitro* translated proteins of *Arabidopsis* mRNA using a wheat germ system containing eIF2α or eIF2α-P would identify plant homologues of GCN4 and ATF4. Sadly, this was not the case; although the presence of eIF2α-P suppressed general protein synthesis, there was no evidence for the synthesis of proteins not found when eIF2α was used for initiation of translation. It is conceivable that such proteins were synthesized but not in sufficient amounts to be detected on protein gels.

A bioinformatics approach was also attempted to identify translationally activated sequences. In these studies the 5'UTR regions of all *Arabidopsis* cDNA was investigated for uORF structures that might be involved in translational control. These studies revealed that approximately one-third (>8,000) of *Arabidopsis* genes encode a 5'UTR uORF peptide with at least 2 codons and contain a *bone fide* start and stop codon. This large set of cDNAs were then refined using search criteria for uORF structure broadly similar to those found in ScGCN4 and HsATF4; both the number of uORFs and their relative position in the 5′UTR were considered. From this filter a list of 50 transcription factors was prepared although none of these showed particularly close similarity to ScGCN4 or HsATF4 5′UTR uORF structure (Appendix 18; group 4 sequences). Further studies are required to determine if any of these transcription factors are activated by AtGCN2.

The sequences that showed highest homology to the 5′ UTR of ScGCN4 was not transcription factors but a glycosyl transferase / cellulose synthase, and a methyl transferase (Fig. 5.6A&B) among others (Appendix 18; group 3 sequences). Genomic DNA methylation has long been implicated in regulating gene expression and it is tempting to speculate that the translation of the methyl transferase identified here (At1g58120) is regulated through the phosphorylation of eIF2α which in turn regulates transcriptional activity, but at this stage there is no direct evidence to support this contention. The transcription of glycosyl transferases are often affected by abiotic stress factors in plants and it would not be surprising, therefore, for them to be activated at the translational level as well. Whether the sequence identified here (At4g31590) is involved in ER stress responses or stress responses further downstream remains unknown. The sequence containing a 5′UTR uORF most closely related to HsATF4 (At3g47750) encodes a RING/ Zn finger protein. Analysis of its transcriptional expression profile using the e-FP Browser facility shows that it is transcriptionally regulated by cold and heat stress, and by UV irradiation. Clearly, with a Zn finger domain it is possible that this protein is a transcription factor, indeed the TAIR reports its cellular location to be in the nucleus, but there is no direct evidence that it directly regulates transcription.

The endogenous levels of protein of the sequences listed in Appendix 18 may well be regulated at the translational level but further experiments will be required to establish this. One option would be to investigate the protein profile of WT Col-0 and the GCN2 null line *Atgcn2-1* in response to abiotic stress. If these sequences are indeed regulated at the protein level by the activity of GCN2, it should be apparent.

6.7 Significance of GCN2 Signalling Pathway in Plants

The GCN2 signalling pathway has attracted a lot of attention due to its importance in fungal and mammalian metabolism. It has great potential in addressing human health issues, and has been a probable target for drug development for common human disease such as diabetes mellitus, osteoporosis, cancer, virus infection and diabetes (Nayak & Pintel, 2007; Ron & Harding, 2007). Translational control seems to play a key role in numerous developmental and physiological processes in plants, and has been reported to regulate specific genes in response to environmental stress cues, such as water and heat stress (Gallie *et al.*, 1997; Szick-Miranda *et al.*, 2003). Despite differences with the mammalian system, elucidation of GCN2-mediated stress response mechanism and its interaction with other signalling pathway(s) may provide opportunities for developing multi-stress tolerant crops. Since no strong phenotype was observed with a functional AtGCN2 null line, despite being activated under different stress condition suggested that it may be a sensory or receptor-like kinase induced in response to temperature, amino acid and salinity stress. However determination of its role in *Arabidopsis* as a sensor kinase or its involvement in cross-talk between amino acid and carbon signalling pathways (Halford *et al.*, 2004), and endoplasmic reticulum (ER) based unfolded protein response (UPR) pathway (Chen & Brandizzi, 2012) need to be established.

6.8 Conclusions

- *Arabidopsis* eIF2α is phosphorylated at serine 56 located in the SEL**S** domain conserved across all eukaryotes; in yeast and mammalian systems it is serine 51 within the SEL**S** domain that is the target for phosphorylation. This was demonstrated by the ClustalW2 alignment of

the eIF2α protein sequences from *Arabidopsis*, Oryza *sativa*, *Picea abies*, *Homo sapiens*, *Mus musculus,* and *Saccharomyces cerivisiae*.

- GCN2 is the kinase that phosphorylates serine 56 of *Arabidopsis* eIF2α. *Arabidopsis* lacks mammalian PKR, HRI and PERK kinase homologues. The results obtained during *in silico* search for presence of other eIF2α kinases, the inability of truncated AtGCN2 kinase to phosphorylate eIF2α (*Atgcn2-1* mutant seedlings), and functional complementation of *Atgcn2-1* by ectopic expression of *AtGCN2* ORF clearly demonstrated that AtGCN2 kinase is responsible for phosphorylation of AteIF2α (ser56) in *Arabidopsis*.

- The CT-domain is important in activation of the AtGCN2 kinase. The inability to activate AtGCN2 kinase in *Atgcn2-1* seedlings under different stress conditions (N-starvation, NaCl, Cold, and heat stress clearly demonstrates that HisRs (CT-domain) is critical in the activation of the AtGCN2 kinase *in planta* and maybe *in vitro* too.

- Abiotic stresses including salinity, N-starvation and acclimation to extremes of temperature (4 and 37^{o}C) activates the AtGCN2 kinase *in planta*, unlike biotic stresses (Cauliflower Mosaic Virus, *Pseudomonas syringe* DC3000) suggesting that activation of the AtGCN2 kinase does not evoke response in, and is not activated by, the jasmonate and salicylate stress response pathways.

- The results obtained with the AtGCN2 null mutation, ectopic expression experiments, and tissue specific localisation suggests that the AtGCN2 kinase is involved in root growth, and the WT sequence is responsive to PEG-induced osmotic stress, and low temperatures. Salinity stress and high temperatures also lead to an activation of WT AtGCN2 but this did not appear to confer a stress tolerant phenotype on seedlings.

- Phosphorylation of AteIF2α and WGeIF2α suppressed proteins synthesis *in planta* and *in vitro,* respectively.

- Bioinformatic studies have identified several putative translation regulated transcripts homologous to yeast GCN4 and human ATF4

suggesting *Arabidopsis* possesses a translation control mechanisms that is regulated by the AtGCN2 kinase. There is some evidence that an alternative translational control mechanism independent of AtGCN2 kinase is also present.

6.9 Future Work

This study has attempted to dissect translation regulation mechanism in *Arabidopsis* using *in planta*, *in vitro* and gene mutation techniques (*Atgcn2* mutants) and using *in silico* tools. However, more needs to be done to elucidate this mechanism further and to determine its importance or function in plants. The root and cold phenotypes obtained with the AtGCN2 kinase mutants and tissue specific localisation of AtGCN2 protein, especially in root tips/zones suggested that AtGCN2 kinase is required for growth and development. Further work is therefore needed to investigate the localisation of GFP:AtGCN2 fusion protein under the control of either a native or inducible promoter and a smaller or different fusion tag to determine whether AtGCN2 localisation observed in this study was due to the influence of the 2×35S constitutive promoter and GFP tag (mis-location). In addition, localisation of GFP:AtGCN2 fusions under stress (activated kinase) and non-stress (inactivated kinase) conditions are required to determine any change in cellular localisation. Further work on the role of AtGCN2 on root growth is required, as is its effect on tolerance of abiotic stress factors including osmotic, cold and heat stress; particular attention should be paid to the activity of AtGCN2 in meristematic tissues such as root tips. This will help address the question 'does *in planta* phosphorylation of AteIF2α reduce cell proliferation or growth in *Arabidopsis* root tips?'.

Direct AtGCN2 interaction with the components of other signalling pathways could be investigated by pull-down assays using lines ectopically expressing epitope-tagged AtGCN2 kinase. Further, interaction analysis may have to be conducted using the yeast two-hybrid system. Attempts to identify putative *Arabidopsis* ScGCN4 homologues using the bioinformatics techniques are in their infancy but the work reported in this thesis suggests this may be a fruitful avenue to pursue. Further work is required to determine if the uORF present in these putative homologues have a regulatory role in translation. If they are

regulatory, then further *in vitro* and *in planta* studies are required to establish if they are regulated at the translational level by phosphorylation of AteIF2α or WGeIF2α. Failure to produce strong phenotypes in AtGCN2 mutants suggests the presence of an alternative mechanism that is capable of inducing translation of putative *Arabidopsis* ScGCN4 homologues without the involvement of AtGCN2; hence there is a need to investigate these possibilities. The *in vitro* phosphorylation of AteIF2α or WGeIF2α by mPKR suggested functional complementation and conservation of the translation control mechanism through phosphorylation of plants eIF2α. It would be interesting, however, to determine whether ectopic expression of mPKR can functionally complement AtGCN2 null lines, as *Arabidopsis* has only AtGCN2 kinase which is activated through a different mechanism.

7 References

Albert B, Johnson J, Lewis J, Raff M, Roberts K & Walter P. (2002). Molecular biology of the cell. 4 edn, pp. 348-364. Garland Science, New York.

Algire MA, Maag D & Lorsch JR. (2005). P_i release from eIF2, not GTP hydrolysis, is the step controlled by start-site selection during eukaryotic translation initiation *Molecular and Cellular Biochemistry* **20,** 251-262.

Aoyama T, Dong CH, Wu Y, Carabelli M, Sessa G, Ruberti I, Morelli G & Chua NH. (1995). Ectopic expression of the *Arabidopsis* transcriptional activator Athb-1 alters leaf cell fate in tobacco. *Plant Cell* **7,** 1773 - 1785.

Asano K, Clayton J, Shalev A & Hinnebusch AG. (2000). A multifactor complex of eukaryotic initiation factors, eIF1, eIF2, eIF3, eIF5, and initiator tRNA (Met) is an important translation initiation intermediate *in vivo*. *Genes and Developement* **14,** 2534-2546.

Asano K & Sachs MS. (2007). Translation factor control of ribosome conformation during start codon selection. *Genes & Developement* **21,** 1280-1287.

Bailey-Serres J. (1999). Selective translation of cytoplasmic mRNAs in plants. *Trends in Plant Science* **4,** 142-148.

Bertolotti A, Zhang Y, Hendershot LM, Harding HP & Ron D. (2000). Dynamic interraction of BiP and ER stress transducers in the unfolded protein response *Nature Cell Biology* **2,** 326-332.

Bostock RM. (2005). Signal crosstalk and induced resistance: straddling the line between cost and benefit. *Annual Review of Phytopathology* **43,** 545-580.

Bradford MM. (1976). A rapid and sensitive method for quantitation of microgram qauntities of protein utilizing the principle of protein-dye-binding. *Analytical Biochemistry* **72,** 248-254.

Branco-Price C, Kawaguchi R, Ferreira RB & Bailey-Serres J. (2005). Genome-wide analysis of transcript abundance and translation in Arabidopsis seedlings subjected to oxygen deprivation. *Annals of Botany (Lond)* **96,** 647 - 660.

Bray EA, Bailey-Serres J & Weretilnyk E. (2000). Responses to abiotic stresses. *In Biochemistry and Molecular Biology of Plants* ed. B. B. Buchanan, W. Gruissem & R. L. Jones, pp. 1158-1203 American Society of Plant Physiologists, Rockville, Md.

Browne GJ & Proud CG. (2002). Regulation of peptide-chain elongation in mammalian cells. *European Journal of Biochemistry* **269,** 5360-5368.

Browning KS. (2004). Plant translation initiation factors: it is not easy to be green. *Biochemical Society Transactions* **32,** 589-591.

Bruce WB, Edmeades GO & Barker TC. (2002). Molecular and physiological approaches to maize improvement for drought tolerance. *Journal of Experimental Botany* **53,** 13-25.

Buysse W, Stern R, Coe R & Matere C. (2007). *GenStat Discovery Edfition 3 for everyday use*. ICRAF Nairobi, Kenya.

Carnevalli LS, Pereira CM, Jaqueta CB, Alves VS, Paiva VN, Vattem KM, Wek RC, Mello LAM & Castilho BA. (2006). Phosphorylation of the α–subunit of translation initiation factor-2 by PKR mediates protein synthesis inhibition in the mouse brain during status epilepticus. *Biochemistry Journal* **397,** 187-194.

Chang C, Kwok SF, Bleecker AB & Meyerowitz EM. (1993). *Arabidopsis* ethylene-response gene ETR1: similarity of product to two-component regulators. *Science* **262,** 539-544.

Chang L-Y, Yang WY, Browning K & Roth D. (1999). Specific *in vitro* phosphorylation of plant eIF2α by eukaryotic eIF2α kinase. *Plant Molecular Biology* **41,** 363-370.

Chang L-Y, Yang WY & Roth D. (2000). Functional complementation by wheat eIF2α in the yeast GCN2-mediated pathway. *Biochemical and Biophysical Research Communications* **279,** 468-474.

Chapman SC & Edmeades GO. (1999). Selection improves drought tolerance in tropical maize populations: II. Direct and correlated responses among secondary traits. *Crop Science* **39,** 1315-1324.

Chaves MM, Flexas J & Pinheiro C. (2009). Photosynthesis under drought and salt stress: regulation mechanisms from whole plant to cell. *Annals of Botany* **103,** 551-560.

Chaves MM & Oliveira MM. (2004). Mechanisms underlying plant resilience to water deficits: prospects for water-saving agriculture. *Journal of Experimental Botany* **55,** 2365-2384.

Chen JJ. (2000). Heme-regulated eIF2α–kinase. In *Translational control of gene expression*, ed. Sonenberg N, Hershey JWB & Mathews MB. Cold Spring Harbor Laboratory Press, Plainview New York.

Cheung Y-N, Maag D, Mitchell SF, Fekete CA, Algire MA, Takacs JE, Shirokikh N, Pestova T, Lorsch JR & Hinnebusch AG. (2007). Dissociation of eIF1 from the 40S ribosomal subunit in a key step in start codon selection *in vivo*. *Genes and Developement* **21,** 1217-1230.

Chinnusamy V, Zhu J & Zhu J-K. (2007). Cold stress regulation of gene expression in plants. *Trends in Plant Science* **12,** 444-451.

Clemens M. (1996). Protein kinases that phosphorylate eIF2α and eIF2B, and their role in eukaryotic cell translational control. In *Translational control*, ed. Hershey JWB, Mathews MB & Sonenberg N, pp. 139-172. Cold Spring Harbor Press, Plainview New York.

Clemens MJ. (1997). PKR-a protein kinase regulated by double-stranded RNA. *The International Journal of Biochemistry and Cell Biology* **29,** 945 - 949.

Coca MA, Almoguera C, Thomas TL & Jordano J. (1996). Differential regulation of small heat-shock genes in plants: analysis of a water-stress-inducible and developmentally activated sunflower promoter. *Plant Molecular Biology* **31,** 863 - 876.

Condon AG, Richards RA, Rebetzke GJ & Farquhar GD. (2004). Breeding for high water-use efficiency. *Journal of Experimental Botany* **55,** 2447-2460.

Conn GL. (2003). Expression of active RNA-activated protein kinase (PKR) in bacteria. *Biotechniques* **35,** 682-686.

Curtis MD & Grossniklaus U. (2003). A Gateway cloning vector set for high-through put functional analysis of genes *in planta*. *Plant Physiology* **133,** 462-469.

Damiani RD & Wessler SR. (1993). An upstream open reading frame represses expression of Lc, a member of the R/B family of maize transcriptional activators. *Proceedings of National Academy of Science USA* **90** 8244–8248.

Dar AC, Dever TE & Sicheri F. (2005). Higher order substrate recognition of eIF2α by the RNA-depended protein kinase PKR. *Cell* **122,** 887-900.

Dey M, Cao C, Dar AC, Tamura T, Ozato K, Sicheri F & Dever TE. (2005). Mechanistic link between PKR dimerization, autophosphorylation, and eIF2α substrate recognition. *Cell* **122,** 901-913.

Dey M, Cao C, Sicheri F & Dever TE. (2007). Conserved intermolecular salt bridge required for activation of protein kinases PKR, GCN2 and PERK. *Journal of Biological Chemistry* **282,** 6653-6660.

FAO. (2009). Profile for climate change. In *Climate change and food security*, ed. FAO, pp. 28. FAO, Natural Resources Management and Enviromental Department.

Fernandez J, Yaman I, Huang C, Liu H, Lopez AB, Komar AA, Caprara MG, Merrick WC, Snider MD, Kaufman RJ, Lamers WH & Hatzoglou M. (2005). Ribosome stalling regulates IRES-mediated translation in eukaryotes, a parallel to prokaryotic attenuation. *Molecular Cell* **17,** 405 - 416.

Flowers TJ. (2004). Improving crop salt tolerance. *Journal of Experimental Botany* **55** 207-319.

Fujii H, Verslues PE & Zhu J-K. (2007). Identification of two protein kinases required for abscisic acid regulation of seed germination, root growth, and gene expression in *Arabidopsis*. *Plant Cell* **19,** 485-494.

Fujita M, Fujita Y, Noutoshi Y, Takahashi F, Narusaka Y, Yamaguchi-Shinozaki K & Shinozaki K. (2006). Crosstalk between abiotic and biotic stress responses: a current view from the points of convergence in the stress signaling networks. *Current Opinion in Plant Biology* **9,** 436-442.

Futterer J & Hohn T. (1992). Role of an upstream open reading frame in the translation of polycistronic mRNAs in plant cells. *Nucleic Acids Research* **20,** 3851 - 3857.

Gallie DR, Le H, Caldwell C, Tanguay RL, Hoang NX & Browning KS. (1997). The Phosphorylation State of Translation Initiation Factors Is Regulated Developmentally and following Heat Shock in Wheat. *Journal of Biological Chemistry* **272,** 1046-1053.

Geer LY, Domrachev M, Lipman DJ, Bryant SH & (2002). CDART: Protein Homology by Domain Architecture. *Genome Research* **12,** 1619-1623.

Hai Lan P, Jeong Hwa L, Soo Jin K, Gang-Won C & Inhwan H. (2001). Constitutive over-expression of AtGSK1 induces NaCl stress responses in the absence of NaCl stress and results in enhanced NaCl tolerance in *Arabidopsis*. *The Plant Journal* **27,** 305-314.

Halford NG, Hey S, Jhurreea D, Laurie S, McKibbin RS, Zhang Y & Paul MJ. (2004). Highly conserved protein kinases involved in the regulation of carbon and amino acid metabolism. *Journal of Experimental Botany* **55,** 35-42.

Hamilton A, Voinnet O, Chappell L & Baulcombe D. (2002). Two classes of short interfering RNA in RNA silencing. *EMBO Journal* **21,** 4671-4679.

Hartwell LH, Hood L, Goldberg ML, Reynolds AE, Silver LM & Veres RC. (2008). *Genetic from genes to genome*. McGraw-Hill, New York.

Heazlewood JL, Tonti-Filippini J, Verboom RE & Millar AH. (2005). Combining experimental and predicted datasets for determination of the subcellular location of proteins in *Arabidopsis*. *Plant Physiology* **139,** 598-609.

Hennig L, Köhler C, Viczián A & Kircher S. (2010). Luciferase and green fluorescent protein reporter genes as tools to determine protein abundance and intracellular dynamics. In *Plant Developmental Biology*, ed. Walker JM, pp. 293-312. Humana Press.

Hinnebusch AG. (1988). Mechanisms of gene regulation in the general control of amino acid biosynthesis in Saccharomyces cerevisiae. *Microbiology Review* **52,** 248-273.

Hinnebusch AG. (1992). General and pathway-specific regulatory mechanisms controlling the synthesis of amino acid biosynthetic enzymes in *Saccharomyces cerevisiae*. In *The molecular and cellular biology of the yeast Saccharomyces*, ed. Jones EW, Pringle JR & Broach JR, pp. 319–414. Cold Spring Harbor Press New York.

Hinnebusch AG. (1996). Translational control of GCN4: gene specific regulation by phosphorylation of eIF2. In *Translational Control*, ed. Hershey JWB, Mathews MB & Sonenberg N, pp. 199-244. Cold Spring Harbor Laboratory Press, New York.

Hinnebusch AG. (1997a). Translational regulation of yeast GCN4. *Journal of Biological Chemistry* **272,** 21661 - 21664.

Hinnebusch AG. (1997b). Translational regulation of yeast GCN4. *Journal of Biological Chemistry* **272,** 21661 - 21664.

Hinnebusch AG. (2005). Translational regulation of GCN4 and the general amino acid control of yeast. *Annual Review of Microbiology* **59,** 407-450.

Hinnebusch AG. (2006). eIF3: A varsatile scaffold for translation initiation complexes. *Trends in Biochemical Sciences* **31,** 553-562.

Hinnebusch AG, Asano K, Olsen DS, Phan LON, Nielsen KH & Valasek L. (2004). Study of Translational Control of Eukaryotic Gene Expression Using Yeast. *Annals of the New York Academy of Science* **1038,** 60-74.

Hinnebusch AG & Natarajan K. (2002). Gcn4p, a master regulator of gene expression, is controlled at multiple levels by diverse signals of starvation and stress. *Eukaryotic Cell* **1,** 22-32.

Hoffmann B, Valerius O, Andermann M & Braus GH. (2001). Transcriptional autoregulation and inhibition of mRNA translation of amino acid regulator gene *cpcA* of filamentous fungus *Aspergillus nidulans*. *Molecular Biology of the Cell* **12,** 2846-2857.

Ichikawa T, Nakazawa M, Kawashima M, Iizumi H, Kuroda H, Kondou Y, Tsuhara Y, Suzuki K, Ishikawa A, Seki M, Fujita M, Motohashi R, Nagata N, Takagi T, Shinozaki K & Matsui M. (2006). The FOX hunting system: an alternative gain-of-function gene hunting technique. *The Plant Journal* **48,** 974-985.

Ichikawa T, Nakazawa M, Kawashima M, Muto S, Gohda K, Suzuki K, Ishikawa A, Kobayashi H, Yoshizumi T, Tsumoto Y, Tsuhara Y, Iizumi H, Goto Y & Matsui M. (2003). Sequence database of 1172 T-DNA insertion sites in Arabidopsis activation-tagging lines that showed phenotypes in T1 generation. *The Plant Journal* **36,** 421-429.

Iida K, Li Y, McGrath B, Frank A & Cavener D. (2007). PERK eIF2 alpha kinase is required to regulate the viability of the exocrine pancreas in mice. *BMC Cell Biology* **8,** 38.

Imataka H & Sonenberg N. (1997). Human eukaryotic translation initiation factor-4G (eIF4G) posesses two indipendent binding sites for eIF4A. *Molecular and Cellular Biology* **17,** 6940-6947.

Jiang H-Y & Wek RC. (2005). Phosphorylation of the alpha-subunit of the eukaryotic initiation factor-2 (eIF2alpha) reduces protein synthesis and enhances apoptosis in response to proteasome inhibition. *Journal of Biological Chemistry* **280,** 14189-14202.

Karaba A, Dixit S, Greco R, Aharoni A, Trijatmiko KR, Marsch-Martinez N, Krishnan A, Nataraja KN, Udayakumar M & Pereira A. (2007). Improvement of water use efficiency in rice by expression of HARDY, an Arabidopsis drought and salt tolerance gene. *Proceedings of the National Academy of Sciences* **104,** 15270-15275.

Karimi M, Depicker A & Hilson P. (2007). Recombinational Cloning with Plant Gateway Vectors. *Plant Physiology* **145,** 1144-1154.

Karimi M, Inzé D & Depicker A. (2002). GATEWAY™ vectors for Agrobacterium-mediated plant transformation. *Trends in Plant Science* **7,** 193-195.

Kaufman RJ. (1999). Double-stranded RNA-activated protein kinase mediates virus-induced apoptosis: A new role for an old actor. *Proceedings of the National Academy of Sciences* **96,** 11693-11695.

Kaufman RJ. (2000). Double-stranded RNA-activated protein kinase PKR In *Transalational control of gene expression*, ed. Sonenberg N, Hershey JWB & Mathews MB, pp. 503-527. Cold Spring Harbor Laboratory Press, Plainview New York.

Kaufman RJ. (2004). Regulation of mRNA translation by protein folding in the endoplasmic reticulum. *Trends in Biochemical Sciences* **29,** 152-158.

Ke Y, Sierzputowska-Gracz H, Gdaniec Z & Theil EC. (2000). Internal loop/bulge and hairpin loop of the iron-responsive element of ferritin mRNA contribute to maximal iron regulatory protein 2 binding and translational regulation in the Iso-iron-responsive element/Iso-iron regulatory protein family. *Biochemistry* **39,** 6235-6242.

Kim TH, Kim BH, Yahalom A, Chamovitz DA & von Arnim AG. (2004). Translational regulation via 5' mRNA leader sequences revealed by mutational analysis of the Arabidopsis translation initiation factor subunit eIF3h. *Plant Cell* **16,** 3341 - 3356.

Kochetov AV, Ahmad S, Ivanisenko V, Volkova OA, Kolchanov NA & Sarai A. (2008). uORFs, reinitiation and alternative translation start sites in human mRNAs. *FEBS Letters* **582,** 1293 - 1297.

Kozak M. (1978). How do eukaryotic ribosomes select initiation regions in messenger RNA? *Cell* **15,** 1109-1123.

Kozak M. (1983). Comparison of initiation of protein synthesis in procaryotes, eucaryotes, and organelles. *Microbiological Reviews* **47,** 1-45.

Kozak M. (1987a). Effects of intercistronic length on the efficiency of reinitiation by eucaryotic ribosomes. *Moecular and Cellular Biology* **7,** 3438 - 3445.

Kozak M. (1987b). Effects of intercistronic length on the efficiency of reinitiation by eucaryotic ribosomes. *Molecular and Cellular Biology* **7,** 3438 - 3445.

Kozak M. (1991). Effects of long 5' leader sequences on initiation by eukaryotic ribosomes in vitro. *Gene Expression* **1,** 117 - 125.

Kozak M. (2005). Regulation of translation via mRNA structure in prokaryotes and eukaryotes. *Gene* **361,** 13-37.

Kregel KC. (2002). Heat shock proteins: modifying factors in physiological stress responses and acquired thermotolerance. *Journal of Applied Physiology* **92,** 2177 - 2186.

Krummeck G, Göttenof T & Rödel G. (1991). AUG codons in the RNA leader sequences of the yeast PET genes CBS1 and SCO1 have no influence on translation efficiency. *Current Genetics* **20,** 465-469.

Krysan PJ, Young JC & Sussman MR. (1999). T-DNA as an insertional mutagen in *Arabidopsis*. *Plant Cell* **11,** 2283-2290.

Kumar R, Azam S, Sullivan JM, Owen C, Cavener DR, Zhang P, Ron D, Harding HP, Chen JJ & Han AP. (2001). Brain ischemia and reperfusion activates the eukaryotic initiation factor 2α kinase, PERK. *Journal of Neurochemistry* **77,** 1418-1421.

Kuromori T, Takahashi S, Kondou Y, Shinozaki K & Matsui M. (2009). Phenome analysis in plant species using Loss-of-function and gain-of-function Mutants. *Plant and Cell Physiology* **50,** 1215-1231.

Lageix S, Lanet E, Pouch-Pelissier M-N, Espagnol M-C, Robaglia C, Deragon J-M & Pelissier T. (2008). *Arabidopsis* eIF2 alpha kinase GCN2 is essential for growth in stress conditions and is activated by wounding. *BMC Plant Biology* **8,** 134.

Lamaire PA, Lary J & Cole JL. (2005). Mechanism of PKR activation: Dimerization and Kinase Activation in the Absence of Double-stranded RNA. *Journal of Molecular Biology* **345,** 81-90.

Lamphear B, Kirchenweger R, Skern T & Rhoads R. (1995). Mapping functional domains in eukaryotic protein synthesis initiation factor 4G (eIF4G) with picornaviral proteases; implications for cap-dependent and cap-indipendent translation initiation *Journal of Biological Chemistry* **270,** 21975-21983.

Langland JO, Langland L, Zeman C, Saha D & Roth DA. (1996). Phosphorylation of plant eukaryotic initiation factor-2 by the plant encoded double-stranded RNA-depended protein kinase, pPKR, and inhibition of protein synthesis *in vitro*. *The Journal of Biological Chemistry* **271,** 4539-4544.

Larkin R. (2007). Extraction of total protein from Arabidopsis. *Cold Spring Harbor Protocols* **doi :10.1101/pdb.prot4680**.

Liang S-H, Zhang W, McGrath BC, Zhang P & Cavener DR. (2006). PERK (eIF2α kinase) is required to activate the stress-activated MAPKs and induce the expression of immediate-early genes upon disruption of ER calcium homoeostasis. *Biochemical Journal* **393,** 201-209.

Lohmer S, Maddaloni M, Motto M, Salamini F & Thompson RD. (1993). Translation of the mRNA of the maize transcriptional activator Opaque-2 is inhibited by upstream open reading frames present in the leader sequence. *Plant Cell* **5,** 65 - 73.

Lomakin IB, Hellen CUT & Pestova TV. (2000). Physical association of eukaryotic initiation factor 4G (eIF4G) with eIF4A strongly enhances binding of eIF4G to the internal ribosomal entry site of encephalomyocarditis virus and is required for internal initiation of translation. *Molecular and Cellular Biology* **20,** 6019-6029.

Lorenzo O & Solano R. (2005). Molecular players regulating the jasmonate signalling network. *Current Opinion in Plant Biology* **8,** 532-540.

Lu L, Han A-P & Chen J-J. (2001). Translation initiation control by heme-regulated eukaryotic initiation factor 2 alpha kinase in erythroid cells under cytoplasmic stresses. *Molecular and Cellular Biology* **21,** 7971-7980.

Lu PD, Harding HP & Ron D. (2004). Translation re-initiation at alternative open reading frames regulates gene expression in an integrated stress response. *Journal of Cell Biology* **167,** 27-33.

Lukaszewicz M, Je´ rouville B & Boutry M. (1998). Signs of translational regulation within the transcript leader of a plant plasma membrane HF-ATPase gene. *The Plant Journal* **14,** 413–423.

Maag D, Fekete CA, Gryczynski Z & Lorsch JR. (2005). A conformational change in the eukaryotic translation preinitiation complex and release of eIF1 signal recognition of the start codon. *Molecular and Cellular Biochemistry* **17,** 265-275.

Majumdar R & Maitra U. (2005). Regulation of GTP hydrolysis prior to ribosomal AUG selection during eukaryotic translation initiation. *EMBO Journal* **24,** 3737-3746.

Mathews MB & Shenk T. (1991). Adenovirus virus-associated RNA translational control. *Journal of Virology* **65,** 5657-5662.

Matsui T, Tanihara K & Date T. (2001). Expression of un-phosphorylated form of human double-stranded RNA-activated protein kinase in *Escherichia coli*. *Biochemical and Biophysical Research Communications* **284,** 798-807.

Mauch-Mani B & Mauch F. (2005). The role of abscisic acid in plant-pathogen interactions. *Current Opinion in Plant Biology* **8,** 409-414.

McElver J, Tzafrir I, Aux G, Rogers R, Ashby C, Smith K, Thomas C, Schetter A, Zhou Q, Cushman MA, Tossberg J, Nickle T, Levin JZ, Law M, Meinke D & Patton D. (2001). Insertional mutagenesis of genes required for seed development in *Arabidopsis thaliana*. *Genetics* **159,** 1751-1763.

Meijer HA & Thomas AA. (2002). Control of eukaryotic protein synthesis by upstream open reading frames in the 5'-untranslated region of an mRNA. *Biochemical Journal* **367,** 1 - 11.

Meister G & Tuschl T. (2004). Mechanisms of gene silencing by double-stranded RNA. *Nature* **431,** 343-349.

Meurs E, Chong K, Galabru J, Thomas NSB, Kerr IM, Williams BRG & Hovanessian AG. (1990). Molecular cloning and characterisation of the human double stranded RNA-activated protein kinase induced by interferon. *Cell* **62,** 379-390.

Michel BE & Kaufmann MR. (1973). The osmotic potential of polyethylene glycol 6000. *Plant Physiology* **51** 914-916.

Mignone F, Gissi C, Liuni S & Pesole G. (2002). Untranslated regions of mRNAs. *Genome Biology* **3,** reviews0004.0001-0004.0010.

Miki D, Itoh R & Shimamoto K. (2005). RNA silencing of single and multiple members in a gene family of rice. *Plant Physiology* **138,** 1903-1913.

Mittler R. (2006). Abiotic stress, the field environment and stress combination. *Trends in Plant Science* **11,** 15-19.

Moffat AS. (2002). PLANT GENETICS: Finding new ways to protect drought-stricken plants. *Science* **296,** 1226-1229.

Morris DR & Gaballe AP. (2000). Upstream open reading frames as regulators of mRNA translation. *Molecular and Cellular Biology* **20,** 8635-8642.

Munns R. (2002). Comparative physiology of salt and water stress. *Plant, Cell and Environment* **25,** 239-250.

Munns R & Tester M. (2008). Mechanisms of Salinity Tolerance. *Annual Review of Plant Biology* **59,** 651-681.

Murphy AS, Schulz B, Peer W, Barkla B & Pantoja O. (2011). Plasma Membrane and Abiotic Stress. In *The Plant Plasma Membrane*, pp. 457-470. Springer Berlin / Heidelberg.

Nakamura H, Hakata M, Amano K, Miyao A, Toki N, Kajikawa M, Pang J, Higashi N, Ando S, Toki S, Fujita M, Enju A, Seki M, Nakazawa M, Ichikawa T, Shinozaki K, Matsui M, Nagamura Y, Hirochika H & Ichikawa H. (2007). A genome-wide gain-of-function analysis of rice genes using the FOX-hunting system. *Plant Molecular Biology* **65,** 357-371.

Nakazawa M, Ichikawa T, Ishikawa A, Kobayashi H, Tsuhara Y, Kawashima M, Suzuki K, Muto S & Matsui M. (2003). Activation tagging, a novel tool to dissect the functions of a gene family. *The Plant Journal* **34,** 741-750.

Naranda T, MacMillan SE, Donahue TF & Hershey JW. (1996). SUI1/p16 is required for the activity of translation initiation factor 3 in *Sacccharomyces cerevisiae*. *Molecular and Cellular Biology* **16,** 2307-2313.

Natarajan K, Meyer MR, Jackson BM, Slad D, Roberts C, Hinnebusch AG & Marton MJ. (2001). Transcriptional profiling show that Gcn4p is a master regulator of gene expression during amino acid starvation in yeast. *Molecular and Cellular Biology* **21,** 4347-4368.

Nelson DE, Repetti PP, Adams TR, Creelman RA, Wu J, Warner DC, Anstrom DC, Bensen RJ, Castiglioni PP, Donnarummo MG, Hinchey BS, Kumimoto RW, Maszle DR, Canales RD, Krolikowski KA, Dotson SB, Gutterson N, Ratcliffe OJ & Heard JE. (2007). Plant nuclear factor Y (NF-Y) B subunits confer drought tolerance and lead to improved corn yields on water-limited acres. *Proceedings of the National Academy of Sciences* **104,** 16450-16455.

Penfield S. (2008). Temperature perception and signal transduction in plants. *New Phytologist* **179,** 615-628.

Pesole G, Mignone F, Gissi C, Grillo G, Licciulli F & Liuni S. (2001). Structural and functional features of eukaryotic mRNA untranslated regions. *Gene* **276,** 73-81.

Pestova T, Lorsch JR & Hellen CUT. (2007). The mechanism of translation initiation in eukaryotes In *Translation control in biology and medicine* ed. Mathews MB, Sonenberg N & Hershey JWB, pp. 87-128. Cold Spring Harbor Laboratory Press, New Yok.

Pestova TV & Kolupaeva VG. (2002). The roles of individual eukaryotic translation initiation factors in ribosomal scanning and initiation codon selection. *Genes and Developement* **16,** 2906-2922.

Pestova TV & Kulopaeva VG. (2002). The roles of individual eukaryotic translation initiation factors in ribosoamal scanning and initiation codon selection. *Genes and Developement* **16,** 2906-2922.

Phan L, Zhang X, Asano K, Anderson J, Vornlocher HP, Greenberg JR, Qin J & Hinnebusch AG. (1998). Identification of translation initiation factor 3 (eIF3) core complex, conserved in yeast and mammals, that interact with eIF5. *Molecular and Cellular Biology* **18,** 4935-4946.

Pierrat OA, Mikitova V, Bush MS, Browning KS & Doonan JH. (2007). Control of protein translation by phosphorylation of the mRNA 5'-cap-binding complex. *Biochemical Society Transactions* **035,** 1634-1647.

Pino M-T, Skinner JS, Park E-J, Jeknic Z, Hayes PM, Thomashow MF & Chen THH. (2007). Use of a stress inducible promoter to drive ectopic AtCBF expression improves potato freezing tolerance while minimizing negative effects on tuber yield. *Plant Biotechnology Journal* **5,** 591-604.

Pogorelko GV, Fursova OV, Ogarkova OA & Tarasov VA. (2008). A new technique for activation tagging in *Arabidopsis*. *Gene* **414,** 67-75.

Price J. (2005). An investigation into halotolerance mechanism in *Arabidopsis* thaliana. *PhD thesis*. University of Glasgow, Glasgow.

Price J, Li T-C, Kang SG, Na JK & Jang J-C. (2003). Mechanisms of glucose signaling during germination of *Arabidopsis*. *Plant Physiology* **132,** 1424-1438.

Proud CG. (2005). eIF2 and the control of cell physiology. *Seminars in Cell and Developmental Biology* **16,** 3-12.

Qiu H, Garcia-Barrio MT & Hinnebusch AG. (1998). Dimerization by translation initiation factor 2 kinase GCN2 is mediated by interactions in the C-terminal ribosome-binding region and protein kinase domain *Molecular and Cellular Biology* **18,** 2697-2711.

Quesada V, Ponce MR & Micol JL. (2000). Genetic Analysis of Salt-Tolerant Mutants in *Arabidopsis thaliana*. *Genetics* **154,** 421-436.

Ramirez M, Wek RC & Hinnebusch AG. (1991). Ribosome-association of GCN2 protein kinase, a translational activator of the GCN4 gene of *Saccharomyces cerevisiae*. *Molecular and Cellular Biology* **11,** 3027-3036.

Ray BK, Lawson TG, Kramer JC, Cladaras MH, Grifo JA, Abramson RD, Merrick WC & Thach RE. (1985). ATP-dependent unwinding of messenger RNA srtucture by eukaryotic initiation factor *Journal of Biological Chemistry* **260,** 7651-7658.

Rizhsky L, Liang H & Mittler R. (2002). The combined effect of drought stress and heat shock on gene expression in tobacco. *Plant Physiology* **130,** 1143-1151.

Rizhsky L, Liang H, Shuman J, Shulaev V, Davletova S & Mittler R. (2004). When defense pathways collide. The response of *Arabidopsis* to a combination of drought and heat stress. *Plant Physiology* **134,** 1683-1696.

Rolfes RJ & Hinnebusch AG. (1993). Translation of the yeast transcriptional activator GCN4 is stimulated by purine limitation: implication for activation of the protein kinase GCN2 *Molecular and Cellular Biology* **13,** 5099-5111.

Ron D & Harding HP. (2000). PERK and translation control by stress in the endoplasmic reticulum In *Translation control of gene expression*, ed. Sonenberg N, Hershey JW & Mathews MB, pp. 547-560. Cold Spring Harbor Laboratory Press, Plainview New York.

Saijo Y, Kinoshita N, Ishiyama K, Hata S, Kyozuka J, Hayakawa T, Nakamura T, Shimamoto K, Yamaya T & Izui K. (2001). A Ca^{2+}-dependent protein kinase that endows rice plants with cold- and salt-stress tolerance functions in vascular bundles. *Plant and Cell Physiology* **42,** 1228-1233.

Sambrook J & Russell D. (2001). *Molecular Cloning, A laboratory manual*. Cold Spring Harbor Laboratory Press, Cold Spring Harbor New York.

Sasaki T, Matsumoto T, Yamamoto K, Sakata K, Baba T, Katayose Y, Wu J, Niimura Y, Cheng Z, Nagamura Y, Antonio BA, Kanamori H, Hosokawa S, Masukawa M, Arikawa K, Chiden Y, Hayashi M, Okamoto M, Ando T, Aoki H, Arita K, Hamada M, Harada C, Hijishita S, Honda M, Ichikawa Y, Idonuma A, Iijima M, Ikeda M, Ikeno M, Ito S, Ito T, Ito Y, Ito Y, Iwabuchi A, Kamiya K, Karasawa W, Katagiri S, Kikuta A, Kobayashi N, Kono I, Machita K, Maehara T, Mizuno H, Mizubayashi T, Mukai Y, Nagasaki H, Nakashima M, Nakama Y, Nakamichi Y, Nakamura M, Namiki N, Negishi M, Ohta I, Ono N, Saji S, Sakai K, Shibata M, Shimokawa T, Shomura A, Song J, Takazaki Y, Terasawa K, Tsuji K, Waki K, Yamagata H, Yamane H, Yoshiki S, Yoshihara R, Yukawa K, Zhong H, Iwama H, Endo T, Ito H, Hahn JH, Kim H-I, Eun M-Y, Yano M, Jiang J & Gojobori T. (2002). The genome sequence and structure of rice chromosome 1. *Nature* **420,** 312-316.

Sessions A, Burke E, Presting G, Aux G, McElver J, Patton D, Dietrich B, Ho P, Bacwaden J, Ko C, Clarke JD, Cotton D, Bullis D, Snell J, Miguel T, Hutchison D, Kimmerly B, Mitzel T, Katagiri F, Glazebrook J, Law M & Goff SA. (2002). A high-throughput *Arabidopsis* reverse genetics system. *Plant Cell* **14,** 2985-2994.

Sharon RF, Kelly HC, Lori SB, Ginger JH, John M, Marliese SH, Samuel JP, Lys MB & Franklin RL. (1996). Use of firefly luciferase for ATP measurement: other nucleotides enhance turnover. *Journal of Bioluminescence and Chemiluminescence* **11,** 149-167.

Shi Y, An J, Liang J, Hayes SE, Sandusky GE, Stramm LE & Yang NN. (1999). Characterisation of a mutant pancreatic eIF-2α kinase, PEK, and co-localization with somatostatin in Islet delta cells. *Journal of Biological Chemistry* **274,** 5723-5730.

Singh CR, He H, Li M, Yamamoto Y & Asano K. (2004). Efficient in-corparation of eukaryotic initiation factor 1 into the multifactor complex is critical for formation and functional ribosomal pre-initiation complexes in vivo. *Journal of Biological Chemistry* **279,** 31910-31920.

Sung DY, Kaplan F, Lee KJ & Guy GL. (2003). Acquired tolerance to temperature extremes. *Trends in Plant Science* **8,** 179 - 187.

Szick-Miranda K, Jayachandran S, Tam A, Werner-Fraczek J, Williams AJ & Bailey-Serres J. (2003). Evaluation of translational control mechanisms in response to oxygen deprivation in maize. *Russian Journal of Plant Physiology* **50,** 774-786.

Tabaeizadeh Z & Kwang WJ. (1998). Drought-induced responses in plant cells. In *International Review of Cytology*, pp. 193-247. Academic Press.

Tallo'czy Z, Jiang W, Virgin HW, Leib DA, Scheuner D, Kaufman RJ, Eskelinen E-L & Levin B. (2002). Regulation of starvation- and virus-induced autophagy by the eIF2α kinase signaling pathway. *Proceedings of the National Academy of Sciences* **99,** 190-195.

Tani H, Xinwea C, Pedro N, John JG, Marhorie S, Andrea C, Eleanor G, Paul RJB & Gary JL. (2004). Activation tagging in plants: a tool for gene discovery. *Funcional and Integrative Genomics* **4,** 258-266.

Tax FE & Vernon DM. (2001). T-DNA-Associated Duplication/Translocations in *Arabidopsis*. Implications for Mutant Analysis and Functional Genomics. *Plant Physiology* **126,** 1527-1538.

Thorneycroft D, Sherson SM & Smith SM. (2001). Using gene knockouts to investigate plant metabolism. *Journal of Experimental Botany* **52,** 1593-1601.

Thuiller W, Lavorel S, Arau´ jo MB, Sykes MT & Prentice IC. (2005). Climate change threats to plant diversity in Europe. *Proceedings of the National Academy of Sciences, USA* **102,** 8245-8250.

Tissier AF, Marillonnet S, Klimyuk V, Patel K, Torres MA, Murphy G & Jones JDG. (1999). Multiple independent defective suppressor-mutator transposon insertions in *Arabidopsis*: A tool for functional genomics. *Plant Cell* **11,** 1841-1852.

Toth AM, Devaux P, Cattaneo R & Samuel CE. (2009). Protein kinase PKR mediates the apoptosis induction and growth restriction phenotypes of C protein-deficient measles virus. *Journal of Virology* **83,** 961-968.

Travella S, Klimm TE & Keller B. (2006). RNA interference-based gene silencing as an efficient tool for functional genomics in hexaploid bread wheat. *Plant Physiology* **142,** 6-20.

Valliyodan B & Nguyen HT. (2006). Understanding regulatory networks and engineering for enhanced drought tolerance in plants. *Current Opinion in Plant Biology* **9,** 189-195.

Vattem KM & Wek RC. (2004). Reinitiation involving upstream ORFs regulates ATF4 mRNA translation in mammalian cells. *Proceedings of the National Academy of Sciences* **101,** 11269-11274.

Verslues PE, Agarwal M, Katiyar-Agarway S, Zhu JH & Zhu JK. (2006). Methods and concepts in quantifying resistance to drought, salt and freezing, abiotic stresses that affect plant water status. *Plant Journal* **45,** 523 - 539.

Vilela C, Ramirez CV, Linz B, Rodrigues-Pousada C & McCarthy JE. (1999). Post-termination ribosome interactions with the 5'UTR modulate yeast mRNA stability. *EMBO Journal* **18,** 3139 - 3152.

Vittoria L, Cosimo G, Laura De G & Maria Concetta De P. (2008). Production of reactive species and modulation of antioxidant network in response to heat shock: a critical balance for cell fate. *Plant, Cell & Environment* **31,** 1606-1619.

Wang W, Vinocur B & Altman A. (2003). Plant responses to drought, salinity and extreme temperatures: towards genetic engineering for stress tolerance. *Planta* **218,** 1-14.

Wang W.X, B. V, O. S & A. A. (2001). Biotechnology of plant osmotic stress tolerance:physiological and molecular considerations. *Acta Horticulturae,* 285-292.

Webb S. (2008). Prediction of translationally regulated stress response proteins in *Arabidopsis thaliana*. M.Res. Dessertation, University of Glasgow, Glasgow, UK.

Weigel D, Ahn JH, Blazquez MA, Borevitz JO, Christensen SK, Fankhauser C, Ferrandiz C, Kardailsky I, Malancharuvil EJ, Neff MM, Nguyen JT, Sato S, Wang Z-Y, Xia Y, Dixon RA, Harrison MJ, Lamb CJ, Yanofsky MF & Chory J. (2000). Activation tagging in *Arabidopsis*. *Plant Physiology* **122,** 1003-1014.

Weigel D & Glazebrook J. (2006). Forward genetics in *Arabidopsis*: Finding mutations that cause particular phenotypes. *Cold Spring Harbor Protocols* **2006,** pdb.top1-.

Wek RC, Jiang HY & Anthony TG. (2006). Coping with stress: eIF2 kinases and translational control. *Biochemical Society Transactions* **34,** 7-11.

Wek SA, Zhu S & Wek RC. (1995). The histidyl-tRNA synthetase related sequence in the eIF-2α protein kinase GCN2 interacts with tRNA and is required for activation in response to starvation for different amino acids. *Molecular and Cellular Biology* **15,** 4497-4506.

Westernack C. (2007). Jasmonates: An update of biosynthesis, signal transduction and action in plant stress response, growth and developement. *Annals of Botany* **100,** 681-697.

Wielopolska A, Townley H, Moore I, Waterhouse P & Helliwell C. (2005). A high-throughput inducible RNAi vector for plants. *Plant Biotechnology Journal* **3,** 583-590.

Wilkie GS, Dickson KS & Gray NK. (2003). Regulation of mRNA translation by 5'- and 3'-UTR-binding factors. *Trends in Biochemical Sciences* **28,** 182-188.

Winter D, Vinegar B, Nahal H, Ammar R, Wilson GV & Provart NJ. (2007). An "Electronic Fluorescent Pictograph" Browser for Exploring and Analyzing Large-Scale Biological Data Sets. *PLoS ONE* **2,** e718.

Yadav SK. (2009). Cold stress tolerance mechanisms in plants. A review. *Agronomy for Sustainable Developement* **DOI: 10.1051/agro/2009050**.

Yamaguchi-Shinozaki K & Shinozaki K. (2006). Transcriptional regulatory Networks in cellular responses and tolerance to dehydration and cold stresses. *Annual Review of Plant Biology* **57,** 781-803.

Yamaguchi T & Blumwald E. (2005). Developing salt-tolerant crop plants: challenges and opportunities. *Trends in Plant Science* **10,** 615-620.

Yan W, Frank CL, Korth MJ, Sopher BL, Novoa I, Ron D & Katze MG. (2002). Control of PERK eIF2α kinase activity by the endoplasmic reticulum stress-induced molecular chaperone $P58^{IPK}$. *Proceedings of the National Academy of Sciences* **99,** 15920-15925.

Yang R, Wek SA & Wek RC. (2000). Glucose limitation induces GCN4 translation by activation of Gcn2 protein kinase. *Molecular and Cellular Biology* **20,** 2706-2717.

Yeo A. (1998). Predicting the interaction between the effects of salinity and climate change on crop plants. *Scientia Horticulturae* **78,** 159-174.

Zhang P, McGrath B, Li Sa, Frank A, Zambito F, Reinert J, Gannon M, Ma K, McNaughton K & Cavener DR. (2002a). PERK eukaryotic initiation Factor 2 (alpha) kinase is required for the development of the skeletal system, postnatal growth, and the function and viability of the pancreas. *Molecular and Cellular Biology* **22,** 3864-3874.

Zhang P, McGrath BC, Reinert J, Olsen DS, Lei L, Gill S, Wek SA, Vattem KM, Wek RC & Kimball SR. (2002b). The GCN2 eIF2alpha kinase is required for adaptation to amino acid deprivation in mice. *Molecular and Cellular Biology* **22,** 6681 - 6688.

Zhang X, Henriques R, Lin SS, QW N & NH C. (2006). Agrobactrium-mediated transformation of *Arabidopsis thaliana* using floral dip method. *Nature Protocols* **2,** 1-6.

Zhang Y, Dickinson JR, Paul MJ & Halford NG. (2003). Molecular cloning of an arabidopsis homologue of GCN2, a protein kinase involved in co-ordinated response to amino acid starvation. *Planta* **217,** 668 - 675.

Zhang Y, Wang Y, Kanyuka K, Parry MAJ, Powers SJ & Halford NG. (2008). GCN2-dependent phosphorylation of eukaryotic translation initiation factor-2 alpha in *Arabidopsis*. *Journal of Experimental Botany* **59,** 3131-3141.

Zhu J-K. (2002). Salt and drought stress signal transduction in plants. *Annual Review of Plant Biology* **53,** 247-273.

8 Appendices

Appendix 1. Map of Gateway™ compatible binary expression vector pMDC32 (Curtis & Grossniklaus, 2003) and pH7WGF2.0 (Karimi *et al.*, 2002).

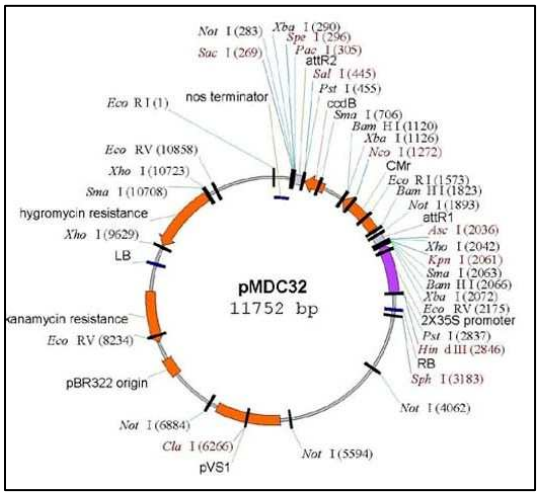

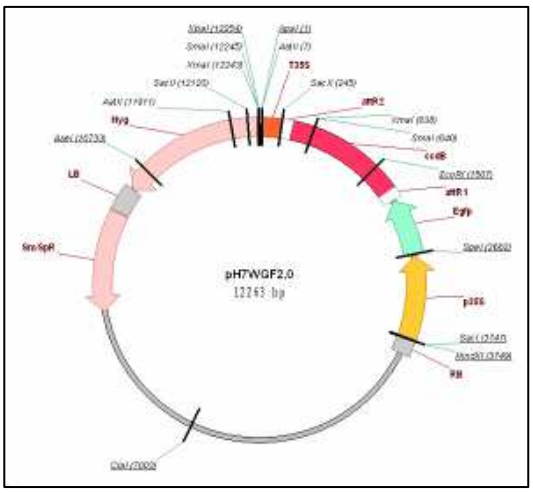

Appendix 2. Full-length ScGCN2 BLAST search on TAIR10 protein.

Sequences producing significant alignments:	Score (bits)	E Value
AT3G59410.2 | Symbols: GCN2 | protein kinase family protein...	230	7e-60
AT3G59410.1 | Symbols: GCN2 | protein kinase family protein...	230	7e-60
AT5G57630.1 | Symbols: CIPK21, SnRK3.4 | CBL-interacting pr...	103	9e-22
AT2G30360.1 | Symbols: CIPK11, PKS5, SIP4, SNRK3.22 | SOS3-...	100	6e-21
AT5G10930.1 | Symbols: CIPK5, SnRK3.24 | CBL-interacting pr...	100	8e-21
AT2G26980.5 | Symbols: CIPK3 | CBL-interacting protein kina...	99	2e-20
AT2G26980.2 | Symbols: CIPK3 | CBL-interacting protein kina...	98	4e-20
AT5G25110.1 | Symbols: CIPK25, SnRK3.25 | CBL-interacting p...	98	5e-20
AT2G26980.1 | Symbols: CIPK3, SnRK3.17 | CBL-interacting pr...	98	5e-20
AT2G26980.3 | Symbols: CIPK3 | CBL-interacting protein kina...	98	6e-20
AT2G26980.4 | Symbols: CIPK3 | CBL-interacting protein kina...	98	6e-20
AT5G01810.3 | Symbols: CIPK15 | CBL-interacting protein kin...	97	8e-20
AT5G01810.2 | Symbols: CIPK15, ATPK10, PKS3 | CBL-interacti...	97	1e-19
AT5G01810.1 | Symbols: CIPK15, ATPK10, PKS3, SNRK3.1, SIP2 ...	97	1e-19
AT5G21222.1 | Symbols: | protein kinase family protein | c...	96	2e-19
AT5G45820.1 | Symbols: CIPK20, SnRK3.6, PKS18 | CBL-interac...	96	3e-19
AT3G15220.1 | Symbols: | Protein kinase superfamily protei...	94	6e-19
AT5G35410.1 | Symbols: SOS2, SNRK3.11, CIPK24, ATSOS2 | Pro...	94	7e-19
AT3G02760.1 | Symbols: | Class II aaRS and biotin syntheta...	93	1e-18
AT5G04510.2 | Symbols: PDK1, ATPDK1 | 3'-phosphoinositide-d...	92	2e-18
AT5G04510.1 | Symbols: PDK1, ATPDK1 | 3'-phosphoinositide-d...	92	4e-18
AT1G48490.3 | Symbols: | Protein kinase superfamily protei...	91	5e-18
AT1G48490.2 | Symbols: | Protein kinase superfamily protei...	91	5e-18
AT1G48490.1 | Symbols: | Protein kinase superfamily protei...	91	5e-18
AT1G30270.1 | Symbols: CIPK23, SnRK3.23, ATCIPK23, LKS1 | C...	91	8e-18
AT1G53165.3 | Symbols: ATMAP4K ALPHA1 | Protein kinase supe...	91	1e-17
AT1G53165.2 | Symbols: ATMAP4K ALPHA1 | Protein kinase supe...	90	1e-17
AT1G53165.1 | Symbols: ATMAP4K ALPHA1 | Protein kinase supe...	90	1e-17
AT3G10540.1 | Symbols: | 3-phosphoinositide-dependent prot...	90	2e-17
AT3G17850.1 | Symbols: | Protein kinase superfamily protei...	89	2e-17
AT1G01140.2 | Symbols: CIPK9, PKS6 | CBL-interacting protei...	88	4e-17
AT1G12580.1 | Symbols: PEPKR1 | phosphoenolpyruvate carboxy...	88	4e-17
AT4G30960.1 | Symbols: CIPK6, SIP3, SNRK3.14, ATCIPK6 | SOS...	88	4e-17
AT5G45810.1 | Symbols: CIPK19, SnRK3.5 | CBL-interacting pr...	88	5e-17
AT3G29160.2 | Symbols: AKIN11, KIN11 | SNF1 kinase homolog ...	87	8e-17
AT3G29160.1 | Symbols: AKIN11, SNRK1.2, KIN11, ATKIN11 | SN...	87	8e-17
AT2G25090.1 | Symbols: CIPK16, SnRK3.18 | CBL-interacting p...	87	9e-17
AT5G21326.1 | Symbols: | Ca2+regulated serine-threonine pr...	87	9e-17
AT5G58380.1 | Symbols: CIPK10, PKS2, SIP1, SNRK3.8 | SOS3-i...	87	1e-16
AT4G14580.1 | Symbols: CIPK4, SnRK3.3 | CBL-interacting pro...	87	1e-16
AT1G01140.3 | Symbols: CIPK9, PKS6 | CBL-interacting protei...	86	2e-16
AT3G29160.3 | Symbols: AKIN11, KIN11 | SNF1 kinase homolog ...	86	2e-16
AT1G01140.1 | Symbols: CIPK9, SnRK3.12, PKS6 | CBL-interact...	86	2e-16
AT1G49180.2 | Symbols: | protein kinase family protein | c...	86	2e-16
AT1G49180.1 | Symbols: | protein kinase family protein | c...	86	3e-16
AT3G07980.1 | Symbols: MAPKKK6, MAP3KE2 | mitogen-activated...	84	7e-16
AT4G18700.1 | Symbols: CIPK12, SnRK3.9, ATWL4, WL4 | CBL-in...	84	8e-16
AT5G24430.1 | Symbols: | Calcium-dependent protein kinase ...	84	8e-16
AT3G01090.3 | Symbols: AKIN10, KIN10 | SNF1 kinase homolog ...	84	1e-15
AT3G01090.1 | Symbols: AKIN10, SNRK1.1, KIN10 | SNF1 kinase...	84	1e-15
AT1G08650.1 | Symbols: PPCK1, ATPPCK1 | phosphoenolpyruvate...	83	2e-15
AT3G01090.2 | Symbols: AKIN10, KIN10 | SNF1 kinase homolog ...	83	2e-15
AT4G24400.1 | Symbols: CIPK8, SnRK3.13, PKS11, ATCIPK8 | CB...	82	2e-15
AT4G24400.2 | Symbols: CIPK8, PKS11 | CBL-interacting prote...	82	2e-15
AT2G40860.1 | Symbols: | protein kinase family protein / p...	82	3e-15
AT3G50530.2 | Symbols: CRK | CDPK-related kinase | chr3:187...	82	3e-15
AT3G49370.1 | Symbols: | Calcium-dependent protein kinase ...	82	3e-15

Appendix 3. Full-length HsGCN2 BLAST search on TAIR10 protein

Sequences producing significant alignments:		Score (bits)	E Value
AT3G59410.2	Symbols: GCN2 | protein kinase family protein...	201	5e-51
AT3G59410.1	Symbols: GCN2 | protein kinase family protein...	200	8e-51
AT3G02760.1	Symbols: | Class II aaRS and biotin syntheta...	119	2e-26
AT1G09000.1	Symbols: ANP1, MAPKKK1, NP1 | NPK1-related pr...	102	2e-21
AT1G54960.1	Symbols: ANP2, MAPKKK2, NP2 | NPK1-related pr...	100	7e-21
AT5G04510.2	Symbols: PDK1, ATPDK1 | 3'-phosphoinositide-d...	100	1e-20
AT5G04510.1	Symbols: PDK1, ATPDK1 | 3'-phosphoinositide-d...	99	2e-20
AT3G06030.1	Symbols: ANP3, MAPKKK12, NP3 | NPK1-related p...	99	2e-20
AT3G10540.1	Symbols: | 3-phosphoinositide-dependent prot...	99	2e-20
AT4G26890.1	Symbols: MAPKKK16 | mitogen-activated protein...	94	1e-18
AT5G55090.1	Symbols: MAPKKK15 | mitogen-activated protein...	91	7e-18
AT2G32510.1	Symbols: MAPKKK17 | mitogen-activated protein...	88	5e-17
AT1G53165.3	Symbols: ATMAP4K ALPHA1 | Protein kinase supe...	87	8e-17
AT1G53165.2	Symbols: ATMAP4K ALPHA1 | Protein kinase supe...	87	9e-17
AT1G53165.1	Symbols: ATMAP4K ALPHA1 | Protein kinase supe...	87	9e-17
AT3G15220.1	Symbols: | Protein kinase superfamily protei...	85	5e-16
AT3G04810.2	Symbols: ATNEK2, NEK2 | NIMA-related kinase 2...	84	1e-15
AT3G04810.1	Symbols: ATNEK2, NEK2 | NIMA-related kinase 2...	84	1e-15
AT3G20860.1	Symbols: ATNEK5, NEK5 | NIMA-related kinase 5...	83	2e-15
AT1G63700.1	Symbols: EMB71, YDA, MAPKKK4 | Protein kinase...	82	4e-15
AT3G44200.1	Symbols: ATNEK6, NEK6, IBO1 | NIMA (never in ...	81	5e-15
AT1G54510.3	Symbols: NEK1 | NIMA-related serine/threonine...	81	5e-15
AT1G54510.2	Symbols: NEK1 | NIMA-related serine/threonine...	81	5e-15
AT1G54510.1	Symbols: ATNEK1, NEK1 | NIMA-related serine/t...	81	5e-15
AT4G08500.1	Symbols: MEKK1, ATMEKK1, MAPKKK8, ARAKIN | MA...	80	2e-14
AT5G58380.1	Symbols: CIPK10, PKS2, SIP1, SNRK3.8 | SOS3-i...	79	2e-14
AT1G49180.1	Symbols: | protein kinase family protein | c...	79	2e-14
AT1G49180.2	Symbols: | protein kinase family protein | c...	79	3e-14
AT3G63280.2	Symbols: ATNEK4, NEK4 | NIMA-related kinase 4...	78	5e-14
AT3G63280.1	Symbols: ATNEK4, NEK4 | NIMA-related kinase 4...	78	5e-14
AT1G53570.3	Symbols: MAP3KA, MAPKKK3 | mitogen-activated ...	78	6e-14
AT1G53570.2	Symbols: MAP3KA, MAPKKK3 | mitogen-activated ...	78	6e-14
AT1G53570.4	Symbols: MAP3KA | mitogen-activated protein k...	78	6e-14
AT1G53570.1	Symbols: MAP3KA, MAPKKK3 | mitogen-activated ...	78	6e-14
AT1G12580.1	Symbols: PEPKR1 | phosphoenolpyruvate carboxy...	78	6e-14
AT4G08480.1	Symbols: MAPKKK9, MEKK2 | mitogen-activated p...	77	8e-14
AT3G08730.1	Symbols: ATPK1, ATPK6, ATS6K1, PK6, PK1, S6K1...	77	9e-14
AT5G28290.1	Symbols: ATNEK3, NEK3 | NIMA-related kinase 3...	77	1e-13
AT5G67080.1	Symbols: MAPKKK19 | mitogen-activated protein...	77	1e-13
AT5G57630.1	Symbols: CIPK21, SnRK3.4 | CBL-interacting pr...	77	1e-13
AT4G10730.1	Symbols: | Protein kinase superfamily protei...	76	2e-13
AT5G18700.1	Symbols: RUK, EMB3013 | Protein kinase family...	76	2e-13
AT2G30360.1	Symbols: CIPK11, PKS5, SIP4, SNRK3.22 | SOS3-...	76	2e-13
AT3G08720.2	Symbols: ATPK19, ATPK2 | serine/threonine pro...	76	3e-13
AT3G08720.1	Symbols: ATPK19, ATS6K2, S6K2, ATPK2 | serine...	76	3e-13
AT3G61960.1	Symbols: | Protein kinase superfamily protei...	75	3e-13
AT3G61960.2	Symbols: | Protein kinase superfamily protei...	75	3e-13
AT4G38470.1	Symbols: | ACT-like protein tyrosine kinase ...	75	3e-13
AT4G24100.1	Symbols: | Protein kinase superfamily protei...	75	4e-13
AT1G01140.3	Symbols: CIPK9, PKS6 | CBL-interacting protei...	75	4e-13
AT5G45820.1	Symbols: CIPK20, SnRK3.6, PKS18 | CBL-interac...	75	4e-13
AT2G34650.1	Symbols: PID, ABR | Protein kinase superfamil...	75	5e-13
AT1G01140.1	Symbols: CIPK9, SnRK3.12, PKS6 | CBL-interact...	75	5e-13
AT1G01140.2	Symbols: CIPK9, PKS6 | CBL-interacting protei...	75	5e-13
AT4G24400.1	Symbols: CIPK8, SnRK3.13, PKS11, ATCIPK8 | CB...	75	5e-13
AT4G24400.2	Symbols: CIPK8, PKS11 | CBL-interacting prote...	75	5e-13
AT4G12020.3	Symbols: WRKY19, ATWRKY19, MAPKKK11, MEKK4 | ...	74	6e-13

Appendix 4. Full-length HsPKR BLAST Search on TAIR10 protein

Sequences producing significant alignments:		Score (bits)	E Value
AT3G59410.2	Symbols: GCN2 | protein kinase family protein...	123	3e-28
AT3G59410.1	Symbols: GCN2 | protein kinase family protein...	123	3e-28
AT1G54510.3	Symbols: NEK1 | NIMA-related serine/threonine...	104	1e-22
AT1G54510.2	Symbols: NEK1 | NIMA-related serine/threonine...	104	1e-22
AT1G54510.1	Symbols: ATNEK1, NEK1 | NIMA-related serine/t...	104	1e-22
AT3G44200.1	Symbols: ATNEK6, NEK6, IBO1 | NIMA (never in ...	100	3e-21
AT3G20860.1	Symbols: ATNEK5, NEK5 | NIMA-related kinase 5...	100	3e-21
AT5G28290.1	Symbols: ATNEK3, NEK3 | NIMA-related kinase 3...	94	3e-19
AT1G51660.1	Symbols: ATMKK4, MKK4, ATMEK4 | mitogen-activ...	92	6e-19
AT3G04810.2	Symbols: ATNEK2, NEK2 | NIMA-related kinase 2...	92	9e-19
AT3G04810.1	Symbols: ATNEK2, NEK2 | NIMA-related kinase 2...	92	9e-19
AT1G50240.2	Symbols: FU | Protein kinase family protein w...	91	2e-18
AT3G21220.1	Symbols: ATMKK5, ATMAP2K_ALPHA, MAP2K_A, MKK5...	90	4e-18
AT3G01490.1	Symbols: | Protein kinase superfamily protei...	88	2e-17
AT3G22750.1	Symbols: | Protein kinase superfamily protei...	86	5e-17
AT3G63280.2	Symbols: ATNEK4, NEK4 | NIMA-related kinase 4...	85	1e-16
AT3G63280.1	Symbols: ATNEK4, NEK4 | NIMA-related kinase 4...	85	1e-16
AT1G02970.1	Symbols: WEE1, ATWEE1 | WEE1 kinase homolog |...	84	2e-16
AT4G14780.1	Symbols: | Protein kinase superfamily protei...	84	2e-16
AT1G14000.1	Symbols: VIK | VH1-interacting kinase | chr1:...	83	5e-16
AT3G63260.1	Symbols: ATMRK1 | Protein kinase superfamily ...	83	5e-16
AT4G27300.1	Symbols: | S-locus lectin protein kinase fam...	83	6e-16
AT3G29160.2	Symbols: AKIN11, KIN11 | SNF1 kinase homolog ...	82	7e-16
AT3G29160.1	Symbols: AKIN11, SNRK1.2, KIN11, ATKIN11 | SN...	82	7e-16
AT3G63260.2	Symbols: ATMRK1 | Protein kinase superfamily ...	82	7e-16
AT5G39440.1	Symbols: SnRK1.3 | SNF1-related protein kinas...	82	1e-15
AT1G18350.1	Symbols: ATMKK7, BUD1, MKK7 | MAP kinase kina...	82	1e-15
AT3G29160.3	Symbols: AKIN11, KIN11 | SNF1 kinase homolog ...	82	1e-15
AT2G01820.1	Symbols: | Leucine-rich repeat protein kinas...	82	1e-15
AT3G61960.1	Symbols: | Protein kinase superfamily protei...	81	2e-15
AT3G01090.3	Symbols: AKIN10, KIN10 | SNF1 kinase homolog ...	81	2e-15
AT3G61960.2	Symbols: | Protein kinase superfamily protei...	81	2e-15
AT3G01090.1	Symbols: AKIN10, SNRK1.1, KIN10 | SNF1 kinase...	81	2e-15
AT3G01090.2	Symbols: AKIN10, KIN10 | SNF1 kinase homolog ...	81	2e-15
AT1G61460.1	Symbols: | S-locus protein kinase, putative ...	81	2e-15
AT2G11520.1	Symbols: CRCK3 | calmodulin-binding receptor-...	81	2e-15
AT2G25220.2	Symbols: | Protein kinase superfamily protei...	80	2e-15
AT5G64960.1	Symbols: CDKC2, CDKC;2 | cyclin dependent kin...	80	3e-15
AT2G25220.1	Symbols: | Protein kinase superfamily protei...	80	4e-15
AT5G50000.1	Symbols: | Protein kinase superfamily protei...	80	5e-15
AT1G70520.1	Symbols: CRK2 | cysteine-rich RLK (RECEPTOR-l...	79	8e-15
AT1G73500.1	Symbols: ATMKK9, MKK9 | MAP kinase kinase 9 |...	79	9e-15
AT3G06230.1	Symbols: ATMKK8, MKK8 | MAP kinase kinase 8 |...	78	2e-14
AT1G70110.1	Symbols: | Concanavalin A-like lectin protei...	78	2e-14
AT1G31420.1	Symbols: FEI1 | Leucine-rich repeat protein k...	78	2e-14
AT3G12200.1	Symbols: AtNek7, Nek7 | NIMA-related kinase 7...	77	2e-14
AT1G61420.1	Symbols: | S-locus lectin protein kinase fam...	77	2e-14
AT4G31170.3	Symbols: | Protein kinase superfamily protei...	77	2e-14
AT4G31170.2	Symbols: | Protein kinase superfamily protei...	77	2e-14
AT4G31170.1	Symbols: | Protein kinase superfamily protei...	77	2e-14
AT4G35780.1	Symbols: | ACT-like protein tyrosine kinase ...	77	3e-14
AT5G10270.1	Symbols: CDKC;1 | cyclin-dependent kinase C;1...	77	3e-14
AT2G37050.3	Symbols: | Leucine-rich repeat protein kinas...	77	4e-14
AT2G37050.1	Symbols: | Leucine-rich repeat protein kinas...	77	4e-14
AT1G69220.1	Symbols: SIK1 | Protein kinase superfamily pr...	77	4e-14
AT1G70130.1	Symbols: | Concanavalin A-like lectin protei...	77	5e-14
AT2G24360.1	Symbols: | Protein kinase superfamily protei...	76	7e-14

Appendix 5. Full-length HsPEKR BLAST search on TAIR10 protein

Sequences producing significant alignments:		Score (bits)	E Value
AT3G59410.2	Symbols: GCN2 | protein kinase family protein...	111	2e-24
AT3G59410.1	Symbols: GCN2 | protein kinase family protein...	111	3e-24
AT1G62400.1	Symbols: HT1 | Protein kinase superfamily pro...	85	2e-16
AT1G02970.1	Symbols: WEE1, ATWEE1 | WEE1 kinase homolog |...	84	8e-16
AT3G04810.2	Symbols: ATNEK2, NEK2 | NIMA-related kinase 2...	80	7e-15
AT3G04810.1	Symbols: ATNEK2, NEK2 | NIMA-related kinase 2...	80	7e-15
AT3G44200.1	Symbols: ATNEK6, NEK6, IBO1 | NIMA (never in ...	80	8e-15
AT5G28290.1	Symbols: ATNEK3, NEK3 | NIMA-related kinase 3...	80	9e-15
AT1G01140.2	Symbols: CIPK9, PKS6 | CBL-interacting protei...	80	1e-14
AT3G63280.2	Symbols: ATNEK4, NEK4 | NIMA-related kinase 4...	79	2e-14
AT3G63280.1	Symbols: ATNEK4, NEK4 | NIMA-related kinase 4...	79	2e-14
AT1G30270.1	Symbols: CIPK23, SnRK3.23, ATCIPK23, LKS1 | C...	79	3e-14
AT5G04510.2	Symbols: PDK1, ATPDK1 | 3'-phosphoinositide-d...	78	3e-14
AT5G04510.1	Symbols: PDK1, ATPDK1 | 3'-phosphoinositide-d...	78	4e-14
AT3G10540.1	Symbols: | 3-phosphoinositide-dependent prot...	78	5e-14
AT1G01140.1	Symbols: CIPK9, SnRK3.12, PKS6 | CBL-interact...	76	1e-13
AT1G01140.3	Symbols: CIPK9, PKS6 | CBL-interacting protei...	76	1e-13
AT5G01810.3	Symbols: CIPK15 | CBL-interacting protein kin...	76	2e-13
AT1G54510.3	Symbols: NEK1 | NIMA-related serine/threonine...	75	2e-13
AT1G54510.2	Symbols: NEK1 | NIMA-related serine/threonine...	75	2e-13
AT1G54510.1	Symbols: ATNEK1, NEK1 | NIMA-related serine/t...	75	2e-13
AT5G57630.1	Symbols: CIPK21, SnRK3.4 | CBL-interacting pr...	75	2e-13
AT5G01810.2	Symbols: CIPK15, ATPK10, PKS3 | CBL-interacti...	75	2e-13
AT5G01810.1	Symbols: CIPK15, ATPK10, PKS3, SNRK3.1, SIP2 ...	75	2e-13
AT1G50240.2	Symbols: FU | Protein kinase family protein w...	75	3e-13
AT5G58380.1	Symbols: CIPK10, PKS2, SIP1, SNRK3.8 | SOS3-i...	74	6e-13
AT5G45820.1	Symbols: CIPK20, SnRK3.6, PKS18 | CBL-interac...	74	8e-13
AT5G12480.1	Symbols: CPK7 | calmodulin-domain protein kin...	73	9e-13
AT3G20860.1	Symbols: ATNEK5, NEK5 | NIMA-related kinase 5...	73	1e-12
AT5G19450.2	Symbols: CDPK19, CPK8 | calcium-dependent pro...	73	1e-12
AT5G19450.1	Symbols: CDPK19, CPK8 | calcium-dependent pro...	73	1e-12
AT3G08720.2	Symbols: ATPK19, ATPK2 | serine/threonine pro...	73	1e-12
AT3G08720.1	Symbols: ATPK19, ATS6K2, S6K2, ATPK2 | serine...	73	1e-12
AT3G08730.1	Symbols: ATPK1, ATPK6, ATS6K1, PK6, PK1, S6K1...	72	2e-12
AT4G29810.2	Symbols: ATMKK2, MKK2, MK1 | MAP kinase kinas...	72	2e-12
AT2G01820.1	Symbols: | Leucine-rich repeat protein kinas...	72	2e-12
AT5G21222.1	Symbols: | protein kinase family protein | c...	72	3e-12
AT4G29810.1	Symbols: ATMKK2, MKK2, MK1 | MAP kinase kinas...	72	3e-12
AT5G39440.1	Symbols: SnRK1.3 | SNF1-related protein kinas...	72	3e-12
AT5G35410.1	Symbols: SOS2, SNRK3.11, CIPK24, ATSOS2 | Pro...	72	3e-12
AT1G74740.1	Symbols: CPK30, CDPK1A, ATCPK30 | calcium-dep...	72	3e-12
AT3G61960.1	Symbols: | Protein kinase superfamily protei...	72	3e-12
AT3G61960.2	Symbols: | Protein kinase superfamily protei...	72	3e-12
AT3G53930.1	Symbols: | Protein kinase superfamily protei...	71	3e-12
AT3G53930.2	Symbols: | Protein kinase superfamily protei...	71	3e-12
AT3G15354.1	Symbols: SPA3 | SPA1-related 3 | chr3:5169327...	71	4e-12
AT3G63260.2	Symbols: ATMRK1 | Protein kinase superfamily ...	71	5e-12
AT4G31170.3	Symbols: | Protein kinase superfamily protei...	71	5e-12
AT4G31170.2	Symbols: | Protein kinase superfamily protei...	71	5e-12
AT4G31170.1	Symbols: | Protein kinase superfamily protei...	71	5e-12
AT4G35780.1	Symbols: | ACT-like protein tyrosine kinase ...	71	5e-12
AT2G24360.1	Symbols: | Protein kinase superfamily protei...	71	6e-12
AT1G49180.1	Symbols: | protein kinase family protein | c...	70	6e-12
AT4G29810.3	Symbols: ATMKK2, MKK2, MK1 | MAP kinase kinas...	70	7e-12
AT3G63260.1	Symbols: ATMRK1 | Protein kinase superfamily ...	70	7e-12
AT5G50000.1	Symbols: | Protein kinase superfamily protei...	70	7e

Appendix 6. ClustalW2 alignment of the cloned AtGCN2 sequence on pENTR/D vector (pDGCN2) an AtGCN2 sequence deposited in TAIR

```
GCN2TAIR        ------------------------------------------------------------
pDGCN2          GCATATGATTTTATTTTGACTGATAGTGACCTGTTCGTTGCAACAAATTGATGAGCAATG 60

GCN2TAIR        ------------------------------------------------------------AT 2
pDGCN2          CTTTTTTATAATGCCAACTTTGTACAAAAAAGCAGGCTCCGCGGCCGCCCCCTTCACCAT 120
                                                                          **

GCN2TAIR        GGGTCGCAGCAGTTCGAAGAAAAAGAAGAAACGAGGAGGTAGCGGAAGAAGGGGTCAGCT 62
pDGCN2          GGGTCGCAGCAGTTCGAAGAAAAAGAAGAAACGAGGAGGTAGCGGAAGAAGGGGTCAGCT 180
                ************************************************************

GCN2TAIR        GAAAGACCATGGATCTAATGCTGATGAAGATAATGAACTTCTATCTGAGGAGATCACTGC 122
pDGCN2          GAAAGACCATGGATCTAATGCTGATGAAGATAATGAACTTCTATCTGAGGAGATCACTGC 240
                ************************************************************

GCN2TAIR        TCTCTCTGCAATATTTCAAGAGGACTGCAAAGTTGTTTCTGATTCGCGTTCGCCTCCGCA 182
pDGCN2          TCTCTCTGCAATATTTCAAGAGGACTGCAAAGTTGTTTCTGATTCGCGTTCGCCTCCGCA 300
                ************************************************************

GCN2TAIR        AATAGCAATCAAGCTCAGGCCGTACTCAAAGGACATGGGATATGAAGACACCGACATATC 242
pDGCN2          AATAGCAATCAAGCTCAGGCCGTACTCAAAGGACATGGGATATGAAGACACCGACATATC 360
                ************************************************************

GCN2TAIR        TGCTATGCTTATAGTTAGGTGCTTACCAGGATATCCTTACAAGTGCCCCAAGCTTCAGAT 302
pDGCN2          TGCTATGCTTATAGTTAGGTGCTTACCAGGATATCCTTACAAGTGCCCCAAGCTTCAGAT 420
                ************************************************************

GCN2TAIR        TACTCCAGAACAAGGGTTGACAACAGCTGATGCTGAGAAGCTTTTATCTCTTCTCGAGGA 362
pDGCN2          TACTCCAGAACAAGGGTTGACAACAGCTGATGCTGAGAAGCTTTTATCTCTTCTCGAGGA 480
                ************************************************************

GCN2TAIR        CCAGGCAAATTCCAATGCTCGTGAAGGTCGGGTTATGATATTCAACCTGGTGGAGGCTGC 422
pDGCN2          CCAGGCAAATTCCAATGCTCGTGAAGGTCGGGTTATGATATTCAACCTGGTGGAGGCTGC 540
                ************************************************************

GCN2TAIR        TCAAGAGTTTTTATCAGAAATCATTCCGGAAAGTCATGATGAGGAATCTGTTCCATGCTT 482
pDGCN2          TCAAGAGTTTTTATCAGAAATCATTCCGGAAAGTCATGATGAGGAATCTGTTCCATGCTT 600
                ************************************************************

GCN2TAIR        GACTGCACATCGAAGCACTCAGTTCATTGAGCAACCTATGCTTTCAAATATAGCAAAATC 542
pDGCN2          GACTGCACATCGAAGCACTCAGTTCATTGAGCAACCTATGCTTTCAAATATAGCAAAATC 660
                ************************************************************

GCN2TAIR        CTGTTCTGGTGGACCTTTTGTGTATGGTTTTATAGACCTATTTAGTGGCTTGGAAGATGC 602
pDGCN2          CTGTTCTGGTGGACCTTTTGTGTATGGTTTTATAGACCTATTTAGTGGCTTGGAAGATGC 720
                ************************************************************

GCN2TAIR        AAGAAATTGGAGTCTGACTCCAGATGAAAATAGGGGAATCGTATCTTCAGTACAATCTCA 662
pDGCN2          AAGAAATTGGAGTCTGACTCCAGATGAAAATAGGGGAATCGTATCTTCAGTACAATCTCA 780
                ************************************************************

GCN2TAIR        CCCACTAGACACTTCAAGAATTTTGCATCAGAAGCCAGACAAGAATCTGAAGCGATTTGA 722
pDGCN2          CCCACTAGACACTTCAAGAATTTTGCATCAGAAGCCAGACAAGAATCTGAAGCGATTTGA 840
                ************************************************************

GCN2TAIR        AGACCATGCTAAAGAAGAAGTTGCACTGCCTGCTCCCATTGCCAAACTGAATACTGTTCA 782
pDGCN2          AGACCATGCTAAAGAAGAAGTTGCACTGCCTGCTCCCATTGCCAAACTGAATACTGTTCA 900
                ************************************************************

GCN2TAIR        AGAGGAGAATGTTGATGATACAAGCATCTCTTCTTTTGACTCAAGTAAATCTACTGACGA 842
pDGCN2          AGAGGAGAATGTTGATGATACAAGCATCTCTTCTTTTGACTCAAGTAAATCTACTGACGA 960
                ************************************************************

GCN2TAIR        TGTGGAATCTGGATTATTCCAAAATGAGAAGAAGGAATCAAATCTTCAAGATGATACAGC 902
pDGCN2          TGTGGAATCTGGATTATTCCAAAATGAGAAGAAGGAATCAAATCTTCAAGATGATACAGC 1020
                ************************************************************

GCN2TAIR        TGAAGATGACAGCACTAACTCCGAAAGTGAGTCGCTGGGGTCATGGTCTTCTGATTCCTT 962
pDGCN2          TGAAGATGACAGCACTAACTCCGAAAGTGAGTCGCTGGGGTCATGGTCTTCTGATTCCTT 1080
                ************************************************************

GCN2TAIR        AGCTCAAGATCAAGTGCCTCAGATTAGCAAGAAAGATCTGTTGATGGTCCATTTACTTCG 1022
pDGCN2          AGCTCAAGATCAAGTGCCTCAGATTAGCAAGAAAGATCTGTTGATGGTCCATTTACTTCG 1140
                ************************************************************

GCN2TAIR        AGTAGCTTGCACTTCCCGAGGACCTTTGGCTGATGCATTACCTCAGATAACTGATGAACT 1082
pDGCN2          AGTAGCTTGCACTTCCCGAGGACCTTTGGCTGATGCATTACCTCAGATAACTGATGAACT 1200
                ************************************************************

GCN2TAIR        GCATGAGCTTGGTATATTGTCTGAAGAAGTGTTGGATTTAGCTTCCAAATCATCTCCAGA 1142
pDGCN2          GCATGAGCTTGGTATATTGTCTGAAGAAGTGTTGGATTTAGCTTCCAAATCATCTCCAGA 1260
                ************************************************************

GCN2TAIR        CTTTAATAGAACCTTTGAACATGCATTCAATCAAAACATGGCCTCAACCAGTGTTCCTCA 1202
pDGCN2          CTTTAATAGAACCTTTGAACATGCATTCAATCAAAACATGGCCTCAACCAGTGTTCCTCA 1320
                ************************************************************

GCN2TAIR        GTTTTGGGAGCCACCTTCTGATTCTTGCGAGCCAAATGCATCACTCCCAAGCTCGCGATA 1262
pDGCN2          GTTTTGGGAGCCACCTTCTGATTCTTGCGAGCCAAATGCATCACTCCCAAGCTCGCGATA 1380
                ************************************************************

GCN2TAIR        TCTCAATGATTTTGAAGAGTTGAAACCCCTTGGCCAAGGTGGTTTCGGCCACGTTGTGTT 1322
pDGCN2          TCTCAATGATTTTGAAGAGTTGAAACCCCTTGGCCAAGGTGGTTTCGGCCACGTTGTGTT 1440
                ************************************************************
```

```
GCN2TAIR        GTGCAAAAATAAACTGGATGGAAGACAATATGCAGTGAAGAAAATTCGACTGAAGGACAA 1382
pDGCN2          GTGCAAAAATAAACTGGATGGAAGACAATATGCAGTGAAGAAAATTCGACTGAAGGACAA 1500
                ************************************************************

GCN2TAIR        AGAGATACCTGTCAACAGTCGGATAGTTCGAGAAGTAGCAACACTTTCCCGTTTGCAGCA 1442
pDGCN2          AGAGATACCTGTCAACAGTCGGATAGTTCGAGAAGTAGCAACACTTTCCCGTTTGCAGCA 1560
                ************************************************************

GCN2TAIR        TCAGCATGTTGTACGTTACTATCAGGCCTGGTTCGAAACAGGAGTTGTTGATCCCTTTGC 1502
pDGCN2          TCAGCATGTTGTACGTTACTATCAGGCCTGGTTCGAAACAGGAGTTGTTGATCCCTTTGC 1620
                ************************************************************

GCN2TAIR        TGGCGCAAATTGGGGATCAAAAACTGCAGGGAGTTCAATGTTCAGCTACTCAGGTGCAGT 1562
pDGCN2          TGGCGCAAATTGGGGATCAAAAACTGCAGGGAGTTCAATGTTCAGCTACTCAGGTGCAGT 1680
                ************************************************************

GCN2TAIR        GTCAACTGAAATTCCTGAGCAGGACAATAATCTTGAGTCGACTTATCTATATATTCAAAT 1622
pDGCN2          GTCAACTGAAATTCCTGAGCAGGACAATAATCTTGAGTCGACTTATCTATATATTCAAAT 1740
                ************************************************************

GCN2TAIR        GGAATATTGTCCCAGGACTCTCCGCCAGGTTTTTGAATCATATAACCACTTCGACAAAGA 1682
pDGCN2          GGAATATTGTCCCAGGACTCTCCGCCAGGTTTTTGAATCATATAACCACTTCGACAAAGA 1800
                ************************************************************

GCN2TAIR        CTTTGCATGGCATTTAATTCGCCAAATTGTGGAAGGCTTAGCTCATATCCATGGACAAGG 1742
pDGCN2          CTTTGCATGGCATTTAATTCGCCAAATTGTGGAAGGCTTAGCTCATATCCATGGACAAGG 1860
                ************************************************************

GCN2TAIR        AATAATTCATCGGGATTTTACACCTAACAATATTTTCTTTGACGCTCGGAATGATATTAA 1802
pDGCN2          AATAATTCATCGGGATTTTACACCTAACAATATTTTCTTTGACGCTCGGAATGATATTAA 1920
                ************************************************************

GCN2TAIR        AATTGGGGATTTTGGTCTTGCAAAGTTCTTGAAGCTGGAACAGTTGGATCAAGATGGGGG 1862
pDGCN2          AATTGGGGATTTTGGTCTTGCAAAGTTCTTGAAGCTGGAACAGTTGGATCAAGATGGGGG 1980
                ************************************************************

GCN2TAIR        TTTCTCTACGGATGTGGCTGGAAGCGGAGTCGATAGTACTGGTCAAGCTGGTACTTACTT 1922
pDGCN2          TTTCTCTACGGATGTGGCTGGAAGCGGAGTCGATAGTACTGGTCAAGCTGGTACTTACTT 2040
                ************************************************************

GCN2TAIR        TTACACAGCACCTGAAATTGAGCAAGATTGGCCTAAGATTGATGAAAAGGCCGACATGTA 1982
pDGCN2          TTACACAGCACCTGAAATTGAGCAAGATTGGCCTAAGATTGATGAAAAGGCCGACATGTA 2100
                ************************************************************

GCN2TAIR        TAGCTTAGGGGTTGTGTTCTTTGAACTTTGGCATCCTTTTGGAACCGCCATGGAGAGACA 2042
pDGCN2          TAGCTTAGGGGTTGTGTTCTTTGAACTTTGGCATCCTTTTGGAACCGCCATGGAGAGACA 2160
                ************************************************************

GCN2TAIR        CGTTATTTTAACTAACCTGAAGCTGAAAGGGGAGCTACCTCTCAAATGGGTAAATGAATT 2102
pDGCN2          CGTTATTTTAACTAACCTGAAGCTGAAAGGGGAGCTACCTCTCAAATGGGTAAATGAATT 2220
                ************************************************************

GCN2TAIR        TCCCGAACAGGCGTCTCTACTGCGGCGTTTGATGTCTCCAAGTCCATCTGATCGTCCCTC 2162
pDGCN2          TCCCGAACAGGCGTCTCTACTGCGGCGTTTGATGTCTCCAAGTCCATCTGATCGTCCCTC 2280
                ************************************************************

GCN2TAIR        TGCCACAGAACTTCTTAAGCATGCATTTCCTCCCAGAATGGAATCTGAGTTACTGGACAA 2222
pDGCN2          TGCCACAGAACTTCTTAAGCATGCATTTCCTCCCAGAATGGAATCTGAGTTACTGGACAA 2340
                ************************************************************

GCN2TAIR        TATTCTAAGAATAATGCAAACTTCTGAAGATTCAAGTGTTTATGATAGAGTAGTAAGTGT 2282
pDGCN2          TATTCTAAGAATAATGCAAACTTCTGAAGATTCAAGTGTTTATGATAGAGTAGTAAGTGT 2400
                ************************************************************

GCN2TAIR        GATATTTGATGAAGAAGTATTAGAGATGAAAAGCCATCAGTCTAGTAGATCGAGACTCTG 2342
pDGCN2          GATATTTGATGAAGAAGTATTAGAGATGAAAAGCCATCAGTCTAGTAGATCGAGACTCTG 2460
                ************************************************************

GCN2TAIR        TGCAGATGATAGTTATATTCAATACACAGAGATAAATACAGAGCTTCGTGATTATGTTGT 2402
pDGCN2          TGCAGATGATAGTTATATTCAATACACAGAGATAAATACAGAGCTTCGTGATTATGTTGT 2520
                ************************************************************

GCN2TAIR        TGAAATAACAAAAGAAGTCTTTAGGCAGCATTGTGCGAAGCATCTAGAGGTCATACCAAT 2462
pDGCN2          TGAAATAACAAAAGAAGTCTTTAGGCAGCATTGTGCGAAGCATCTAGAGGTCATACCAAT 2580
                ************************************************************

GCN2TAIR        GCGCTTACTTAGTGATTGCCCCCAGTTTAGCAGGAAAACTGTAAAGCTTTTGACCAATGG 2522
pDGCN2          GCGCTTACTTAGTGATTGCCCCCAGTTTAGCAGGAAAACTGTAAAGCTTTTGACCAATGG 2640
                ************************************************************

GCN2TAIR        AGGAGATATGCTTGAACTATGCTATGAGCTACGACTGCCTTTTGTGCATTGGATAAGCGT 2582
pDGCN2          AGGAGATATGCTTGAACTATGCTATGAGCTACGACTGCCTTTTGTGCATTGGATAAGCGT 2700
                ************************************************************

GCN2TAIR        AAATCAGAAATCCTCATTCAAGCGATATGAAATATCTCATGTCTACAGGAGAGCAATTGG 2642
pDGCN2          AAATCAGAAATCCTCATTCAAGCGATATGAAATATCTCATGTCTACAGGAGAGCAATTGG 2760
                ************************************************************

GCN2TAIR        CCATTCTCCACCAAATCCGTGTCTTCAGGCGGACTTTGACATTGTTGGAGGCACACTATC 2702
pDGCN2          CCATTCTCCACCAAATCCGTGTCTTCAGGCGGACTTTGACATTGTTGGAGGCACACTATC 2820
                ************************************************************

GCN2TAIR        CCTGACAGAGGCAGAAGTTCTCAAGGTGATAGTAGACATCACAACCCACATCTTTCATCG 2762
pDGCN2          CCTGACAGAGGCAGAAGTTCTCAAGGTGATAGTAGACATCACAACCCACATCTTTCATCG 2880
                ************************************************************

GCN2TAIR        CGGATCTTGTGACATTCATTTGAATCATGGAGATTTGCTGGATGCGATTTGGTCCTGGGC 2822
pDGCN2          CGGATCTTGTGACATTCATTTGAATCATGGAGATTTGCTGGATGCGATTTGGTCCTGGGC 2940
                ************************************************************

GCN2TAIR        AGGAATTAAGGCAGAGCATAGACGAAAGGTTGCAGAGCTTCTTTCCATGATGGGATCCTT 2882
pDGCN2          AGGAATTAAGGCAGAGCATAGACGAAAGGTTGCAGAGCTTCTTTCCATGATGGGATCCTT 3000
                ************************************************************

GCN2TAIR        GCGTCCTCAGTCATCTGAGCGGAAGCTAAAATGGGTTTTCATAAGGCGTCAACTTCTTCA 2942
pDGCN2          GCGTCCTCAGTCATCTGAGCGGAAGCTAAAATGGGTTTTCATAAGGCGTCAACTTCTTCA 3060
                ************************************************************
```

```
GCN2TAIR        GGAGTTGAAGTTACCTGAAGCTGTTGTCAATAGACTGCAGACTGTTGCTTCAAGGTTTTG 3002
pDGCN2          GGAGTTGAAGTTACCTGAAGCTGTTGTCAATAGACTGCAGACTGTTGCTTCAAGGTTTTG 3120
                ************************************************************

GCN2TAIR        TGGAGATGCAGATCAAGCACTTCCTCGTTTAAGAGGGGCTCTGCGTGCTGATAGACCTAC 3062
pDGCN2          TGGAGATGCAGATCAAGCACTTCCTCGTTTAAGAGGGGCTCTGCGTGCTGATAGACCTAC 3180
                ************************************************************

GCN2TAIR        CCGCAAAGCACTCGATGAGTTGTCAAACCTCTTAACCTACCTGAGAGTCTGGAGGATAGA 3122
pDGCN2          CCGCAAAGCACTCGATGAGTTGTCAAACCTCTTAACCTACCTGAGAGTCTGGAGGATAGA 3240
                ************************************************************

GCN2TAIR        AGAGCATGTTCATATTGATGTTCTGATGCCACCAACTGAAAGTTATCACCGGAATTTGTT 3182
pDGCN2          AGAGCATGTTCATATTGATGTTCTGATGCCACCAACTGAAAGTTATCACCGGAATTTGTT 3300
                ************************************************************

GCN2TAIR        TTTTCAGGTTTTCTTAACCAAAGAAAATAGCTCTGGGACATCTAATGATGGCGTTTTACT 3242
pDGCN2          TTTTCAGGTTTTCTTAACCAAAGAAAATAGCTCTGGGACATCTAATGATGGCGTTTTACT 3360
                ************************************************************

GCN2TAIR        TGCTGTTGGTGGTCGTTATGATTGGTTGGTGCAGGAAGTGTGTGATCGTGAACATAAAAT 3302
pDGCN2          TGCTGTTGGTGGTCGTTATGATTGGTTGGTGCAGGAAGTGTGTGATCGTGAACATAAAAT 3420
                ************************************************************

GCN2TAIR        GAACCTCCCTGGTGCTGTTGGAGTTAGTCTTGCACTGGAGACAATATTTCAGCATCTTCC 3362
pDGCN2          GAACCTCCCTGGTGCTGTTGGAGTTAGTCTTGCACTGGAGACAATATTTCAGCATCTTCC 3480
                ************************************************************

GCN2TAIR        TATGGATCTAAGGCCTATTAGAAATGAAGTCAGCACCAGTGTACTTGTTTGTTCAAGAGG 3422
pDGCN2          TATGGATCTAAGGCCTATTAGAAATGAAGTCAGCACCAGTGTACTTGTTTGTTCAAGAGG 3540
                ************************************************************

GCN2TAIR        AGGTGGTGGTTTACTGGTCCAGCGCATGGAACTAGTTGCGGAACTATGGGAAAAAAGTAT 3482
pDGCN2          AGGTGGTGGTTTACTGGTCCAGCGCATGGAACTAGTTGCGGAACTATGGGAAAAAAGTAT 3600
                ************************************************************

GCN2TAIR        AAAGGCTGAGTTTGTTCCAACACCTGATCCAAGTCTTACTGAGCAGTACGAATATGCAAA 3542
pDGCN2          AAAGGCTGAGTTTGTTCCAACACCTGATCCAAGTCTTACTGAGCAGTACGAATATGCAAA 3660
                ************************************************************

GCN2TAIR        TGAACATGAAATCAAATGTCTAGTGATCATCACAGAGTCTGGAGTAGCTCAAAATCAAAT 3602
pDGCN2          TGAACATGAAATCAAATGTCTAGTGATCATCACAGAGTCTGGAGTAGCTCAAAATCAAAT 3720
                ************************************************************

GCN2TAIR        AGAGTTTGTAAAGGTTCGTCACCTTGAACTGAAGAAGGAGAAAGTGGTAGGAAGAGAAGA 3662
pDGCN2          AGAGTTTGTAAAGGTTCGTCACCTTGAACTGAAGAAGGAGAAAGTGGTAGGAAGAGAAGA 3780
                ************************************************************

GCN2TAIR        ACTTGTCAAATTTCTGCTGGATGCAATGGCTGTTCAATTTAGAAACCCCTCTGTTTGGAG 3722
pDGCN2          ACTTGTCAAATTTCTGCTGGATGCAATGGCTGTTCAATTTAGAAACCCCTCTGTTTGGAG 3840
                ************************************************************

GCN2TAIR        CTAA------------------------------------------------------- 3726
pDGCN2          CTAAAAGGGTGGGCGCGCCGACCCAGCTTTCTTGTACAAAGTTGGCATTATAAGAAAGCA 3900
                ****

GCN2TAIR        ------------------------------------------------------------
pDGCN2          TTGCTTATCAATTTGTTGCAACGAACAGGTCACTATCAGTCAAAATAAAATCATTATTGC 3960

GCN2TAIR        ----------------
pDGCN2          CATCCAGCTGATTCCC 3976
```

Appendix 7. ANOVA for germination of WT Col-0, *Atgcn2-1* and *p35S:AtGCN2* seeds on ½ MS media supplemented with 0, 100 and 150mM NaCl

Variate: %Germination
Day 2

Source of variation	d.f.	s.s.	m.s.	v.r.	F pr.
Genotype	2	355.03	177.51	3.17	0.066
NaCl_mM	2	25391.20	12695.60	226.49	<.001
Genotype.NaCl_mM	4	359.61	89.90	1.60	0.216
Residual	18	1008.96	56.05		
Total	26	27114.79			

Day 3

Source of variation	d.f.	s.s.	m.s.	v.r.	F pr.
Genotype	2	366.89	183.44	2.97	0.077
NaCl_mM	2	27782.89	13891.44	224.73	<.001
Genotype.NaCl_mM	4	683.56	170.89	2.76	0.059
Residual	18	1112.67	61.81		
Total	26	29946.00			

Day 4

Source of variation	d.f.	s.s.	m.s.	v.r.	F pr.
Genotype	2	819.9	409.9	2.39	0.120
NaCl_mM	2	18212.7	9106.4	53.08	<.001
Genotype.NaCl_mM	4	488.4	122.1	0.71	0.595
Residual	18	3088.0	171.6		
Total	26	22609.0			

Appendix 8. ANOVA for primary root growth of WT Col-0, *Atgcn2-1* and *p35S:AtGCN2* seedlings on MS media supplemented with 0, 50, and 100mM NaCl

Variate: Primary root growth

Source of variation	d.f.(m.v.)	s.s.	m.s.	v.r.	F pr.
Genotype	2	12.3466	6.1733	55.24	<.001
NaCl_mM	2	20.9416	10.4708	93.70	<.001
Genotype.NaCl_mM	4	0.4557	0.1139	1.02	0.398
Residual	250(11)	27.9374	0.1117		
Total	258(11)	60.1835			

Appendix 9. ANOVA for germination of WT Col-0, *Atgcn2-1* and *p35S:AtGCN2* seeds on ½ MS media supplemented with 0, 50,100 and 150mM KCl

Variate: %Germination
Day 2

Source of variation	d.f.(m.v.)	s.s.	m.s.	v.r.	F pr.
Genotype	2	692.8	346.4	2.45	0.108
KCl_mM	3	42837.2	14279.1	101.06	<.001
Genotype.KCl_mM	6	227.6	37.9	0.27	0.946
Residual	23(1)	3249.8	141.3		
Total	34(1)	44502.7			

Day 3

Source of variation	d.f.	s.s.	m.s.	v.r.	F pr.
Genotype	2	72.17	36.08	1.17	0.327
KCl_mM	3	2407.67	802.56	26.03	<.001
Genotype.KCl_mM	6	223.17	37.19	1.21	0.337
Residual	24	740.00	30.83		
Total	35	3443.00			

Day 4

Source of variation	d.f.	s.s.	m.s.	v.r.	F pr.
Genotype	2	139.56	69.78	5.79	0.009
KCl_mM	3	463.44	154.48	12.81	<.001
Genotype.KCl_mM	6	256.89	42.81	3.55	0.012
Residual	24	289.33	12.06		
Total	35	1149.22			

Appendix 10. ANOVA for primary root growth of WT Col-0, *Atgcn2-1* and *p35S:AtGCN2* seedlings on MS media supplemented with 0, 50, 100 and 150mM KCl

Variate: Primary root growth

Source of variation	d.f.	s.s.	m.s.	v.r.	F pr.
KCl_mM	3	19.77280	6.59093	98.60	<.001
Genotype	2	1.86151	0.93075	13.92	<.001
KCl_mM.Genotype	6	0.46127	0.07688	1.15	0.365
Residual	24	1.60435	0.06685		
Total	35	23.69993			

Appendix 11. ANOVA for germination of WT Col-0, *Atgcn2-1* and *p35S:AtGCN2* seeds on ½ MS media supplemented with 0, 50,100, 200 and 300mM Mannitol

Variate: %Germination
Day 2

Source of variation	d.f.	s.s.	m.s.	v.r.	F pr.
Genotype	2	748.088	374.044	176.45	<.001
Mannitol	4	934.414	233.604	110.20	<.001
Genotype.Mannitol	8	690.100	86.263	40.69	<.001
Residual	30	63.593	2.120		
Total	44	2436.196			

Day 3

Source of variation	d.f.	s.s.	m.s.	v.r.	F pr.
Genotype	2	1590.67	795.34	53.36	<.001
Mannitol	4	30266.35	7566.59	507.67	<.001
Genotype.Mannitol	8	440.55	55.07	3.69	0.004
Residual	30	447.13	14.90		
Total	44	32744.70			

Day 4

Source of variation	d.f.	s.s.	m.s.	v.r.	F pr.
Genotype	2	62.15	31.07	2.14	0.136
Mannitol	4	42042.67	10510.67	722.65	<.001
Genotype.Mannitol	8	175.08	21.88	1.50	0.197
Residual	30	436.34	14.54		
Total	44	42716.23			

Appendix 12. ANOVA for primary root growth of WT Col-0, *Atgcn2-1* and *p35S:AtGCN2* seedlings on MS media supplemented with 0, 50, 100, 200 and 300mM mannitol

Variate: Primary root growth

Source of variation	d.f.	s.s.	m.s.	v.r.	F pr.
Mannitol_mM	4	20.42111	5.10528	58.94	<.001
Genotype	2	2.95150	1.47575	17.04	<.001
Mannitol_mM.Genotype	8	0.96362	0.12045	1.39	0.241
Residual	30	2.59847	0.08662		
Total	44	26.93471			

Appendix 13. ANOVA for germination of WT Col-0, *Atgcn2-1* and *p35S:AtGCN2* seeds on ½ MS media infused with 0, 20 and 40% PEG6000 solution.

Variate: %Germination
Day 2

Source of variation	d.f.	s.s.	m.s.	v.r.	F pr.
Genotype	2	452.4	226.2	1.65	0.210
%_PEG	2	6483.9	3242.0	23.70	<.001
Genotype.% PEG	4	130.5	32.6	0.24	0.914
Residual	27	3693.4	136.8		
Total	35	10760.1			

Day3

Source of variation	d.f.	s.s.	m.s.	v.r.	F pr.
Geno	2	1534.5	767.2	4.88	0.015
%PEG	2	3052.4	1526.2	9.71	<.001
Genotype.% PEG	4	337.7	84.4	0.54	0.709
Residual	27	4242.5	157.1		
Total	35	9167.0			

Day4

Source of variation	d.f.	s.s.	m.s.	v.r.	F pr.
Genotype	2	478.04	239.02	4.13	0.027
%PEG4	2	2370.01	1185.00	20.49	<.001
Genotype.%PEG	4	195.96	48.99	0.85	0.508
Residual	27	1561.81	57.84		
Total	35	4605.81			

Appendix 14. ANOVA for primary root growth of WT Col-0, *Atgcn2-1* and *p35S:AtGCN2* seedlings on MS media infused with 0, 70% PEG6000 solution

Variate: Primary root growth

Source of variation	d.f.(m.v.)	s.s.	m.s.	v.r.	F pr.
%PEG	1	9.74678	9.74678	159.75	<.001
Genotype	2	0.21720	0.10860	1.78	0.177
%PEG.Genotype	2	0.65235	0.32618	5.35	0.007
Residual	65(1)	3.96576	0.06101		
Total	70(1)	14.44930			

Appendix 15. Germination kinetics of WT Col-0, *Atgcn2-1* and *p35S:AtGCN2* seeds assessed at 2, 3 and 4 days after incubation on ½ MS supplemented with 0-2µM ABA.

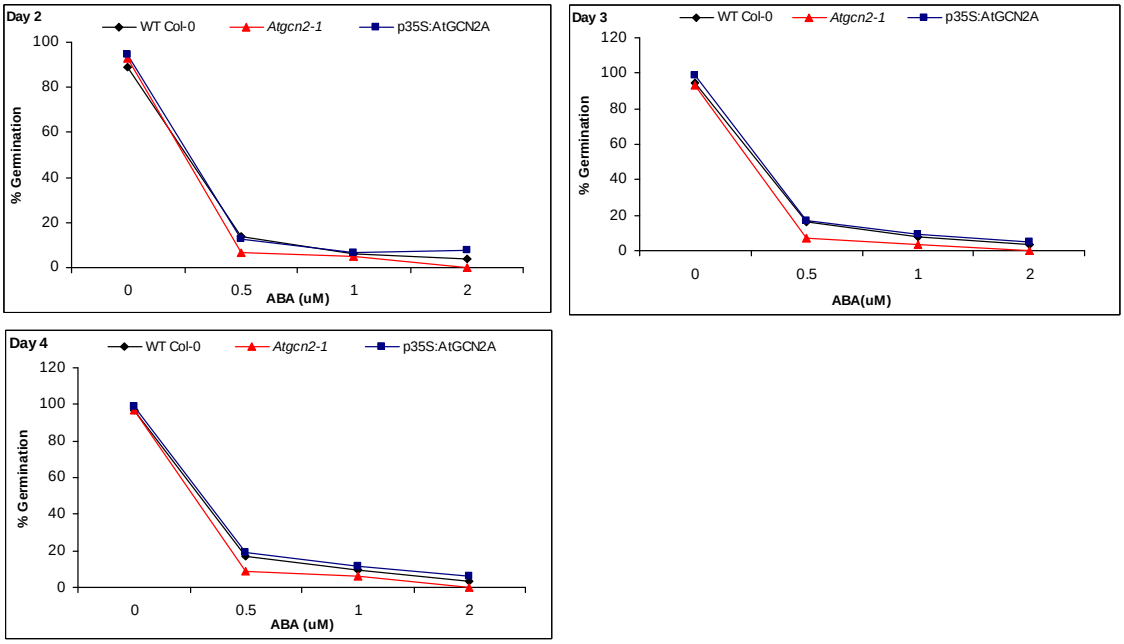

Appendix 16. ANOVA for survival for survival of acclimated 14-day old WT Col-0, *Atgcn2-1* and *p35S:AtGCN2* seedlings 12 days after -20°C cold shock treatments

Variate: %Survival

Source of variation	d.f.	s.s.	m.s.	v.r.	F pr.
Genotype	2	1782.52	891.26	14.91	0.001
Residual	9	537.81	59.76		
Total	11	2320.33			

Appendix 17. Confirmation of AteIF2α insert sequences cloned in pCR4®-TOPO sequencing vector. **(A)** ClustalW2 alignment of cloned At2G40290.1 and CDS sequence deposited in TAIR

```
AteIF290        GCGCGATTCGCCCTTGCAGTATCGAAATCTACCAATCATGGCGAGTCAAACACCGAATCT 60
TAIR_CDS        ------------------------------------ATGGCGAGTCAAACACCGAATCT 23
                                                     **********************

AteIF290        CGAGTGTCGGATGTACGAGGCGAAATACCCAGAGGTGGATATGGCGGTGATGATCCAGGT 120
TAIR_CDS        CGAGTGTCGGATGTACGAGGCGAAATACCCAGAGGTGGATATGGCGGTGATGATCCAGGT 83
                ************************************************************

AteIF290        GAAGAACATTGCCGATATGGGAGCTTATGTTTCTCTCCTCGAGTACAACAACATCGAAGG 180
TAIR_CDS        GAAGAACATTGCCGATATGGGAGCTTATGTTTCTCTCCTCGAGTACAACAACATCGAAGG 143
                ************************************************************

AteIF290        CATGATCCTTTTCTCCGAGCTCTCTCGTCGTCGGATCCGAAGTGTTAGCAGTTTGATTAA 240
TAIR_CDS        CATGATCCTTTTCTCCGAGCTCTCTCGTCGTCGGATCCGAAGTGTTAGCAGTTTGATTAA 203
                ************************************************************

AteIF290        GGTCGGAAGAATTGAGCCTGTCATGGTTCTCCGTGTTGACAAAGAGAAAGGTTACATTGA 300
TAIR_CDS        GGTCGGAAGAATTGAGCCTGTCATGGTTCTCCGTGTTGACAAAGAGAAAGGTTACATTGA 263
                ************************************************************

AteIF290        TCTGAGCAAACGTAGAGTCAGCGAGGAAGATATTCAGACTTGTGAAGAGAGGTATAACAA 360
TAIR_CDS        TCTGAGCAAACGTAGAGTCAGCGAGGAAGATATTCAGACTTGTGAAGAGAGGTATAACAA 323
                ************************************************************

AteIF290        GAGCAAACTTGTTCATTCTATCATGCGCCATGTTGCTGAGACTCTTTCAATTGATTTGGA 420
TAIR_CDS        GAGCAAACTTGTTCATTCTATCATGCGCCATGTTGCTGAGACTCTTTCAATTGATTTGGA 383
                ************************************************************

AteIF290        GGACTTGTATGTGAACATTGGTTGGCCTTTGTATCGACGACATGGTCATGCTTTTGAGGC 480
TAIR_CDS        GGACTTGTATGTGAACATTGGTTGGCCTTTGTATCGACGACATGGTCATGCTTTTGAGGC 443
                ************************************************************

AteIF290        TTTCAAGATCTTAGTGACGGATCCTGATTCAGTGTTGGGTCCTCTCACCCGTGAGATCAA 540
TAIR_CDS        TTTCAAGATCTTAGTGACGGATCCTGATTCAGTGTTGGGTCCTCTCACCCGTGAGATCAA 503
                ************************************************************

AteIF290        AGAAGTTGGGCCTGATGGGCAAGAGGTGACTAAGGTTGTACCTGCTGTTACGGAAGAAGT 600
TAIR_CDS        AGAAGTTGGGCCTGATGGGCAAGAGGTGACTAAGGTTGTACCTGCTGTTACGGAAGAAGT 563
                ************************************************************

AteIF290        GAAAGATGCACTTGTGAAGAACATTAGGAGGAGAATGACACCACAACCAATGAAAATCCG 660
TAIR_CDS        GAAAGATGCACTTGTGAAGAACATTAGGAGGAGAATGACACCACAACCAATGAAAATCCG 623
                ************************************************************

AteIF290        GGCTGATATCGAATTGAAGTGTTTTCAGTTTGATGGAGTTGTTCACATTAAGGAGGCTAT 720
TAIR_CDS        GGCTGATATCGAATTGAAGTGTTTTCAGTTTGATGGAGTTGTTCACATTAAGGAGGCTAT 683
                ************************************************************

AteIF290        GAAAAATGCTGAAGCCGCTGGAAATGAAGACTGTCCTGTTAAGATTAAATTGGTTGCTCC 780
TAIR_CDS        GAAAAATGCTGAAGCCGCTGGAAATGAAGACTGTCCTGTTAAGATTAAATTGGTTGCTCC 743
                ************************************************************

AteIF290        ACCTCTGTATGTCCTTACTACTCAGACACTTGACAAGGAACAAGGGATTGAAATTCTAAA 840
TAIR_CDS        ACCTCTGTATGTCCTTACTACTCAGACACTTGACAAGGAACAAGGGATTGAAATTCTAAA 803
                ************************************************************

AteIF290        CAAAGCCATAGCAGCATGCACTGAGACAATTGAGACACACAAAGGCAAGCTTGTCGTTAA 900
TAIR_CDS        CAAAGCCATAGCAGCATGCACTGAGACAATTGAGACACACAAAGGCAAGCTTGTCGTTAA 863
                ************************************************************

AteIF290        GGAGGGGGCTAGAGCTGTGAGTGAACGTGATGAAAAGATGCTGACAGAACACATGGCTAA 960
TAIR_CDS        GGAGGGGGCTAGAGCTGTGAGTGAACGTGATGAAAAGATGCTGACAGAACACATGGCTAA 923
                ************************************************************

AteIF290        GCTACGTCTTGACAATGAAGAAATGAGCGGCGATGAAGATAGCGGAGACGAAGAAGAGGA 1020
TAIR_CDS        GCTACGTCTTGACAATGAAGAAATGAGCGGCGATGAAGATAGCGGAGACGAAGAAGAGGA 983
                ************************************************************

AteIF290        CACTGGTATGGGCGAAGTGGATCTCGATGCAGGTGCCGGAATCATCGAGTAAGATTGCCG 1080
TAIR_CDS        CACTGGTATGGGCGAAGTGGATCTCGATGCAGGTGCCGGAATCATCGAGTAA-------- 1035
                ************************************************** 

AteIF290        GATTTTTCTTTCTATTAAATCTACCCAATCTCAACAGTCCCAGTATTTTGGTTTAAGCTT 1140
TAIR_CDS        ------------------------------------------------------------

AteIF290        TGACAAGGCAGTAGAAAAACCTCCGAGAGGATTTATGTGCTTTTTGATGACTCTGAGGCA 1200
TAIR_CDS        ------------------------------------------------------------

AteIF290        TTTTATTTTACCCATAGGGGGTGGTTACATATCAATCATACATTCATGGTTTTATAAAAG 1260
TAIR_CDS        ------------------------------------------------------------

AteIF290        ATTTGATTCTTTGCATATGTTACTACTGCTCAAGAATATGTTGCTCCACCACATGAAGGG 1320
TAIR_CDS        ------------------------------------------------------------

AteIF290        CGAATTCGTA 1330
TAIR_CDS        ----------
```

(B). ClustalW2 alignment of cloned At5G05470.1 and CDS sequence deposited in TAIR

```
AteIF270        CGCGATTCGCCCTTCATCCTCGACGCTCTCTACTAAGAAACTCAATCTTACTTTCTCTGT 60
TAIR_CDS        ------------------------------------------------------------

AteIF270        AATTCGTAGCTTCCGAAATCTTTTCTCAAGAATCTCATAACCATGGCGAATCCTGCTCCG 120
TAIR_CDS        -----------------------------------------ATGGCGAATCCTGCTCCG 18
                                                         ******************

AteIF270        AATCTAGAATGTCGTATGTACGAATCGAGATACCCTGATGTAGACATGGCGGTGATGATT 180
TAIR_CDS        AATCTAGAATGTCGTATGTACGAATCGAGATACCCTGATGTAGACATGGCGGTGATGATT 78
                ************************************************************

AteIF270        CAGGTGAAGACCATCGCTGACATGGGAGCTTACGTATCTCTCCTTGAATACAACAACATC 240
TAIR_CDS        CAGGTGAAGACCATCGCTGACATGGGAGCTTACGTATCTCTCCTTGAATACAACAACATC 138
                ************************************************************

AteIF270        GAAGGAATGATCCTGTTCTCCGAGCTCTCTCGCCGTCGGATTCGTAGTATCAGTAGCTTA 300
TAIR_CDS        GAAGGAATGATCCTGTTCTCCGAGCTCTCTCGCCGTCGGATTCGTAGTATCAGTAGCTTA 198
                ************************************************************

AteIF270        ATCAAGGTCGGTCGTACCGAGCCTGTTATGGTCCTTCGTGTCGATAGAGAGAGAGGTTAC 360
TAIR_CDS        ATCAAGGTCGGTCGTACCGAGCCTGTTATGGTCCTTCGTGTCGATAGAGAGAGAGGTTAC 258
                ************************************************************

AteIF270        ATTGATCTCAGTAAACGTAGGGTTAGTGATGAGGACAAAGAGGCTTGTGAGGAGAGGTAT 420
TAIR_CDS        ATTGATCTCAGTAAACGTAGGGTTAGTGATGAGGACAAAGAGGCTTGTGAGGAGAGGTAT 318
                ************************************************************

AteIF270        AATAAGAGCAAGCTTGTTCACTCTATCATGCGTCATGTTGCTGAGACTGTTGGTGTCGAT 480
TAIR_CDS        AATAAGAGCAAGCTTGTTCACTCTATCATGCGTCATGTTGCTGAGACTGTTGGTGTCGAT 378
                ************************************************************

AteIF270        TTGGAGGAGCTATACGTAAACATCGGTTGGCCATTGTATAAGAAGCATGGACATGCTTTT 540
TAIR_CDS        TTGGAGGAGCTATACGTAAACATCGGTTGGCCATTGTATAAGAAGCATGGACATGCTTTT 438
                ************************************************************

AteIF270        GAGGCTTTCAAAATTGTTGTCACTGATCCTGATTCAGTTTTCGATGCTCTTACCCGAGAA 600
TAIR_CDS        GAGGCTTTCAAAATTGTTGTCACTGATCCTGATTCAGTTTTCGATGCTCTTACCCGAGAA 498
                ************************************************************

AteIF270        GTTAAAGAAACTGGACCTGATGGTGTGGAGGTGACCAAAGTTGTCCCGGCTGTGTCTGAA 660
TAIR_CDS        GTTAAAGAAACTGGACCTGATGGTGTGGAGGTGACCAAAGTTGTCCCGGCTGTGTCTGAA 558
                ************************************************************

AteIF270        GAATTGAAAGATGCATTTTTGAAGGACATTAGGAGGAGAATGACACCACAGCCAATGAAG 720
TAIR_CDS        GAATTGAAAGATGCATTTTTGAAGGACATTAGGAGGAGAATGACACCACAGCCAATGAAG 618
                ************************************************************

AteIF270        ATTCGTGCTGATATTGAATTGAAGTGTTTTCAGTTTGATGGAGTTCTCCACATCAAGGAA 780
TAIR_CDS        ATTCGTGCTGATATTGAATTGAAGTGTTTTCAGTTTGATGGAGTTCTCCACATCAAGGAA 678
                ************************************************************

AteIF270        GCCATGAAGAAGGCAGAGGCTGTAGGTACTGATGATTGTCCAGTCAAAATCAAGCTCGTT 840
TAIR_CDS        GCCATGAAGAAGGCAGAGGCTGTAGGTACTGATGATTGTCCAGTCAAAATCAAGCTCGTT 738
                ************************************************************

AteIF270        GCTCCACCACTTTATGTACTCACAACTCACACCCATTACAAGGAAAAAGGAATAGTGACT 900
TAIR_CDS        GCTCCACCACTTTATGTACTCACAACTCACACCCATTACAAGGAAAAAGGAATAGTGACT 798
                ************************************************************

AteIF270        CTGAATAAAGCAATTGAAGCATGCATTACTGCAATTGAGGAACACAAGGGTAAACTTGTC 960
TAIR_CDS        CTGAATAAAGCAATTGAAGCATGCATTACTGCAATTGAGGAACACAAGGGTAAACTTGTC 858
                ************************************************************

AteIF270        GTTAAAGAAGGTGCTCGTGCGGTGAGTGAGCGTGATGACAAATTGCTTGCTGAGCACATG 1020
TAIR_CDS        GTTAAAGAAGGTGCTCGTGCGGTGAGTGAGCGTGATGACAAATTGCTTGCTGAGCACATG 918
                ************************************************************

AteIF270        GCTAAGCTTAGAATGGATAATGAAGAAATGAGTGGTGATGAGGGAAGCGAAGATGAAGAA 1080
TAIR_CDS        GCTAAGCTTAGAATGGATAATGAAGAAATGAGTGGTGATGAGGGAAGCGAAGATGAAGAA 978
                ************************************************************

AteIF270        GAAGACACTGGAATGGGAGAAGTCGATATCGATGGAGGTAGCGGGATAATTGAATGAACA 1140
TAIR_CDS        GAAGACACTGGAATGGGAGAAGTCGATATCGATGGAGGTAGCGGGATAATTGAATGA--- 1035
                ************************************************************

AteIF270        AAAGCAAAAGCATTGTAACTGCTGTTTCTGCTTTAGATCCTACAATTTTGTTTCCCTTTG 1200
TAIR_CDS        ------------------------------------------------------------

AteIF270        AGCAAAAACAGAAGGGCGAATTCGTAA 1227
TAIR_CDS        --------------------------
```

Appendix 18. List of 99 *Arabidopsis* loci possessing putative regulatory uORFs generated using the FivePrime Viewer (Shaun, 2008).

*Group 1	Group 2	Group 3	Group 4	Group 4
AT1G58120.1	AT3G47550.2	AT4G31590.1	AT3G13000.1	AT1G19850.1
AT1G58122.1	AT1G55920.1	AT5G58930.1	AT2G30590.1	AT2G04880.1
AT2G04039.2	AT1G68935.1	AT3G01970.1	AT1G22070.1	AT5G62165.1
AT1G74160.1	AT4G28600.1	AT5G42980.1	AT2G46530.2	AT2G23740.1
AT4G20110.1	AT3G26750.1	AT4G27040.3	AT1G01060.1	AT5G59710.1
AT3G21700.1	AT3G45090.2	AT2G42320.2	AT5G61270.2	AT5G65210.1
AT3G21700.3	AT2G02620.1	AT4G27040.1	AT1G09570.2	AT3G54390.1
AT1G78770.1	AT3G54350.1	AT3G54120.1	AT2G46870.1	AT5G56270.1
AT4G02010.1	AT2G05510.4	AT3G07550.1	AT3G01970.1	AT5G07690.1
AT5G63780.1		AT4G23770.1	AT1G43850.1	AT4G21750.2
AT5G18940.1		AT4G10380.1	AT1G52150.1	AT1G75410.2
AT5G18940.2		AT2G39870.1	AT5G67480.2	AT5G60100.1
AT3G53670.1		AT1G50030.1	AT5G47670.2	AT3G04280.1
AT3G53668.1		AT5G48000.2	AT1G72830.1	AT4G30410.2
AT1G25500.3		AT2G30420.1	AT5G66730.1	AT2G47890.1
AT5G08120.1		AT5G63410.1	AT5G42520.3	AT4G04890.1
AT3G13000.1		AT5G48000.4	AT5G06100.3	AT1G20980.1
AT2G05210.2		AT2G02760.1	AT2G30420.1	AT5G67480.1
AT1G09570.2		AT2G36485.1	AT5G08130.2	AT3G62340.1
		AT2G01480.1	AT1G64630.1	AT4G32980.1
		AT3G20870.1	AT5G15310.1	AT2G25650.1
			AT5G50010.1	AT3G12250.3
			AT5G09460.1	AT2G04890.1
			AT5G64340.1	AT1G54830.3
			AT5G15850.1	AT4G16520.2

*Group 1: cDNAs that generally scored highly (98-99), group 2: cDNAs that have physical resemblance to the HsATF4 5′UTRs sequences, group 3: cDNAs that have physical resemblance to the ScGCN4 5′ UTRs sequences, group 4: cDNAs coding for transcriptional factor.